Valorizing and Remediating Synthetic Polymers with Tenacious Backbones

by
Paul Takunda Chazovachii

A dissertation submitted in partial fulfillment
of the requirements for the degree of
Doctor of Philosophy
(Chemistry)
in the University of Michigan
2021

Doctoral Committee:

Professor Anne J. McNeil, Chair
Professor Jinsang Kim
Professor E. Neil G. Marsh
Professor Paul M. Zimmerman

P. Takunda Chazovachii

paulchaz@umich.edu

ORCID iD: 0000-0003-0561-0302

Dedication

To my family and friends back home in Zimbabwe, the family I have made in America, and most importantly, to Jesus Christ, the Master and Sustainer of my soul and Source of grace in my life. Not an ounce of this work would have been possible without your love and support.

Acknowledgments

I knew this would be one of the most challenging parts of my thesis. Acknowledgments are hard for me, not because expressing gratitude is difficult in itself, but because giving adequate praise and honor to the sheer number of people responsible for my being here today is a tremendous feat.

You all deserve a chapter at least, and some of you, perhaps an entire thesis as well, to explain the depths of your love and impact on my progress. God has placed each of you in my life strategically at specific times and places to draft a beautiful yet intricate picture that is now ready to hang on the wall. The credit is not mine alone – it is shared!

Dad and mom, Alexander and Clara Chazovachii, thank you for raising me in a community of strength and dignity. From you both I learned resilience, honest work ethic, and the meaning of sacrifice. I thank you my brother Brendon Dube and my sisters Kundai, Rutendo, and Bridget. We always found a way to be joyful during hard times and remained hopeful. Sometimes it was transport to school, sometimes clothes, sometimes even food… but *nhasi ndezvedu, Takunda veduwe!* Thank you Mbuya Nomusa Dube and Sekuru Robert Dube – without you both the logistics of my coming to America to study would have been close to impossible.

I would like to thank my advisor Anne J. McNeil. Anne, thank you for inviting me to join your lab, and your relentless efforts to chasten me into a good scientist – from learn how to prepare presentation slides to running experiments properly. You know I dreaded the process but today I am grateful. Thank you for giving me the freedom to explore and for being there call me back in when I drifted too far.

I would like to thank Professor Neil Marsh. Neil, thank you for welcoming me into your lab even though my research trajectory was vastly different from yours, it really meant a lot.

I would like to thank Professor Mark Banaszak Holl. Mark, thank you for being my advisor in my first few years of grad school. Thank you for fostering my creativity and teaching me to think.

I would like to thank my committee members Professor Jinsang Kim and Professor Paul Zimmerman. Jinsang, I appreciated the two polymer science classes (Advanced functional polymers and polymer physics) I took from you. A lot of the concepts I learned from those classes were instrumental to my research. Paul, I enjoyed the continued collaborations we have had since my second year. Thank you for all the guidance.

I would like to thank my labmates past and present who contributed many aspects of my growth as a graduate student made each day easier: Dr. Mitchell Smith, Dr. Peter Goldberg, Dr. Kendra Souther, Dr. Ariana Hall, Dr. Chen Kong, Dr. Patrick Lutz, Dr. Danielle Fagnani, Dr. Amanda Leone, Dr. Tan Nguyen, Dr. Woojung Ji, Dr. Justin Harris, Dukhan Kim, Matthew Hannigan, Emily Mueller, Briana Barbu, Jessica Tami, Gloria de la Garza, Vai Shastri, and Isabelle Zelaya.

I would like to thank my former labmates from the Marsh group: Dr. Arti Baban Dumbrepatil, Dr. Soumi Ghosh, Dr. Kyle, Dr. Soumi Ghosh, Dr. Ajitha Cristie-David, Dr. Tim Grunkemeyer, Dr. Karl Koebke, Dr. Hannah Chia, April Kaneshiro, Prathamesh Datar , Srijoni Majhi, and Ayesha Patel.

I would like to thank my former labmates from the Banaszak Holl group: Dr. Ted Ahn, Jinhee Kim, Rachel Wallace, Junjie Chen, Li Zi, and Nathan Ng.

Both before and during this journey, several individuals and organizations were instrumental in supporting me, whether financially, emotionally, or by setting an example in difficult times. It began with the Joshua Nkomo Scholarship foundation, where I fellowshipped with many brilliant

minds and learned the ethos of servant leadership. Next, from the United States Achievers Program, I learned that dreams do come true. Somewhere in the mix, I have picked up lifelong mentors: Rebecca Ziegler Mano (amai), Dr. Allen Chaparadza (who never let me settle for less than greatness), Bill and Paulina Logozzo (who ground me in my faith and identity in Jesus), Dr. Timothy Trygstad (my amazing advisor who would not let me drop my math major and even paid for my grad school application, which I could not afford), Dr. McGahey (who introduced me to the art of scientific research), Dr. Luther Qson (my amazing math professor and advisor), Dr. Timothy Swager (thank you for giving me the opportunity to intern in your lab), and Dr. Myles Herbert (who continues to mentor me during my internship at MIT and introduced me to polymers). I thank all these wise companions for their continued guidance and support.

Mama and baba Baye, thank you for giving me a home in grade 3 as I transitioned to boarding school life.

I would also like to thank Chadwick Boseman, Denzel Washington, Dr. Benjamin Carson, Dr. Thomas Sowell, Strive Masiiwa (sponsored my high education too) and many other black male public figures for using their platforms to set great examples for me and many other young black men.

A shout out to my friends since undergrad Isaac Wakiro (help with GRE fees, help replacing lost phones, and a brother indeed), Ahmed Kemal (the David Goggins of the pack), Aleksander Radakovic (man, very kind to those meals between classes when I was taking 21 credits and couldn’t go to get food), Fitsum Solomon, Hansel Ngwa, Gaurav Adhikari, Raphael Mumba, Akeem Gumbs, Malvern Madondo, Glander Madondo, Michelle Sandisile Dube, Trang Nguyen, and Yevedzo Chipangura.

A shout out to my long-time grad school buddies, Ryan Dodson, Edmond Atindaana, Masimba Hwati, and Kunal Khanna (great researchers, gym buddies, and friends).

A shout out to all my former roommates: Jimmy Hinrichs, Audrey Eshun, James Akinola, Jerreh Jadda, and Matthew Schnizlein – Thank you all for tolerating me as I toiled through tough classes and the horrors of grad school!

I thank all my peers from Gokomere High School, the College of St. Scholastica, and the University of Michigan. To say everyone by name would be similar to counting the grains of sand on the seashore.

Last but not least, I thank my mudiwa wangu, Violet Chazovachii (née Sheffey). Our relationship marked the beginning of a new saga in both my personal life and professional career. You've endured late nights in lab, never-ending questions about grammar edits, hectic scheduling and so much more. This win is ours.

Table of Contents

List of Figures

List of Tables

List of Schemes

List of Appendices

Abstract

Synthetic polymers or plastics are manufactured long-chained molecules primarily sourced from nonrenewable fossil fuels like petroleum. Owing to their superior properties (e.g., durability, impermeability, and high strength to mass ratio), plastics are the most widely used material, replacing traditional materials like metals, wood, and glass. However, the same properties that make plastics desirable are also responsible for their recycling difficulty and biopersistence. As a result, over 79% of the 6.3 billion metric tons of plastics waste generated to date accumulates in landfills or escapes into the environment, persisting for decades or centuries. This thesis highlights the immensity of plastics pollution and contributes polymer chemistry-based solutions in recycling and remediation methodologies.

Chapter 1 emphasizes that the desirable properties of plastics are also responsible for their problematic persistence in the environment, causing a predicament where plastics are indispensable yet detrimental to the environment. Because it is impractical for society to avoid plastics altogether, developing recycling and remediation methods that use waste plastics as feedstocks alleviates their environmental impact. Many polymers, however, cannot be recycled via mechanical processes, and as a result, they are incinerated or landfilled. These waste plastics slowly disintegrate into microplastics, which are significant environmental pollutants and have problematic health effects. One example is the superabsorbent material made of crosslinked sodium polyacrylate used in diapers and feminine hygiene products.

We aimed to develop a chemical recycling solution for the superabsorbent polymer used in Procter and Gamble's (P&G's) hygiene products ($PAA_{P\&G}$). After discussing various chemical recycling methods, we highlight the unavailability of closed-loop recycling methods for $PAA_{P\&G}$. We then transition to chapter 2, where we present an open-loop recycling method inspired by the common acrylic acid origin of $PAA_{P\&G}$ and pressure-sensitive adhesives. This transformation was executed in three steps, namely (i) decrosslinking via hydrolysis, (ii) an optional chain-shortening step via sonication, and (iii) functionalizing via base-mediated esterification. Viscoelastic properties were tuned by adjusting the molar mass using sonication or incorporating amine functional groups, making adhesives spanning various applications, including tapes, bandages, and sticky notes.

Any new recycling methodology requires an unbiased comparative evaluation to determine its processing and environmental impacts—chapter 3 utilized life cycle assessment to evaluate and improve the recycling method presented in chapter 2. The significant improvements to the previously developed process include: (i) replacing the base hydrolysis with acid hydrolysis and (ii) replacing the base-mediated esterification with Fischer esterification. Life cycle assessment suggested that our new approach outperforms the conventional petroleum-based route on nearly every metric, including carbon dioxide emissions and energy usage. Recycling diapers and feminine hygiene products through this method could avoid the disposal of 2 million metric tons of polymer waste annually.

Chapter 4 begins with accidentally discovering that the adhesives developed in chapters 2 and 3 effectively captured micronized rubber, a type of microplastics, in a mixed solvent waste container. Next, we demonstrated the removal of various microplastics using adhesive-coated glass slides followed by quantitatively evaluating removal in suspensions of 10 μm polystyrene as a function

of adhesive molar mass. We successfully quantified polystyrene removal using flow cytometry without fluorescent labeling and confirmed > 99% removal efficiencies.

Chapter 5 summarizes each chapter and recommends future directions, including preliminary work towards developing a one-pot process to recycle $PAA_{P\&G}$ to make PSAs where the idea stems from the similarity between acid hydrolysis and acid-catalyzed esterification.

Chapter 1: Introduction

1.1 Dilemma: Synthetic polymers are indispensable yet problematically persistent

Synthetic polymers and the quality of life experienced by the residents of the 21st century are inextricably tied. Synthetic polymers are derived from petroleum-based resources and include the nylons used in clothing fabric/textiles, polyvinyl chloride in our home pipes, polycarbonate in our cellphone cases, and sealants on our car frames, and a plethora of other consumer applications. Modern consumer goods' evolution parallels discovering new ways to exploit these manufactured, long-chained molecules primarily sourced from petroleum. Despite the best efforts of the green lobby, production and use of plastics shows little sign of slowing down soon.[1] While producing synthetic polymers, also known as plastics, now strikes a chord of dissonance amongst the environmentally conscious, history suggests that corporate and public societies once promoted the rise of these materials.

Except for Bakelite[2] commercialized in 1910, the desperation for resources during World War II fueled the mass production of the first synthetic polymers.[3] Innovative minds developed industrial-scale processes to produce polyethylene to insulate radar cabling, plexiglass to replace aircraft windows, styrene-butadiene copolymer to make tires for military trucks (replacing natural rubber), and nylon to make parachutes (replacing synthetic silk).[4,5] After World War II, the established synthetic polymers market was redirected towards meeting the general public's desire for cheap, light, and durable materials. Thompson et al.[6] quote how Yarsley and Couzens[7] imagined the dwellers of the plastics age in 1941: *"This [imaginary] plastic man will come into a*

world of colour and bright shining surfaces where childish hands find nothing to break, no sharp edges, or corners to cut or graze, no crevices to harbor dirt or germs …. The walls of his nursery, his bath … all his toys, his cot, the molded light perambulator in which he takes the air, the teething ring he bites, the unbreakable bottle he feeds from [all plastic]. As he grows he cleans his teeth and brushes his hair with plastic brushes, clothes himself with plastic clothes, writes his first lesson with a plastic pen and does his lessons in a book bound with plastic. The windows of his school curtained with plastic cloth entirely grease- and dirt-proof … and the frames, like those of his house are of molded plastic, light and easy to open never requiring any paint." War victories and access to convenient lifestyles were such a priority back then that not enough thought was given to the consequences of continually harvesting nonrenewable resources (e.g., petroleum) and pumping out materials that nature had not evolved to digest. Since their commercialization in the early-mid 20th century, synthetic polymers have become indispensable, yet concerningly persistent – we can barely live without synthetic polymers, and yet, our apparent failure to sustainably dispose of them could be dire.

Since the Yarsley and Couzens publication titled *Plastics*, the global annual production of commercial polymers has risen from less than 2 million to approximately 368 million metric tons,[8] and over 75% of all plastics produced are disposed of after a single use.[9] Approximately 6.3 billion metric tons of plastics waste have been generated, with the majority (79%) accumulating in landfills or escaping into the environment.[1] Because these plastics are designed to confer desirable properties like high performance, durability, and impermeability (especially to moisture and air), most synthetic polymers contain tenacious carbon-carbon backbones that do not naturally biodegrade in a reasonable timeframe.[10,11]

1.2 Post-consumer acrylic-based superabsorbent polymers accumulate in landfills

In this work, Procter and Gamble (P&G) tasked us to develop a method to recycle the acrylic-based superabsorbent polymer (SAP) used in their disposable diapers. It is estimated that the global annual production of this SAP is over 2 million metric tons, with disposable diapers accounting for 74% of the market.[12] Unfortunately, like most vinyl polymers, acrylic-based superabsorbents contain unreactive carbon-carbon bonds in the backbone, which can take centuries to degrade in the natural environment.[13]

The SAP provided by P&G is a sodium poly(acrylate) crosslinked via a poly(ethylene glycol) diacrylate co-monomer ($PAA_{P\&G}$), and 1 g of this SAP can absorb at least 100 g of deionized water (Figure 1-1). In addition, the crosslinking improves the material's tensile strength to lock in absorbed fluids under pressure (e.g., when a baby sits on the diaper).

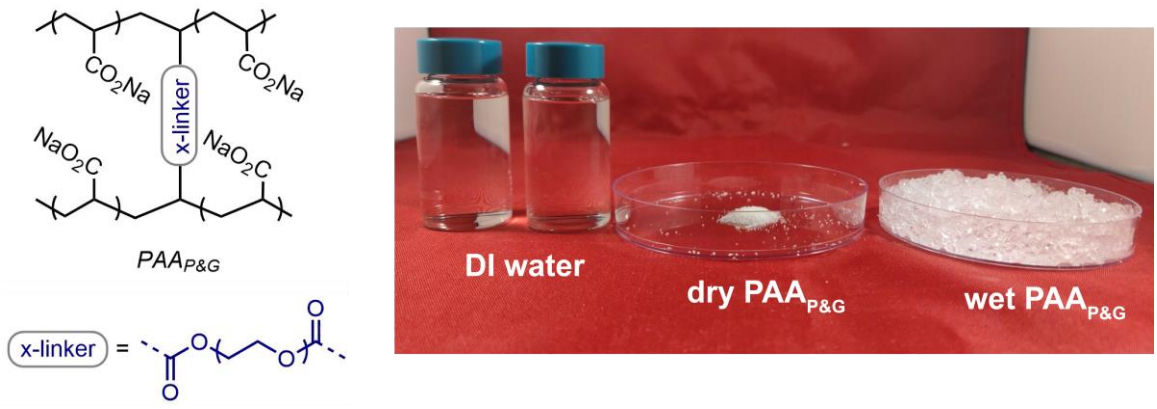

Figure 1-1. Chemical structure (left) and image showing 0.35 g of $PAA_{P\&G}$ before and after absorbing 40 g of DI H_2O (right).

1.3 Chemical recycling conserves the energy consumed in plastics production

There are several solutions to plastics waste addressed in the literature, namely: i) energy recovery (or waste-to-energy), ii) biodegradable alternatives, and iii) mechanical and chemical recycling.

The Environment Protection Agency defines Waste-to-energy (WtE) as "conversion of **non-recyclable** waste materials into usable heat, electricity, or fuel".[14] However, WtE is not a preferred solution to plastics waste because it releases toxic combustion by-products like bottom ash and organic volatiles (e.g., the known carcinogenic phosgene generated from burning polyvinyl chloride).[15]

Replacing plastics with biodegradable alternatives seems appealing; however, for effective and timely biodegradation in the environment, hydrolyzable or oxidizable chemical linkages must be incorporated within the polymer, which may compromise the polymer's performance.[16] Even so, the presence of hydrolyzable linkages within the polymer structure does not guarantee timely biodegradation. Most plastics containing hydrolyzable functional groups (e.g., nylon, polylactic acid, polyethylene terephthalate, etc.) also have relatively strong intermolecular interactions (i.e., glass transition temperatures > 70 °C) which impede penetration of degradation agents like moisture, air, and enzymes.[17] Although this impermeability is key to preventing spoilage in packaging applications, it is also responsible for the resistance to biodegradation post-use. Furthermore, biodegradation of plastics in the landfill leads to no recovery of the energy consumed (mostly nonrenewable) during production.

A more sustainable approach would be to use post-consumer plastics as feedstock for recycling.[18] For decades, recovering some value from waste polymer has been achieved via mechanical recycling, although recycling rates are low[19] and the material quality is often reduced. Moreover, polymers that do not reversibly melt (e.g., crosslinked polymers) cannot be recycled mechanically. An alternative recycling route known as chemical recycling was developed to address these challenges.[20,21,22,23]

Scheme 1-1. Closed loop recycling of water bottles (left) and open-loop recycling of diapers to make adhesives as demonstrated in this work (right).

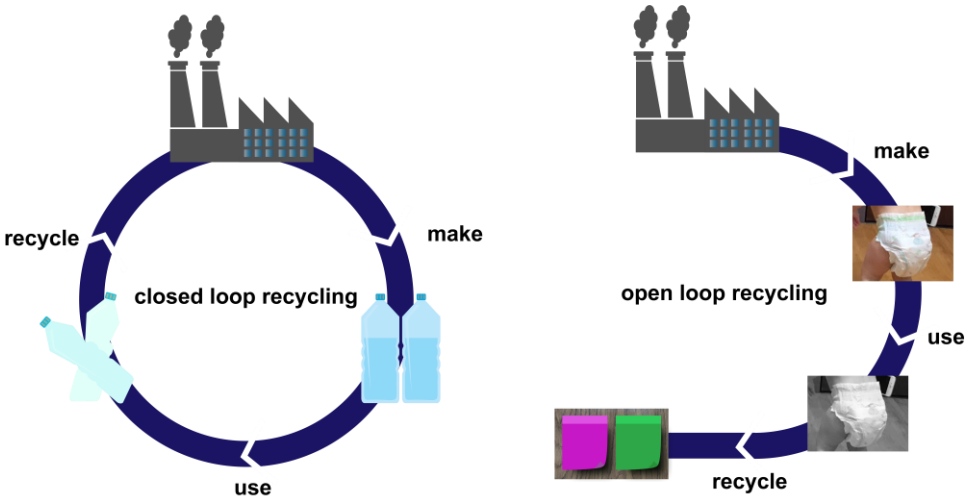

In closed-loop chemical recycling, polymers are chemically cleaved into their monomers (depolymerization) or create a material with equivalent function (Scheme 1-1, left).[24] Polyethylene terephthalate (PET) is one of the few commercial polymers that can be recycled both mechanically and chemically, making it one of the most recycled plastics (~18%).[25] PET is recycled chemically via ester linkage chemolysis methods like base or acid-mediated hydrolysis, alcoholysis, aminolysis, ammonolysis, and glycolysis (Scheme 1-1).[26]

Scheme 1-2. Closed loop recycling of polyethylene terephthalate via various chemolysis methods (see reference for detailed experimental conditions).[26]

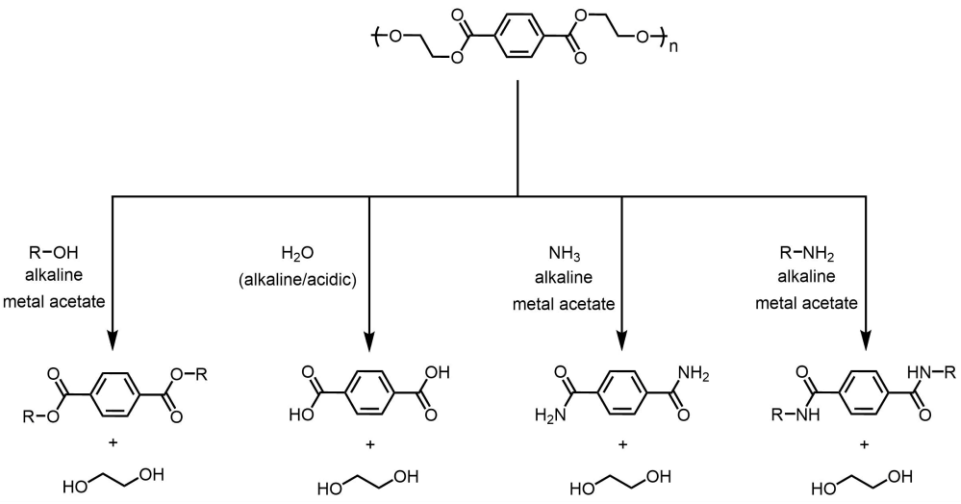

When closed-loop chemical processes are unavailable, an alternative known as open-loop chemical recycling can be utilized (Scheme 1-1, right). Here, chemical transformations convert waste polymers into other value-added materials, delaying their entry into the waste stream. Jia et al. developed an open-loop chemical recycling method to make low molar mass alkanes (i.e., liquid fuels and waxes) from post-consumer polyethylene (PE).[27] This recycling approach uses a cross-alkane metathesis (CAM) method where a feed of n-alkanes reacts via a dual catalyst system in three steps (i.e., dehydrogenation, olefin metathesis, and hydrogenation) to make new scrambled n-alkanes. The dual catalyst system comprises a dehydrogenation catalyst (e.g., iridium complexes 2 and 3 in Scheme 1-3) and a cross-metathesis catalyst (e.g., Re_2O_7/Al_2O_3). In their recycling approach, the iridium complex dehydrogenates the polyethylene and light alkanes. Dehydrogenation is followed by producing shorter scrambled unsaturated polymer chains via cross-metathesis of the unsaturated PE and light alkanes via a rhenium catalyzed olefin-metathesis. Finally, the Iridium complex reduced during the dehydrogenation step hydrogenates the unsaturated scrambled polymers. After multiple iterations of this CAM cycle, they achieved low molar mass n-alkanes (6–20 repeat units).

Scheme 1-3. Open-loop recycling of polyethylene to make liquid fuels and waxes via a tandem catalytic cross-alkane metathesis (CAM). *Modified with permission from the American Association for the Advancement of Science (AAAS).*[27]

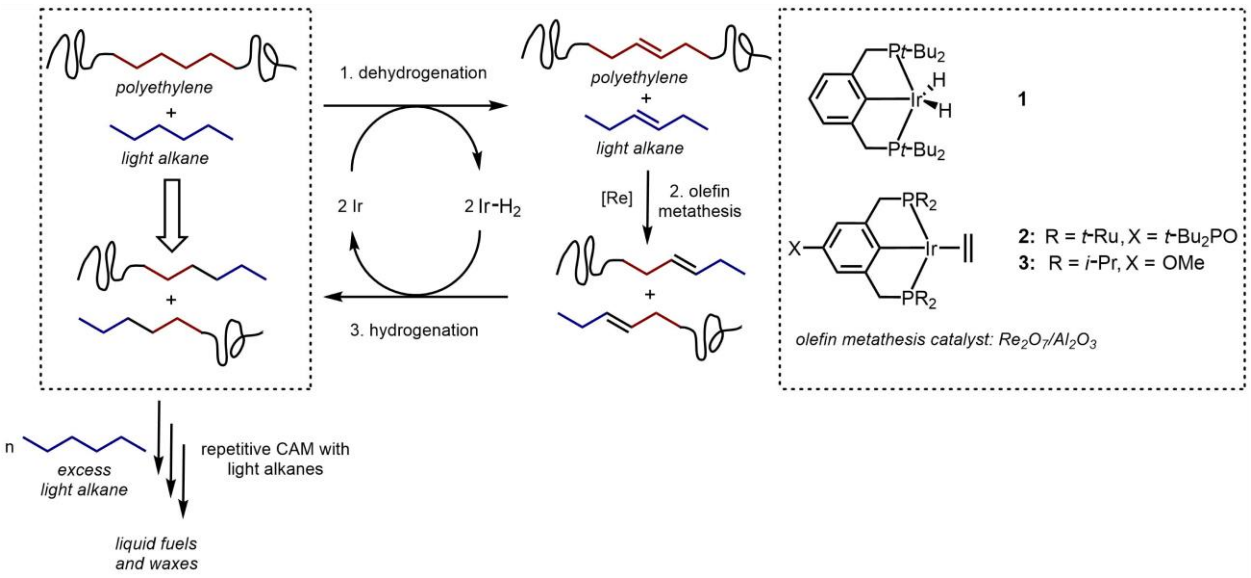

Closed-loop chemical recycling via thermal depolymerization to monomer is not feasible for acrylic-based superabsorbent materials because side-chain degradation outcompetes depolymerization. For example, polyacrylic acid undergoes dehydration and decarboxylation in bulk[28] and solution[29] upon heating. Recent efforts to sidestep this degradation using microwaves and added radical initiators led to oligomeric products with 50–60% decarboxylation.[30]

Catalytic depolymerization of some vinyl polymers (e.g., acrylamides and alkyl acrylates) have also been reported in the literature.[31] In one example, Li et al. reported reversible polymerization of acrylamide monomers in an atom transfer radical polymerization (ATRP) system.[32] In this work, N-isopropylacrylamide (NIPAM) was successfully polymerized in the presence of CuCl and tris(2-dimethylaminoethyl)amine (Me_6TREN). Upon adding 2,2,6,6-tetramethylpiperidinooxy radical (TEMPO) or 1,4-benzoquinone (BQ), up to 34% depolymerization to monomer was observed. In a control experiment where 2,2′-azobisisobutyronitrile (AIBN) was used as the radical initiator, no depolymerization was observed after adding TEMPO, which suggested that the copper catalyst was a vital component. In the end, they propose a depolymerization mechanism where the living radicals on the polymer chain act as sites for β-alkyl elimination (Scheme 1-4).

Scheme 1-4. TEMPO mediated in situ depolymerization of poly(NIPAM). *Modified with permission from Elsevier*.[32]

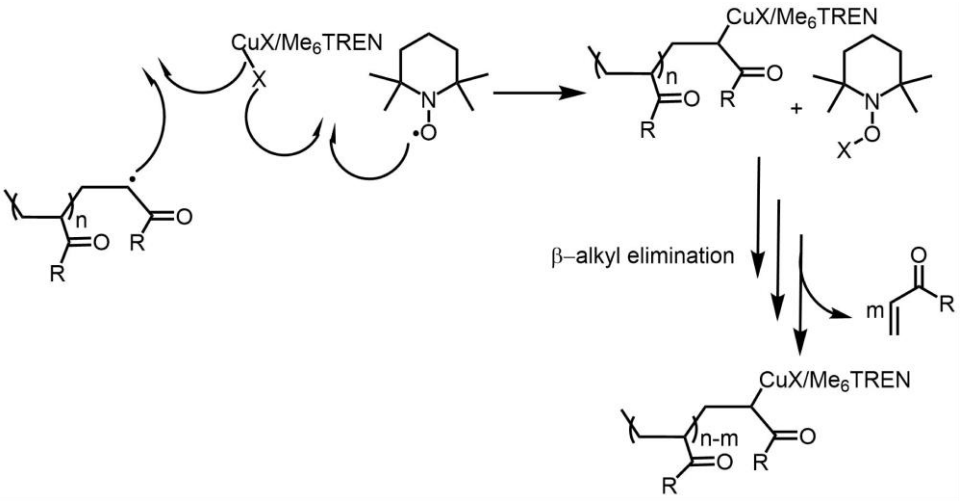

Lloyd et al. also demonstrated a reversible polymerization of acrylamide and acrylate monomers via a copper-catalyzed ATRP system in a CO_2 saturated aqueous environment.[33] The CO_2 saturated water was used to exclude oxygen successfully, and complete polymerization of NIPAM was achieved with 10 min. Without direct perturbation to the system, 52% depolymerization to monomer was observed over the next 30 min. Bubbling nitrogen into the system over 30 min resulted in repolymerization. Apart from probing pH effects on the reaction, they did not provide a mechanistic or thermodynamic explanation for these observations.

Scheme 1-5. CO_2 mediated in situ depolymerization of poly(NIPAM). *Modified with permission from Royal Society of Chemistry (RSC).*[33]

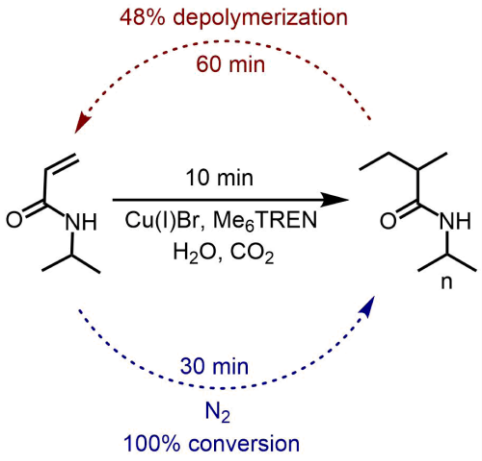

While the aforementioned catalytic depolymerization methods can, in principle, proceed without side-chain degradation, they have not yet been demonstrated for commercial sources of sodium polyacrylate. It is important to note that both depolymerizations highlighted above were done on relatively short polymers with living chain ends, which will not be the case for post-consumer superabsorbent polymers. Furthermore, the copper-mediated ATRP systems used are incompatible with sodium polyacrylate due to the inevitable catalyst poisoning caused by carboxylate chelation.

Chapter 2 demonstrates an open-loop chemical recycling approach to make pressure-sensitive adhesives (PSAs) from acrylic-based superabsorbent polymers. A life cycle assessment[34] must be performed to evaluate the energy and environmental implications of any recycling effort. In a recent perspective, Fagnani et al. pointed out that although there has been an increase in publications on "sustainable polymers" since 1990, less than 5% mention or perform any life cycle analysis.[35] This perspective inspired us to evaluate and optimize our open-loop recycling method in chapter 3. Guided by our life cycle analysis (LCA) tools, we improved our method and demonstrated that our optimized method to make PSAs outcompetes the conventional petroleum-based route.

1.4 A new application for pressure-sensitive adhesives discovered serendipitously

Pressure-adhesive adhesives (PSAs) are used conventionally in removable adhesive applications like tape, bandages, and sticky notes. PSAs exhibit three critical properties for these applications: i) enough tack wet to a substrate with minimal pressure, ii) strong intermolecular interactions with the substrate for good adhesion, and iii) enough cohesiveness to peel from the substrate without leaving residue. After fortuitously noticing that micronized rubber suspended in a solvent waste container readily adhered blobs of PSA waste (Figure 1-2), we decided to explore a new application for adhesives as agents to capture microplastic underwater.[36] Owing to the potential

and novelty of this discovery, we filed joint patents with P&G[37] and earned an NSF-EFRI grant[38] towards our new research center, SuMuP (Sequestering Microplastics Using Upcycled Plastic Waste)[39].

Figure 1-2. Image showing micronized rubber particles adhered onto a blob of pressure-sensitive adhesives in a solvent waste container.

1.5 The concerning ubiquity of microplastics and remediation efforts

Microplastics (MPs) are plastic particles with dimensions smaller than 5 mm. These particulates are introduced into the environment either as additives in consumer products (primary MPs) or by the physical degradation of existing plastic materials (secondary MPs). As with the persistence of plastics discussed earlier, MPs' ubiquitous distribution and environmental persistence are due to the same features (e.g., inertness, impermeability, and durability) that make plastics desirable in consumer goods applications.

A large portion of the MPs pollution in the environment is traced back to washing textiles where over 20 km^3 of MPs contaminated water is generated globally[40] and disposed of in wastewater treatment plants.[41] During the wastewater treatment process, 90–98% of the MPs in the influent are trapped physically in biosolids sludge, and most of the MPs remaining in the effluent were

regularly shaped microbeads (i.e., primary MPs).[42] The MPs contaminated sludge is subsequently distributed to farmers as organic fertilizers, consequently introducing MPs into the environment.[43]

While investigating the abundance of MPs in soils amended with sludge-based biosolids, Zhang et al. noted over 500 particulates/kg in amended fields, whereas unamended fields only contained about 5.0 particulates/kg.[44] In a similar investigation, Crossman et al. studied the transport and retention of MPs in fields amended with biosolids over seven months.[45] In the end, they noted that > 99% of the MPs applied from biosolids were uncounted for, which suggested that MPs were not permanently stored in the soil but potentially exported to the aquatic environment by wind and rainfall.

Accumulation of MPs in oceans and other surface water bodies as a final destination is a cause for concern.[46] Apart from the primary suspect pathway of drinking water,[47] several other vectors transfer MPs from the aquatic environment to humans. For example, MPs have been detected in beer[48] (12–109 particles/L^{-1}) and sea salts[49] (550–681 particles/kg). Another worrisome vector of MPs is seafood, where bivalves like mussels and oysters contain about 0.36 and 0.47 particles/gram of tissue.[50] Based on these findings, it was estimated that the average European consumer has an annual dietary exposure of 11,000 MPs.

Although there is substantial literature investigating MPs' effects on aquatic fauna, fewer efforts have been invested towards studying the effects on mammalian species, which explains the lack of consensus on this topic among the scientific community.[51, 52, 53] In 1998, Pauly et al. investigated the presence of inhaled plastic fibers (i.e., MPs) in diseased (malignant) and healthy (nonneoplastic) human lungs.[54] They observed that inhaled MPs were present in 83% of nonneoplastic lung samples (n = 67/81) and 97% of malignant lung samples (n 32/33). Based on the observed correlation between malignancy and MPs, which are biopersistent and often contain

toxic compounds (e.g., residual monomer, dyes, and additives), they may be a suspect contributor to pulmonary diseases like lung cancer. These results challenged the claims that plastic particles cannot accumulate in human lungs due to their large size (relative to cells) and the body's ability to eject them naturally (e.g., mucociliary escalator, macrophage phagocytosis, dissolution). In another study on the effects of ingested polystyrene MPs (5 and 20 μm) on mice, Deng et al. reported size-dependent tissue-accumulation kinetics of MPs in the liver and kidney and gut.[55]

While ongoing efforts have been made to understand the occurrence, ubiquity, diversity (e.g., size and chemical identity), and hazards of MPs, comparatively little has been done to develop remediation solutions. As of January 2021, from the 4,663 Web Of Science research articles, we found addressing MPs or nanoplastics, less than 2% (i.e., 71 articles) include remediation or a similar term (e.g., capture, removal, remediation) in their titles. Chapter 4 will discuss some of the remediation methods and demonstrate MPs removal from water using our first-generation adhesives (i.e., unmodified poly(2-ethylhexyl acrylate)).

1.6 References

1 Geyer, R. Production, Use, and Fate of Synthetic Polymers. In *Plastic Waste and Recycling*; Elsevier, 2020; pp 13–32. https://doi.org/10.1016/B978-0-12-817880-5.00002-5.

2 American Chemical Society National Historic Chemical Landmarks. Bakelite: The World's First Synthetic Plastic. http://www.acs.org/content/acs/en/education/whatischemistry/landmarks/bakelite.html (accessed May 31, 2021).

3 Scientific American. A Brief History of Plastic's Conquest of the World. https://www.scientificamerican.com/article/a-brief-history-of-plastic-world-conquest/ (Accessed May 31, 2021).

4 Rånby, B. Plastics and Rubber. In *Macromolecular Concept and Strategy for Humanity in Science, Technology and Industry*; Springer Berlin Heidelberg: Berlin, Heidelberg, 1996; pp 29–36. https://doi.org/10.1007/978-3-642-61036-3_5.

5 Spitz, P. H. Fuels and Chemicals Research Helps Win World War II. In *Primed for Success: The Story of Scientific Design Company*; Springer International Publishing: Cham, 2019; pp 25–42. https://doi.org/10.1007/978-3-030-12314-7_3.

6 Thompson, R. C.; Swan, S. H.; Moore, C. J.; vom Saal, F. S. Our Plastic Age. *Philos. Trans. R. Soc. B Biol. Sci.* **2009**, *364*, 1973–1976. https://doi.org/10.1098/rstb.2009.0054.

7 Yarsley, V. E.; Couzens, E. G. *Plastics*; Pelican books; A. Lane, Penguin books, 1941.

8 https://www.statista.com/statistics/282732/global-production-of-plastics-since-1950 (Accessed Apr 6, 2020).

9 *Advancing Sustainable Materials Management*, 2017 fact sheet (EPA 530-F-19-007); United States Environmental Protection Agency (EPA) – Office of Land and Emergency Management. (5306P), 2019. https://www.epa.gov/sites/production/files/2019-11/documents/2017_facts_and_figures_fact_sheet_final.pdf

10 Hong, M.; Chen, E. Y.-X. Chemically Recyclable Polymers: A Circular Economy Approach to Sustainability. *Green Chem.* **2017**, *19*, 3692–3706. https://doi.org/10.1039/C7GC01496A.

11 Barnes, D. K. A.; Galgani, F.; Thompson, R. C.; Barlaz, M. Accumulation and Fragmentation of Plastic Debris in Global Environments. *Philos. Trans. R. Soc. B Biol. Sci.* **2009**, *364*, 1985–1998. https://doi.org/10.1098/rstb.2008.0205.

12 Future Market Insights. Super Absorbent Polymer Market: Global Industry Analysis and Opportunity Assessment 2015 - 2020 https://www.futuremarketinsights.com/reports/super-absorbent-polymer-market.

13 Barnes, D. K. A.; Galgani, F.; Thompson, R. C.; Barlaz, M. Accumulation and Fragmentation of Plastic Debris in Global Environments. *Philos. Trans. R. Soc. B Biol. Sci.* **2009**, *364* (1526), 1985–1998. https://doi.org/10.1098/rstb.2008.0205.

14 https://www.epa.gov/smm/energy-recovery-combustion-municipal-solid-waste-msw (accessed June 1, 2021).

15 Cole-Hunter, T.; Johnston, F. H.; Marks, G. B.; Morawska, L.; Morgan, G. G.; Overs, M.; Porta-Cubas, A.; Cowie, C. T. The Health Impacts of Waste-to-Energy Emissions: A Systematic Review of the Literature. *Environ. Res. Lett.* **2020**, *15*, 123006. https://doi.org/10.1088/1748-9326/abae9f.

16 Haider, T. P.; Völker, C.; Kramm, J.; Landfester, K.; Wurm, F. R. Plastics of the Future? The Impact of Biodegradable Polymers on the Environment and on Society. *Angew. Chemie Int. Ed.* **2019**, *58* (1), 50–62. https://doi.org/10.1002/anie.201805766.

17 Min, K.; Cuiffi, J. D.; Mathers, R. T. Ranking Environmental Degradation Trends of Plastic Marine Debris Based on Physical Properties and Molecular Structure. *Nat. Commun.* **2020**, *11* (1), 727. https://doi.org/10.1038/s41467-020-14538-z.

18 Hong, M.; Chen, E. Y.-X. Chemically Recyclable Polymers: A Circular Economy Approach to Sustainability. *Green Chem.* **2017**, *19*, 3692–3706. https://doi.org/10.1039/C7GC01496A.

19 Advancing Sustainable Materials Management: 2017 Fact Sheet. EPA 530-F-19-001, Nov 2019. https://www.epa.gov/sites/production/files/2019-11/documents/2017_facts_and_figures_fact_sheet_final.pdf (accessed Apr 6, 2021).

20 Hong, M.; Chen, E. Y.-X. Chemically Recyclable Polymers: A Circular Economy Approach to Sustainability. *Green Chem.* **2017**, *19*, 3692–3706. https://doi.org/10.1039/C7GC01496A.

21 Rahimi, A.; García, J. M. Chemical Recycling of Waste Plastics for New Materials Production. *Nat. Rev. Chem.* **2017**, *1*, 46.

22 Thiounn, T.; Smith, R. C. Advances and Approaches for Chemical Recycling of Plastic Waste. *J. Polym. Sci.* **2020**, *58*, 1347–1364. https://onlinelibrary.wiley.com/doi/full/10.1002/pol.20190261

23 Coates, G. W.; Getzler, Y. D. Y. L. Chemical Recycling to Monomer for an Ideal, Circular Polymer Economy. *Nat. Rev. Mater.* **2020** DOI: https://doi-org.proxy.lib.umich.edu/10.1038/s41578-020-0190-4

24 Ellen MacArthur Foundation. The new plastics economy: rethinking the future of plastics & catalyzing action. Ellen MacArthur Foundation, 2017. https://www.ellenmacarthurfoundation.org/publications/the-new-plastics-economy-rethinking-the-future-of-plastics-catalysing-action (accessed on Apr 6, 2021).

25 Plastic has a Problem; is Chemical Recycling the Solution? https://cen.acs.org/environment/recycling/Plastic-problem-chemical-recycling-solution/97/i39 (accessed on June 7, 2021).

26 Raheem, A. B.; Noor, Z. Z.; Hassan, A.; Abd Hamid, M. K.; Samsudin, S. A.; Sabeen, A. H. Current Developments in Chemical Recycling of Post-Consumer Polyethylene Terephthalate Wastes for New Materials Production: A Review. *J. Clean. Prod.* **2019**, *225*, 1052–1064. https://doi.org/10.1016/j.jclepro.2019.04.019.

27 Jia, X.; Qin, C.; Friedberger, T.; Guan, Z.; Huang, Z. Efficient and Selective Degradation of Polyethylenes into Liquid Fuels and Waxes under Mild Conditions. *Sci. Adv.* **2016**, *2*, 1–8. https://doi.org/10.1126/sciadv.1501591.

28 McNeill, I. C.; Sadeghi, S. M. T. Thermal Stability and Degradation Mechanisms of Poly(Acrylic Acid) and Its Salts: Part 1-Poly(Acrylic Acid). *Polym. Degrad. Stab.* **1990**, *29*, 233–246. https://doi.org/10.1016/0141-3910(90)90034-5.

29 Lépine, L.; Gilbert, R. Thermal Degradation of Polyacrylic Acid in Dilute Aqueous Solution. *Polym. Degrad. Stab.* **2002**, *75*, 337–345. https://doi.org/10.1016/S0141-3910(01)00236-1.

30 Ching, T. W.; Zhang, J.; Collias, D.; McDaniel, J.; Simonyan, A.; Tanksale, A.; Banaszak Holl, M. M. *ACS Sustainable Chem. Eng.* **2020**, *8*, 14504–14510.

31 Tang, H.; Luan, Y.; Yang, L.; Sun, H. A Perspective on Reversibility in Controlled Polymerization Systems: Recent Progress and New Opportunities. *Molecules* **2018**, *23*, 2870.

32 Li, L.; Shu, X.; Zhu, J. Low Temperature Depolymerization from a Copper-Based Aqueous Vinyl Polymerization System. *Polymer (Guildf).* **2012**, *53*, 5010–5015.

33 Lloyd, D. J.; Nikolaou, V.; Collins, J.; Waldron, C.; Anastasaki, A.; Bassett, S. P.; Howdle, S. M.; Blanazs, A.; Wilson, P.; Kempe, K.; et al. Controlled Aqueous Polymerization of Acrylamides and Acrylates and "in Situ" Depolymerization in the Presence of Dissolved CO2. *Chem Commun* **2016**, *52* (39), 6533–6536. https://doi.org/10.1039/c6cc03027k.

34 Bjørn, A.; Owsianiak, M.; Molin, C.; Laurent, A. Main characteristics of LCA. In *Life Cycle Assessment*; Hauschild, M. Z., Rosenbaum, R. K., Olsen, S. I., Eds.; Springer International Publishing AG: Switzerland, **2018**; pp 9– 16.

35 Fagnani, D. E.; Tami, J. L.; Copley, G.; Clemons, M. N.; Getzler, Y. D. Y. L.; McNeil, A. J. 100th Anniversary of Macromolecular Science Viewpoint: Redefining Sustainable Polymers. *ACS Macro Lett.* **2021**, *10*, 41–53.

36 U-M group gets $2 million NSF grant for turning diapers into devices to capture microplastics. https://news.umich.edu/u-m-group-gets-2-million-nsf-grant-for-turning-diapers-into-devices-to-capture-microplastics/ (accessed June 7, 2021).

37 Collias, D. I.; Chazovachii, P. T.; McNeil, A. J. Microplastics Removal Using Adhesives. US Provisional Patent Application, 2020.

38 National Science Foundation. Award Abstract # 2029251 EFRI E3P: Sequestering Microplastics Using Upcycled Plastic Waste. https://www.nsf.gov/awardsearch/showAward?AWD_ID=2029251&HistoricalAwards=false. (accessed June 6, 2021).

39 SuMuP (Sequestering Microplastics Using Upcycled Plastic Waste). https://sumup.squarespace.com/

40 De Falco, F.; Di Pace, E.; Cocca, M.; Avella, M. The Contribution of Washing Processes of Synthetic Clothes to Microplastic Pollution. *Sci. Rep.* **2019**, *9*, 6633. https://doi.org/10.1038/s41598-019-43023-x.

41 Hernandez, E.; Nowack, B.; Mitrano, D. M. Polyester Textiles as a Source of Microplastics from Households: A Mechanistic Study to Understand Microfiber Release During Washing. *Environ. Sci. Technol.* **2017**, *51*, 7036–7046. https://doi.org/10.1021/acs.est.7b01750

42 Nizzetto, L.; Futter, M.; Langaas, S. Are Agricultural Soils Dumps for Microplastics of Urban Origin? *Environ. Sci. Technol.* **2016**, *50* (20), 10777–10779. https://doi.org/10.1021/acs.est.6b04140.

43 Weithmann, N.; Möller, J. N.; Löder, M. G. J.; Piehl, S.; Laforsch, C.; Freitag, R. Organic Fertilizer as a Vehicle for the Entry of Microplastic into the Environment. *Sci. Adv.* **2018**, *4*, eaap8060. https://doi.org/10.1126/sciadv.aap8060.

44 Zhang, L.; Xie, Y.; Liu, J.; Zhong, S.; Qian, Y.; Gao, P. An Overlooked Entry Pathway of Microplastics into Agricultural Soils from Application of Sludge-Based Fertilizers. *Environ. Sci. Technol.* **2020**, *54*, 4248–4255. https://doi.org/10.1021/acs.est.9b07905.

45 Crossman, J.; Hurley, R. R.; Futter, M.; Nizzetto, L. Transfer and Transport of Microplastics from Biosolids to Agricultural Soils and the Wider Environment. *Sci. Total Environ.* **2020**, *724*, 138334. https://doi.org/10.1016/j.scitotenv.2020.138334.

46 Rochman, C. M.; Browne, M. A.; Halpern, B. S.; Hentschel, B. T.; Hoh, E.; Karapanagioti, H. K.; Rios-Mendoza, L. M.; Takada, H.; Teh, S.; Thompson, R. C. Classify Plastic Waste as Hazardous. *Nature* **2013**, *494*, 169–171. https://doi.org/10.1038/494169a.

47 Mason, S. A.; Welch, V. G.; Neratko, J. Synthetic Polymer Contamination in Bottled Water. *Front. Chem.* **2018**, *6*. https://doi.org/10.3389/fchem.2018.00407.

48 Liebezeit, G.; Liebezeit, E. Synthetic Particles as Contaminants in German Beers. *Food Addit. Contam. Part A* **2014**, *31*, 1574–1578. https://doi.org/10.1080/19440049.2014.945099.

49 Yang, D.; Shi, H.; Li, L.; Li, J.; Jabeen, K.; Kolandhasamy, P. Microplastic Pollution in Table Salts from China. *Environ. Sci. Technol.* **2015**, *49*, 13622–13627. https://doi.org/10.1021/acs.est.5b03163.

50 Van Cauwenberghe, L.; Janssen, C. R. Microplastics in Bivalves Cultured for Human Consumption. *Environ. Pollut.* **2014**, *193*, 65–70. https://doi.org/10.1016/j.envpol.2014.06.010.

51 Braeuning, A. Uptake of Microplastics and Related Health Effects: A Critical Discussion of Deng et Al., Scientific Reports 7:46687, 2017. *Arch. Toxicol.* **2019**, *93*, 219–220. https://doi.org/10.1007/s00204-018-2367-9.

52 Deng, Y.; Zhang, Y. Response to Uptake of Microplastics and Related Health Effects: A Critical Discussion of Deng et Al., Scientific Reports 7: 46687, 2017. *Arch. Toxicol.* **2019**, *93*, 213–215. https://doi.org/10.1007/s00204-018-2384-8.

53 World Health Organization. Information sheet: Microplastics in drinking-water. https://www.who.int/water_sanitation_health/water-quality/guidelines/microplastics-in-dw-information-sheet/en/ (accessed June 9, 2021).

54 Pauly, J. L.; Stegmeier, S.J.; Allaart, H. A.; Cheney, R. T.; Zhang, P. J.; Mayer, A. G.; Streck, R. J. Inhaled Cellulosic and Plastic Fibers Found in Human Lung Tissue. *Cancer Epidemiology, Biomarkers & Prevention*. **1998**, *7*, 419–428.

55 Deng, Y.; Zhang, Y.; Lemos, B.; Ren, H. Tissue Accumulation of Microplastics in Mice and Biomarker Responses Suggest Widespread Health Risks of Exposure. *Sci. Rep.* **2017**, 46687. https://doi.org/10.1038/srep46687.

Chapter 2: Repurposing Acrylic-Based Absorbents via Post-Polymerization Modifications Part I

Portions of this chapter have been published:

Chazovachii, P. T.; Somers, M. J.; Robo, M. T.; Collias, D. I.; James, M. I.; Marsh, E. N. G.; Zimmerman, P. M.; Alfaro, J. F.; McNeil, A. J. Giving Superabsorbent Polymers a Second Life as Pressure-Sensitive Adhesives. *Nat. Commun.* **2021**, *12*, 4524. https://doi.org/10.1038/s41467-021-24488-9.

Chazovachii et al. Depolymerization of polymers. US Patent Application, 2021.

2.3 Introduction

Commercial polymers are ubiquitous, with a global annual production of approximately 368 million metric tons.[1] Unfortunately, most of the feedstocks currently used come from nonrenewable resources,[2] and approximately 75% of plastics are disposed of after a single use.[3] Although durability and strength are advantages of synthetic polymers, these properties are also responsible for their environmental persistence.[4, 5, 6] The synthetic polymer community created these impactful materials, and now, we must turn our attention towards technologies that facilitate their collection and recycling to create a circular economy that is more sustainable.[7]

We report an open-loop method to recycle the superabsorbent materials used in disposable diapers and feminine hygiene products. The global annual production of this superabsorbent material is estimated to be over 2 million metric tons, with disposable diapers claiming 74% of the market.[8] Unfortunately, most used diapers sit in landfills without substantial biodegradation[3] or are incinerated. To date, most diaper recycling efforts[9] have focused on the cellulosic components, which can be biodegraded, incinerated to generate steam, pyrolyzed, or fermented to generate

bioethanol.[10] In contrast, few studies have examined the recycling of sodium polyacrylate superabsorbent polymers. Mechanical recycling is not feasible because the crosslinks prevent melting. Decrosslinking has been reported using ozonolysis,[11] though not for the purposes of mechanical recycling.

In this work, we report an open-loop recycling approach for the acrylic-based superabsorbent material used in diapers. Specifically, using a 3 step synthetic process, the sodium polyacrylate is converted into a pressure-sensitive adhesive (PSA), which has a significant global market (expected to be $13 billion by 2023).[12] This approach was inspired by the similar structures of sodium polyacrylate (superabsorbent polymer) and polyacrylates (pressure-sensitive adhesives) used in tapes, bandages, and sticky notes, among others.[13] Commercial polyacrylate-based PSAs are often accessed via petroleum-sourced monomers (Scheme 2-1 left).[14, 15, 16] Instead, we envisioned a 3 step method starting with crosslinked sodium polyacrylate: (i) base-mediated decrosslinking to generate water-soluble polymers, (ii) sonication to lower the molar mass, and (iii) functionalizing via esterification to generate tack (Scheme 2-1 right).

Scheme 2-1. Comparing syntheses of pressure-sensitive adhesives from petroleum versus waste diapers as the feedstock.

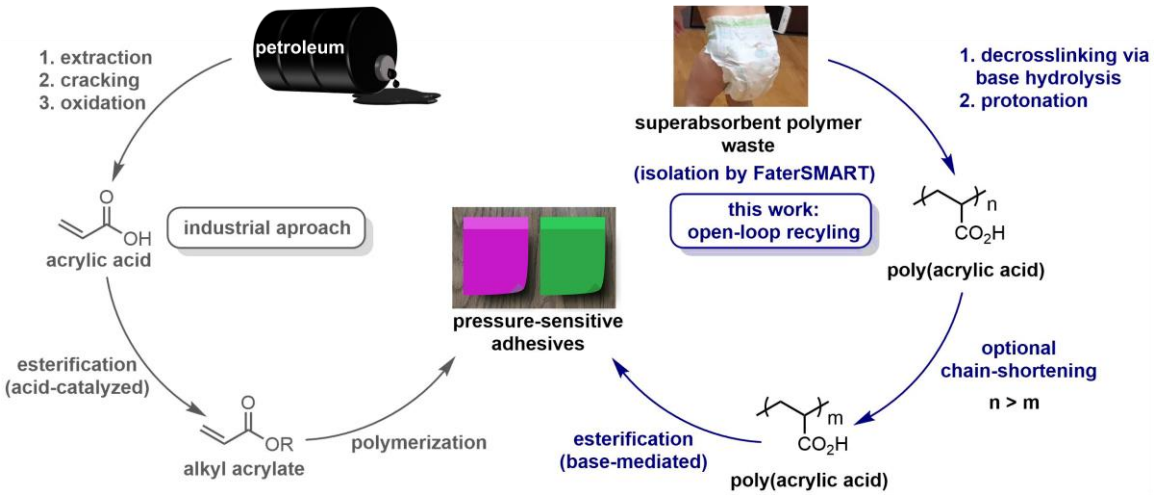

2.4 Isolation from post-consumer waste

Globally, there have been significant efforts towards recycling the components of diapers.[17] For example, FaterSMART, a Proctor and Gamble (P&G) affiliated company, has developed and implemented a diaper recycling facility that includes used diaper acquisition, steam sterilization, shredding, and separation into the purified raw materials (cellulosics, superabsorbent polymer, and polyolefins).[18] We have included these important steps in our life cycle assessments; however, our syntheses utilized the more readily accessible samples of superabsorbent polymer used to manufacture diapers at P&G.

2.5 Decrosslinking via base-mediated hydrolysis

The superabsorbent polymer provided by P&G is a sodium poly(acrylate) crosslinked via a poly(ethylene glycol) diacrylate co-monomer ($PAA_{P\&G}$). The crosslinks were hydrolyzed using 3 M aq. NaOH and mild heating (80 °C). The initially heterogeneous reaction mixture became a homogeneous solution over 3 h due to the chemical change from a superabsorbent gel-like substance into soluble, linear polymer products (Appendix 1, pg. 96). We further optimized this step by monitoring the decrosslinking process at a lower concentration of base (i.e., 0.3 M). Within the first 15 h, we observed a substantial drop (more than two orders of magnitude) in viscosity, after which point no further changes were observed (Appendix 1, Figure A1-8). This result suggests that the majority of crosslinks had been hydrolyzed within 15 h.

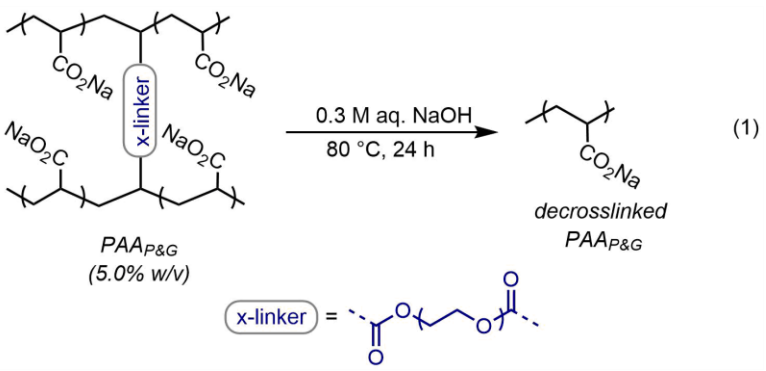

2.6 Chain-shortening via sonication

To demonstrate that pressure-sensitive adhesives with varying degrees of viscoelastic properties could be achieved, we needed a method to shorten the linear polymers obtained after the decrosslinking step. Sonication has previously been used to chain-shorten high-molar mass polymers with various backbone architectures[19, 20] including polyacrylic acid,[21] and has been used at scale.[22] This process is visually demonstrated in Scheme 2-2. During sonication, the ultrasound frequencies create microscopic cavitation bubbles in the solution. Upon collapse, the bubbles generate solvodynamic shear forces, which cleave entangled polymer chains into shorter fragments while maintaining the polymer's chemical identity. The rate of chain scission during sonication is directly proportional to the amount of chain entanglement during sonication.[23] As a consequence, there is an intrinsic, limiting molar mass for each polymer below which further chain scissions are unlikely to occur. Experimentally, a plateau is observed in the plot of weight-average molar mass (M_w) versus sonication time.

Scheme 2-2. Chain-shortening of high molar mass polymers using ultrasound.

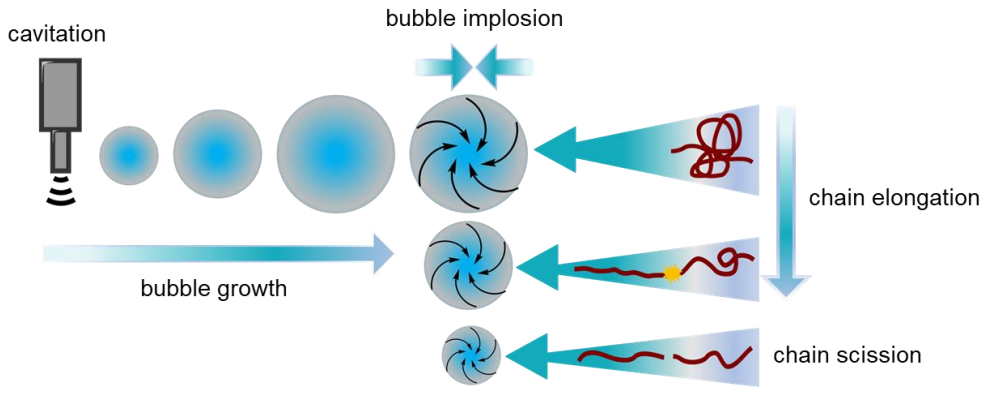

2.7 Chain-shortening PAA_{spp}

As a model system, linear polyacrylic acid was purchased from Scientific Polymer Products (PAA_{SPP}). The reported M_w was 750 kg/mol; however, we suspected that some crosslinking was present, as no peak was observed in the size-exclusion chromatography (SEC) trace after passing

the sample through a syringe filter (1.0 μm). Different concentrations of PAA_{SPP} solutions were prepared in deionized water with sodium chloride added to reduce the viscosity.[24] These solutions were sonicated using a 20 kHz sonication horn operating at full (100%) amplitude. Aliquots were collected at time points spanning 1–10 min (Appendix 1, pgs. 86–95). The maximum specific energy (w_{max}) was calculated at each time point using the maximum power drawn from the outlet and the mass of added PAA, and the molar masses (M_w) were determined using size-exclusion chromatography.

Overall, the shortest fragments achievable within 10 min of sonication exhibited a M_w ~90 kg/mol at 0.5% w/v (Appendix 1, pg. 88). However, to achieve the necessary cohesive and holding strength for a PSA, the polymer should have a M_w > 400 kg/mol.[25, 26, 27] Considering this factor, the optimized conditions involved sonicating a 5.0% w/v solution for t < 5 min to give a M_w of ~340 kg/mol and w_{max} = 70 MJ/kg (Appendix 1, pg. 98–100).

2.8 Chain-shortening $PAA_{P\&G}$

With these conditions in hand, we next evaluated the chain-shortening of decrosslinked $PAA_{P\&G}$. Sonicating 5% w/v solutions for up to 10 min revealed a substantially faster chain-shortening process for $PAA_{P\&G}$ compared to PAA_{SPP} (Figure 2-1). For example, $PAA_{P\&G}$ could be chain-shortened to a M_w ~330 kg/mol within 5 min with a w_{max} of 38 MJ/kg. This faster chain-shortening relative to PAA_{SPP} may be due to the decrosslinked state of $PAA_{P\&G}$. The resulting chain-shortened $PAA_{P\&G}$ polymers were dialyzed to remove the excess base, protonated using ion exchange resin, and concentrated under reduced pressure to remove water. The resulting polymers were isolated in ~90% yield.[28]

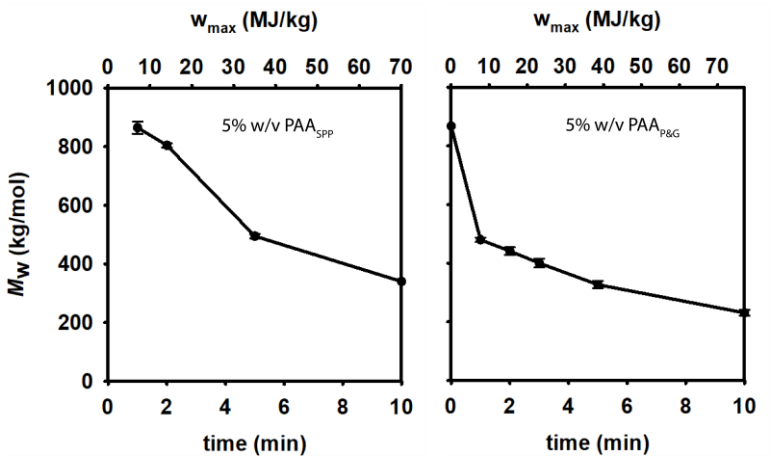

Figure 2-1. Plot of molar mass (M_w) and specific energy versus time for sonicating PAA_{SPP} (left) and $PAA_{P\&G}$ (right) at 5% w/v.

2.9 Esterifying to generate tack

The protonated polymers were functionalized over 12 h with 2-ethylhexyl bromide (2-EHBr) via a tetramethylguanidine (TMG) mediated esterification.[29] The reaction was quenched using acetic acid, and the polymer was precipitated by adding MeOH. The polymer was purified by dissolving in minimal amounts of THF, precipitating with MeOH twice, and drying under high vacuum. To access more than one type of PSA, incorporating polar functional groups (i.e., primary amine) was also explored. Fragments sonicated for 2 min ($PAA_{P\&G\text{-}2min}$) were co-esterified using 2-EHBr and 2-(BOC-amino)ethyl bromide (2-BAEBr) to incorporate amine groups (eq 2). The BOC group was deprotected over 12 h using *p*-toluenesulfonic acid and confirmed by FT-IR, ^{1}H NMR, and DOSY (Appendix 1, pg. 109–114). We observed that within 24 h after drying, the polymer sets into an insoluble material. We believe that the setting was caused by physical crosslinking induced by hydrogen bonding.

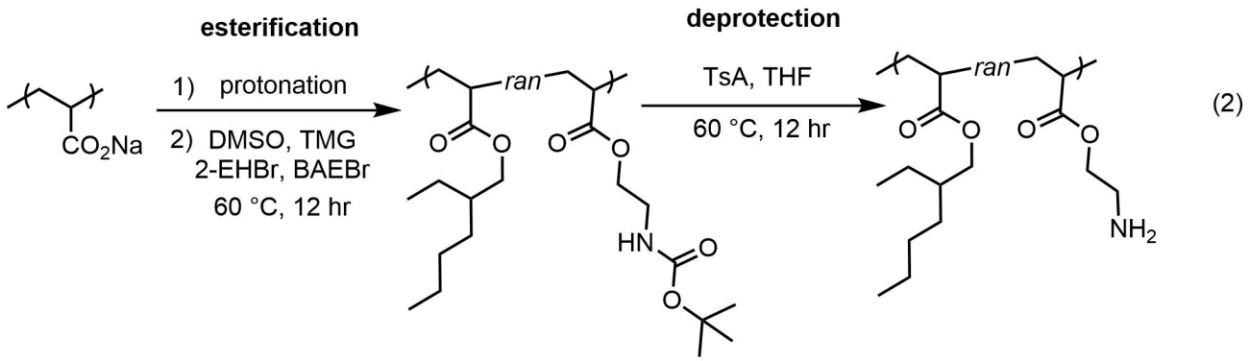

(2)

2.10 Characterizing the adhesive properties

The adhesive properties of the synthesized polyacrylates were analyzed using rheology and evaluated based on Chang's viscoelastic window (VW) concept, which classifies different adhesive types.[30] In this approach, the PSA's VW is constructed using the dynamic storage (G′) and loss (G″) moduli at the representative bonding (0.01 Hz) and debonding (100 Hz) frequencies. The corresponding VW for each adhesive is the rectangular region bounded by these four moduli (Figure 2-2). Chang noted that most existing PSAs appear between the G′ and G″ bounds of 10^3 and 10^6 Pascals (Pa) at the abovementioned frequency bounds and can be grouped into the quadrants (and central region) highlighted in Figure 2-2. The G′ at each frequency describes an adhesive's resistance to shear, and this term generally increases in samples with more chain entanglements (e.g., with increasing M_w). The G″ at each frequency describes an adhesive's ability to dissipate energy. Most consumer PSA-based products are in either quad 3 (e.g., office tape and bandages) or the central region (e.g., sticky notes and removable labels), signified by low-to-medium G′ and G″.

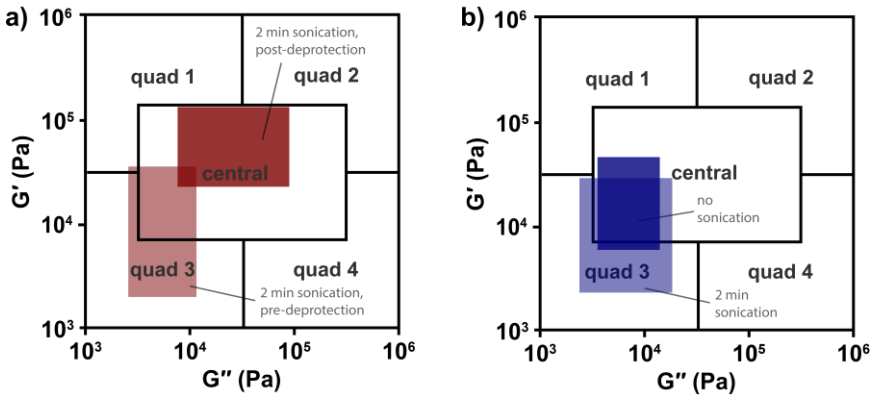

Figure 2-2. Plots of storage (G′) versus loss (G″) moduli for synthesized polyacrylate adhesives, including visualization of Chang's viscoelastic window. a) Properties for PSAs made from chain-shortened (2 min) with Boc incorporation before and after deprotection. b) Properties for PSAs made from chain-shortened (2 min) and unshortened $PAA_{P\&G}$.

The synthesized adhesives span quad 3 and the central region (Figure 2-2). That is, the PSAs are soft enough to flow and wet a substrate at the bonding frequency while hard enough to hold onto a substrate and peel cleanly at the debonding frequency. As expected, the lower M_w adhesive (2 min sonication, pre-deprotection) occupied the lesser elastic region of the VW (quad 3) due to its lower degree of entanglements relative to higher M_w adhesive (no sonication, homopolymer). Similarly, the post-deprotection (2 min sonication) adhesive exhibited the highest elastic character (upper central region) due to the higher degree of entanglements induced by the hydrogen bonding.

2.11 Conclusions

In summary, we developed a 3-step method to synthesize PSAs by repurposing superabsorbent poly(acrylic acid). Because this process uses waste polymer as the feedstock, it provides an alternative to using petroleum resources and avoids disposal in a landfill or incineration. The synthesized adhesives fall within the viscoelastic windows utilized in most commercial PSAs. One can target a specific window simply by varying molecular weights via sonication or incorporating polar functional groups. Overall, this work demonstrates the open-loop chemical recycling of

landfill-destined post-consumer polymers into other consumer polymers. To confirm real-world practicability, the developed recycling process must be compared with the conventional petroleum-based route used to manufacture PSAs

2.12 References

1 https://www.statista.com/statistics/282732/global-production-of-plastics-since-1950 (Accessed Apr 6, 2020)

2 Geyer, R.; Jambeck, J. R.; Law, K. L. Production, Use, and Fate of All Plastics Ever Made. *Sci. Adv.* **2017**, *3*, 1–6. https://doi.org/10.1126/sciadv.1700782.

3 *Advancing Sustainable Materials Management*, 2017 fact sheet (EPA 530-F-19-007); United States Environmental Protection Agency (EPA) – Office of Land and Emergency Management. (5306P), 2019. https://www.epa.gov/sites/production/files/2019-11/documents/2017_facts_and_figures_fact_sheet_final.pdf

4 *Plastics and the Environment*; Andrady, A. L., Ed.; John Wiley & Sons, Inc.: Hoboken, NJ, USA, 2003. https://doi.org/10.1002/0471721557.

5 Rochman, C. M. Microplastics Research-from Sink to Source. *Science*. April 6, 2018, pp 28–29. https://doi.org/10.1126/science.aar7734.

6 Barnes, D. K. A.; Galgani, F.; Thompson, R. C.; Barlaz, M. Accumulation and Fragmentation of Plastic Debris in Global Environments. *Philos. Trans. R. Soc. B Biol. Sci.* **2009**, *364*, 1985–1998. https://doi.org/10.1098/rstb.2008.0205.

7 Fagnani, D. E.; Tami, J. L.; Copley, G.; Clemons, M. N.; Getzler, Y. D. Y. L.; McNeil, A. J. 100th Anniversary of Macromolecular Science Viewpoint: Redefining Sustainable Polymers. *ACS Macro Lett.* **2021**, *10*, 41–53.

8 Future Market Insights (FMI). Super Absorbent Polymer (SAP) Market- Global Industry Analysis, Size and Forecast, 2015 to 2020.

https://www.futuremarketinsights.com/reports/super-absorbent-polymer-market (accessed Mar 21, 2020).

9 Khoo, S. C.; Phang, X. Y.; Ng, C. M.; Lim, K. L.; Lam, S. S.; Ma, N. L. Recent Technologies for Treatment and Recycling of Used Disposable Baby Diapers. *Process Saf. Environ. Prot.* **2019**, *123*, 116-129. https://doi.org/10.1016/j.psep.2018.12.016

10 Liang, L.; Li, C.; He, Q.; Tachea, F.; Tanjore, D.; Luong, T.; Somma, M.; D'Alessio, N.; Pray, T. R.; Sun, N. Upgrading of Postconsumer Absorbent Hygiene Products for Bioethanol Production. *ACS Sustain. Chem. Eng.* **2018**, *6*, 3589–3595. https://doi.org/10.1021/acssuschemeng.7b03931.

11 Ichiura, H.; Nakaoka, H.; Konishi, T. Recycling Disposable Diaper Waste Pulp After Dehydrating the Superabsorbent Polymer Through Oxidation Using Ozone. *J. Clean. Prod.* **2020**, *276*, 123350.

12 https:// www.alliedmarketresearch.com/pressure-sensitive-adhesives-market (Accessed Apr 7, 2021).

13 Creton, C. Pressure-Sensitive Adhesives: An Introductory Course. *MRS Bull.* **2003**, *28*, 434–439. https://doi.org/10.1557/mrs2003.124.

14 For example, see: Fornof, A. R.; DiZio, J. P. Self-Wetting Adhesive Composition. U.S. Patent 9,822,286. November 21, 2017.

15 Pocious, A. V. *Adhesion and Adhesives Technology*, 3rd ed.; Carl Hanser Verlag: Münich, 2012. https://doi.org/10.3139/9783446431775

16 Lehmann, A. Glacial acrylic acid (GAA), Methyl acrylate (MA), Ethyl acrylate (EA), n-Butyl acrylate (BA) and 2-Ethylhexyl acrylate (2-EHA) EABM July 15; Cefic European

Basic Acrylic Monomers Sector group (EBAM): Brussels, 2015; 17. https://www.petrochemistry.eu/wp-content/uploads/2018/01/150727_EBAM-Eco-profile-Acrylic-Monomers-1.pdf.

17 Takaya, C. A.; Cooper, I.; Berg, M.; Carpenter, J.; Muir, R.; Brittle, S.; Sarker, D. K. Offensive Waste Valorisation in the UK: Assessment of the Potentials for Absorbent Hygiene Product (AHP) Recycling. *Waste Management* **2019**, *88*, 56–70.

18 FaterSMART https://www.fatersmart.com/ (Accessed on Apr 6, 2021).

19 Caruso, M. M.; Davis, D. A.; Shen, Q.; Odom, S. A.; Sottos, N. R.; White, S. R.; Moore, J. S. Mechanically-Induced Chemical Changes in Polymeric Materials. *Chem. Rev.* **2009**, *109*, 5755–5798. https://doi.org/10.1021/cr9001353.

20 Li, J.; Nagamani, C.; Moore, J. S. Polymer Mechanochemistry: From Destructive to Productive. *Acc. Chem. Res.* **2015**, *48*, 2181–2190. https://doi.org/10.1021/acs.accounts.5b00184.

21 Prajapat, A. L.; Gogate, P. R. Intensification of Depolymerization of Polyacrylic Acid Solution Using Different Approaches Based on Ultrasound and Solar Irradiation with Intensification Studies. *Ultrason. Sonochem.* **2016**, *32*, 290–299. https://doi.org/10.1016/j.ultsonch.2016.03.022.

22 Bystryak, S.; Santockyte, R.; Peshkovsky, A. S. Cell Disruption of S. Cerevisiae by Scalable High-Intensity Ultrasound. *Biochem. Eng. J.* **2015**, *99*, 99–106.

23 Chubarova, E. V.; Melenevskaya, E. Y.; Shamanin, V. V. Chain Degradation under Low-Intensity Sonication of Polymer Solutions in the Presence of Filler: Mechanism of Ultrasonic Degradation of Flexible Chain Macromolecules. *J. Macromol. Sci. Part B* **2013**,

52, 873–896. https://doi.org/10.1080/00222348.2012.738576.

24 Markovitz, H.; Kimball, G. E. The Effect of Salts on the Viscosity of Solutions of Polyacrylic Acid. *J. Colloid Sci.* **1950**, *5* (2), 115–139. https://doi.org/10.1016/0095-8522(50)90014-6.

25 Creton, C. Pressure-Sensitive Adhesives: An Introductory Course. *MRS Bull.* **2003**, *28*, 434–439. https://doi.org/10.1557/mrs2003.124.

26 Pocious, A. V. *Adhesion and Adhesives Technology*, 3rd ed.; Carl Hanser Verlag: Münich, 2012. https://doi.org/10.3139/9783446431775

27 Tobing, S. D.; Klein, A. Molecular Parameters and Their Relation to the Adhesive Performance of Acrylic Pressure-Sensitive Adhesives. *J. Appl. Polym. Sci.* **2001**, *79*, 2230–2244. https://doi.org/10.1002/1097-4628(20010321)79:12%3C2230::AID-APP1030%3E3.0.CO;2-2

28 Collias, D. I.; Zimmerman, P. M.; Chazovachii, P. T.; Robo, M. T.; McNeil, A. J. Depolymerization of Polymers. U.S. Patent Application 62/890,880, August 23, 2019.

29 Li, Q.; Bao, Y.; Wang, H.; Du, F.; Li, Q.; Jin, B.; Bai, R. A Facile and Highly Efficient Strategy for Esterification of Poly(Meth)Acrylic Acid with Halogenated Compounds at Room Temperature Promoted by 1,1,3,3-Tetramethylguanidine. *Polym. Chem.* **2013**, *4* (9), 2891–2897. https://doi.org/10.1039/c3py00155e.

30 Chang, E. P. Viscoelastic Windows of Pressure-Sensitive Adhesives. *J. Adhes.* **1991**, *34*, 189–200. https://doi.org/10.1080/00218469108026513.

Chapter 3: Repurposing Acrylic-Based Absorbents via Post-Polymerization Modification Part II

Portions of this chapter have been published:

Chazovachii, P. T.; Somers, M. J.; Robo, M. T.; Collias, D. I.; James, M. I.; Marsh, E. N. G.; Zimmerman, P. M.; Alfaro, J. F.; McNeil, A. J. Giving Superabsorbent Polymers a Second Life as Pressure-Sensitive Adhesives. *Nat. Commun.* **2021**, *12*, 4524. https://doi.org/10.1038/s41467-021-24488-9.

Chazovachii et al. Depolymerization of polymers. US Patent Application, 2021.

Chazovachii et al. Preparation of Pressure Sensitive Adhesives from Post-Consumer Superabsorbent Polymers. US Patent Application, 2021.

Michael Robo from the Zimmerman lab performed atomistic simulations and Madeline Somers from the Zimmerman lab performed the life cycle assessment.

3.1 Introduction

The previous chapter demonstrated that the sodium polyacrylate superabsorbent polymer provided by Procter and Gamble ($PAA_{P\&G}$) could be chemically recycled into pressure-sensitive adhesives (PSAs) via a 3-step process. In this chapter, we used the life cycle assessment (LCA) to evaluate the previously developed open-loop recycling method and guide the optimization. Life cycle assessment is used to factually evaluate the potential environmental impacts associated with a commercial product, process, or activity over its entire life cycle. Life cycle assessment provides comprehensive (i.e., thousands of variables are accounted for) results by mapping: (1) all emissions and resource uses (including the respective geographical locations where possible), and (2) utilization factors derived from cause/effect models to calculate potential impacts on the environment from these emissions and resource uses.[1] A complete LCA includes the environmental impacts of all processes from raw materials extraction to product disposal (i.e.,

cradle-to-grave), whereas a partial LCA ends right after production (cradle-to-product or cradle-to-gate). Although LCA cannot objectively determine if a product environmentally friendly, the assessment tool can comparatively deduce the better option.

Guided by LCA tools, we demonstrate that our improved method outcompetes the petroleum-derived syntheses on nearly every metric, including global warming potential and cumulative energy demand. The significant improvements to the previously developed process include: (i) replacing the base hydrolysis with acid hydrolysis and (ii) replacing the base-mediated esterification with Fischer (i.e., acid-catalyzed) esterification (Scheme 3-1). Moreover, a route involving just decrosslinking and esterification (i.e., no sonication) was discovered, which has the potential to be industrially scalable, providing a sustainable solution to a longstanding waste problem.

Scheme 3-1. Comparing syntheses of pressure-sensitive adhesives from petroleum versus waste diapers as the feedstock.

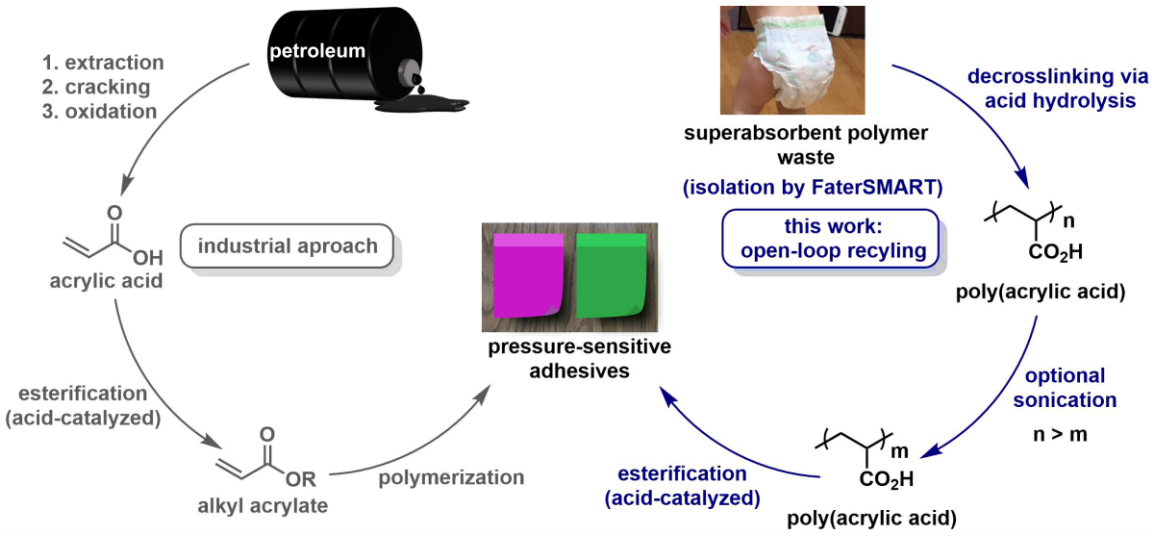

3.2 Decrosslinking via hydrolysis

The superabsorbent polymer provided by P&G is a sodium poly(acrylate) crosslinked via a poly(ethylene glycol) diacrylate co-monomer ($PAA_{P\&G}$). In chapter 2, the crosslinks were

hydrolyzed using 0.3 M aq. NaOH and mild heating (Scheme 3-2, top). For comparison, we also evaluated the hydrolysis using 0.8 M aq. H_2SO_4 with heating (Scheme 3-2 bottom). The complex viscosity again dropped several orders of magnitude over 24 h, at which point no further changes were observed, suggesting that the majority of crosslinks had been hydrolyzed (Appendix 2, Figure A2-2). To determine whether the base-mediated or acid-catalyzed pathway was better, the two routes were compared using a cradle-to-product life cycle assessment (Appendix 2, Figure A2-3). The acid-catalyzed hydrolysis outperformed the base-mediated hydrolysis by a factor of 10 on both global warming potential and cumulative energy demand. The resulting acidic polymer solutions were used directly in the subsequent experiments without any isolation steps.

Scheme 3-2. Hydrolysis reactions examined synthetically and analyzed using life cycle assessment.

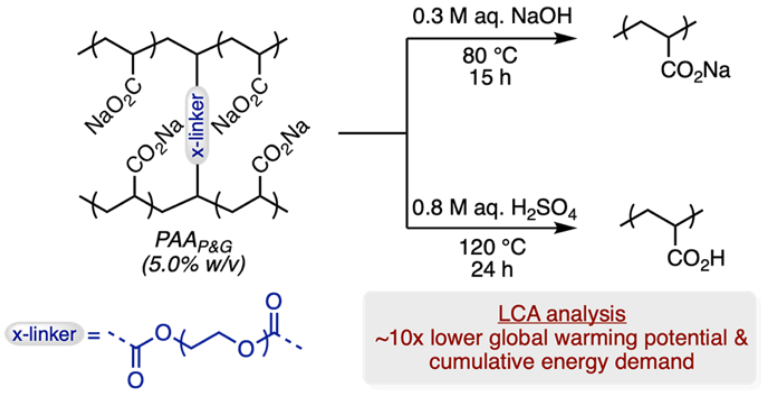

3.3 Chain-shortening via sonication

In pressure-sensitive adhesive (PSA) applications, tuning the molar mass of the polymeric component confers variations in the PSA's viscoelastic properties. Sonication was used to chain-shorten the decrosslinked polymer chains to access a range of molar masses. Sonicating 2.5% and 5.0% w/v solutions of decrosslinked $PAA_{P\&G}$ for 0–10 min using a 20 kHz sonication horn operating at full amplitude (100%) revealed rapid chain-shortening for the decrosslinked $PAA_{P\&G}$ (Figure 3-1). At each time point, the maximum specific energy (w_{max}) was calculated using the

maximum power drawn from the outlet and the mass of added PAA (Appendix 2, eq. 1), and the molar masses (M_w) were determined using size-exclusion chromatography (Appendix 2, pgs. 127–131).

Acrylate-based PSAs confer appropriate cohesion and shear holding strength at M_w > 400 kg/mol. [2, 3, 4] therefore our optimized conditions involved sonicating a 2.5% w/v solution for 1 min to give an M_w ~360 kg/mol, and a 5.0% w/v solution for 2 min to give a M_w of ~330 kg/mol.[5] The resulting chain-shortened $PAA_{P\&G}$ fragments were then dialyzed to remove excess acid, lyophilized, and then ground into a powder. The resulting polymers were isolated in ~90% yield (over the two steps). A life cycle assessment was used to compare the routes that involved (i) no sonication, (ii) sonication for 1 min (2.5% w/v) and (iii) sonication for 2 min (5.0% w/v), including the workup steps, and will be described in more detail below.

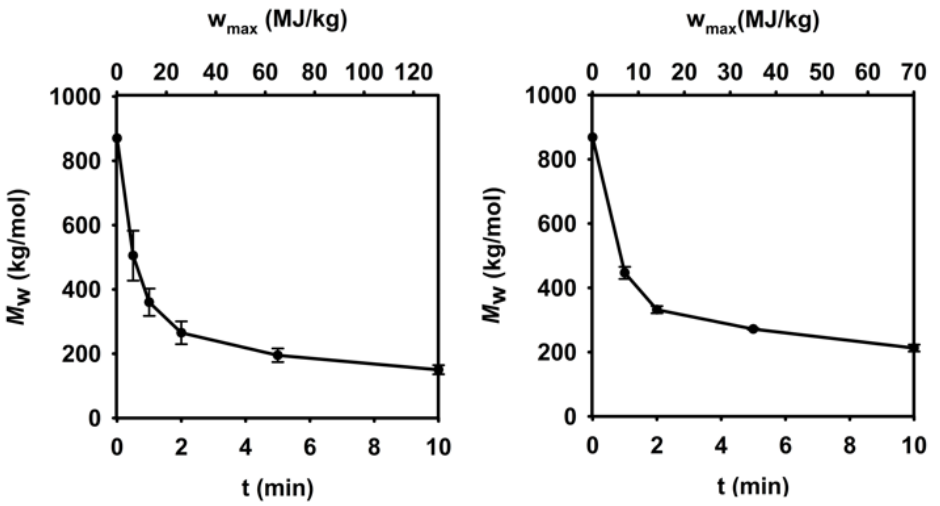

Figure 3-1. Plot of weight-average molar mass (M_w) versus time and maximum specific energy (w_{max}) for sonicating $PAA_{P\&G}$ at 2.5% w/v (left) and 5.0% w/v (right).

3.4 Esterification of polymer fragments

Several routes for converting the polyacrylic acid into a polyacrylate were compared. Esterification of polyacrylic acid using alkyl halides under basic conditions had already been

reported[6] and was used in the previous chapter. However, this process utilizes expensive solvents (e.g., dimethylsulfoxide = $47/L) and reagents (e.g., 2-ethyl hexyl bromide = $222/kg and tetramethyl guanidine = $213/kg), which would likely be too costly for large-scale recycling of waste superabsorbent materials (Appendix 2, Table A2-1). In contrast, a common approach used in industry to convert acrylic acids into acrylate esters uses inexpensive alcohols (e.g., 2-ethylhexanol = $12/L) (Appendix 2, Table A2-1) as both the reagent and solvent.[7,8] However, this approach can lead to low yields due to competitive ester hydrolysis[9,10] and catalyst deactivation by water.[11] To circumvent these challenges, the water by-product can be selectively removed via azeotropic distillation, or a large excess of alcohol can be employed.[12,13]

We hypothesized that we could potentially eliminate the need to actively remove water because once produced, the water phase separates from hydrophobic polymer backbone and alcohol solvent. [14] To interrogate this hypothesis, we measured the percent esterification under different conditions. For example, high degrees of esterification were observed via ^{1}H NMR and IR spectroscopy when using only 3 equiv. of 2-ethylhexanol and H_2SO_4 as a catalyst (Scheme 3-3 and Appendix 2, pgs. 132–134). Surprisingly, even when excess H_2O was intentionally added (3 equiv), high conversions were still observed (Appendix 2, pgs. 135–136). The results from both of these experiments demonstrate that the equilibrium lies far towards the esterification product.

To understand why esterification is so favored, we turned to small molecule model systems (Appendix 2, pgs. 137–147). To probe the role of both solvent and substrate hydrophobicity, we used two different substrates (acetic versus undecanoic acid) and solvents (ethanol versus 2-ethylhexanol). When acetic acid was reacted with 2-ethylhexanol/water, we observed a 94% conversion. In contrast, when acetic acid was reacted with ethanol/water, the conversion was only 67%. These results demonstrate that solvent hydrophobicity improves conversion to the ester.

Next, undecanoic acid was esterified under the same conditions, yielding 100% ester for 2-ethylhexanol/water and 83% for ethanol/water. When compared to the acetic acid reactions, these results suggest that the substrate hydrophobicity also favors conversion to the ester. From these studies, we conclude that the quantitative esterification of the polymer results from the hydrophobic reaction environment created by the polymer backbone and the 2-ethylhexanol solvent.

Scheme 3-3. Acid-catalyzed esterification of poly(acrylic acid), acetic acid, and undecanoic acid with 2-ethylhexanol/water or ethanol/water mixtures.

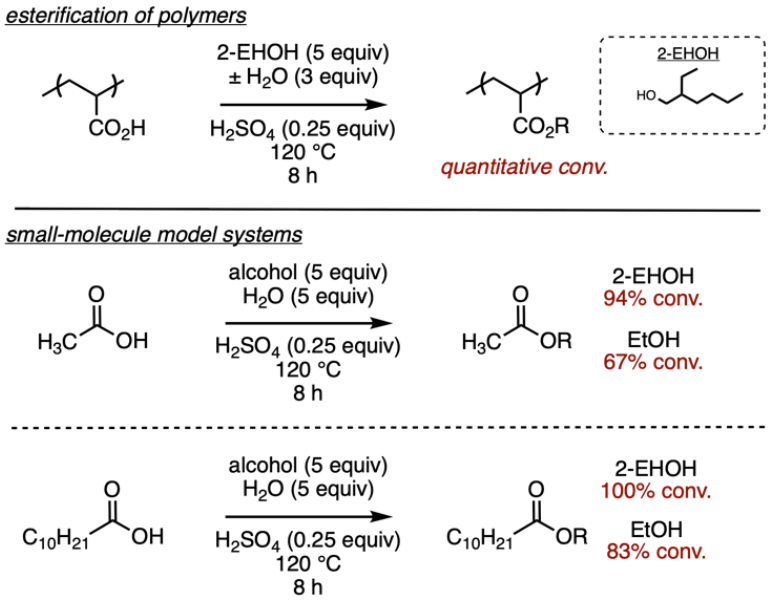

To probe whether the hydrophobic side chains also push the equilibrium towards esterification, atomistic simulations were performed by Dr. Michael Robo (Zimmerman lab) (Scheme 3-4 and Appendix 2, pgs. 148–153).[15,16] Briefly, nonamers of polyacrylic acid were used as a model system along with butyl alcohol. Comparison of the reaction free energies was made between the first esterification and the final esterification. In both cases, the nonamers were solvated in a 3:1 butanol/water mixture to mimic the most challenging esterification conditions. The change in the Helmholtz free energy of esterification for these two steps (ΔΔA) was found to be −0.7 ± 0.1

kcal/mol. This value suggests that the increase in polymer hydrophobicity provides a significant thermodynamic driving force towards further esterification, perhaps counteracting the buildup of water that was otherwise expected to limit conversion.

Scheme 3-4. Comparing the computed free energies for the first and last esterification.

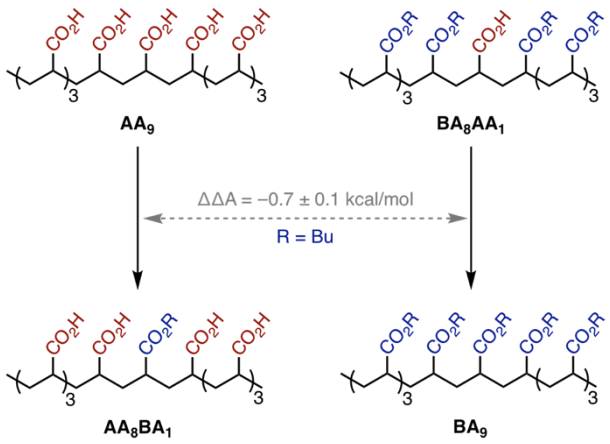

3.5 Characterizing the adhesive properties

All the adhesives synthesized from $PAA_{P\&G}$ fall within quad 3 and the central region (Figure 3-2) of the viscoelastic window (VW).[17,18] This suggests that the PSAs exhibit enough softness to wet a substrate at the bonding frequency, while also having enough hardness to hold onto a substrate, and peel cleanly without leaving residue at the debonding frequency. As expected, the VWs are higher with larger M_w, which is due to the increased chain entanglements. Overall, the viscoelastic properties of the synthesized PSAs suggest they would be useful for applications such as removable general-purpose adhesives, including tapes, bandages, and sticky notes. Excitingly, a viable "central" region pressure-sensitive adhesive is accessible without any sonication.

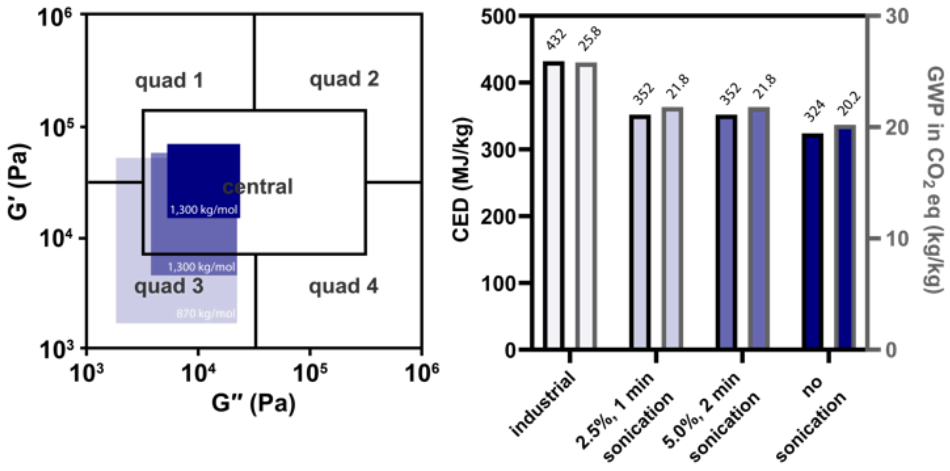

Figure 3-2. Plots of storage (G′) versus loss (G″) moduli for poly(2-ethylhexylacrylate) (left), including visualization of Chang's viscoelastic window, and of the cumulative energy demand (CED) and global warming potential (GWP) for each route.

3.6 Life cycle assessments

Life cycle assessments (LCA) were performed in collaboration with Madeline Somers (Alfaro lab) to assess the cumulative energetic and environmental impacts of producing 1 kg of adhesive via our open-loop recycling method. More specifically, we compared four different cradle-to-production LCA scenarios: poly(2-ethylhexylacrylate) production in the conventional industrial approach and three variations of the recycling process: (i) sonicating the 2.5% w/v polymer solution for 1 min, (ii) sonicating the 5.0% w/v polymer solution for 2 min, and (iii) no sonication of the 5% w/v polymer solution. All environmental data were gathered from experiments, literature, or the ecoinvent database (version 3.5),[19] and implemented in SimaPro v. 9.0.0.48,[19] as described in detail within the appendix (Appendix 2, pgs. 160–165). Several environmental impact categories were examined, but particular attention was paid to the global warming potential (GWP) and cumulative energy demand (CED). We found a 15.3% and 15.1% decrease in GWP when

replacing the industrial route with either the 1 min or 2 min sonication scenario, respectively, and an impressive 21.5% decrease when sonication was avoided altogether. From an energetic standpoint, the CED is reduced by 18.8% and 18.6% with the sonication scenarios, and further reduced (by 24.8%) by the scenario without sonication. Combined, these data indicate that open-loop recycling of the superabsorbent poly(acrylic acid) to synthesize PSAs is both energetically and environmentally favorable compared to petroleum-derived syntheses in our assessment.

Given a growing emphasis on sustainability within the polymer industry, including calls to increase the circularity of polymer production,[20] LCA provides an important metric for evaluating new approaches to polymer recycling. At present, the environmental benefits of diaper recycling (including superabsorbent poly(acrylic acid) recovery) are dependent on the avoided material burdens.[21] One of the pitfalls of diaper recycling pilots is the low demand for recovered diaper materials, which depreciates the environmental potentiality of such endeavors.[9] Therefore, efforts to introduce synergy between superabsorbent poly(acrylic acid) recovery and PSA production may provide much-needed demand for diaper recycling end-products, which in-turn may improve environmental performance for both processes on a large scale.

3.7 Conclusions

To summarize, we developed a facile and potentially scalable method to synthesize commercially relevant PSAs by open-loop recycling poly(acrylic acid) sourced from a leading diaper manufacturer. The transformation relies on an (i) acid-catalyzed hydrolysis, (ii) optional chain-shortening via sonication, and (iii) a highly efficient esterification drive by hydrophobicity. Different PSAs were targeted simply by varying the sonication times. Moreover, the life cycle assessments, which utilized soiled diapers as the starting point, demonstrated that these open-loop recycling methods outperform the conventional routes from petroleum-derived feedstocks on

nearly every metric, including for the key LCA metrics of global warming potential and cumulative energy demand. Because this recycling method should be amenable to waste polymer as the feedstock, it offers a more sustainable alternative to diaper disposal in a landfill or incineration.

3.8 References

1 Bjørn, A.; Owsianiak, M.; Molin, C.; Laurent, A. Main characteristics of LCA. In Life Cycle Assessment; Hauschild, M. Z., Rosenbaum, R. K., Olsen, S. I., Eds.; Springer International Publishing AG: Switzerland, 2018; pp 9−16.

2 Creton, C. Pressure-Sensitive Adhesives: An Introductory Course. *MRS Bull.* **2003**, *28*, 434–439. https://doi.org/10.1557/mrs2003.124.

3 Pocious, A. V. *Adhesion and Adhesives Technology*, 3rd ed.; Carl Hanser Verlag: Münich, 2012. https://doi.org/10.3139/9783446431775

4 Tobing, S. D.; Klein, A. Molecular Parameters and Their Relation to the Adhesive Performance of Acrylic Pressure-Sensitive Adhesives. *J. Appl. Polym. Sci.* **2001**, *79*, 2230–2244. https://doi.org/10.1002/1097-4628(20010321)79:12%3C2230::AID-APP1030%3E3.0.CO;2-2

5 Collias, D. I.; Zimmerman, P. M.; Chazovachii, P. T.; Robo, M. T.; McNeil, A. J. Depolymerization of Polymers. U.S. Patent Application 62/890,880, August 23, 2019.

6 Li, Q.; Bao, Y.; Wang, H.; Du, F.; Li, Q.; Jin, B.; Bai, R. A Facile and Highly Efficient Strategy for Esterification of Poly(Meth)Acrylic Acid with Halogenated Compounds at Room Temperature Promoted by 1,1,3,3-Tetramethylguanidine. *Polym. Chem.* **2013**, *4*, 2891–2897. https://doi.org/10.1039/c3py00155e.

7 Bauer, W. Acrylic Acid and Derivatives. In *Kirk-Othmer Encyclopedia of Chemical Technology*; John Wiley & Sons, Inc.: Hoboken, NJ, USA, 2003. https://doi.org/10.1002/0471238961.0103182502012105.a01.pub2.

8 Ohara, T.; Sato, T.; Shimizu, N.; Prescher, G.; Schwind, H.; Weiberg, O.; Marten, K.; Greim, H. Acrylic Acid and Derivatives. In *Ullman's Encyclopedia* of *Industrial Chemistry.* Wiley-VCH Verlag GmbH & Co: Weinheim, 2012. https://onlinelibrary.wiley.com/doi/epdf/10.1002/14356007.a01_161.pub3

9 Roberts, I.; Urey, H. C. The Mechanisms of Acid Catalyzed Ester Hydrolysis, Esterification and Oxygen Exchange of Carboxylic Acids. *J. Am. Chem. Soc.* **1939**, *61*, 2584–2587. https://doi.org/10.1021/ja01265a003.

10 Raber, D. J.; Gariano, P.; Brod, A. O.; Gariano, A.; Guida, W. C.; Guida, A. R.; Herbst, M. D. Esterification of Carboxylic Acids with Trialkyloxonium Salts. *J. Org. Chem.* **1979**, *44*, 1149–1154. https://doi.org/10.1021/jo01321a027.

11 Liu, Y.; Lotero, E.; Goodwin, Jr, J. G. Effect of Water on Sulfuric Acid Catalyzed Esterification. *J. Mol. Catal. A* **2006**, *245*, 132–140. https://www.sciencedirect.com/science/article/pii/S1381116905007004

12 Carlyle, R. L. Process for the Production of Acrylic Acid Esters. U.S. Patent 2,917,538, December 15, 1959.

13 Alarifi, A. S.; Aouak, T. Synthesis of Acrylic or Methacrylic Acid/Acrylate or Methacrylate Ester Polymers Using Pervaporation. US Patent 9,321,868 B2, April 26, 2016.

14 McNeil, A. J.; Chazovachii, P. T.; Robo, M. T.; Marsh, N. G.; Zimmerman, P. M.; James, M. I.; Collias, D. I. Esterifying Polyacrylic Acid with High Conversion. U.S. Patent Application 62/947,363, December 12, 2019.

15 Vilseck, J. Z.; Sohail, N.; Hayes, R. L.; Brooks, C. L. Overcoming Challenging Substituent Perturbations with Multisite λ-Dynamics: A Case Study Targeting β-Secretase 1. *J. Phys. Chem. Lett.* **2019**, *10*, 4875–4880. https://doi.org/10.1021/acs.jpclett.9b02004.

16 Hayes, R. L.; Armacost, K. A.; Vilseck, J. Z.; Brooks, C. L. Adaptive Landscape Flattening Accelerates Sampling of Alchemical Space in Multisite λ Dynamics. *J. Phys. Chem. B* **2017**, *121*, 3626–3635. https://doi.org/10.1021/acs.jpcb.6b09656

17 Collias, D. I.; Zimmerman, P.; Chazovachii, P. T.; Robo, M. T.; McNeil, A. J. Super Absorbent Polymer Recycling to Pressure Sensitive Adhesives. U.S. Patent Application 62/890,943, August 23, 2019.

18 Chazovachii, P. T.; Somers, M.; Robo, M. T.; Marsh, E. N. G.; Zimmerman, P. M.; Alfaro, J.; McNeil, A. J. Preparation of Pressure-Sensitive Adhesives from Post-Consumer Superabsorbent Polymers. US Provisional Patent Application No. 63/174,000 (filed April 13, 2021).

19 Wernet, G.; Bauer, C.; Steubing, B.; Reinhard, J.; Moreno-Ruiz, E.; Weidema, B., The ecoinvent database version 3 (part I): overview and methodology. *The International Journal of Life Cycle Assessment* **2016,** *21* (9), 1218-1230.

20 Ellen MacArthur Foundation. The New Plastics Economy: Rethinking the Future of Plastics & Catalyzing Action. *Ellen MacArthur Foundation*, 2017. https://www.ellenmacarthurfoundation.org/publications/the-new-plastics-economy-rethinking-the-future-of-plastics-catalysing-action (accessed on Apr 9, 2021).

21 Arena, U.; Ardolino, F.; Gregorio, F. D., Technological, Environmental and Social Aspects of a Recycling Process of Post-Consumer Absorbent Hygiene Products. *Journal of Cleaner Production* **2016,** *127*, 289-301. https://doi.org/10.1016/j.jclepro.2016.03.164

Chapter 4: Removing Microplastics Pollutants from Water via Adhesive-Induced Van der Waals Interactions

Portions of this chapter have been published:

Chazovachii, P.T.; Rieland, J. M.; Sheffey, V.V.; Jugovic, T. M. E.; Zimmerman, P. M.; Eniola-Adefeso, O.; Love, B. J.; McNeil, A. J.; Using Adhesives to Capture Microplastics from Water. *(submitted)*

Chazovachii et al. Microplastics Removal Using Adhesives. US Provisional Patent Application, 2021.

P. Takunda Chazovachii and Anne McNeil conceived the research project. P. Takunda Chazovachii synthesized the adhesives, performed the scoping/preliminary experiments, coated the beads, and led the capture experimental effort. Julie Rieland from the Love lab assisted in the capture experiments while Violet Sheffey from the Eniola-Adefeso lab assisted with the flow cytometry analysis. Timothy Jugovic from the Zimmerman lab performed the atomistic simulations. Brian Love provided valuable insight throughout the entire project duration.

4.1 Introduction

Accumulation of microplastics (MPs) in oceans and other surface water bodies is a cause for concern.[1] Microplastics dominate marine particulates with seas and oceans acting as major sinks for most MPs released into the environment.[2,3] A majority of MPs are generated from the erosion of car tires[4,5] (e.g., micronized rubber)[4,5] and the wear and tear of synthetic textiles[6,7] (i.e., microfibers).[8] Before reaching the oceans, micronized rubber and textile fibers find their way into sewers as suspended particulates in road runoff and laundry effluent, respectively. Sewage water, which contains MPs from other sources (e.g., microbeads from cosmetics), passes through the wastewater treatment plant where biosolids capture 90–98% of the MPs.[3] These biosolids are often distributed to farmers as nutrient-rich organic fertilizers, introducing the MPs into the terrestrial environment.[3] Natural elements[9] like rainfall and wind eventually transport most of these MPs to the marine environment, where remediation is complex.[10]

The notion that society can wholly avoid using plastics altogether is impractical. One feasible solution is to develop efficient remediation methods to remove MPs before entering wastewater treatment plants. Most of the few commercialized remediation technologies are used to remove microfibers from laundry effluent (e.g., CORA ball[11], GuppyFriend[12], etc.).[13] These methods are based on physical entrapment, therefore, MPs smaller than a specific threshold are not captured (~50–100 μm).

In recent years, there has been growing efforts towards developing solutions to remove MPs from the environment.[3,14] In one example, Wang et al. investigated incorporating biochar in sand filters to enhance MPs removal.[15] Using hemocytometry to evaluate capture efficiency, they observed >95% removal efficiency (RE) of polystyrene (PS) microbeads (10 μm) while the unmodified sand filter only removed 60–80%. They suggested that the biochar's unique ability to trap MPs in its honeycomb structure and bind with MPs via π interactions improved removal efficiency. Sun et al. also reported removing unfunctionalized, carboxylate- and amine-functionalized polystyrene fluorescent beads (1 μm) using chitin sponges functionalized with graphene oxides.[16] Using a fluorescence spectrophotometer, they observed RE values of ~90% for the unfunctionalized, ~72% carboxylate, and ~89% for the amine-functionalized PS beads. They attributed the capture efficiency to electrostatic, hydrogen-bonding, and π interactions between graphene oxide and PS. In another study, Chen et al. developed a method to remove MPs from simulated suspensions (water/ethanol, 3:1 ratio) using zirconium metal-organic frameworks loaded into melamine foam.[17] By measuring the change in mass, they determined RE of ~90% for poly(vinylidene difluoride) (~260 nm), ~88% for polystyrene (~300 nm), and ~85% for poly(methyl methacrylate) (~183 nm).

The efforts towards developing MPs remediation methodologies are still at their infant stages (i.e., most publications demonstrating MPs remediation emerged in 2020); therefore, there is a need for innovation. Most of the approaches highlighted above utilize π interactions, which may not apply to most biopersistent MPs (e.g., polyethylene, polypropylene, and nylon). Also, the MPs removal reported above may (understandably) lack accuracy due to the high detection limits of the methodologies used. Therefore, the MPs scientific community benefits from innovative discovery-focused work introducing removal methodologies, accompanied by improved detection and quantification methods. This chapter demonstrates MPs removal using pressure-sensitive adhesives, a new approach discovered serendipitously, and demonstrates quantification using flow cytometry, a technique that enables rapid analysis of MPs removal efficiencies. [18]

4.2 Adhesives in the context of underwater adhesion to microplastics

The pressure-sensitive adhesives (PSAs) market is a rapidly growing adhesives sector due to their application in various removable articles (e.g., tape, bandages, and sticky notes).[19] One of the critical features of PSAs is their softness, which enables them to wet a substrate spontaneously with minimal external pressure.[20] The intimate contact between the surfaces allows many short-range noncovalent interactions to develop, resulting in strong adhesion. PSAs contain highly entangled long-chain or crosslinked polymers, which allows clean peeling from the substrate.

Surface energy (γ) is a parameter used to predict wetting between an adhesive and a substrate. This parameter is the excess energy that manifests at the material's surface due to the absence of stabilizing interactions present in bulk. The surface energy parameter can be divided into polar (γ^p) and dispersive (γ^d) components.[21] Strong adhesion should be achieved when the adhesive and microplastic have similar ratios of these components. In addition, adhesion should be strengthened when the adhesive/water and microplastic/water surface energies are dissimilar. One way to

compare the values is to look at the percent polar contribution (% polar = γ^p /(γ^d + γ^p) x 100). Advantageously, the surface energy of water is highly polar (69% polar), whereas most microplastics are much lower (i.e., 0–34% polar)[22] (Table 4-1). Based on this analysis, we chose poly(2-ethylhexyl acrylate) (P(2-EHA)) homopolymers because % polar value (~7% polar) lies right in the middle of the targeted microplastics. Computational simulations of an atomistic P(2-EHA) model in contact with common plastic surfaces were used to estimate adhesive ability (Appendix 3, Table A3-1). The simulated work of adhesion provided values in the range of 20–30 mN/m, suggesting that P(2-EHA) will have moderate adhesive ability underwater. These results are consistent with experimental values for similar PSAs interacting with those same plastic surfaces.[23]

Table 4-1. Surface energies of materials used herein.

Material	γ^d (mN/m)	γ^p (mN/m)	% polar
water[24]	21.8	51.0	70
PE[25]	25.9	0	0
PS[26]	34.5	6.1	15
rubber (SBR)[27]	28.9	2.4	7.6
PET[28]	39.3	4.2	9.6
nylon 12[29]	30.3	5.5	15
P(2-EHA)[29]	27.1	2.2	7.5

4.3 Selection and synthesis of adhesives

Molar mass is a key variable in designing acrylate-based PSAs for any application, which requires an informed compromise between desired properties. Low molar mass confers good wetting (i.e., tack or flow), while shear holding strength and cohesion require high degrees of chain entanglements only achievable at high molar mass. For this reason, we decided to explore the implications of molecular weight.

We started with poly(2-ethylhexyl acrylate) (P(2-EHA)) homopolymers because 2-ethyl hexyl acrylate is the primary repeat in most acrylate-based PSAs, and its $\frac{\gamma^d}{\gamma^p}$ (i.e., ~18% polar) lies right in the middle of the range for most biopersistent synthetic polymers (i.e., 0–30% polar). Poly(2-ethylhexyl acrylate)s of varying molar masses were either purchased or accessed as follows: 92 kg/mol P(2-EHA)$_{\text{Sigma-93k}}$ solution in toluene purchased from Sigma Aldrich, 450 kg/mol P(2-EHA)$_{\text{Sigma-370k}}$ made by esterifying 240 kg/mol poly(acrylic acid) purchased from Sigma Aldrich, 950 kg/mol P(2-EHA)$_{\text{SPP-950k}}$ synthesized by esterifying 500 kg/mol poly(acrylic acid) prepared by chain-shortening 1,000 kg/mol poly(acrylic acid) purchased from Scientific Polymer Products, and 450 kg/mol P(2-EHA)$_{\text{P\&G-590k}}$ was synthesized by esterifying 260 kg/mol poly(acrylic acid) prepared by decrosslinking, chain-shortening, and esterifying PAA$_{\text{P\&G}}$. Details about the decrosslinking, chain-shortening, and esterification processes were discussed in chapters 2 and 3.

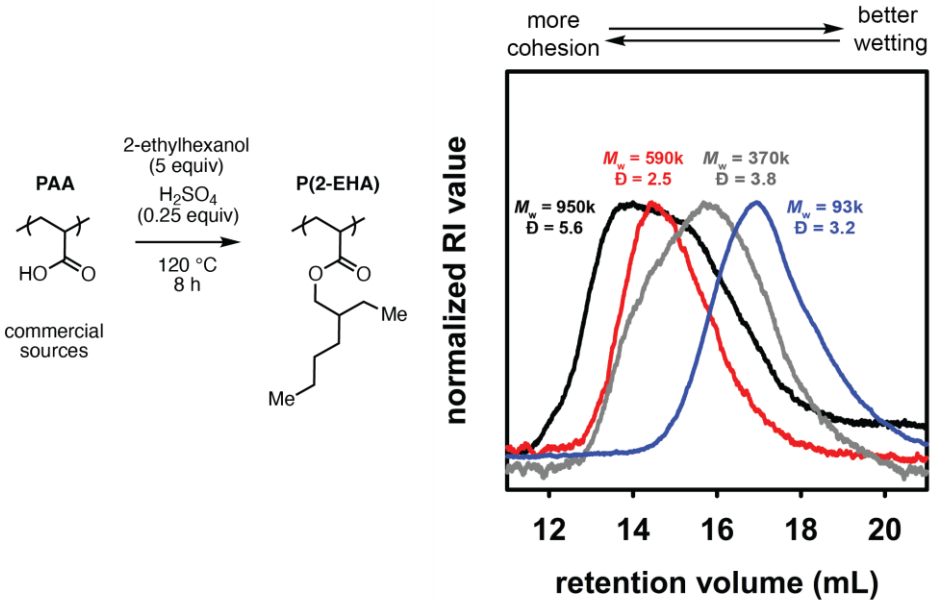

Figure 1-1. Synthesis procedure and size-exclusion chromatography traces of the synthesized P(2-EHA).

4.4 Evaluating microplastics removal in water

First, we decided to evaluate the observed results in water after observing the accidental capture of micronized rubber in the liquid waste container, which contained a plethora of solvents and reagents waste detailed in earlier (Chapter 1, pg. 10). We reevaluated the previously observed capture in the liquid waste container using suspensions of micronized rubber in water. As expected, the stir bar coated with $P(2\text{-EHA})_{Sigma\text{-}93k}$ captured the micronized rubber, whereas nothing adhered to the bare stir bar (Figure 4-2 and Appendix 3, pg. 182). Micronized rubber primarily consists of C-C bonds and contains carbon black, making it hydrophobic.

Figure 4-2. Preliminary experiments demonstrating MPs removal from water using an adhesive-coated stir bar to capture micronized rubber (~100 μm) suspended in water

After verifying our initial observations, we demonstrated that this method is generalizable to other types of MPs, including those with heteroatomic structures (Figure 4-3). In one example, using adhesive-coated glass slides and optical microscopy, a wide range of materials were captured with $P(2\text{-EHA})_{590k}$, including polar (i.e., nylon and polyethylene terephthalate) and non-polar microplastics (i.e., rubber and polyethylene). Optimistically, these sampled plastics include the highest production volume material (PE) as well as key components of environmental

microplastics (micronized rubber and synthetic textiles (PET, nylon)). In addition, microplastics with varying sizes (from 30–300 μm) and irregular shapes were captured.

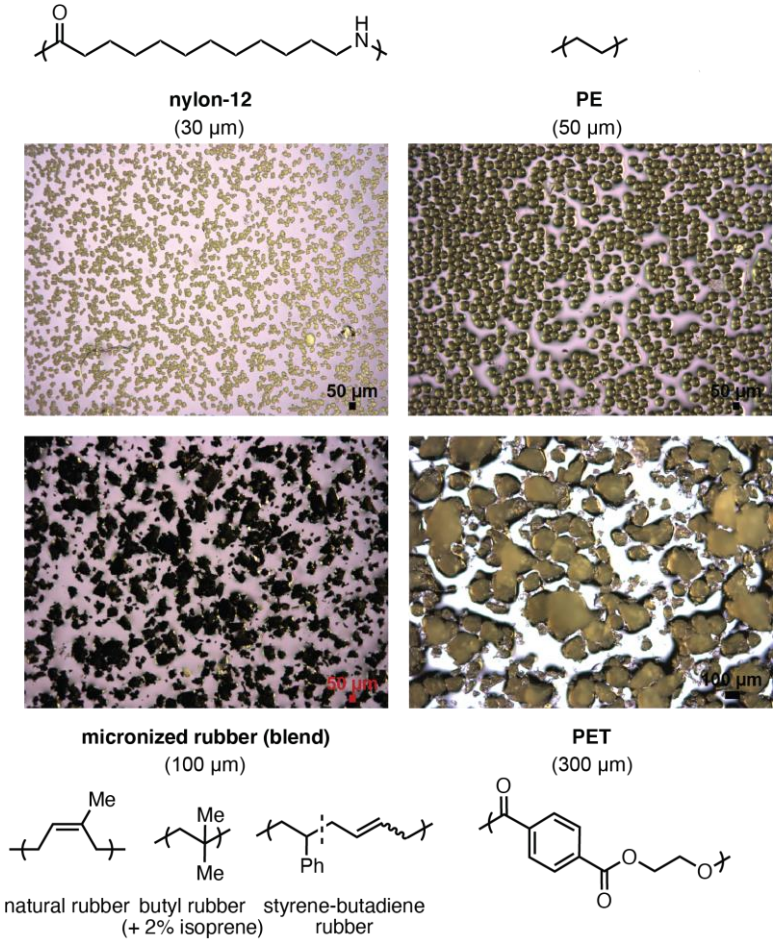

Figure 4-3. Optical microscope images of adhesive-coated glass slides that captured other microplastics, as well as their chemical structures and average size.

4.5 Adhesive coated beads as substrates for efficient MPs removal

We next explored methods to improve our MPs RE by increasing the frequency of PSA-MPs collisions. We imagined that using adhesive-coated small spherical objects would increase the frequency of collisions due to the increased available surface area and increased mobility relative to the flat and immobile glass slides in the previous examples. While exploring this idea, we found that the beads can be too small to the point of not generating enough force to disaggregate from

the clumping that occurs after the adhesive is applied. In preliminary experiments, we dip-coated post-use molecular sieves (2 mm) found in the lab and tested capturing 300 µm PET and 90 µm PS (Appendix 3, pgs. 183–185). Although the adhesive-coated sieves initially aggregated, we observed immediate disaggregation within 30 s of mild hand-shaking (3 shakes per second). The disaggregation was likely due to the obstruction of the adhesive surface by the captured MPs. The sieves were analyzed using scanning electron microscopy (SEM) by Violet Sheffey, and indeed, the sieves were effective at capturing both PET (Figure 4-4 B and C) and PS (Figure 4-4, D and E). After noting some debris released by the sieves, we switched to zirconium silicate beads (0.5 mm) for our subsequent experiments. The dense metallic beads are less prone to material shedding, even with high impact, such as ball milling.

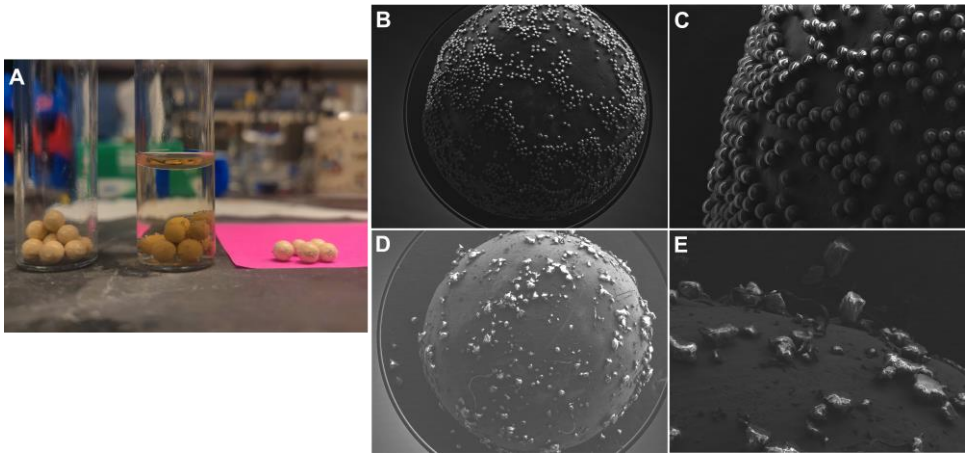

Figure 4-4. Preliminary experiments investigating spherical beads as substrates for MPs removal. (A) adhesive-coated sieves initially aggregated before and later disaggregated after MPs capture experiments. (B) and (C) SEM images of sieves after capturing 300 µm PET in water. (D) and (E) SEM images of sieves after capturing 90 µm PS in water.

Using adhesive-coated zirconium beads, we further investigated removing 90 µm PS as a function of time under saturation conditions (i.e., using a large excess of MPs) (Appendix 3, pg. 186). MPs removal was induced by vortex mixing the samples 0.5–2 min, and the results were analyzed using optical microscopy. Based on the optical microscope images, we confirmed MPs

removal using adhesive-coated zirconium silicate beads (0.5 mm), which are of different chemical composition and smaller than the sieves used earlier.

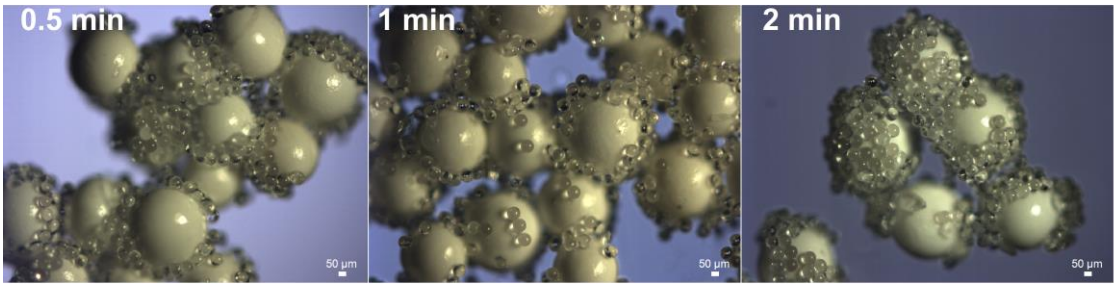

Figure 4-5. Optical microscopic images showing 90 µm PS captured by $PAA_{SPP\text{-}950k}$ coated 0.5 mm beads at different time points.

4.6 Identifying flow cytometry as a method for quantifying removal efficiency

We primarily analyzed MPs captured by the adhesive-coated substrate using optical and scanning electron microscopy in the previous examples. From there, we aimed to evaluate our method's MPs RE. Due to the small sizes and low concentrations (i.e., post-remediation) of MPs in removal tests, we needed to identify a reliable method for quantification. As with the examples highlighted earlier, the quantification methods generally used in the field to evaluate MPs removal widely vary, making it challenging to compare results wholistically. UV-Vis spectroscopy had been used for MPs quantification[30,31] although this approach may provide inaccurate results because suspended particles tend to scatter light rather than absorb it.[32] Although hemocytometry has also been used for MPs quantification and can be very accurate within its detection bounds, the lower limit of detection is too high (i.e., ~2.5×10^5 counts/mL) to accurately determine MPs post-removal tests.[33]

Flow cytometry is a practical and precise method for quantifying MPs concentration in aqueous suspensions.[34] The flow cytometer we employed, an Attune NxT, can analyze concentrations as low as 500 particles/mL to as high as 1,000,000 particles/mL. This technique is most commonly

applied in microbiology and biomedical engineering, and it allows researchers to analyze single-cell populations and rapidly retrieve data about many parameters concerning those cells (i.e., cell type, size, surface characteristics, morphology, and immunological activity).[35,36] The working principle of the flow cytometry technique involves using a sheath fluid to hydrodynamically focus a stream of events (these can be cells, particles, or other discrete matter) single file in front of a laser where they are subsequently detected, counted, or sorted.

For our application, fluorescence staining was unnecessary as the only population in the samples was the monodisperse MPs. Thus, the forward scatter (FSC) detector, a photomultiplier that analyzes particles in proportion to their size, was employed. The forward scattered light is detected along the direction of the laser beam and results from light diffracting from the event's perimeter. Another detector, the side scatter detector, measures scatter perpendicular to the laser beam and provides information on the internal complexity of the particle. We opted to use the forward scatter detector for data analysis because the MPs have a simplistic internal structure consisting of solid, densely packed polystyrene (PS) material.

After much trial and error, we finalized the instrument's settings to be the following: laser voltage: 200, sample flow rate: 25 μL/min (for 5 and 10 μm sized particles), sample volume: 30 μL. To calculate concentration, we divided the number of particles by the collected sample volume and scaled it to find the number of particles per milliliter.

The total number of particles includes not only the singlets, which are the single particles the detector picks up as particles pass by one by one but also *doublets* and *triplets*. Although flow cytometry analysis intends to analyze events one by one as they pass through the laser interrogation point (so that all events can be represented as singlets), at times, two or three particles (m and 2m particles, Figure 4-6 A) cluster with one another during analysis, leading to the presence of

doublets or triplets on the dot plots. Doublets and triplets can be recognized by the magnitude of the FSC-area (m and 2m particles, Figure 4-6 B). Although the event peak has the same FSC-height (intensity) as a singlet due to its similar size, the peak area doubles or triples the singlet area due to aggregation of particles (Figure 4-6). The other particles (n particles, Figure 4-6) have a different chemical identity and size and therefore scatter light differently.

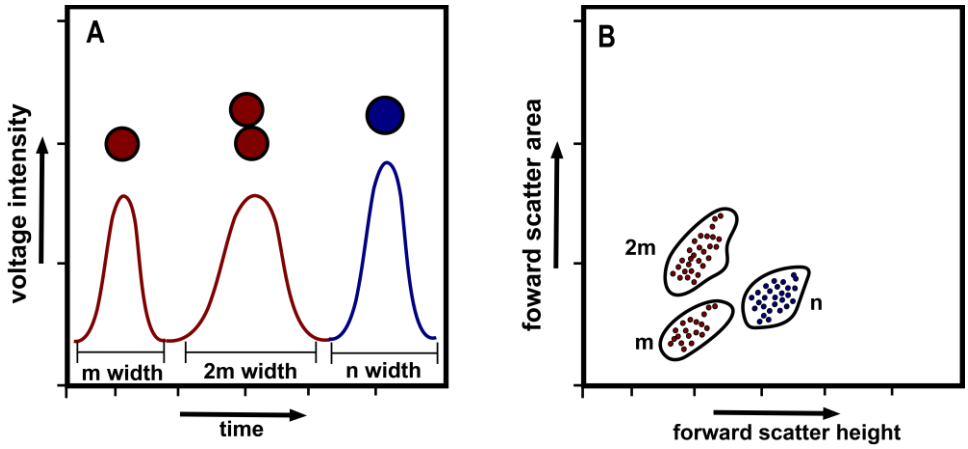

Figure 4-6. Graphical representation of how: (A) particles of type m (red) and other type n (blue) are interpreted at the detector (e.g., doublets (2m) have the same scatter height but double the area.) (B) dot plot displaying the distribution of particle according to their identities (m or n) aggregative state(s)

4.7 Effect of time and adhesive molar mass on removal efficiency

As discussed above, the molar mass is key to the performance of a pressure-sensitive adhesive. The softness required for a PSA to quickly wet a substrate is most conferrable at low molar mass (e.g., < 400 kg/mol), whereas high molar mass (e.g., > 500 kg/mol) is required for shear holding power and cohesion. For this reason, we comparatively investigated MPs removal using 4 PSAs with molecular weights spanning 92–950 kg/mol.

Polystyrene was selected as the model microplastic because it can be purchased as monodisperse spheres in multiple sizes. The dimensions of environmental microplastics typically range from 0.1–5000 μm, with smaller particles called nanoplastics. We selected 10 μm PS beads because they are close to the middle of the microplastics range. Moreover, as highlighted in Table 1, the %

polar for PS is also right in the middle of the range for the most common environmental microplastics. We also chose polystyrene because it can be purchased as monodisperse samples, making it easier to identify singlets and multiplets, and differentiate them from foreign particles in flow cytometry analysis. Clearly, there are other differences among these and other microplastics, including composition, particle size, shape, and potentially surface charge; however, PS serves as a good and commonly used model system.

To achieve uniform MPs suspensions for more accurate quantification, we added 20% ethanol to our formulations to reduce the surface tension of water.[17] The samples were hand-shaken for a specific amount of time (0.5, 1, 3, and 5 min) at 3 shakes per sec, and the suspensions were transferred into Eppendorf's tubes using an 18-gauge needle and syringe (3 mL) (Appendix 3, pgs. 191–193). Then the aliquots (1 mL) were analyzed using flow cytometry (Appendix 3, pg. 194). Removal efficiency (RE) was calculated by comparing the particle counts in the sample relative to the control (stock dispersion).

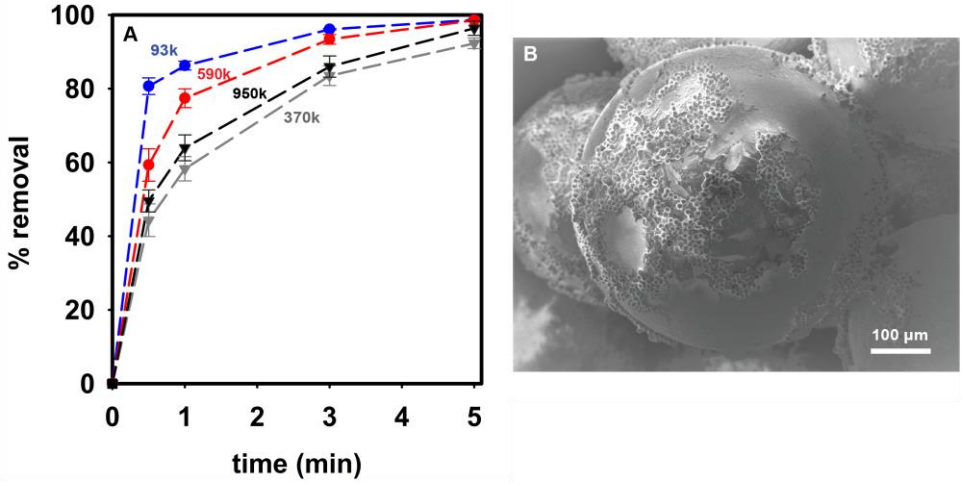

Figure 4-7. (A) Removal efficiency of PS microplastics versus time for P(2-EHA)-coated on beads with varying molar masses. (B) SEM image of $P(2\text{-EHA})_{P\&G\text{-}590k}$ coated beads after a 5 min exposure to the PS microplastic solution.

As highlighted in Figure 4-7, P(2-EHA)$_{\text{Sigma-93k}}$ reproducibly exhibited a remarkable RE at early time points (e.g., RE = 81% at 0.5 min), whereas the other adhesive ranged from 40–60%. The observed trend is likely due to the P(2-EHA)$_{\text{Sigma-93k}}$ superior tack properties conferred by its low molar mass. This result can be rationalized based on the adhesive's capacity to wet the microplastic surface quickly. Within 5 min, however, all adhesives showed > 92% removal efficiencies of the PS particles. There were no other apparent trends based on molar mass, indicating that above a certain threshold, the adhesives perform similarly. In some cases, we observed an additional particle grouping at sizes smaller than the PS particles. Flow cytometry experiments on the PS stock solutions only showed a small fraction of these particles. In contrast, the samples with the lowest molar mass (P(2-EHA)$_{\text{Sigma-93k}}$) showed the most signal in these smaller dimensions (Figure 4-8). We suspect that these signals arise from delaminated adhesive, which likely occurred during agitation.

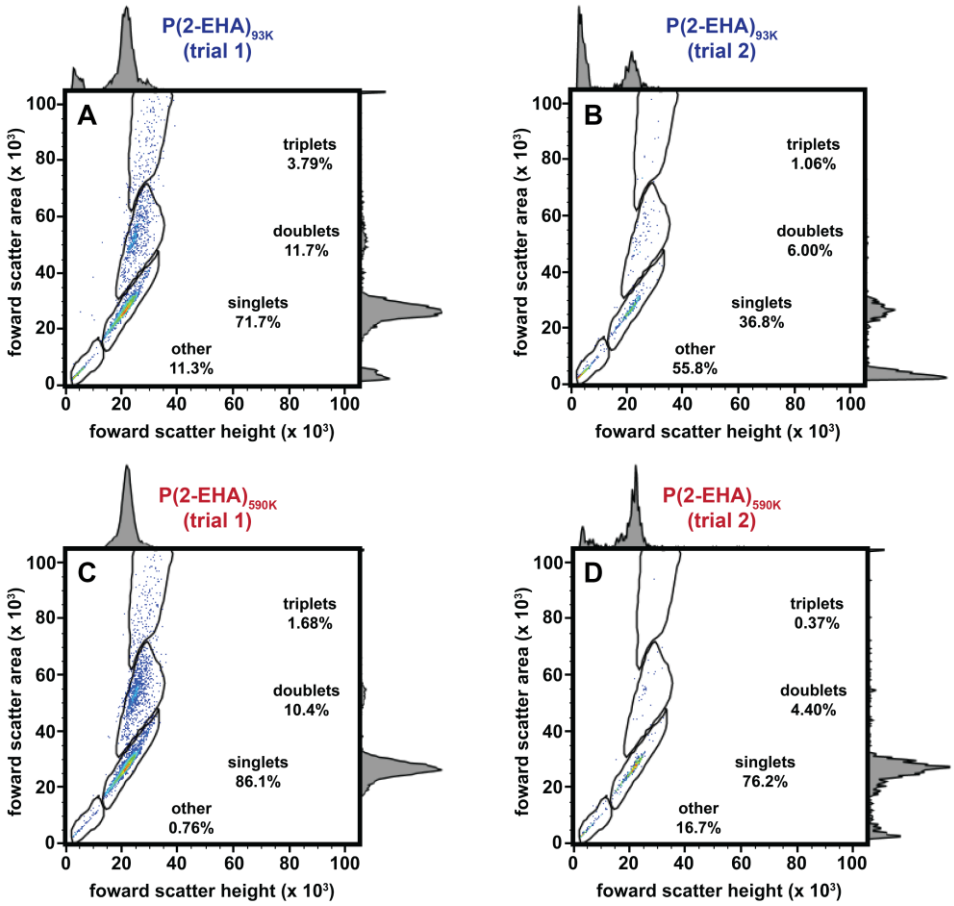

Figure 4-8. Flow cytometry data for capturing PS microplastics using P(2-EHA)$_{93K}$ (A and B) and P(2-EHA)$_{590K}$ (C and D) coated onto beads.

4.8 Conclusions

In summary, we fortuitously discovered that pressure-sensitive adhesives efficiently captured micronized rubber in a liquid waste container. We confirmed the result using other MPs types, including polystyrene, polyethylene terephthalate, and nylon. Intrigued by the preliminary results, we explored MPs removal efficiency using poly(2-ethylhexy acrylate) adhesives spanning 92–950 kg/mol coated onto zirconium silicate beads. The lowest molar mass adhesive, Sigma-93k, dominated MPs removal efficiency by removing 81% within 0.5 min, whereas the other adhesives removed 40–60%. Ultimately the removal efficiencies for P(2-EHA)$_{Sigma-93k}$, P(2-EHA)$_{P\&G-590k}$, P(2-EHA)$_{Sigma-370k}$, and P(2-EHA)$_{SPP-950k}$ were 99, 99, 92, and 96%, respectively. Although Sigma-

93k exhibited the best MPs removal kinetics, we suspect that P(2-EHA)$_{\text{Sigma-93k}}$ suffered adhesive peeling, which introduced new MPs. Although low molar mass improved MPs removal kinetics, adhesive peeling may occur due to lack of cohesion.

Future studies will expand on this work to include quantitative studies, alternative adhesive structures, and different microplastic substrates. Moreover, the complexities that arise when working with authentic environmental samples containing mixed microplastics, likely some with surface degradation,[22] along with salts, surfactants, and other natural particulates, need to be evaluated.

4.9 References

1 Rochman, C. M.; Browne, M. A.; Halpern, B. S.; Hentschel, B. T.; Hoh, E.; Karapanagioti, H. K.; Rios-Mendoza, L. M.; Takada, H.; Teh, S.; Thompson, R. C. Classify Plastic Waste as Hazardous. *Nature* **2013**, *494*, 169–171. https://doi.org/10.1038/494169a.

2 Woodall, L. C.; Sanchez-Vidal, A.; Canals, M.; Paterson, G. L. J.; Coppock, R.; Sleight, V.; Calafat, A.; Rogers, A. D.; Narayanaswamy, B. E.; Thompson, R. C. The Deep Sea Is a Major Sink for Microplastic Debris. *R. Soc. Open Sci.* **2014**, *1* (4), 140317. https://doi.org/10.1098/rsos.140317.

3 Nizzetto, L.; Futter, M.; Langaas, S. Are Agricultural Soils Dumps for Microplastics of Urban Origin? *Environ. Sci. Technol.* **2016**, *50* (20), 10777–10779. https://doi.org/10.1021/acs.est.6b04140.

4 Baensch-Baltruschat, B.; Kocher, B.; Stock, F.; Reifferscheid, G. Tyre and road wear particles (TRWP) – A review of generation, properties, emissions, human health risk, ecotoxicity, and fate in the environment. *Sci. Total Environ.* **2020**, *733*, 127823.

5 Knight, L. J.; Parker-Jurd, F. N. F.; Al-Sid-Cheikh, M.; Thompson, R. C. Tyre wear particles: an abundant yet widely unreported microplastic? *Environ. Sci. Pollut. Res.* **2020**, *27*, 18345–18354.

6 Zhang, Y.-Q.; Lykaki, M.; Alrajoula, M. T.; Markiewicz, M.; Kraas, C.; Kolbe, S.; Klinkhammer, K.; Rabe, M.; Klauer, R.; Bendt, E.; Stolte, S. Microplastics from textile origin – emission and reduction measures. *Green Chem.* **2021**, ASAP.

7 Belzagui, F.; Crespi, M.; Álvarez, A.; Gutiérrez-Bouzán, C.; Vilaseca, M. Microplastics' emissions: Microfibers' detachment from textile garments. *Environ. Pollut*. **2019**, *248*, 1028–1035.

8 Boucher, J.; Friot, D. *Primary microplastics in the oceans: a global evaluation of sources*. IUCN: Gland, Switzerland; 2017.

9 Crossman, J.; Hurley, R. R.; Futter, M.; Nizzetto, L. Transfer and Transport of Microplastics from Biosolids to Agricultural Soils and the Wider Environment. *Sci. Total Environ.* **2020**, *724*, 138334. https://doi.org/10.1016/j.scitotenv.2020.138334.

10 Phelan, M. American Association for the Advancement of Science. Science: Tiny Plastics Cause Big Problems for Marine Environments. https://www.aaas.org/news/science-tiny-plastics-cause-big-problems-marine-environments (accessed June 6, 2021).

11 https://coraball.com (accessed June 3, 2021).

12 https://guppyfriend.com (accessed June 3, 2021).

13 McIlwraith, H. K.; Lin, J.; Erdle, L. M.; Mallos, N.; Diamond, M. L.; Rochman, C. M. Capturing Microfibers – Marketed Technologies Reduce Microfiber Emissions from Washing Machines. *Mar. Pollut. Bull.* **2019**, *139*, 40–45. https://doi.org/10.1016/j.marpolbul.2018.12.012.

14 Zhang, Y.; Jiang, H.; Bian, K.; Wang, H.; Wang, C. A Critical Review of Control and Removal Strategies for Microplastics from Aquatic Environments. *J. Environ. Chem. Eng.* **2021**, *9* (4), 105463. https://doi.org/10.1016/j.jece.2021.105463.

15 Wang, Z.; Sedighi, M.; Lea-Langton, A. Filtration of Microplastic Spheres by Biochar: Removal Efficiency and Immobilisation Mechanisms. *Water Res.* **2020**, *184*, 116165. https://doi.org/10.1016/j.watres.2020.116165.

16 Sun, C.; Wang, Z.; Chen, L.; Li, F. Fabrication of Robust and Compressive Chitin and Graphene Oxide Sponges for Removal of Microplastics with Different Functional Groups. *Chem. Eng. J.* **2020**, *393*, 124796. https://doi.org/10.1016/j.cej.2020.124796.

17 Chen, Y.-J.; Chen, Y.; Miao, C.; Wang, Y.-R.; Gao, G.-K.; Yang, R.-X.; Zhu, H.-J.; Wang, J.-H.; Li, S.-L.; Lan, Y.-Q. Metal–Organic Framework-Based Foams for Efficient Microplastics Removal. *J. Mater. Chem. A* **2020**, *8* (29), 14644–14652. https://doi.org/10.1039/D0TA04891G.

18 U-M Group Gets $2 Million NSF Grant for Turning Diapers into Devices to Capture Microplastics. https://news.umich.edu/u-m-group-gets-2-million-nsf-grant-for-turning-diapers-into-devices-to-capture-microplastics/ (accessed June 7, 2021).

19 Sinha, B. Pressure sensitive adhesives market by chemical composition (acrylic, rubber, ethylene vinyl acetate (EVA), silicone, polyurethane, and others), type (water based, hot melts, solvent based, and radiation based), application (labels, medical, graphics, tapes, and others) and end-use industry (automotive, packaging, building & construction, electronics, medical, consumer goods, and others) - global opportunity analysis and industry forecast, 2017–2023. https://www.alliedmarketresearch.com/pressure-sensitive-adhesives-market (accessed June 10, 2021).

20 Creton, C. Pressure-Sensitive Adhesives: An Introductory Course. *MRS Bull.* **2003**, *28*, 434–439. https://doi.org/10.1557/mrs2003.124

21 KRUSS Scientific. Dispersive part. https://www.kruss-scientific.com/en-US/know-how/glossary/dispersive-part (accessed June 10, 2021)

22 Min, K.; Cuiffi, J. D.; Mathers, R. T. Ranking Environmental Degradation Trends of Plastic Marine Debris Based on Physical Properties and Molecular Structure. *Nat. Commun.* **2020**, *11* (1), 727. https://doi.org/10.1038/s41467-020-14538-z.

23 Kowalski, A.; Czech, Z.; Byczyński, Ł. How does the Surface Free Energy Influence the Tack of Acrylic Pressure-Sensitive Adhesives (PSAs). *J. Coat. Technol. Res.*, **2013**, 10, 879-885. https://doi.org/10.1007/s11998-013-9522-2.

24 Ren, Z.; Chen, G.; Wei, Z.; Sang, L.; Qi, M. Hemocompatibility evaluation of polyurethane film with surface-grafted poly(ethylene glycol) and carboxymethyl-chitosan. *J. Appl. Polym. Sci*. **2013**, *127*, 308–315.

25 Sumita, M.; Sakata, K.; Asai, S.; Miyasaka, K.; Nakagawa, H. Dispersion of fillers and the electrical conductivity of polymer blends filled with carbon black. *Polym. Bull.* **1991**, 265–271.

26 Elias, L.; Fenouillot, F.; Majeste, J. C.; Cassagnau, Ph. Morphology and rheology of immiscible polymer blends filled with silica nanoparticles. *Polymer* **2007**, *48*, 6029–6040.

27 Ansarifar, A; Critchlow, G. W.; Guo, R.; Ellis, R. J.; Kirtley, S. P.; Seymour, B. Effect of rubber chemicals on the surface free energy of NR and NR-SBR rubber blends. *J. Rubb. Res.* **2007**, *10*, 143–155.

28 Gonzalez, E.; Barankin, M. D.; Guschl, P. C.; Hicks, R. F. Remote atmospheric-pressure plasma activation of the surfaces of polyethylene terephthalate and polyethylene naphthalate. *Langmuir* **2008**, *24*, 12636–12643.

29 Wu, S. In *Polymer Handbook, 4th Ed.*; Brandrup, J., Immergut, E.H., Grulke, E.A. eds.; John Wiley & Sons: Hoboken, NJ, 2003, p. VI: 521–535.

30 Zhang, Q.; Qu, Q.; Lu, T.; Ke, M.; Zhu, Y.; Zhang, M.; Zhang, Z.; Du, B.; Pan, X.; Sun, L.; et al. The Combined Toxicity Effect of Nanoplastics and Glyphosate on Microcystis Aeruginosa Growth. *Environ. Pollut.* **2018**, *243*, 1106–1112. https://doi.org/10.1016/j.envpol.2018.09.073.

31 Mitzel, M. R.; Sand, S.; Whalen, J. K.; Tufenkji, N. Hydrophobicity of Biofilm Coatings Influences the Transport Dynamics of Polystyrene Nanoparticles in Biofilm-Coated Sand. *Water Res.* **2016**, *92*, 113–120. https://doi.org/10.1016/j.watres.2016.01.026.

32 Chemistry LibreTexts. 2021. Raja, P. M. V; Barron, A. R. UV-Visible Spectroscopy. https://chem.libretexts.org/@go/page/55881 (accessed June 13, 2021).

33 Bio-Rad. Hemocytometer vs. Automated Cell Counter. https://www.bio-rad.com/featured/en/hemocytometer.html (accessed June 14, 2021).

34 Jaroszeski, M. J.; Radcliff, G. Fundamentals of Flow Cytometry. *Mol. Biotechnol.* **1999**, *11*, 37–53. https://doi.org/10.1007/BF02789175.

35 Colson, B. C.; Michel, A. P. M. Flow-Through Quantification of Microplastics Using Impedance Spectroscopy. *ACS Sensors* **2021**, *6*, 238–244. https://doi.org/10.1021/acssensors.0c02223.

36 Kaile, N.; Lindivat, M.; Elio, J.; Thuestad, G.; Crowley, Q. G.; Hoell, I. A. Preliminary Results From Detection of Microplastics in Liquid Samples Using Flow Cytometry. *Front. Mar. Sci.* **2020**, *7*. https://doi.org/10.3389/fmars.2020.552688.

Chapter 5: Conclusions and Future Directions

Since the inception of their mass production during WWII, the global annual production of synthetic polymers, also known as plastics, has risen from less than 2 million to approximately 368 million metric tons.[1] The desirable superior performance properties (e.g., impermeability, high strength/mass ratio, and durability) of plastics are responsible for the sustained increase in their global market and, unfortunately, their biopersistence as well. [2,3] Despite the problematic consequences to the environment (e.g., petroleum depletion and pollution), these plastics have become so integral to human life that, though possible, existing without them is inconceivable.

Procter and Gamble (P&G) tasked us to develop methods to recycle the acrylic-based superabsorbent polymer ($PAA_{P\&G}$) used in their disposable diapers as an alternative to allowing them to meet their current fate (primarily incineration and landfilling). Like most plastics, acrylic-based superabsorbents can persist in the environment for centuries, if not incinerated.

Chapter 2 considered potential recycling methods, including depolymerization to monomer via thermal unzipping or catalytic pathways (closed-loop recycling) and recycling into another consumer polymer (open-loop recycling).[4] However, because the decarboxylation of side groups outcompetes backbone depropagation, efficient thermal unzipping methods are unavailable for poly(acrylic acid).[5,6] Though appealing, copper-catalyzed depolymerization pathways presented by Li[7] and Lloyd et al.[8] would not work on $PAA_{P\&G}$ due to catalyst poisoning by carboxylic acid groups. Also, these pathways require living free radical chain ends on the polymer, which is atypical in commercial polymers.

The common acrylic acid origin of $PAA_{P\&G}$ and PSAs inspired our open-loop recycling solution, which comprised of (i) decrosslinking via alkaline hydrolysis to make water-soluble polymers (ii) optional chain-shortening via sonication to a lower molar mass, and (iii) functionalizing via base-mediated esterification to generate tack. Furthermore, because chain entanglements are critical to PSA performance and application, we postulated a spectrum of PSA applications that could be achieved by altering molar mass and incorporating polar functional groups (i.e., amines). Indeed, chain-shortened $PAA_{P\&G}$ yielded softer PSAs in the 3rd quadrant of the Chang viscoelastic window, whereas unshortened $PAA_{P\&G}$ yielded a more elastic central region PSA. Similarly, the chain-shortened $PAA_{P\&G}$ esterified with amine groups yielded an elastic PSA within the upper region of the central window.

An unbiased comparative assessment is necessary to evaluate conventional approaches' processing and environmental implications for any new recycling methodology developed. Fagnani et al. performed a survey of publications on "sustainable polymers" since 1990 and noted that less than 5% either mentioned or performed a life cycle assessment. Inspired by this perspective, in Chapter 3, we aimed to evaluate and optimize the 3-step recycling method presented above with the assistance of the LCA methodology performed in collaboration with Madeline Somers (Alfaro lab).[9] Overall, the key improvements were (i) substituting the alkaline hydrolysis with acid hydrolysis and (ii) substituting the base-mediated esterification with acid-catalyzed esterification.

On the hydrolysis step, by performing a cradle-to-gate LCA to compare using sodium hydroxide versus sulfuric acid, we noted that sulfuric acid outperformed sodium hydroxide by a factor of 10 in both cumulative energy demand and global warming potential. Next, we compared base-mediated esterification with acid-catalyzed esterification, which is the primary method used in

industry. Reviewing reagent costs using a Fisher scientific quote (Appendix 2, Table A2-1), we noted that 2-ethyl hexanol, which serves as a reagent and solvent in acid-catalyzed esterification, only cost $12/L. In contrast, the reagents used in the base mediated process were relatively expensive (e.g., dimethylsulfoxide = $47/L and 2-ethylhexyl bromide = $222/kg).

Although the inexpensiveness of acid-catalyzed esterification is attractive, the process can lead to low yields due to the competing ester hydrolysis pathway and catalyst deactivation by the water by-product. [10,11] While selective removal of water or use of excess alcohol can circumvent the problem, we postulated that the hydrophobicity of 2-ethyl hexanol and the polymer backbone would result in phase separation, thereby eliminating the need to remove water actively. This hypothesis was confirmed by performing polymer and small molecule experiments and atomistic simulations to probe the effect of water on the acid-catalyzed esterification.

The PSAs synthesized via acid-catalyzed esterification of chain-shortened and unchain-shortened PAA spanned the 3rd quadrant and central region of the viscoelastic windows, which suggested applications in removable (e.g., sticky notes) and general-purpose adhesives (i.e., bandages), respectively. In our cradle-to-product LCA evaluation of the conventional industrial route versus the three variations of the recycling process, we noted that the recycling process outperformed the industrial route in cumulative energy demand (up to 24.8%) and global warming potential (up to 21.5%).

We also explored performing $PAA_{P\&G}$ open-loop recycling to make PSAs in one pot (Appendix 2, pgs. 167–170).[12] Doing a one-pot reaction can result in economic and environmental benefits. Because acid hydrolysis and acid-catalyzed esterification are similar reactions, we hypothesized a one-pot methodology for decrosslinking and functionalizing $PAA_{P\&G}$ to make PSAs.

We initially tested esterifying $PAA_{P\&G}$ with 2-ethylhexanol (8 equiv) and sulfuric acid (2 equiv) at 130 °C, but the reaction gradually turned black (Figure 5-1 b, left). We suspected that the oxidation of reagents by sulfuric acid was responsible for observed color change. When purging the reaction with nitrogen did not rid the suspected oxidation side reactions, we hypothesized that the crystalline and oleophobic state of $PAA_{P\&G}$ impeded 2-ethylhexanol from penetrating. Therefore, in addition to purging with nitrogen, we added ethanol (2 equiv), and we achieved the one-pot synthesis of PSA within 24 h.

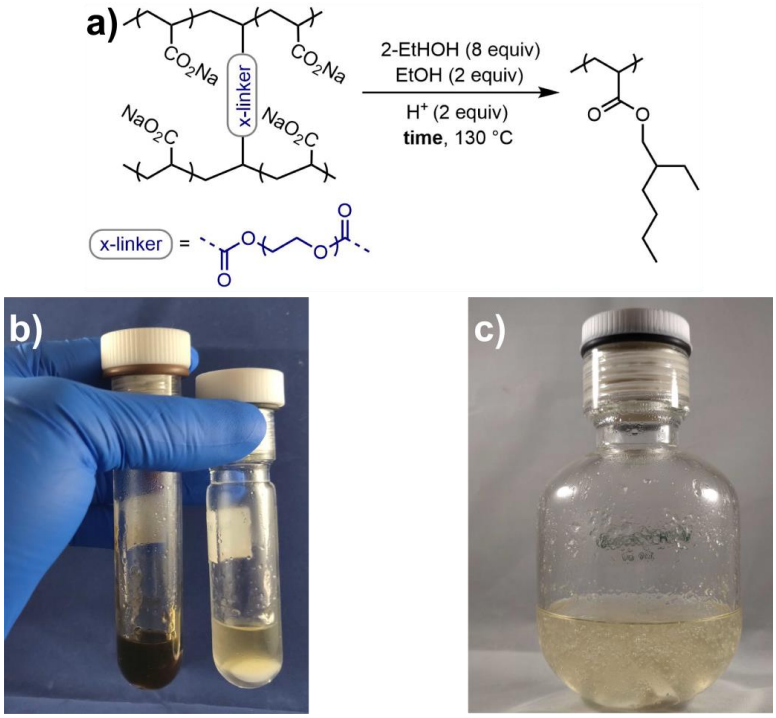

Figure 5-1. One-pot esterification of $PAA_{P\&G}$ to make PSAs. a) Chemical equation for the one-pot esterification method. b) Visual comparing esterifying in the absence (left) versus in the presence (right) of nitrogen and ethanol. c) A scaled-up reaction esterifying 2500 mg of $PAA_{P\&G}$ to make PSAs.

The developed one-pot method was further tested by evaluating the adhesive product's viscoelastic properties (i.e., G′ and G″ as a function of frequency) at different reaction time points (i.e., 9, 15, 21, and 25 h). All the adhesive products resided in the central portion of Chang's viscoelastic window, and we observed no significant changes in the viscoelastic properties after

15 h of esterifying (Figure 5-2). The presented preliminary results for one-pot esterification are another critical step towards industrial pertinence. What remains is to perform further optimizations guided by a life cycle assessment.

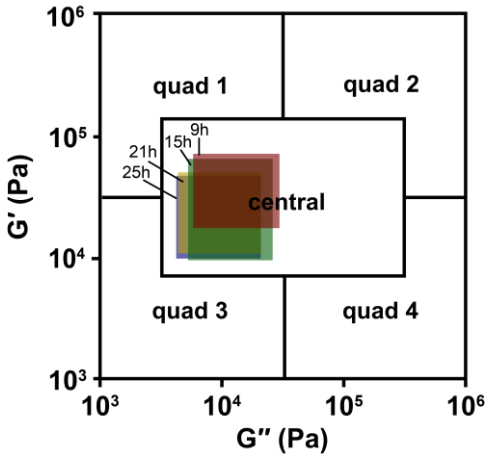

Figure 5-2. Plots of storage (G′) versus loss (G″) moduli for esterifying $PAA_{P\&G}$ to make adhesives in one-pot, including visualization of Chang's viscoelastic window.

While developing the recycling process described above, we fortuitously discovered that the PSAs synthesized from recycled $PAA_{P\&G}$ captured micronized rubber, a ubiquitous microplastics (MPs) type, in a solvent waste container. MPs have become a global concern due to their ubiquity, health effects[13,14] and biopersistence.

In chapter 4, we first confirmed the accidental discovery by capturing other MPs in deionized water including, polyethylene terephthalate, polystyrene, and nylon. Because molar mass is key to the performance of any PSA, we next evaluated the effect of molar mass on MPs removal using 4 PSAs (Sigma-93k, P&G-590k, Sigma-370k, and SPP-950k) coated onto zirconium silicate beads. We successfully used the flow cytometry to quantify removal efficiency for monodisperse 10 μm polystyrene (PS) spherical particles. As we had hypothesized, the tackier low molar mass Sigma-93k kinetically outperformed all the other PSAs by removing 81% within the 30s compared to the other adhesives that only removed 40–60%.

At 5min, the removal efficiencies for Sigma-93k, P&G-590k, Sigma-370k, and SPP-950k were 99, 99, 92, and 96%, respectively. Because we prepared P&G-590k and Sigma-370k differently, we believe that structural differences (e.g., branching) or residual carboxylic acids caused the discrepancy in MPs removal. In addition, although Sigma-93k dominated in removal efficiency kinetics, the adhesive's rating was compromised by its poor cohesion and shear holding strength, which manifested peeling from the substrate, thereby introducing new particulates.

In addition to exploring the effect of PSA molar mass on MPs removal, various PSA chemical structures should be explored next (Scheme 5-1). As highlighted in chapter 4, surface energy (γ) plays a crucial role in MPs capture underwater. More specifically, stronger adhesion between a PSA and a substrate is achieved when polar (γ^p) and dispersive (γ^d) components ratio ($\frac{\gamma^d}{\gamma^p}$) of surface energy are similar between the two materials.[15] In support of this hypothesis, though not directly stated, Messersmith[16] and Ahn[17] demonstrated that poly(2-ethylhexyl acrylate co benzyl acrylate) copolymer exhibited improved adhesion to a steel substrate underwater. An increase in the polar component conferred by the incorporated benzyl groups likely improved adhesion, thereby making the $\frac{\gamma^d}{\gamma^p}$ between the steel and PSA more comparable. This concept can also be used to improve the interactions between the adhesive and substrates (e.g., zirconium silicate) used to capture MPs, which will most likely reduce adhesive peeling – even for the low molar mass PSAs (e.g., < 400 kg/mol). Recently, Woojung Ji (post-doctoral fellow in the McNeil group), who is continuing the project, successfully used the esterification method developed in chapter 3 to synthesize poly(2-ethylhexyl acrylate) copolymers with other functionalities incorporated (e.g., benzyl, per-fluoro, and polyethylene oxide)

Scheme 5-1. Synthesizing pressure-sensitive adhesives with targeted surface energy parameters using acid-catalyzed esterification.

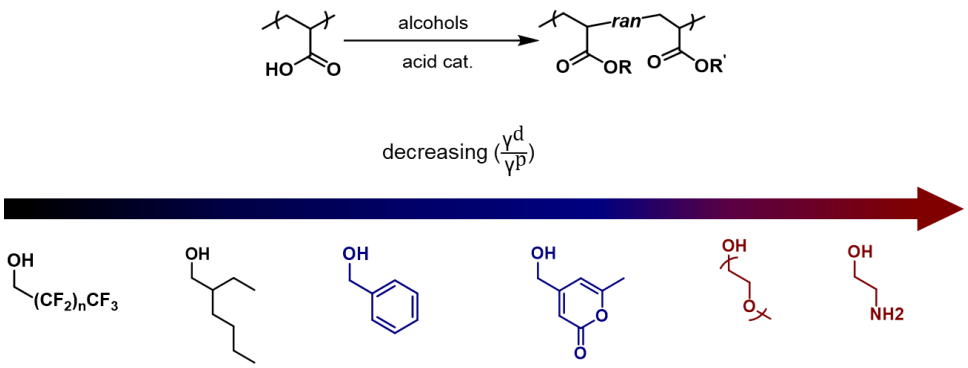

Preliminary studies also explored MPs removal in surfactant (i.e., sodium dodecyl sulfate) with concentrations spanning 0.01–0.1% w/v (Appendix 3, pgs. 219–220). The MPs removal efficiency was evaluated based on MPs coverage on the glass slides, which were analyzed using optical microscopy (Figure 5-3). The results suggested that MPs removal is not negatively affected by sodium dodecyl sulfate (SDS). In fact, adding surfactant actually increased MPs coverage by over 50%. Although the removal of PS MPs in the presence of surfactant is evident, this experiment should be repeated in more replications to confirm the improved MPs removal. Plasticization of the adhesive surface by the small surfactant molecules, which improves tack, is a potential explanation if SDS truly enhances MPs removal efficiency. This hypothesis can be confirmed by running the same experiment using a polymeric surfactant (e.g., high molar mass polyvinyl alcohol), less likely to act as a plasticizer.

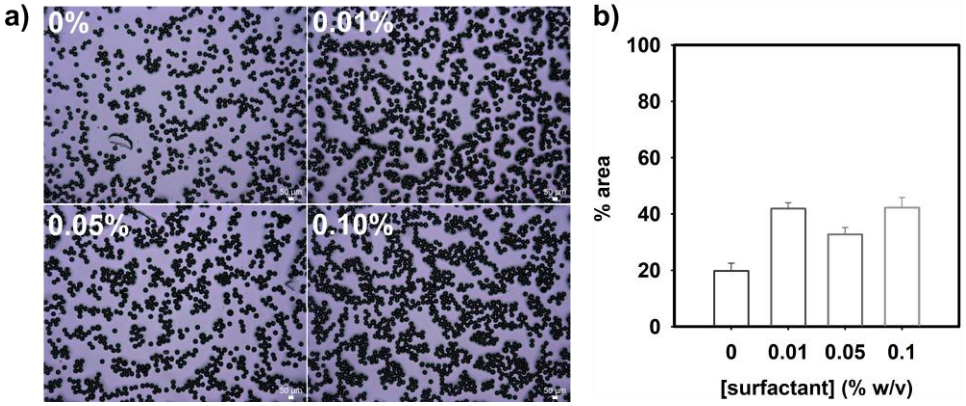

Figure 5-3. Preliminary results on the effect of surfactant (sodium dodecyl sulfate) concentration on MPs (40 μm PS) removal. a) Optical microscopic images showing MPs removal at various SDS concentrations. b) Bar graph showing percent are coverage calculated using ImageJ software.

Briefly, this thesis first describes an open-loop recycling method to make pressure-sensitive adhesives (PSAs) from post-consumer superabsorbent polymer ($PAA_{P\&G}$). Guided by life cycle assessment, we developed an improved $PAA_{P\&G}$-to-PSAs recycling method which outperformed the conventional petroleum-based route to make PSAs. Serendipitously, we discovered that the pressure-sensitive adhesives we developed were effective at removing MPs from aqueous environments. We demonstrated that poly(2-ethylhexyl acrylate) adhesive-coated substrates efficiently remove both polar and nonpolar microplastics from aqueous solutions.

5.1 References

1 https://www.statista.com/statistics/282732/global-production-of-plastics-since-1950 (Accessed Apr 6, 2020).

2 Hong, M.; Chen, E. Y.-X. Chemically Recyclable Polymers: A Circular Economy Approach to Sustainability. *Green Chem.* **2017**, *19*, 3692–3706. https://doi.org/10.1039/C7GC01496A.

3 Barnes, D. K. A.; Galgani, F.; Thompson, R. C.; Barlaz, M. Accumulation and Fragmentation of Plastic Debris in Global Environments. *Philos. Trans. R. Soc. B Biol. Sci.* **2009**, *364*, 1985–1998. https://doi.org/10.1098/rstb.2008.0205.

4 Ellen MacArthur Foundation. The new plastics economy: rethinking the future of plastics & catalyzing action. Ellen MacArthur Foundation, 2017. https://www.ellenmacarthurfoundation.org/publications/the-new-plastics-economy-rethinking-the-future-of-plastics-catalysing-action (accessed on Apr 6, 2021).

5 Lépine, L.; Gilbert, R. Thermal Degradation of Polyacrylic Acid in Dilute Aqueous Solution. *Polym. Degrad. Stab.* **2002**, *75*, 337–345. https://doi.org/10.1016/S0141-3910(01)00236-1.

6 McNeill, I. C.; Sadeghi, S. M. T. Thermal Stability and Degradation Mechanisms of Poly(Acrylic Acid) and Its Salts: Part 1-Poly(Acrylic Acid). *Polym. Degrad. Stab.* **1990**, *29*, 233–246. https://doi.org/10.1016/0141-3910(90)90034-5.

7 Li, L.; Shu, X.; Zhu, J. Low Temperature Depolymerization from a Copper-Based Aqueous Vinyl Polymerization System. *Polymer (Guildf).* **2012**, *53*, 5010–5015.

8 Lloyd, D. J.; Nikolaou, V.; Collins, J.; Waldron, C.; Anastasaki, A.; Bassett, S. P.; Howdle, S. M.; Blanazs, A.; Wilson, P.; Kempe, K.; et al. Controlled Aqueous Polymerization of Acrylamides and Acrylates and "in Situ" Depolymerization in the Presence of Dissolved CO2. *Chem Commun* **2016**, *52* (39), 6533–6536. https://doi.org/10.1039/c6cc03027k.

9 Fagnani, D. E.; Tami, J. L.; Copley, G.; Clemons, M. N.; Getzler, Y. D. Y. L.; McNeil, A. J. 100th Anniversary of Macromolecular Science Viewpoint: Redefining Sustainable Polymers. *ACS Macro Lett.* **2021**, *10*, 41–53.

10 Carlyle, R. L. Process for the Production of Acrylic Acid Esters. U.S. Patent 2,917,538, December 15, 1959.

11 Alarifi, A. S.; Aouak, T. Synthesis of Acrylic or Methacrylic Acid/Acrylate or Methacrylate Ester Polymers Using Pervaporation. US Patent 9,321,868 B2, April 26, 2016.

12 Hayashi, Y. Pot Economy and One-Pot Synthesis. *Chem. Sci.* **2016**, *7* (2), 866–880. https://doi.org/10.1039/C5SC02913A.

13 Pauly, J. L.; Stegmeier, S.J.; Allaart, H. A.; Cheney, R. T.; Zhang, P. J.; Mayer, A. G.; Streck, R. J. Inhaled Cellulosic and Plastic Fibers Found in Human Lung Tissue. *Cancer Epidemiology, Biomarkers & Prevention*. **1998**, *7*, 419–428.

14 Deng, Y.; Zhang, Y.; Lemos, B.; Ren, H. Tissue Accumulation of Microplastics in Mice and Biomarker Responses Suggest Widespread Health Risks of Exposure. *Sci. Rep.* **2017**, 46687. https://doi.org/10.1038/srep46687.

15 KRUSS Scientific. Dispersive part. https://www.kruss-scientific.com/en-US/know-how/glossary/dispersive-part (accessed June 10, 2021)

16 Tiu, B. D. B.; Delparastan, P.; Ney, M. R.; Gerst, M.; Messersmith, P. B. Enhanced Adhesion and Cohesion of Bioinspired Dry/Wet Pressure-Sensitive Adhesives. *ACS Appl. Mater. Interfaces* **2019**, *11* (31), 28296–28306. https://doi.org/10.1021/acsami.9b08429.

17 Clancy, S. K.; Sodano, A.; Cunningham, D. J.; Huang, S. S.; Zalicki, P. J.; Shin, S.; Ahn, B. K. Marine Bioinspired Underwater Contact Adhesion. *Biomacromolecules* **2016**, *17* (5), 1869–1874. https://doi.org/10.1021/acs.biomac.6b00300.

Appendices

Appendix 1: Supporting Information for Chapter 2. Repurposing Acrylic-Based Absorbents via Post-Polymerization Modifications Part I.

Materials

All chemicals were used as received unless otherwise mentioned. Dowex® Marathon™ MSC hydrogen form (23–27 μm), *p*-toluenesulfonic acid (*p*-TsOH), 2-ethylhexyl bromide (2-EHBr), dimethyl sulfoxide (DMSO), 2-(Boc-amino)ethyl bromide (2-BAEB), tetramethylguanidine (TMG), sodium hydroxide, and sodium nitrate were purchased from Millipore Sigma. Methanol (MeOH) and sodium chloride were purchased from Fisher Scientific. Tetrahydrofuran (THF) was purchased from OmniSolv. Glacial acetic acid was purchased from Acros Organics. Sodium polyacrylate based crosslinked superabsorbent polymer ($PAA_{P\&G}$) (get more specifications from P&G) was provided by Procter & Gamble. Sonicated polymer fragments were dialyzed in deionized (DI) water (dripping from the lab faucet at approximately 3.5 L/h) using Spectra/Por molecular porous membrane tubing (molecular weight cut-off: 3.5 kg/mol).

General Experimental and Instrumentation

Sonication – Sonication was performed at 100% amplitude (amp) using a Sonics and Materials Vibra-cell VCX 600 Ultrasonic Liquid Processor equipped with a 13 mm replaceable tip probe. Polymer solutions were placed in a jacketed beaker with 3.5 cm internal diameter during jacket and monitored using a thermocouple inserted into the polymer solution.

NMR Spectroscopy – Unless otherwise noted, ^{1}H NMR spectra for all compounds were acquired at room temperature. Chemical shift data are reported in units of δ (ppm) relative to tetramethylsilane (TMS) and referenced with residual solvent. Multiplicities are reported as follows: singlet (s), doublet (d), doublet of doublets (dd), triplet (t), quartet (q), multiplet (m), broad resonance (br). Residual water is denoted by an asterisk (*).

Gel-Permeation Chromatography (GPC) for sonicated PAA_{750} and $PAA_{P\&G}$ – Polymer molecular weights were determined by comparison with PEG/PEO EasiVial standards from Agilent at 40 °C in 0.1 M $NaNO_3$ (aq) on a Waters GPC equipped with 120 (part#: WAT011565), 250 (part#: WAT011525), 500 (part#: WAT011530) and 1000 (part#: WAT011535) Ultrahydrogel columns (with Waters 1515 Isocratic HPLC pump, 717plus autosampler, RI detector Model 214 and UV-PDA detector Model 487). Peaks are normalized to the polymer peak, when traces are presented in series, the normalized peaks are offset vertically.

GPC for polyacrylate based PSAs (pressure sensitive adhesives) – Polymer molecular weights were determined by comparison with polystyrene standards (1,000,000, 675,000, 115,000, 68,000, 7,600 and 1,050 g/mol from Polymer Laboratories, Ltd.; 20,000 and 4,000 g/mol from PolySciences, Inc.; 44,000 g/mol from Millipore Sigma) at 40 °C in THF on a Shimadzu GPC (Shimadzu LC-20AD HPLC pump, SIL-20AC autosampler, RID-10A RI detector and SPD-M20A UV-PDA detector) equipped with a Phenogel 10 μm Linear(2) column (part#: 00H-3260-K0).

Rheological measurements on PSAs – Rheological measurements were taken on an AR2000ex rheometer (TA Instruments) with a 25 mm serrated parallel plate. Samples were loaded at 1,250 μm layer thickness and measurements were taken at 25 °C. The frequency sweep was performed between 0.1 and 100 Hz and performed in duplicate.

Sonicated PAA and $PAA_{P\&G}$ GPC sample preparation – Sonicated $PAA_{P\&G}$ was dialyzed overnight in DI water to remove NaOH. The PAA_{750} and $PAA_{P\&G}$ fragments were then diluted with 0.1 M $NaNO_3$ (aq) /ethylene glycol (99:1 v/v) and filtered through a Titan3™ Nylon syringe filter (0.45 μm) into a GPC vial.

General PSA work-up for GPC – Esterifications were quenched using glacial acetic acid and the polymer was precipitated using MeOH. The polymer was purified by dissolving in THF with mild heating and then redissolved (~1 mg/mL polymer) in THF/toluene (99:1 v/v) with mild heating and filtered through a PTFE filter (0.2 μm) into a GPC vial.

General sonication procedure – Polymer solution was added to a jacketed beaker (3.5 cm inner diameter, 9 cm height) equipped with a stir bar. Cold water (10–15 °C) was flowed through the jacket while stirring the polymer solution at 500 rpm. A thermocouple was immersed into the polymer solution to monitor temperature. The power into the polymer solution was monitored using the meter on the ultrasound unit. The ultrasound unit was set to 100% amp and the polymer solution was sonicated for the indicated time.

Rheology – Rheological measurements were taken on an AR2000ex rheometer (TA Instruments) with a 25 mm serrated parallel plate. PSA (~650 mg) was loaded to achieve a 1,250 μm layer thickness and measurements were taken at 25 °C. The frequency sweeps were performed between 0.1 and 100 Hz.

Evaluating polymer recovery and chemical structure after sonication

Three batches of 0.50% w/v PAA solution were prepared by dissolving PAA_{SPP} (750 kg/mol, 250 mg, 3.47 mmol) with DI H_2O (50.0 mL each) in jacketed beakers equipped with stir bars. The PAA solutions were stirred at 300 rpm for 15 h at rt. Then, the PAA solutions were sonicated for 20 min. Next, the polymer solutions were concentrated under reduced pressure to dryness, spiked with a known amount of DMSO (1.14, 1.16, and 1.09 mmol, respectively) and redissolved with D_2O for quantitative ^{1}H-NMR spectroscopic analysis. An average recovery of 87% was determined based on relative integrations.

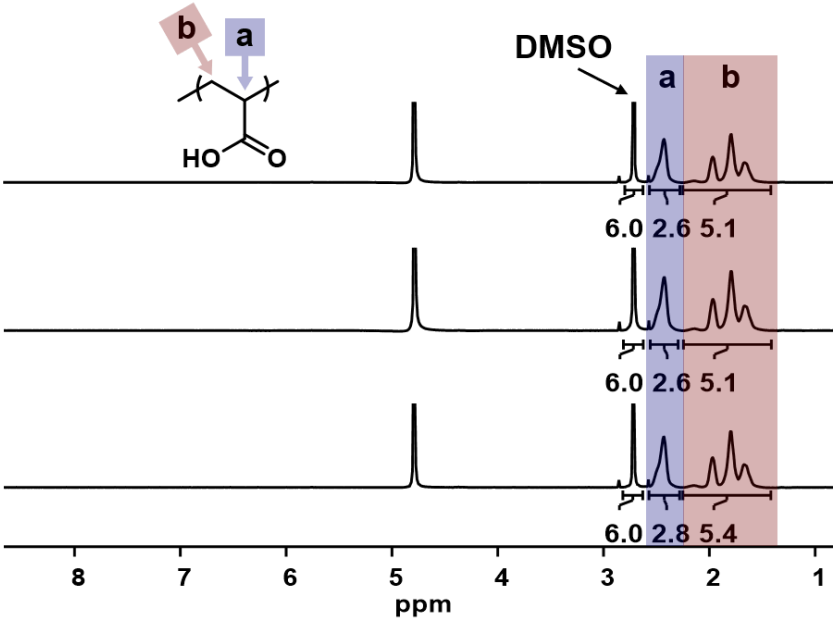

Figure A1-1. ^{1}H NMR spectra of sonicated PAA_{SPP} spiked with known amounts of DMSO (500 MHz, H_2O).

Table A1-1. Average recovery after sonication determined from three trials based on amount of DMSO (mmol), normalized integration for peak a (I_a), mass of polymer sonicated (250 mg), and molar mass of PAA repeat unit (72.06 g/mol).

trial	**DMSO (mmol)**	I_a	**recovery (%)**
1	1.14	2.6	85
2	1.16	2.6	87
3	1.09	2.8	88
avg			87

$$\text{recovery (\%)} = \frac{\text{DMSO(mmol)} \times I_a \times 72.06 \frac{\text{g}}{\text{mol}}}{250 \text{ mg}} \times 100 \qquad (2)$$

Effect of time and concentration on sonicating of PAA_{SPP}

Duplicate batches of PAA_{SPP} solution (0.50, 1.0, and 2.5% w/v) were prepared by dissolving PAA (250, 500, and 1250 mg) with DI H_2O (50.0 mL each) in jacketed beakers equipped with stir bars. NaCl (100 mg, 1.71 mmol) was added to the 1% and 2.5% w/v solutions to lower the solution viscosity. The PAA solutions were stirred at 300 rpm for 15 h at rt.

The 5.0% w/v sample was dissolved differently due to the need for more vigorous stirring. While stirring with a large stir bar, PAA_{SPP} (7500 mg) was slowly added to a 500 mL glass bottle with DI H_2O (150 mL). NaCl (300 mg, 5.13 mmol) was added to lower the solution viscosity. The PAA solutions were stirred at 300 rpm for 24 h at rt. Thereafter, portions of this solution (50 mL) were transferred to jacketed beakers.

The PAA solutions were sonicated for 20 min while collecting 0.50–1.0 mL aliquots at 1, 2, 5, 10, 15, and 20 min. The aliquots were diluted (to 1–1.5 mg/mL) with 0.1 M $NaNO_3$ (aq)/ethylene glycol (99:1 v/v) and analyzed via SEC.

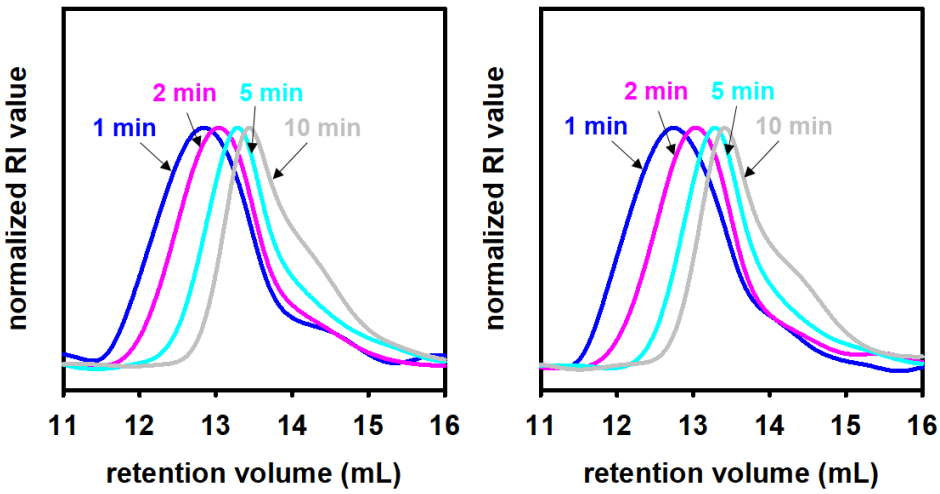

Figure A1-2. SEC traces for sonications of PAA_{SPP} at 0.50% w/v.

Table A1-2. Maximum power (P_{max}) consumed during sonication for PAA_{SPP} at 0.50% w/v.

[PAA] (w/v %)	**mass (mg)**	**mmol**	**run 1** P_{max} (W)	**run 2** P_{max} (W)
0.5	0.25	3.47	220	230

Maximum specific energy (w_{max}) values were determined using equation 1 (pg S3).

Table A1-3. Weight average molecular weight (M_w), dispersity (Đ), and specific energy (w_{max}) data for sonications of PAA_{SPP} at 0.50% w/v.

time (min)	**run 1**			**run 2**		
	M_w (kg/mol)	**Đ**	w_{max}	M_w (kg/mol)	**Đ**	w_{max}
1	320	2.2	53	291	2	55
2	210	1.6	110	210	1.7	110
5	130	1.4	260	123	1.6	280
10	93	1.4	530	86	1.5	550

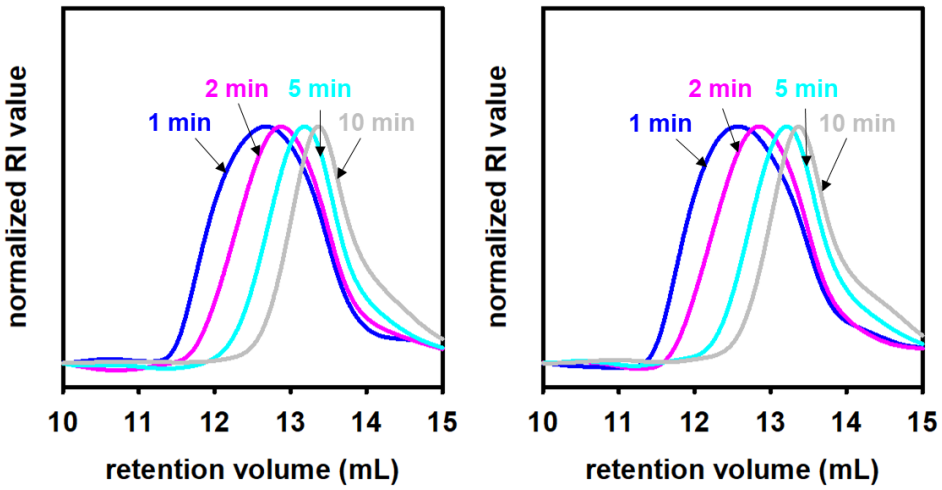

Figure A1-3. SEC traces for sonications of PAA_{SPP} at 1.0% w/v.

Table A1-4. Maximum power (P_{max}) consumed during sonication for PAA_{SPP} at 1.0% w/v.

[PAA] (w/v %)	**mass (mg)**	**mmol**	**run 1** P_{max} (W)	**run 2** P_{max} (W)
1	500	6.94	240	240

Maximum specific energy (w_{max}) values were determined using equation 1 (pg S3).

Table A1-5. Weight average molecular weight (M_w), dispersity (Đ), and specific energy (w_{max}) data for sonications of PAA_{SPP} at 1.0% w/v.

time (min)	**run 1**			**run 2**		
	M_w (kg/mol)	**Đ**	w_{max}	M_w (kg/mol)	**Đ**	w_{max}
1	420	2.9	29	410	2.8	29
2	280	2.3	58	270	2.6	58
5	160	1.8	140	150	1.8	140
10	110	1.5	290	110	1.6	290

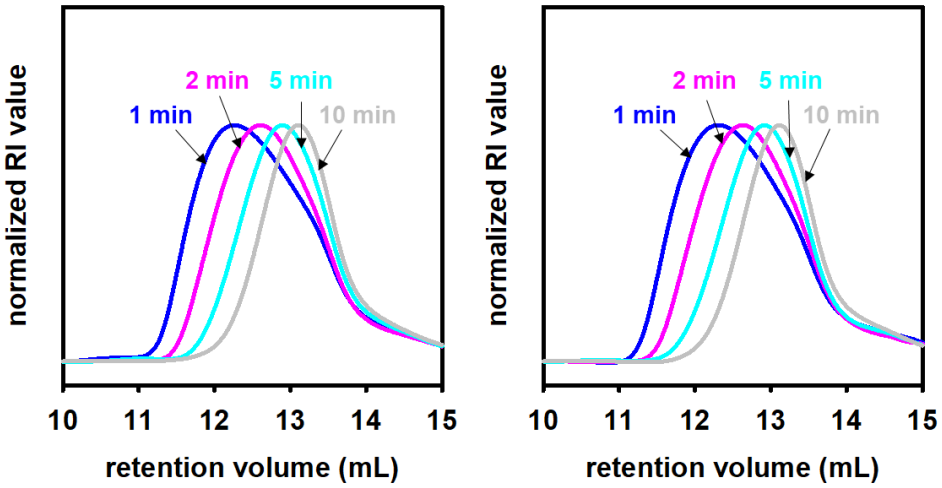

Figure A1-4. SEC traces for sonications of PAA_{SPP} at 2.5% w/v.

Table A1-6. Maximum power (P_{max}) consumed during sonication for PAA_{SPP} at 2.5% w/v.

[PAA] (w/v %)	**mass (mg)**	**mmol**	**run 1** P_{max} (W)	**run 2** P_{max} (W)
2.5	1,250	17.3	260	260

Maximum specific energy (w_{max}) values were determined using equation 1 (pg S3).

Table A1-7. Weight average molecular weight (M_w), dispersity (Đ), and specific energy (w_{max}) data for sonications of PAA_{SPP} at 2.5% w/v.

time (min)	**run 1**			**run 2**		
	M_w (kg/mol)	**Đ**	w_{max}	M_w (kg/mol)	**Đ**	w_{max}
1	580	2.4	12	570	2.4	12
2	370	2.2	25	390	2.0	25
5	250	1.7	62	250	1.8	62
10	190	1.6	120	180	1.6	120

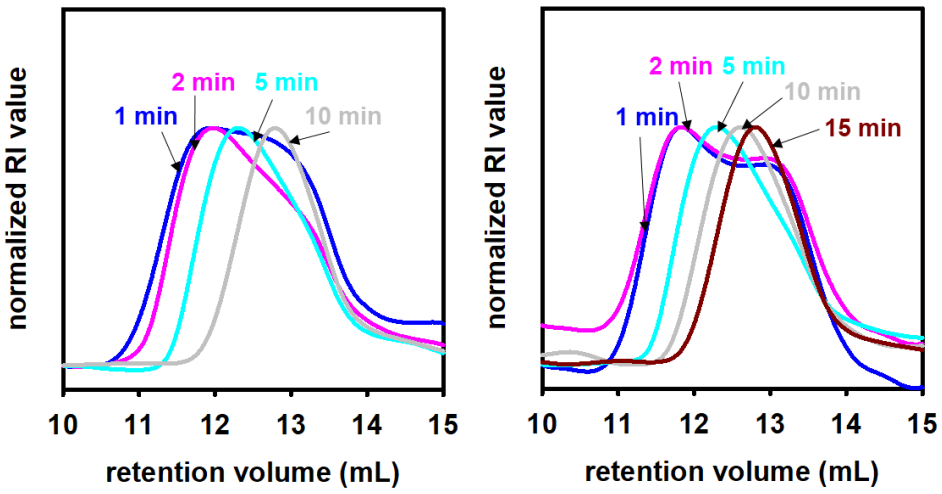

Figure A1-5. SEC traces for sonications of PAA_{SPP} at 5.0% w/v.

Table A1-8. Maximum power (P_{max}) consumed during sonication for PAA_{SPP} at 5.0% w/v.

[PAA] (w/v %)	**mass (mg)**	**mmol**	**run 1** P_{max} (W)	**run 2** P_{max} (W)
5	2,500	34.6	290	290

Maximum specific energy (w_{max}) values were determined using equation 1 (pg S3).

Table A1-9. Weight average molecular weight (M_w), dispersity (Đ), and specific energy (w_{max}) data for sonications of PAA_{SPP} at 5.0% w/v.

time (min)	**run 1**			**run 2**		
	M_w (kg/mol)	**Đ**	w_{max}	M_w (kg/mol)	**Đ**	w_{max}
1	880	3.4	7	850	3.1	7
2	810	2.9	14	800	3.0	14
5	500	2.1	35	490	2.3	35
10	340	1.7	70	340	2.3	70

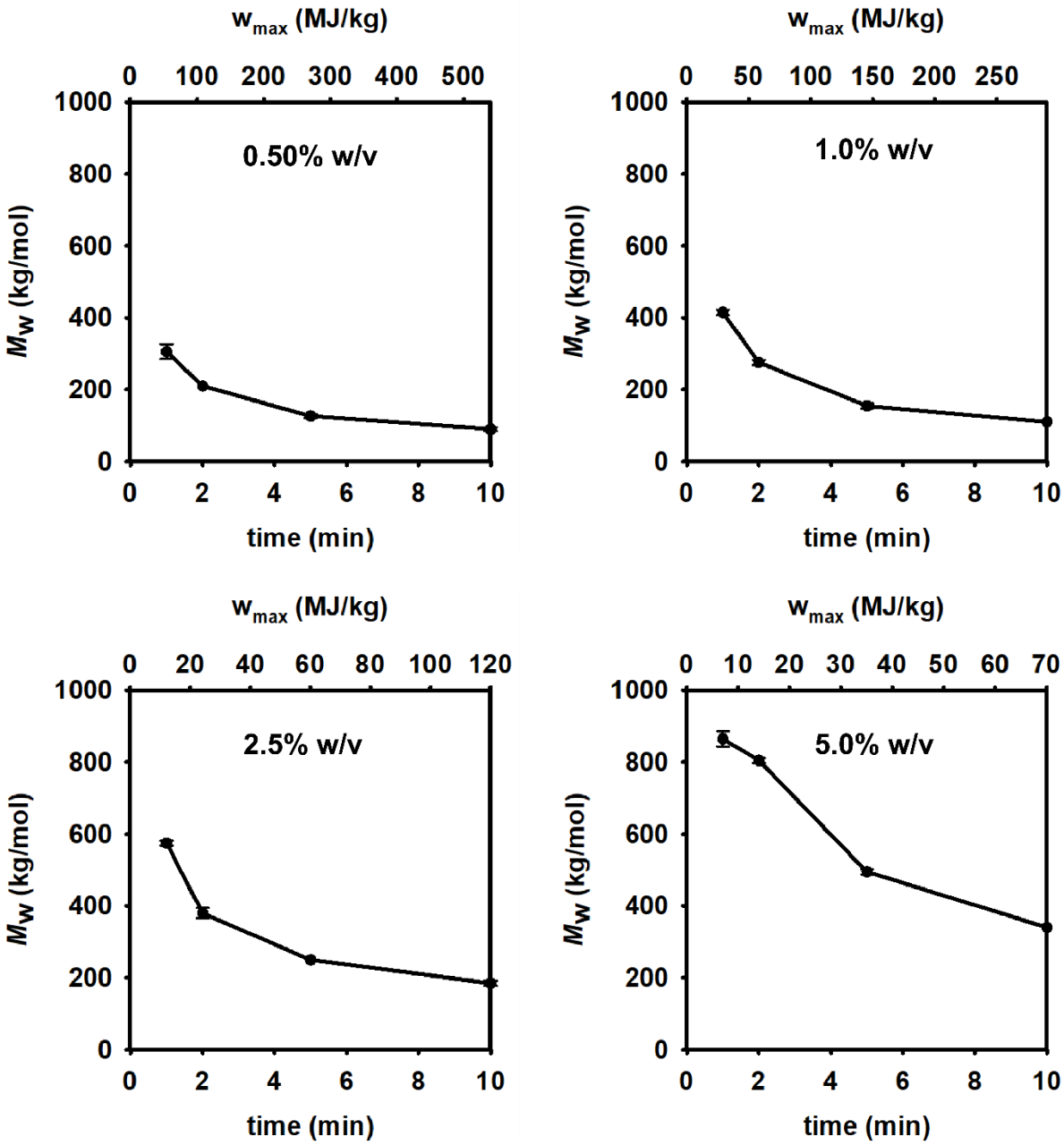

Figure A1-6. Weight average molecular weight (M_w) and maximum specific energy (w_{max}) versus time for PAA_{SPP} sonication at different concentrations.

Effect of time on sonicating $PAA_{P\&G}$ at 5% w/v

Decrosslinking $PAA_{P\&G}$ using 3 M NaOH

To a 20 mL vial, 0.25 g of $PAA_{P\&G}$ and 5 mL if DI H_2O, 0.1 M NaCl or 3 M NaOH was added to make 5% w/v. The samples were equipped with a stir bar and stirred at 300 rpm at 80 °C. The reaction was monitored visually over 24 h. Within 3 h, the opaque crosslinked $PAA_{P\&G}$ becomes homogenous and clear.

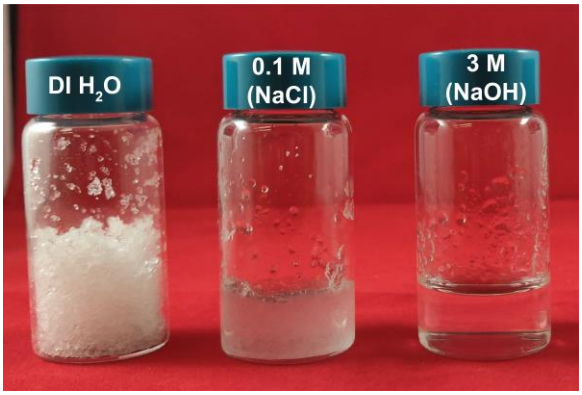

Figure A1-7. $PAA_{P\&G}$ in DI H2O (left), 0.1 M aq. NaCl (middle), and 3 M aq. NaOH (right) after stirring at 80 °C for 3 h.

Monitoring decrosslinking at 0.3 M NaOH. A 0.3 M aq. NaOH stock solution was prepared by adding NaOH (600 mg, 15 mmol) to a 50 mL volumetric flask followed by DI H_2O. $PAA_{P\&G}$ (250 mg) was added to separate 20 mL vials equipped with stir bars followed by aq. NaOH (0.3 M, 5.0 mL). The vials were stirred at 350 rpm on a hot plate at 80 °C for the appropriate time (i.e., 1, 2, 12, 15, 18, and 25 h). Then, the reaction mixture was cooled to rt in a water bath at 25 °C followed by adding acetic acid (90 µL, 1.5 mmol) to quench the NaOH. A pH of 6–7 was observed using pH paper.

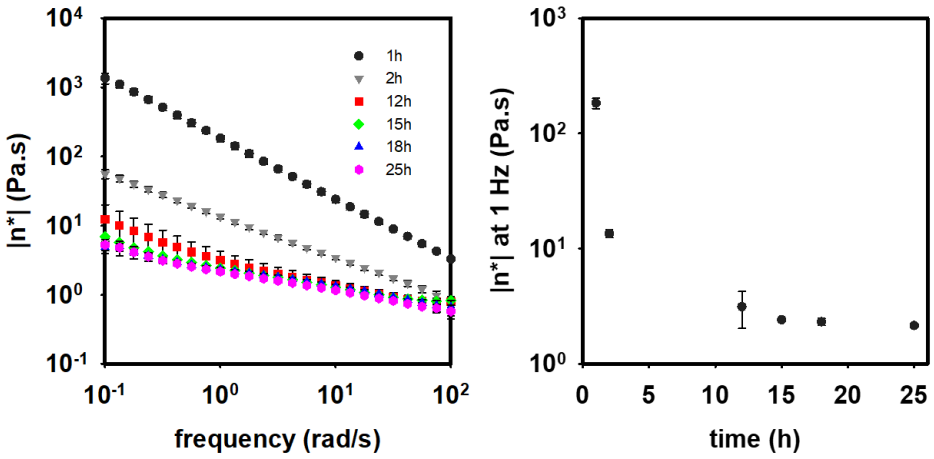

Figure A1-8. Plot of complex viscosity versus frequency (left) and complex viscosity at 1 Hz versus time (right) for decrosslinking $PAA_{P\&G}$ (5% w/v) using 0.3 M aq. NaOH at 80 °C.

A solution of 5% w/v decrosslinked $PAA_{P\&G}$ was prepared by stirring $PAA_{P\&G}$ (12.5 g) in NaOH(aq) (3 M, 250 mL) in a 500 mL glass bottle equipped with a stir bar at 80 °C for 24 h. PSAs were synthesized in one case using the decrosslinked polymer without sonication and 2 min sonication.

A 5% w/v solution of decrosslinked $PAA_{P\&G}$ was prepared by stirring $PAA_{P\&G}$ (10.0 g) and NaOH(aq) (3 M, 200 mL) in a 500 mL glass bottle at 80 °C for 24 h. A portion of the decrosslinked

$PAA_{P\&G}$ solution (50 mL) was poured into jacketed beakers equipped with a stir bar. Cold water was flowed through the beaker jacket from a faucet while stirring at 500 rpm. A thermocouple was immersed into the PAA solution to monitor temperature. The ultrasound unit was set to 100% amplitude and the PAA solutions were sonicated for 10 min while collecting 0.50–1.00 mL aliquots at 1, 2, 3, 5, 10 min. The temperature was observed to increase to 45–50 °C during irradiation. The sonicated SAP fragments were dialyzed overnight in DI water to remove NaOH. The aliquots were diluted with 0.1 M $NaNO_3$ (aq)/ethylene glycol (99:1 v/v) and analyzed via GPC.

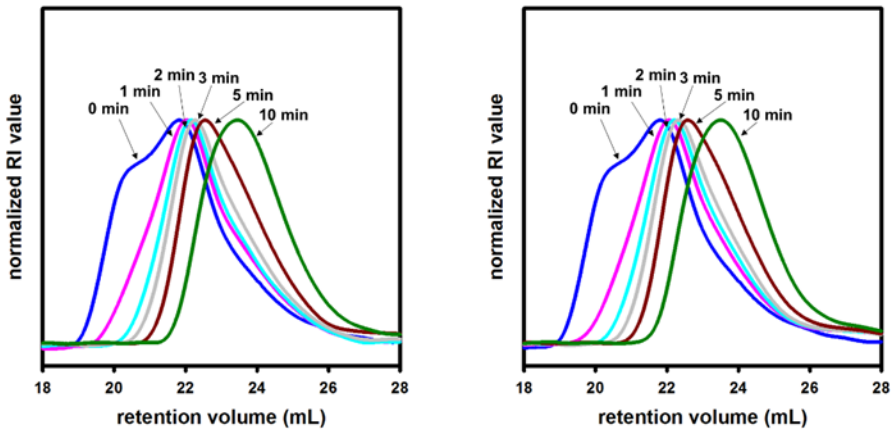

Figure A1-9. GPC traces for the sonication of decrosslinked $PAA_{P\&G}$ at 5% w/v.

Table A1-10. Molecular weight (Mw) and dispersity (Đ) data for the sonication of decrosslinked $PAA_{P\&G}$ at 5% w/v.

time (min)	run 1			run 2		
	M_w (kg/mol)	Đ	w_{max}	M_w (kg/mol)	Đ	w_{max}
0	868	2.8	0	868	2.8	0
1	485	1.8	7.7	475	1.8	7.7
2	451	1.6	15	432	1.7	15
3	411	1.5	23	390	1.7	23
5	336	1.3	38	318	1.7	38
10	238	1.3	77	224	1.5	77

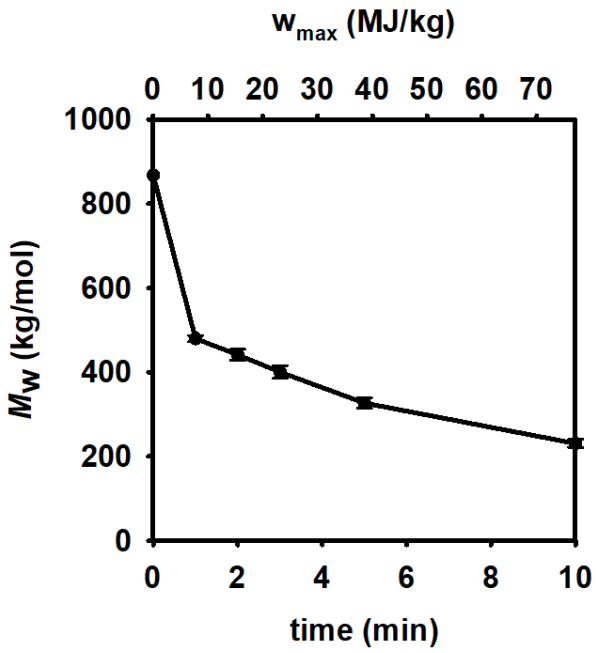

Figure A1-10. Plot of Mw and specific energy versus time for the sonication of decrosslinked $PAA_{P\&G}$ at 5% w/v.

Synthesis of PSAs

Protonation The remaining solution was passed through Dowex® Marathon™ MSC hydrogen form (23–27 μm) column. The protonated polymer solutions were concentrated under reduced pressure to a known volume and two 0.50 mL aliquots were collected for recovery determination and GPC analysis. The concentrated aqueous polymer solution were then diluted with DMSO (70 mL) and concentrated under reduced pressure to leave polymer solution exclusively dissolved in DMSO (1.86% w/v). The mass recovery was 68%.

Sonication – For sonication, 2 batches of the decrosslinked $PAA_{P\&G}$ solution (50 mL) each was poured into separate jacketed beakers equipped with a stir bars. Cold water was flowed through the beaker jacket from a faucet while stirring at 500 rpm. A thermocouple was immersed into the PAA solution to monitor temperature. The ultrasound unit was set to 100% amplitude and the PAA solutions were sonicated for 2 min. The temperature was observed to increase to 45–50 °C during irradiation. The sonicated $PAA_{P\&G}$ fragments were dialyzed overnight in DI water for 10 h to remove NaOH. Aliquots were diluted with 0.1 M $NaNO_3$ (aq)/ethylene glycol (99:1 v/v) and analyzed via GPC.

Protonation – The two batches of sonicated polymer solution were combined and protonated by passing through the Dowex® Marathon™ MSC hydrogen form (23–27 μm) column. The protonated polymer solutions were concentrated under reduced pressure to a known volume, and two 0.50 mL aliquots were collected for recovery determination and GPC analysis. The concentrated aqueous polymer solution was diluted with DMSO (100 mL) and concentrated under reduced pressure to leave the polymer solution exclusively dissolved in DMSO (3.4% w/v). The mass recovery was 90%.

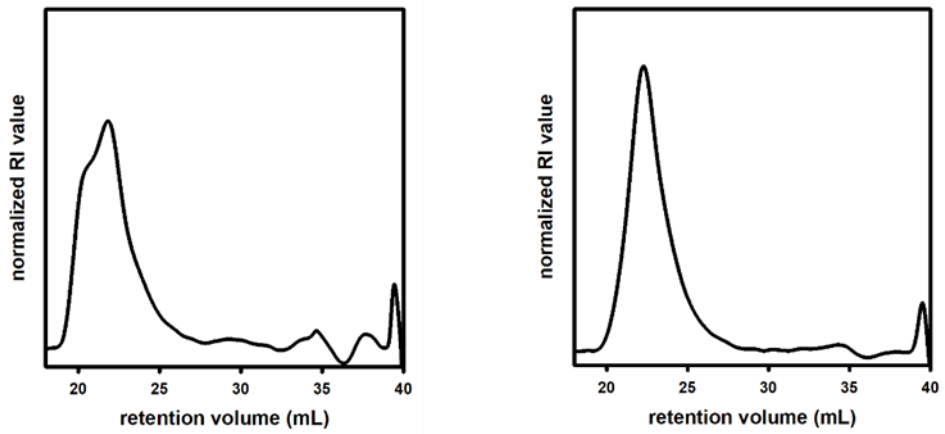

Figure A1-11. GPC traces of decrosslinked $PAA_{P\&G}$ (left) and $PAA_{P\&G}$ sonicated for 2 min (right).

Esterification – $PAA_{P\&G\text{-}0min}$ solution in DMSO (1.86% w/v, 1.30 g, 18 mmol, 1.0 equiv.) and TMG (6.8 mL, 54.1 mmol, 3.0 equiv.) were added to a 150 mL flat bottomed vessel (NB: 250 mL RBF resulted in poor mixing) equipped with a stir bar and stirred at 60 °C for 10 min (or until all precipitated PAA is dissolved). Thereafter, 2-EHBr (6.4 mL, 36.1 mmol, 2.0 equiv.) was added and the reaction was stirred at 60 °C for 15 h. The reaction was cooled to rt then quenched with acetic acid (5 mL) and precipitated by adding MeOH (50 mL). $P(2\text{-}EHA)_{P\&G\text{-}0min}$ was purified by dissolving in minimal amounts of THF (~10 mL) and precipitating with MeOH (~100 mL) twice, followed by drying under high vacuum at 60 °C for 1 h.

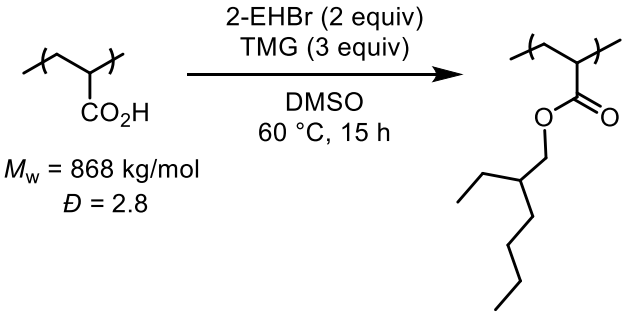

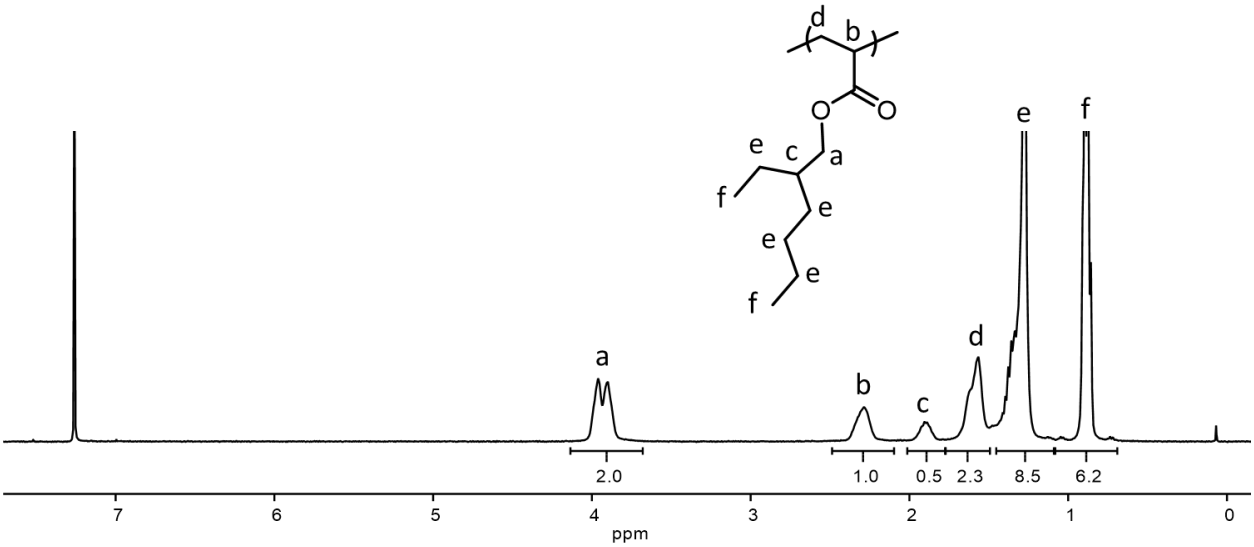

Figure A1-12. ^{1}H NMR spectrum of P(2-EHA)$_{P\&G\text{-}0min}$ (500 MHz, $CDCl_3$).

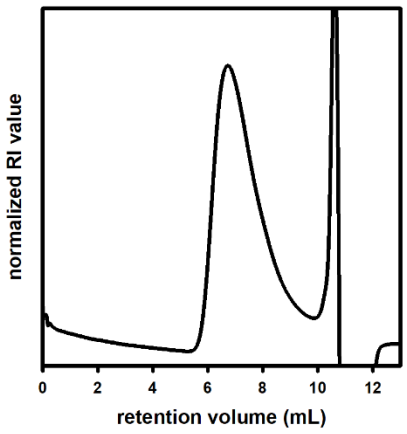

Figure A1-13. GPC chromatogram for P(2-EHA)$_{P\&G\text{-}0min}$.

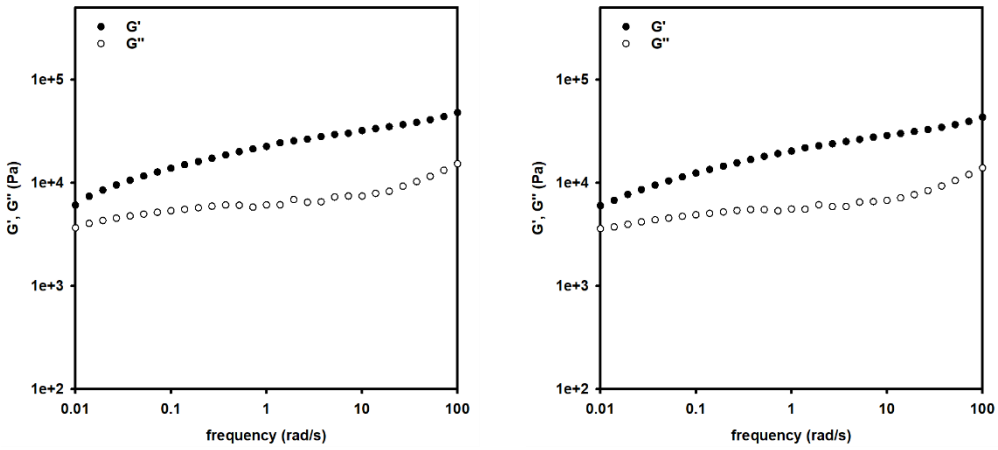

Figure A1-14. Dynamic storage modulus (G′) and dynamic loss modulus (G″) for P(2-EHA)$_{P\&G\text{-}0min}$ in duplicate.

Esterification – $PAA_{P\&G\text{-}2min}$ solution in DMSO (3.4% w/v, 1.70 g, 23.6 mmol, 1.00 equiv.) and TMG (8.9 mL, 70.8 mmol, 3.0 equiv.) were added to a 150 mL flat bottomed vessel (NB: 250 mL RBF resulted in poor mixing) equipped with a stir bar and stirred at 60 °C for 10 min (or until all precipitated PAA is dissolved). Thereafter, 2-EHBr (8.36 mL, 47.2 mmol, 2.0 equiv.) was added and the reaction was stirred at 60 °C for 15 h. The reaction was quenched with acetic acid (5 mL) and precipitated by adding MeOH (50 mL). The polymer was purified by dissolving in minimal amounts of THF (~5 mL) and precipitating with MeOH (~30 mL) twice, followed by drying under high vacuum at 60 °C for 1 h.

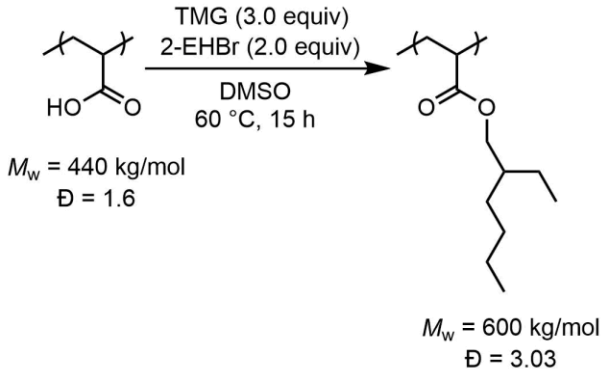

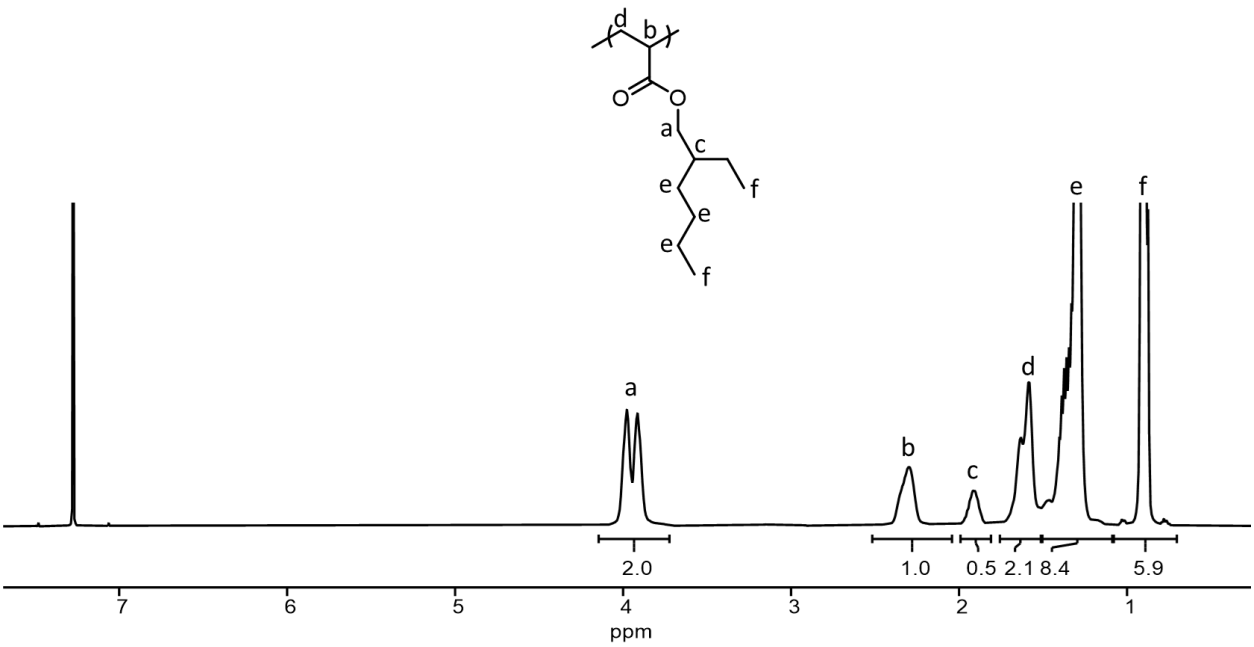

Figure A1-15. ^{1}H NMR spectrum of P(2-EHA)$_{P\&G\text{-}2min}$ (500 MHz, $CDCl_3$).

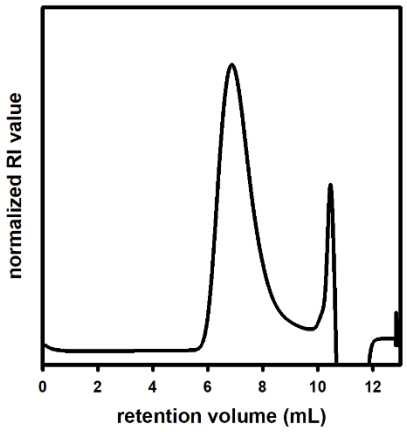

Figure A1-16. GPC chromatogram for P(2-EHA)$_{P\&G\text{-}2min}$.

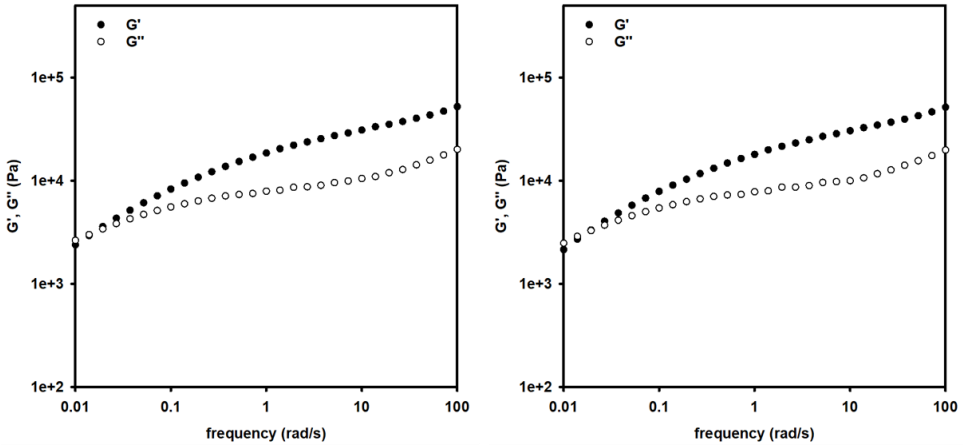

Figure A1-17. Dynamic storage modulus (G′) and dynamic loss modulus (G″) for P(2-EHA)$_{P\&G\text{-}2min}$ in duplicate.

Esterification – $PAA_{P\&G\text{-}2min}$ solution in DMSO (3.4% w/v, 1.70 g, 23.6 mmol, 1.0 equiv.) and TMG (8.9 mL, 70.8 mmol, 3.0 equiv.) were added to a 150 mL flat bottomed vessel (NB: 250 mL RBF resulted in poor mixing) equipped with a stir bar and stirred at 60 °C for 10 min (or until all precipitated PAA is dissolved). Thereafter, 2-EHBr (8.2 mL, 46 mmol, 1.95 equiv.) and 2-BAEB (0.264g, 1.18 mmol, 0.05 equiv.) were added and the reaction was stirred at 60 °C for 15 h. The reaction was quenched with acetic acid (5 mL) and precipitated by adding MeOH (50 mL). The polymer was purified by dissolving in minimal amounts of THF (~5 mL) and precipitating with MeOH (~30 mL) twice, followed by drying under high vacuum at 60 °C for 1 h.

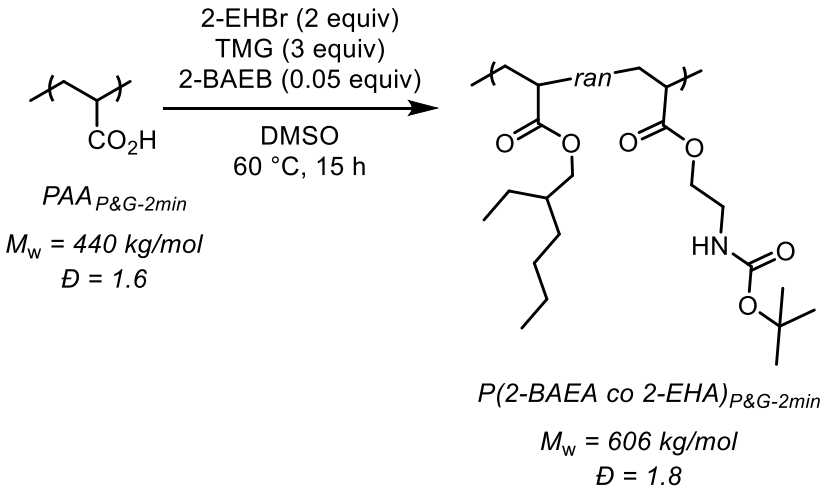

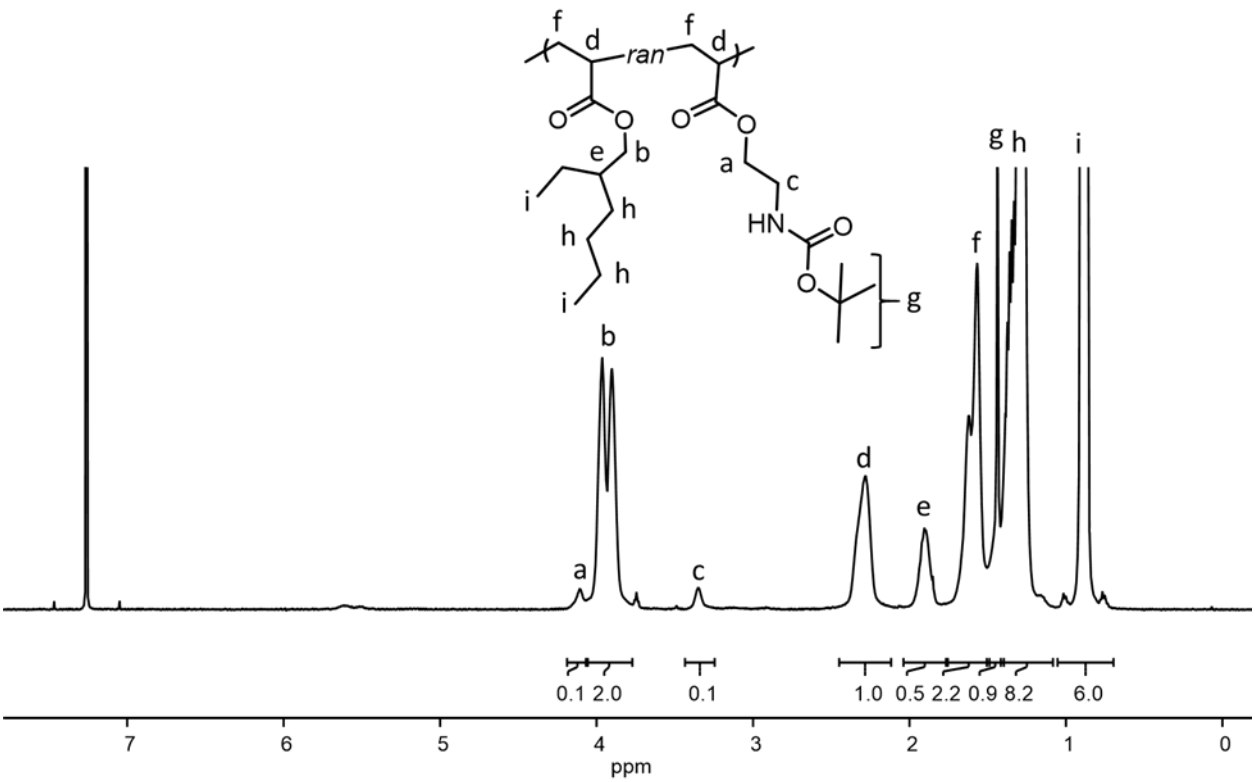

Figure A1-18. ^{1}H NMR spectrum of P(2-AEA *co* 2-EHA)$_{P\&G\text{-}2min}$ before deprotection.

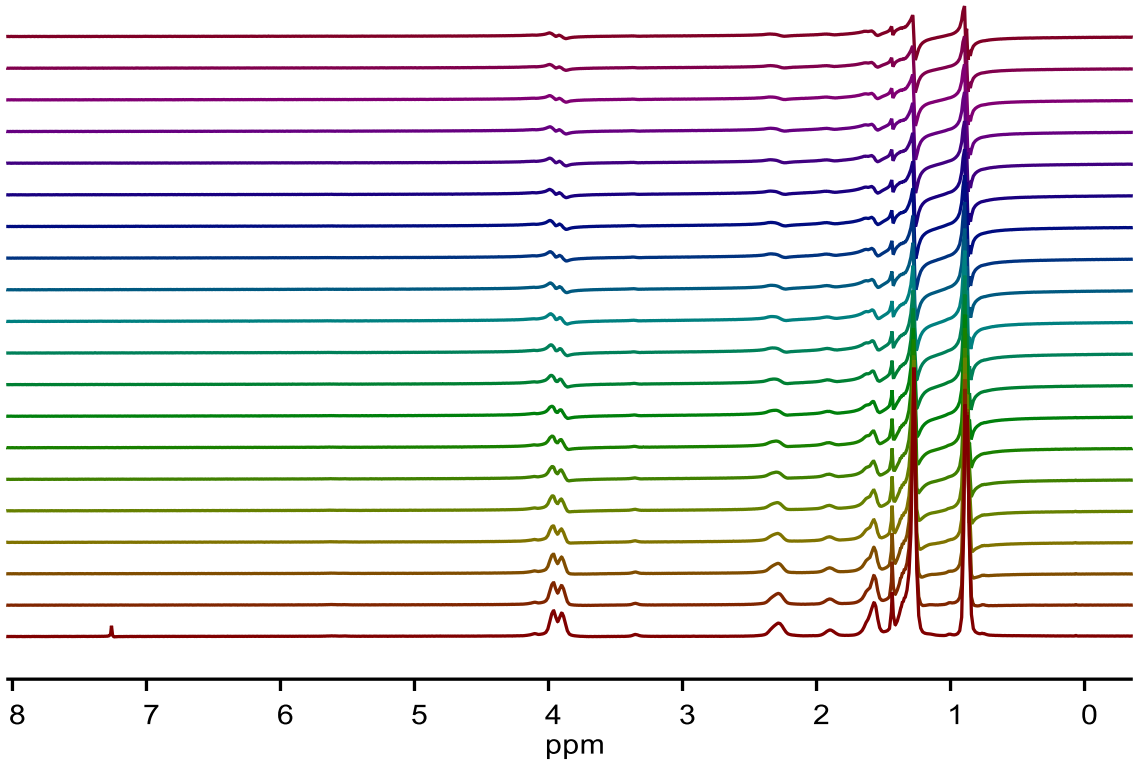

Figure A1-19. DOSY spectrum of P(2-AEA *co* 2-EHA)$_{P\&G\text{-}2min}$ confirming incorporation of Boc group.

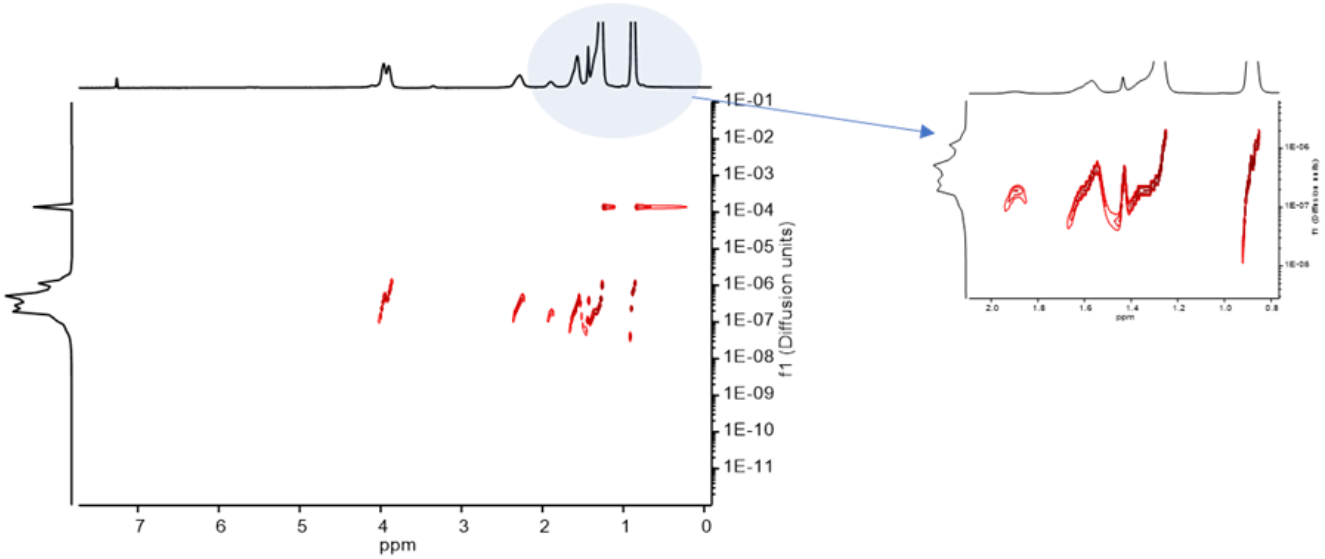

Figure A1-20. DOSY spectrum of P(2-AEA *co* 2-EHA)$_{P\&G\text{-}2min}$ confirming incorporation of Boc group.

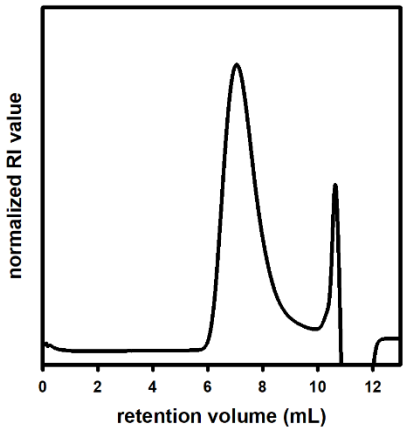

Figure A1-21. GPC chromatogram for P(2-AEA *co* 2-EHA)$_{P\&G\text{-}2min}$ before deprotection.

Deprotection – Poly(2-(Boc-amino)ethyl acrylate *co* 2-ethylhexyl acrylate)$_{P\&G\text{-}2min}$ (P(2-BAEA *co* 2-EHA)$_{P\&G\text{-}2min}$) (3,064 mg, 7.87 mmol, 1 equiv.) was added to 30 mL glass centrifuge tube equipped with a stir bar and dissolved with THF (7 mL). *p*-TsOH (407 mg, 2.36 mmol, 0.3 equiv.) was added to the tube and the reaction was stirred for 12 h at 60 °C. The reaction was quenched by adding TMG (1 mL) and poly(2-amino ethyl acrylate *co* 2-ethylhexyl acrylate)$_{P\&G\text{-}2min}$ P(2-AEA *co* 2-EHA)$_{P\&G\text{-}2min}$ was purified by dissolving in minimal amounts of THF (5 mL) and precipitating with of MeOH twice (25 mL), and then drying under high vacuum at 60 °C for 1 h.

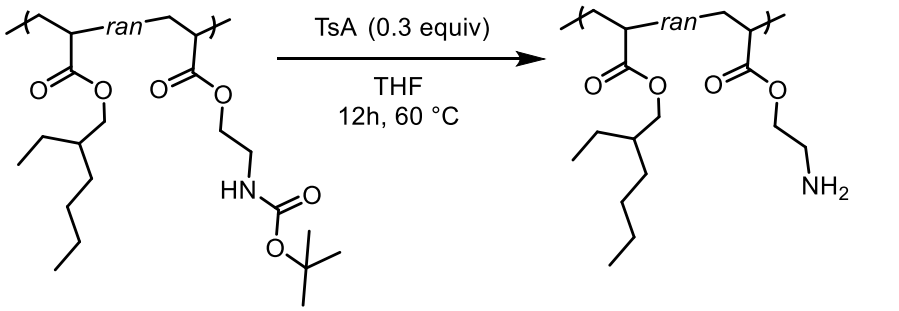

P(2-BAEA co 2-EHA)$_{P\&G\text{-}2min}$
M_w = 606 kg/mol
Đ = 1.8

P(2-AEA co 2-EHA)$_{P\&G\text{-}2min}$
M_w not determined

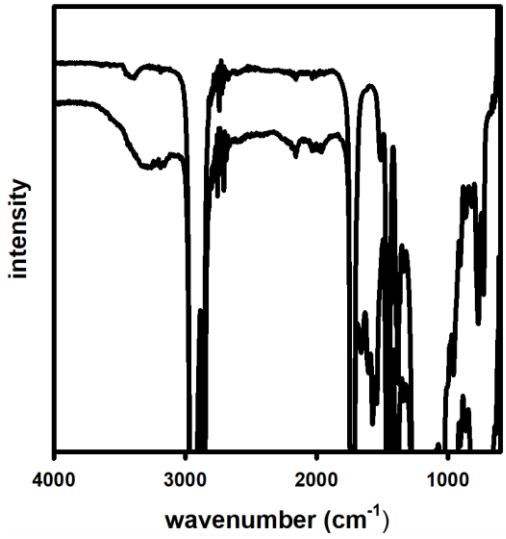

Figure A1-22. IR spectra of P(2-AEA co 2-EHA)P&G-2min before (top) and after (bottom) deprotection.

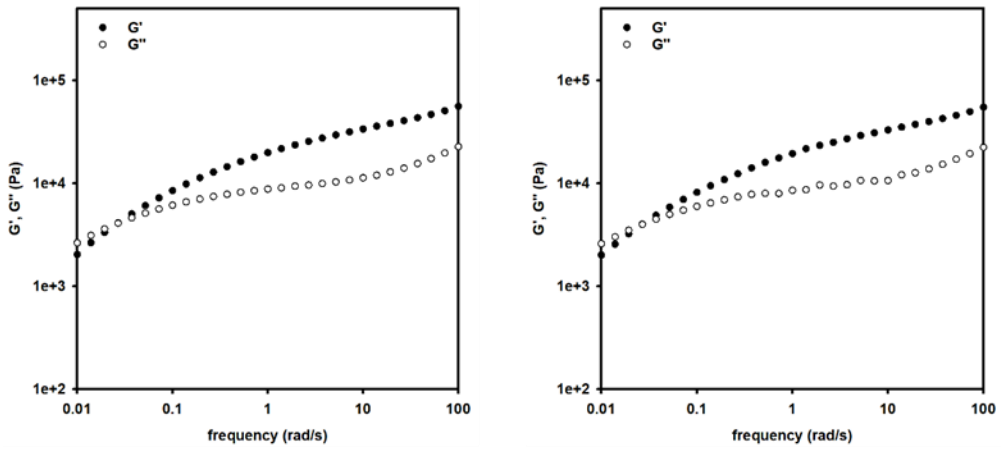

Figure A1-23. Dynamic storage modulus (G′) and dynamic loss modulus (G″) for P(2-AEA *co* 2-EHA)$_{P\&G\text{-}2min}$ before deprotection in duplicate.

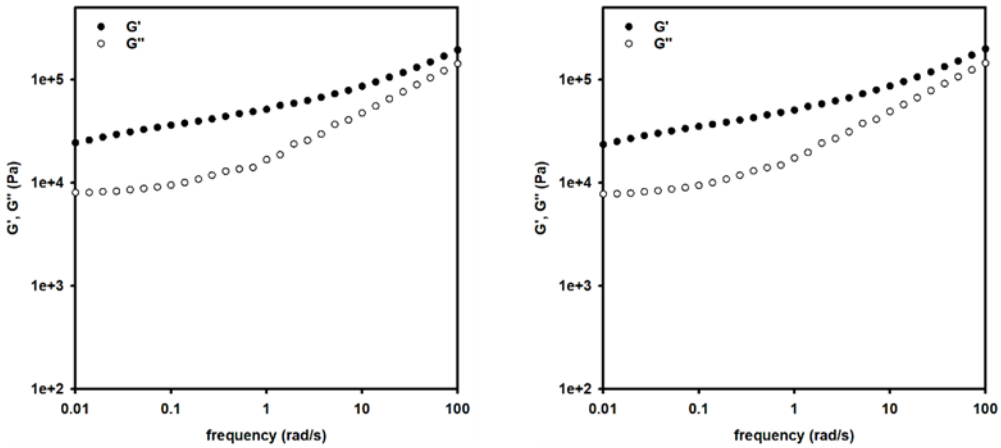

Figure A1-24. Dynamic storage modulus (G′) and dynamic loss modulus (G″) for P(2-AEA *co* 2-EHA)$_{P\&G\text{-}2min}$ after deprotection in duplicate.

Appendix 2: Supporting Information for Chapter 3. Repurposing Acrylic-Based Absorbents via Post-Polymerization Modification Part II

Materials

All chemicals were used as received unless otherwise mentioned. Polyacrylic acid (PAA) with molecular weight listed as 1,033 kg/mol (PAA_{SPP}) was purchased from Scientific Polymer Products. PAA_{SIGMA1} (listed as 240 kg/mol), PAA_{SIGMA2} (listed as 450 kg/mol), *p*-toluenesulfonic acid (*p*-TsOH), decanoic acid, undecanoic acid, 2-ethyl hexanol (2-EHOH), sodium hydroxide (NaOH), sulfuric acid (H_2SO_4), and sodium nitrate were purchased from Millipore Sigma. Methanol (MeOH) was purchased from Fisher Scientific. Tetrahydrofuran (THF) was purchased from OmniSolv. Glacial acetic acid was purchased from Acros Organics. Deuterated solvents: chloroform ($CDCl_3$), pyridine-d_5, and deuterium oxide (D_2O) were purchased from Cambridge Isotopes. The superabsorbent polymer ($PAA_{P\&G}$) provided by Procter & Gamble is 70% neutralized (i.e., % sodium form) and contains up to 1% by weight ethylene glycol diacrylate crosslinker relative to the acrylic acid monomer.[1] Sonicated polymer fragments were dialyzed in deionized (DI) water using Spectra/Por molecular porous membrane tubing (molecular weight cut-off: 3.5 kg/mol). Pressure vessels were purchased from Thomas Scientific. Jacketed beakers were purchased from Sigma Aldrich (cat#: Z202738-1EA).

General experimental

Sonication – Sonication was performed at 100% amplitude (amp) using a Sonics and Materials Vibra-cell VCX 600 Ultrasonic Liquid Processor equipped with a 13 mm replaceable tip probe. A 3.5 cm inner diameter, 9 cm height jacketed beaker was used for all sonication procedures. Cold water (10–15 °C) was flowed through the jacket while stirring the polymer solution at 500 rpm. A thermocouple was immersed into the polymer solution to monitor temperature. The temperature was generally observed to increase from 10–15 °C to 45–50 °C during sonication. The power from the outlet was monitored using a kill-a-watt meter (#P4400). The maximum power (P_{max}) reading observed at the beginning of sonication was recorded. The maximum specific energy (w_{max}) for chain-shortening PAA of mass (m) for time (t) was determined using equation (1).

$$w_{max}\ (J/kg) = \frac{P_{max}\ (W) \times t\ (s)}{m\ (kg)} \qquad (1)$$

NMR Spectroscopy – Unless otherwise noted, ^{1}H and ^{13}C NMR spectra for all compounds were acquired at room temperature. Chemical shift data are reported in units of δ (ppm) relative to tetramethylsilane (TMS) and referenced with residual solvent. Multiplicities are reported as follows: singlet (s), doublet (d), doublet of doublets (dd), triplet (t), quartet (q), multiplet (m), and broad resonance (br). Residual water is denoted by an asterisk (*). For all ^{1}H NMR spectra of polymers, a 3.5 s acquisition time was used with a 10 s relaxation delay between each pulse.

Size Exclusion Chromatography (SEC) for $PAA_{P\&G}$ fragments – Sonicated PAA_{SPP} and $PAA_{P\&G}$ fragments were diluted (to 1–1.5 mg/mL) with 0.2 M $NaNO_3$ (aq)/ethylene glycol (99:1 v/v) and filtered through a Titan3™ Nylon syringe filter (0.45 μm) into a SEC vial.

Polymer molar mass (*M*) and dispersity (Đ) were determined by comparison with PEG/PEO EasiVial standards from Agilent at 40 °C in 0.1 M $NaNO_3$ (aq) on a Waters SEC (Waters 1515 Isocratic HPLC pump, 717plus autosampler, RI detector Model 214 and UV-PDA detector Model 487) equipped with four Ultrahydrogel columns: 120 (WAT011565), 250 (WAT011525), 500 (WAT011530) and 1000 (WAT011535).

Dialyzing, free-drying, and grinding polymer fragments – After sonication, the polymer was dialyzed using DI water (~1 gallon), switching the DI water three times over 12–18 h. Then, the polymer was freeze-dried and ground to a fine powder using a mortar and pestle. More specifically, while wearing cryogenic gloves, a piece of freeze-dried polymer was put into a mortar, which was then immersed into a bath of liquid N_2. A small amount of liquid N_2 was poured into the mortar and the polymer was ground using a pestle. The fine powder was immediately transferred to a 20 mL vial and held under high vacuum for 10 min as the polymer warmed to rt to avoid water condensation.

SEC for polyacrylate-based PSAs (pressure-sensitive adhesives) – The synthesized PSAs were dissolved in THF (1 mg/mL) with mild heating and filtered through a PTFE filter (0.45 μm) into an SEC vial. Polymer molar mass (*M*) and dispersity (Đ) were determined at 40 °C in THF on a SEC: Malvern Viscotek GPCMax VE2001 equipped with two Viscotek LT-5000L 8 mm (ID) × 300 mm (L) columns, and Viscotek TDA 305 and Viscotek RI detectors. Apparent molar masses were calculated using EasiVial PMMA standards (spanning 690–1,944,000 g/mol) provided by Polymer Laboratories.

Rheology – All rheological measurements were taken on an AR2000ex rheometer (TA Instruments). A 40 mm stainless steel parallel plate was used to run frequency sweeps for decrosslinked $PAA_{P\&G}$. First, an aliquot of the reaction mixture (1.2 mL) was added to the bottom

plate. The upper plate/geometry was lowered to a gap of 605 μm. While the geometry rotation was locked, the excess sample was wiped away using a custom-built glass piece that trims the excess sample along the circumference of the geometry. Then, the plate was lowered to the desired gap of 600 μm. For reference, see this TA instruments video (https://www.youtube.com/watch?v=kFiVLSzjUlc). DI water (1.2 mL) was added into the solvent cavity on the plate, followed by the solvent trap. For reference, see this TA instruments video (https://www.youtube.com/watch?v=OQmAtdvYrws). The frequency sweeps were performed between 0.1 and 100 Hz at 1% strain and 25 °C. This process was repeated at least twice for each sample with cleaning and calibration between runs.

A 25 mm serrated parallel plate was used to run frequency sweeps for the PSAs. PSA (~600 mg) was loaded to achieve a 1,250 μm layer thickness. The frequency sweeps were performed between 0.01 and 100 Hz at 1% strain and 25 °C. This process was repeated at least twice for each sample with cleaning and calibration between runs.

Table A2-1. Fisher Scientific quotation displaying costs for chemicals used in base-mediated and acid-catalyzed esterification.

Sales Quotation

*Quote Nbr	Creation Date	Due Date	Page
9273-1563-85	09/30/2019		1 of 3

Payment Terms	Delivery Terms
NET 30 DAYS	DEST
Valid To	Prepared By
11/29/2019	GIGNAC, KATIE
Customer Reference	Sales Representative
BULK CHEMICAL QTE	KATIE GIGNAC

To place an order	Ph: 800-766-7000	Fx: 800-926-1166

Submitted To:	Customer Account: 534920-024
TAKUNDA CHAZOVACHII KATIE.GIGNAC@THERMOFISHER.COM 734- -	UNIVERSITY OF MICHIGAN CHEMISTRY BUILDING 930 N UNIVERSITY AVE ANN ARBOR MI 48109-1001 ATTN: TAKUNDA

Fisher Scientific
Part of Thermo Fisher Scientific

FISHER SCIENTIFIC COMPANY LLC
4500 TURNBERRY DRIVE
HANOVER PARK IL 60133-5491

Review and Place Order

Click here or go through your purchasing system to fishersci.com quotes

*Please reference this Quote Number on all correspondence.

Don't have a profile? Register on fishersci.com

For complete Terms and Conditions, please click here.

Nbr	Qty	UN	Catalog Number	Description	Unit Price	Extended Price
1	1	EA	AC221290025	1,1,3,3-TETRAMETHYLGUANI 2.5KG 1,1,3,3-Tetramethylguanidine 99%, C5H13N3, CAS Number: 80-70-6, 2.5kg Vendor Catalog # 221290025 Hazardous Material This item is being sold as 1 per each	532.29	532.29
2	1	EA	60 090 233	DIMETHYL SULFOXIDE BJ 56LT Vendor Catalog # CS081-56 Hazardous Material This item is being sold as 1 per each	2,641.28	2,641.28
3	1	EA	B228925G	2-(TERT-BUTOXYCARBONYLAMIN 25G 2-(tert-Butoxycarbonylamino)ethyl Bromide,≥98.0% (GC),C7H14BrNO2,39684-80-5,25g,tert-Butyl N-(2-Bromoethyl)carbamate,N-(2-Bromoethyl)carbamic Acid tert-Butyl Ester,2-(Boc-amino)ethyl Bromide Vendor Catalog # B2289-25G Hazardous Material This item is being sold as 1 per each	239.40	239.40
4	1	EA	AC118530250	2-ETHYL-1-HEXANOL, 99% 25LT 2-Ethyl-1-hexanol 99%, C8H18O, CAS Number: 104-76-7, 25L Vendor Catalog # 118530250 This item is being sold as 1 per each	308.04	308.04
5	1	EA	B228925G	2-(TERT-BUTOXYCARBONYLAMIN 25G 2-(tert-Butoxycarbonylamino)ethyl Bromide,≥98.0%	239.40	239.40

Sales Quotation

Fisher Scientific
Part of Thermo Fisher Scientific

Quote Nbr	Customer Reference	Page
9273-1563-85	BULK CHEMICAL QTE	2 of 3

Nbr	Qty	UN	Catalog Number	Description	Unit Price	Extended Price
				(GC),C7H14BrNO2,39684-80-5,25g,tert-Butyl N-(2-Bromoethyl)carbamate,N-(2-Bromoethyl)carbamic Acid tert-Butyl Ester,2-(Boc-amino)ethyl Bromide Vendor Catalog # B2289-25G Hazardous Material This item is being sold as 1 per each		
6	1	EA	AC139020100	P-TOLUENESULFONIC ACID M 10KG p-Toluenesulfonic acid monohydrate 99% PTSA, C7H8O3S.H2O, CAS Number: 6192-52-5, 10kg Vendor Catalog # 139020100 Hazardous Material Shelf Life 3Y This item is being sold as 1 per each	216.71	216.71
7	1	EA	18 604 682	MONOETHANOLAMINE, NF Vendor Catalog # M1322-200LTBL Hazardous Material This item is being sold as 1 per each	4,432.86	4,432.86
8	1	EA	60 017 26	TOLUENE PREP-LC ACS 99. 204LT Vendor Catalog # PP347-204 Hazardous Material This item is being sold as 1 per each	1,695.23	1,695.23
9	1	EA	60 016 76	TETRAHYDROFURAN HPLC GC 200LT Vendor Catalog # CS340-200 Hazardous Material This item is being sold as 1 per each	4,789.37	4,789.37
10	1	EA	MMX048720	METHANOL,SPECIAL ACS 200L Methanol 99.8% min. Methyl Alcohol, CH3OH, CAS Number: 67-56-1, 200L Vendor Catalog # MX0487-20 Hazardous Material This item is being sold as 1 per each	2,165.90	2,165.90
11	1	EA	AC305335000	2-ETHYLHEXYL BROMIDE 95% 500G 2-Ethylhexyl bromide 95% 1-Bromo-2-ethylhexane, C8H17Br, CAS Number: 18908-66-2, 500g Vendor Catalog # 305335000 This item is being sold as 1 per each	111.41	111.41

Sales Quotation

Fisher Scientific
Part of Thermo Fisher Scientific

Quote Nbr	Customer Reference	Page
9273-1563-85	BULK CHEMICAL QTE	3 of 3

Nbr	Qty	UN	Catalog Number	Description	Unit Price	Extended Price

MERCHANDISE TOTAL 17,371.89

NOTES:
DELIVERY: EMAL

We now offer highly competitive financing with low monthly payments. Please contact your local sales representative for more information.

Tell us about your recent customer service experience by completing a short survey. This should take no longer than three minutes. Enter the link into your browser and enter the passcode: USA-PGH-CS2
http://survey.medallia.com/fishersci

Comparing base-mediated versus acid-catalyzed decrosslinking of $PAA_{P\&G}$

Monitoring decrosslinking at 0.3 M NaOH. A 0.3 M aq. NaOH stock solution was prepared by adding NaOH (600 mg, 15 mmol) to a 50 mL volumetric flask followed by DI H_2O. $PAA_{P\&G}$ (250 mg) was added to separate 20 mL vials equipped with stir bars followed by aq. NaOH (0.3 M, 5.0 mL). The vials were stirred at 350 rpm on a hot plate at 80 °C for the appropriate time (i.e., 1, 2, 12, 15, 18, and 25 h). Then, the reaction mixture was cooled to rt in a water bath at 25 °C followed by adding acetic acid (90 µL, 1.5 mmol) to quench the NaOH. A pH of 6–7 was observed using pH paper.

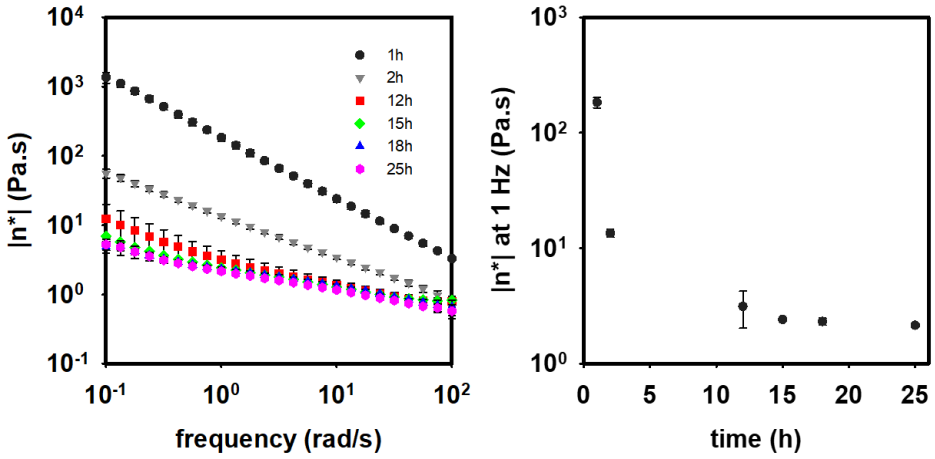

Figure A2-1. Plot of complex viscosity versus frequency (left) and complex viscosity at 1 Hz versus time (right) for decrosslinking $PAA_{P\&G}$ (5% w/v) using 0.3 M aq. NaOH at 80 °C.

Monitoring decrosslinking with 0.8 M aq. H_2SO_4.

A 0.8 M aq. H_2SO_4 stock solution was prepared by adding H_2SO_4 (2.15 mL, 4.0 mmol) to a 50 mL volumetric flask followed by DI water. $PAA_{P\&G}$ (250 mg) and aq. H_2SO_4 (0.8 M, 5.0 mL) were added to a 15 mL pressure vessel equipped with a stir bar. After sealing the vessel, the reaction mixture was heated at 120 °C for the appropriate time (i.e., 1, 2.5, 11.5, 14, and 24 h). Then, the reaction mixture was cooled to rt in a water bath at 25 °C and quenched with aq. Na_2CO_3 (2 mL, 2 M). A pH of approximately 3 was observed using pH paper.

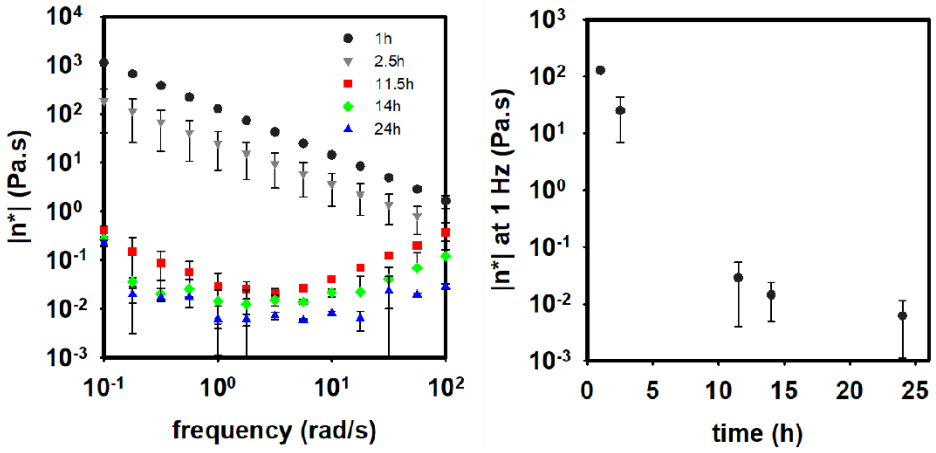

Figure A2-2. Plot of complex viscosity versus frequency (left) and complex viscosity at 1Hz versus time (right) for decrosslinking $PAA_{P\&G}$ (5% w/v) using 0.8 M aq. H_2SO_4 at 120 °C.

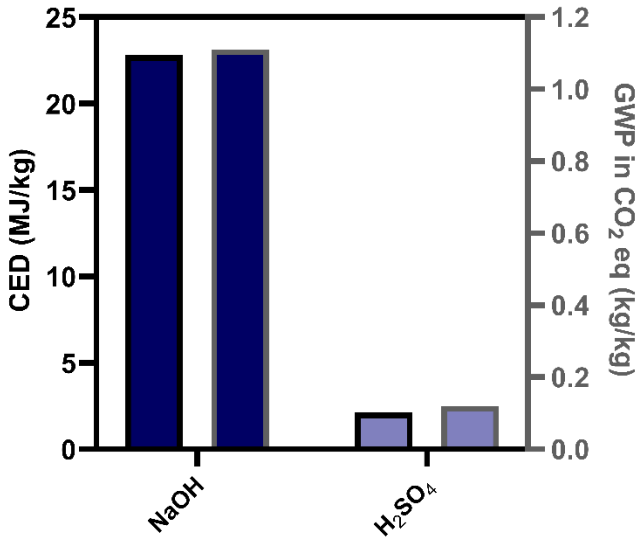

Figure A2-3. Comparing the cumulative energy demand and global warming potential for sulfuric acid versus sodium hydroxide using data from the SimaPro database.

Decrosslinking $PAA_{P\&G}$ for chain-shortening experiments

A 0.8 M aq. H_2SO_4 solution was prepared by adding H_2SO_4 (6.84 mL, 128 mmol, 1.5 equiv) to a 350 mL pressure vessel containing DI H_2O (160 mL) stirring at 350 rpm. Thereafter, $PAA_{P\&G}$ (8,000 mg, 85.1 mmol, 1 equiv) was added. The vessel was sealed, and the reaction stirred at 120 °C for 24 h. The resulting decrosslinked polymer was used for the subsequent sonication experiments (see chain-shortening sections).

Evaluating polymer recovery and chemical structure after sonication

A portion of the decrosslinked $PAA_{P\&G}$ solution (25 mL, 2.5% w/v) and DI H_2O (25 mL) were poured into a jacketed beaker equipped with a stir bar. While flowing cold water through the jacket, the decrosslinked $PAA_{P\&G}$ was sonicated at 100% amplitude (280 W) for 1 min. During sonication, the temperature rose from 10–15 °C to 50 °C. 940 mg (91%) was recovered after dialyzing and freeze-drying (see general experimental).

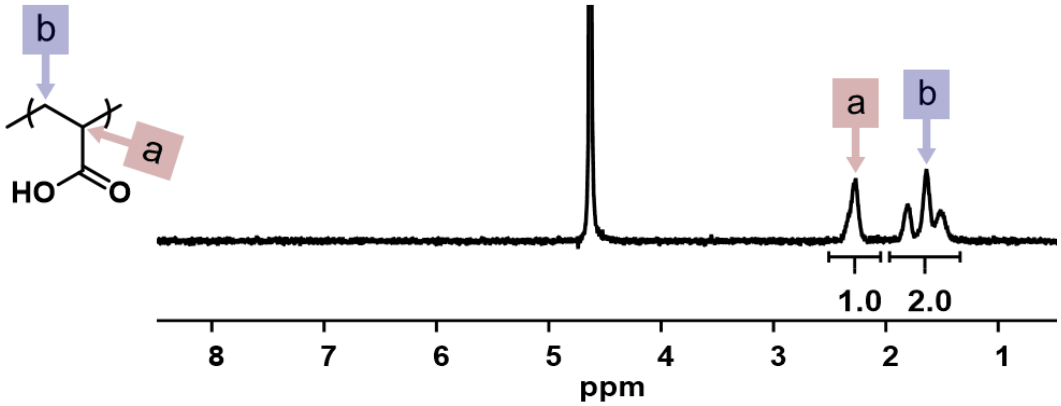

Figure A2-4. ^1H NMR spectra of sonicated $PAA_{P\&G}$ (500 MHz, D_2O).

Monitoring chain-shortening and energy consumption at 2.5 and 5.0% w/v

Monitoring chain-shortening over time of decrosslinked $PAA_{P\&G}$ at 5.0% w/v

Two portions of the decrosslinked $PAA_{P\&G}$ solution (50 mL each) were poured into jacketed beakers equipped with a stir bar. While flowing cold water through the jacket, the decrosslinked $PAA_{P\&G}$ was sonicated at 100% amplitude (290 W) while collecting 1.0 mL aliquots at 1, 2, 5, 10, and 15 min. During sonication, the temperature rose from 10–15 °C to 50 °C. The aliquots were quenched using aq. Na_2CO_3 (2 M, 0.4 mL). The aliquots were diluted (to 1–1.5 mg/mL) with 0.2 M aq. $NaNO_3$/ethylene glycol (99:1 v/v) and analyzed via SEC.

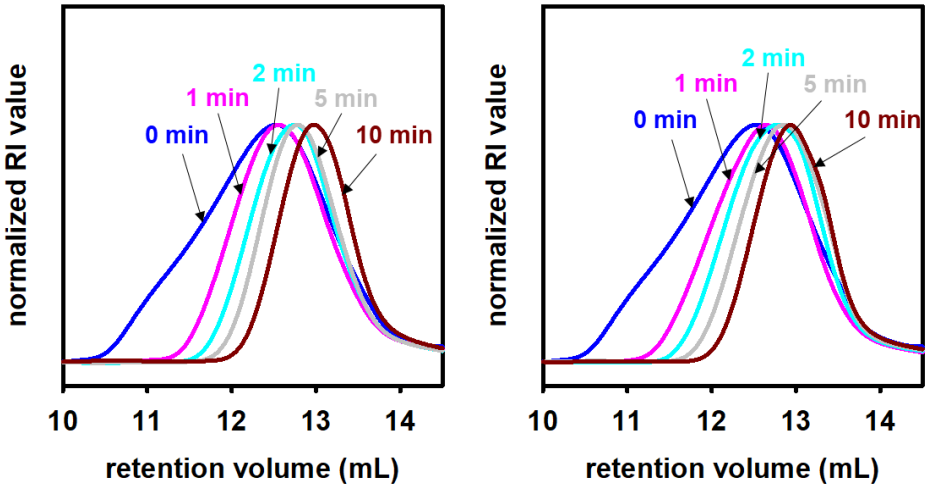

Figure A2-5. SEC traces for the chain-shortening of decrosslinked $PAA_{P\&G}$ at 5.0% w/v.

Table A2-2. Maximum power (P_{max}) consumed during sonication for $PAA_{P\&G}$ at 5% w/v.

[PAA] (w/v %)	mass (mg)	mmol	run 1 P_{max} (W)	run 2 P_{max} (W)
5	2,500	26.6	290	290

Maximum specific energy (w_{max}) values were determined using equation 1 (pg S3).

Table A2-3. Weight average molar mass (M_w), dispersity (Đ) and specific energy (w_{max}) data for sonications of decrosslinked $PAA_{P\&G}$ at 5.0% w/v.

time (min)	run 1			run 2		
	M_w (kg/mol)	Đ	w_{max}	M_w (kg/mol)	Đ	w_{max}
0	870	2.8	0			
1	460	1.8	7	430	1.7	7
2	340	1.6	14	320	1.6	14
5	270	1.3	35	270	1.4	35
10	220	1.3	70	200	1.4	70

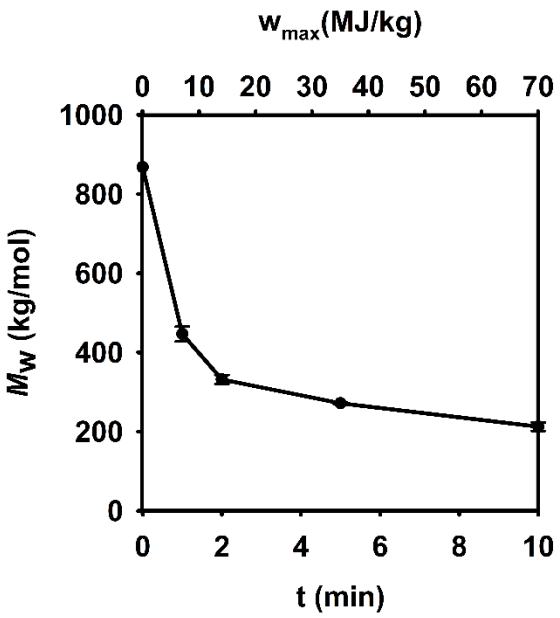

Figure A2-6. Weight average molar mass (M_w) versus time (t) and maximum specific energy (wmax) plot for PAAP&G sonication at 5% w/v.

Monitoring chain-shortening over time of decrosslinked PAA$_{P\&G}$ at 2.5% w/v

A portion of the decrosslinked PAA$_{P\&G}$ solution (50 mL) was diluted to 100 mL using DI water to make 2.5% w/v solution. This solution was poured into two jacketed beakers (50 mL each) equipped with a stir bar. While flowing cold water through the jacket, the decrosslinked PAA$_{P\&G}$ was sonicated at 100% amplitude (280 W) while collecting 1.0 mL aliquots at 0, 0.5, 1, 2, 5, and 10 min. During sonication, the temperature rose from 10–15 °C to 50 °C. The aliquots were quenched using aq. Na_2CO_3 (2 M, 0.2 mL). The aliquots were diluted (to 1–1.5 mg/mL) with 0.2 M aq. $NaNO_3$/ethylene glycol (99:1 v/v) and analyzed via SEC.

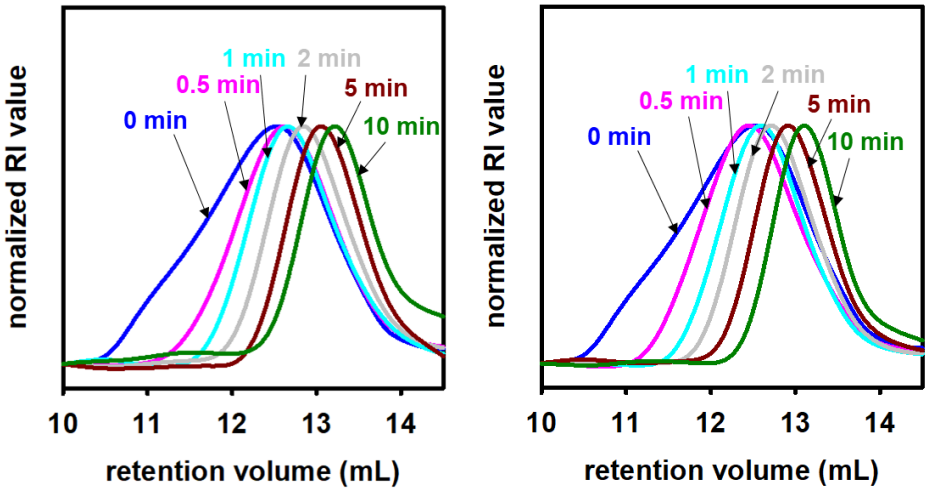

Figure A2-7. SEC traces for the chain-shortening of decrosslinked PAA$_{P\&G}$ at 2.5% w/v

Table A2-4. Maximum power (P_{max}) consumed during sonication for $PAA_{P\&G}$ at 2.5% w/v

[PAA] (w/v %)	mass (mg)	mmol	run 1 P_{max} (W)	run 2 P_{max} (W)
2.5	1,250	13.3	280	280

Maximum specific energy (w_{max}) values were determined using equation 1 (pg S3).

Table A2-5. Weight average molar mass (M_w), dispersity (Đ) and specific energy (w_{max}) data for sonications of decrosslinked $PAA_{P\&G}$ at 2.5% w/v.

time (min)	run 1			run 2		
	M_w (kg/mol)	Đ	w_{max}	M_w (kg/mol)	Đ	w_{max}
0	870	2.8	0	870	2.8	0
0.5	450	1.9	6.7	560	2.0	6.7
1	330	1.7	13	390	1.6	13
2	240	1.5	27	290	1.5	27
5	180	1.4	67	210	1.4	67
10	140	1.3	130	160	1.4	130

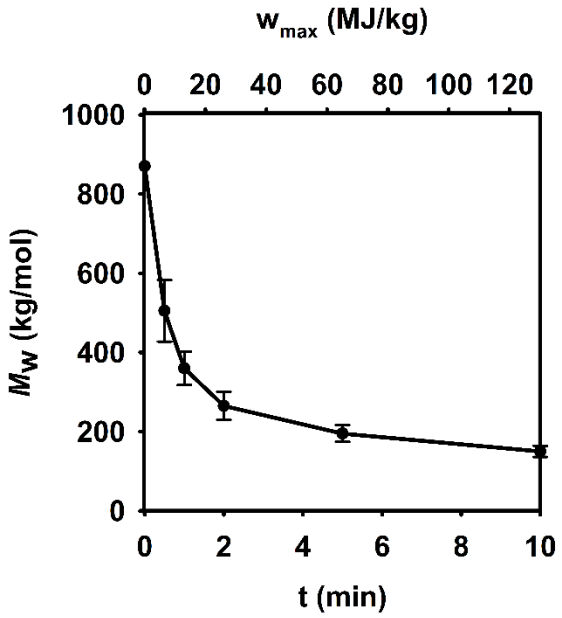

Figure A2-8. Weight average molar mass (M_w) versus time (t) and maximum specific energy (w_{max}) for $PAA_{P\&G}$ sonication at 2.5% w/v.

Fischer esterification studies

Commercial PAAs (i.e., PAA_{SIGMA1} and PAA_{SIGMA2}) are low molecular weight (< 450 kg/mol) relative to the chain-shortened $PAA_{P\&G}$. Consequently, shorter esterification times are needed for commercial PAAs (4 h) relative to the chain-shortened materials (10 h).

Effect of alcohol equivalents on conversion

Reactions were run under identical conditions except for the amounts of 2-ethylhexanol (2-EHOH) (3, 5, 10, 15 equiv.) used relative to PAA_{SIGMA2}. 2-EHOH (2.60 mL, 16.7 mmol, 3.00 equiv.; 4.30 mL, 27.8 mmol, 5.00 equiv.; 8.70 mL, 55.5 mmol, 10.0 equiv.; 13.0 mL, 83.3 mmol, 15.0 equiv.) was added to seperate 20 mL vials equipped with stir bars. *p*-TsOH (527 mg, 2.80 mmol, 0.500 equiv.) was added to each vial and stirred until dissolved. The vials were subsequently heated to 120 °C, then PAA_{SIGMA2} (400 mg, 5.60 mmol, 1.0 equiv.) was added. The vials were capped and stirred for 4 h at 120 °C. The initially heterogeneous reaction mixture becomes homogenous over time (see Figure S9).

Thereafter, the vials were cooled to rt in a water bath. The $poly(2\text{-ethylhexyl acrylate})_{SIGMA2}$ ($P(2\text{-EHA}))_{SIGMA2}$) was isolated by precipitating into MeOH (10 mL) and removing the supernatent. Then, the polymer was purified by dissolving in minimal amounts of THF (1 mL), precipitating into MeOH (10 mL), and removing the supernatent. This process was repeated three times. The resulting solid was dried under high vacuum at 60 °C for 3 h.

The isolated yields were 77% (3 equiv), 77% (5 equiv), 89% (10 equiv), and 89% (15 equiv).

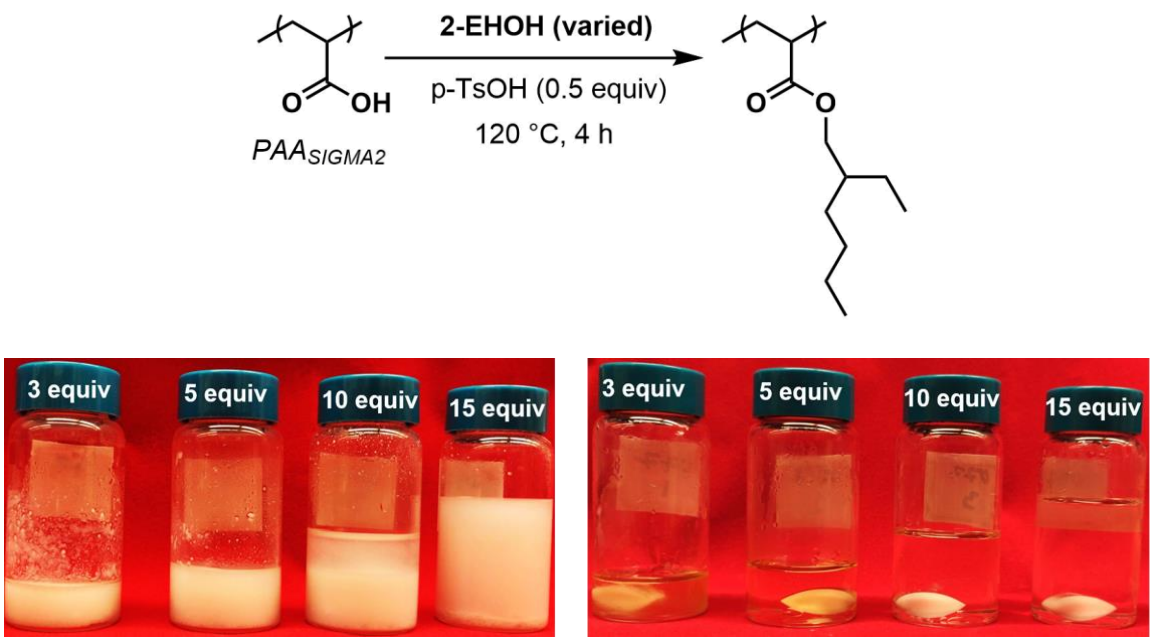

Figure A2-9. Esterification reactions for 3–15 equiv. 2-ethylhexanol before (left) and after (right) heating to 120 °C for 4 h.

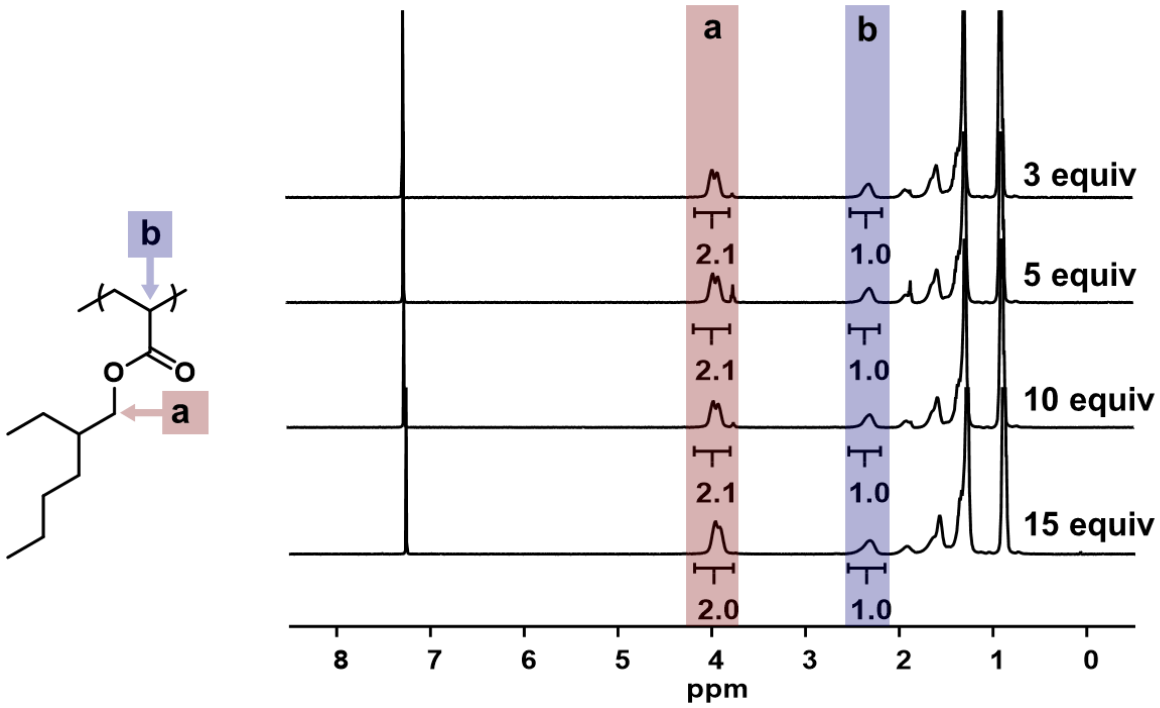

Figure A2-10. ^{1}H NMR spectra of P(2-EHA)$_{SIGMA2}$ made from 3–15 equiv. alcohol (500 MHz, $CDCl_3$).

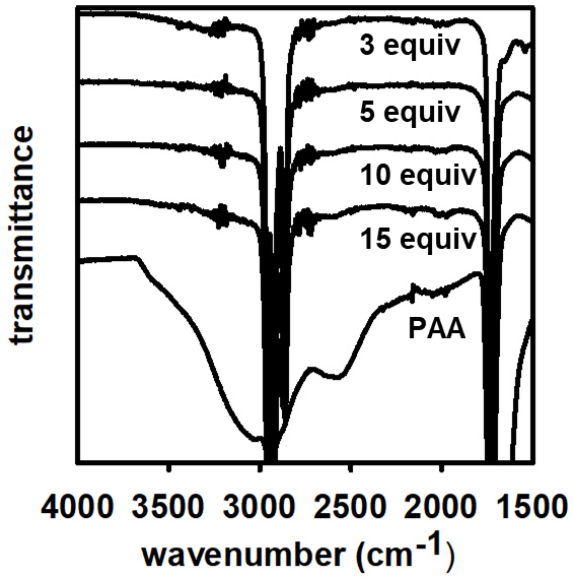

Figure A2-11. IR spectra of P(2-EHA)$_{SIGMA2}$ made from 3–15 equiv. alcohol.

Effect of adding water on conversion

2-ethylhexanol (1.95 mL, 12.49 mmol, 3.00 equiv) was added to 15 mL pressure vessels equipped with stir bars, followed by DI H_2O (0.22 mL, 12.49 mmol, 3.00 equiv). Sulfuric acid (0.055 mL, 1.04 mmol, 0.25 equiv) was then added and the vessel was stirred at 120 °C. PAA_{SPP} (300 mg, 4.20 mmol, 1.00 equiv) was subsequently added and the pressure vessels were immediately sealed and left to run for 6 h. Thereafter, the vials were placed in a water bath to cool and then the polymer was precipitated with MeOH (~10 mL). The $P(2\text{-EHA})_{SPP}$ obtained was purified by dissolving in minimal amounts of THF (~2 mL) and precipitating with MeOH (~10 mL) twice, followed by drying under high vacuum at 60 °C for 3 h. The isolated yield was 79%.

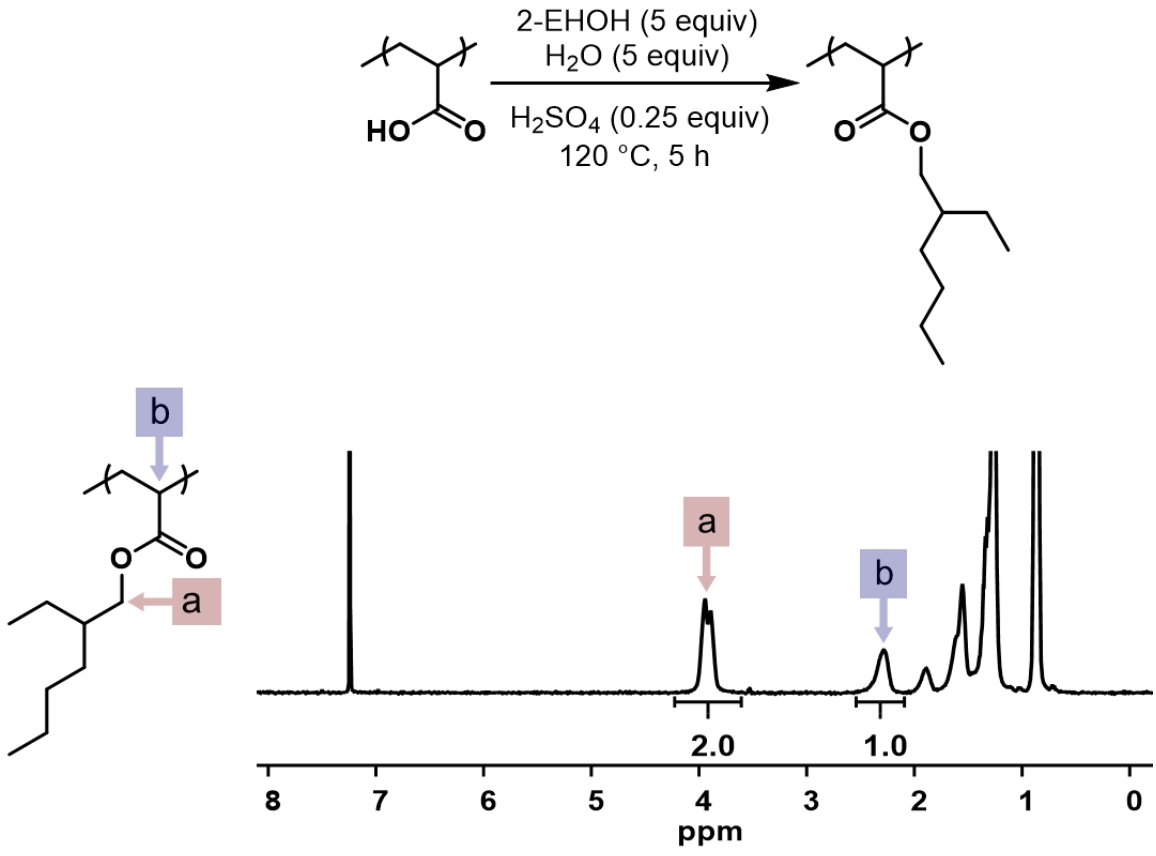

Figure A2-12. ^1H NMR spectra of $P(2\text{-EHA})_{SPP}$ (500 MHz, $CDCl_3$).

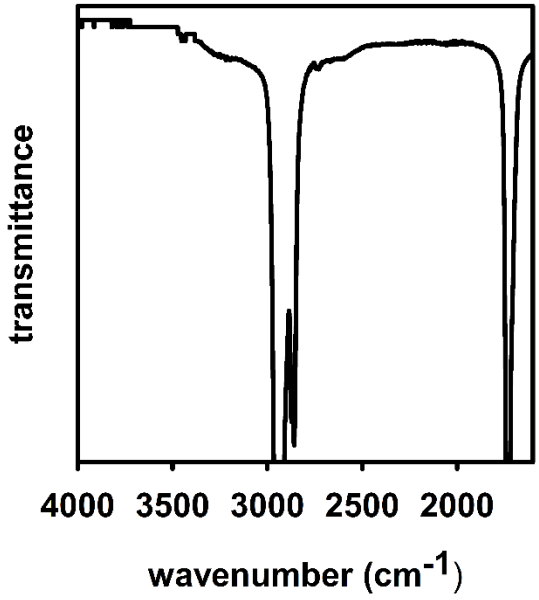

Figure A2-13. IR spectrum of P(2-EHA)$_{SPP}$ made in the presence of added H_2O.

Effect of adding water on conversion for small molecule carboxylic acids

(This experiment was run in duplicate.) To two 15 mL pressure vessels equipped with stir bars, 2-EHOH (3.91 mL, 25 mmol, 5.0 equiv.), sulfuric acid (0.067 mL, 1.25 mmol, 0.25 equiv.), and acetic acid (0.29 mL , 5.0 mmol, 1.0 equiv.) were added. Then, DI H_2O (0.45 mL, 25 mmol, 5.00 equiv.) was added to one vessel. Both vessels were sealed and stirred at 120 °C for 8 h. Thereafter, the vessels were cooled in a rt water bath and aliquots (0.1 mL) were diluted with 2:1 $CDCl_3$/pyridine-d_5 (0.4 mL) for ^1H NMR spectroscopic analysis.

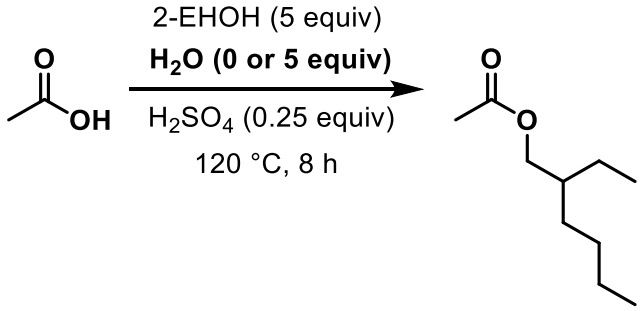

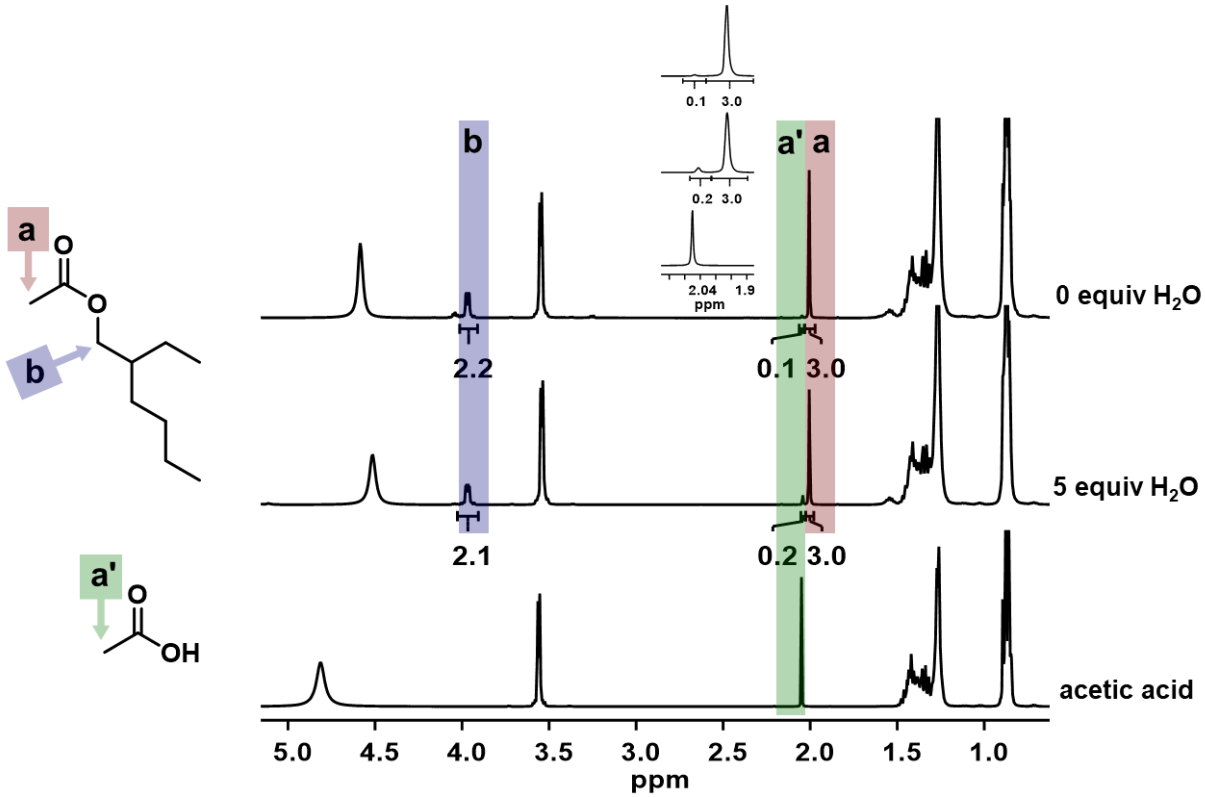

Figure A2-14. ^{1}H NMR spectra of acetic acid esterification with 2-ethylhexanol in the presence (middle) and absence (top) of water (500 MHz, $CDCl_3$/pyridine-d_5 at 2:1).

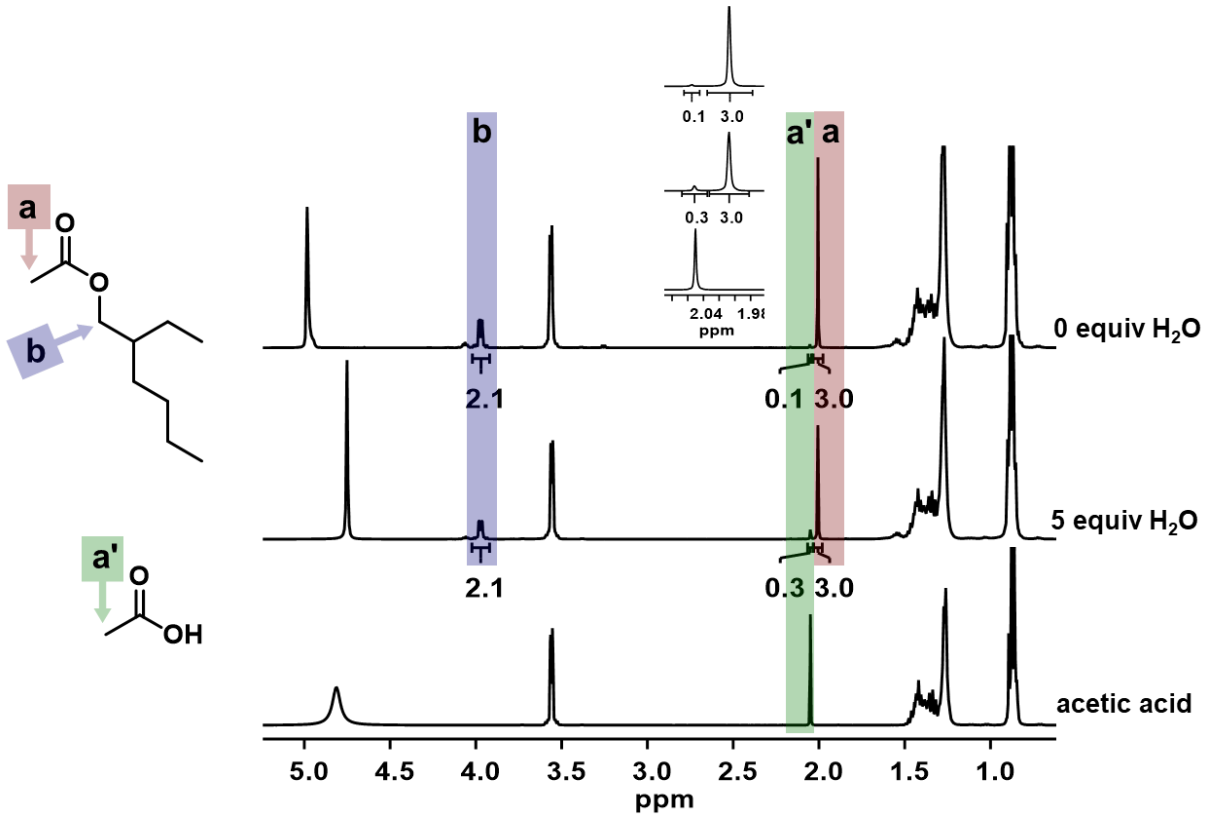

Figure A2-15. ^{1}H NMR spectra of acetic acid esterification with 2-ethylhexanol in the presence (middle) and absence (top) of water (500 MHz, $CDCl_3$/pyridine-d_5 at 2:1).

Table A2-6. Calculated conversions for H_2O (0 or 5 equiv) esterification conditions

	a	a'	% conversion
H_2O (0 equiv)	0.1	3.0	97%
H_2O (5 equiv)	0.2	3.0	94%

	average
H_2O (0 equiv)	97%
H_2O (5 equiv)	94%

	a	a'	% conversion
H_2O (0 equiv)	0.1	3.0	97%
H_2O (5 equiv)	0.2	3.0	94%

(This experiment was run in duplicate.) To two 15 mL pressure vessels equipped with stir bars, EtOH (1.5 mL, 26 mmol, 5.1 equiv.), H_2SO_4 (0.0670 mL, 1.25 mmol, 0.245 equiv.) and acetic acid (0.29 mL, 5.1 mmol, 1.0 equiv.) were added. Then, DI H_2O (0.45 mL, 25 mmol, 4.9 equiv.) was added to one vessel. Both vessels were sealed and stirred at 120 °C for 8 h. Thereafter, the vessels were cooled to rt in a water bath and aliquots (0.1 mL) were diluted with 2:1 $CDCl_3$/pyridine-d_5 (0.4 mL) for ^{1}H NMR spectroscopic analysis.

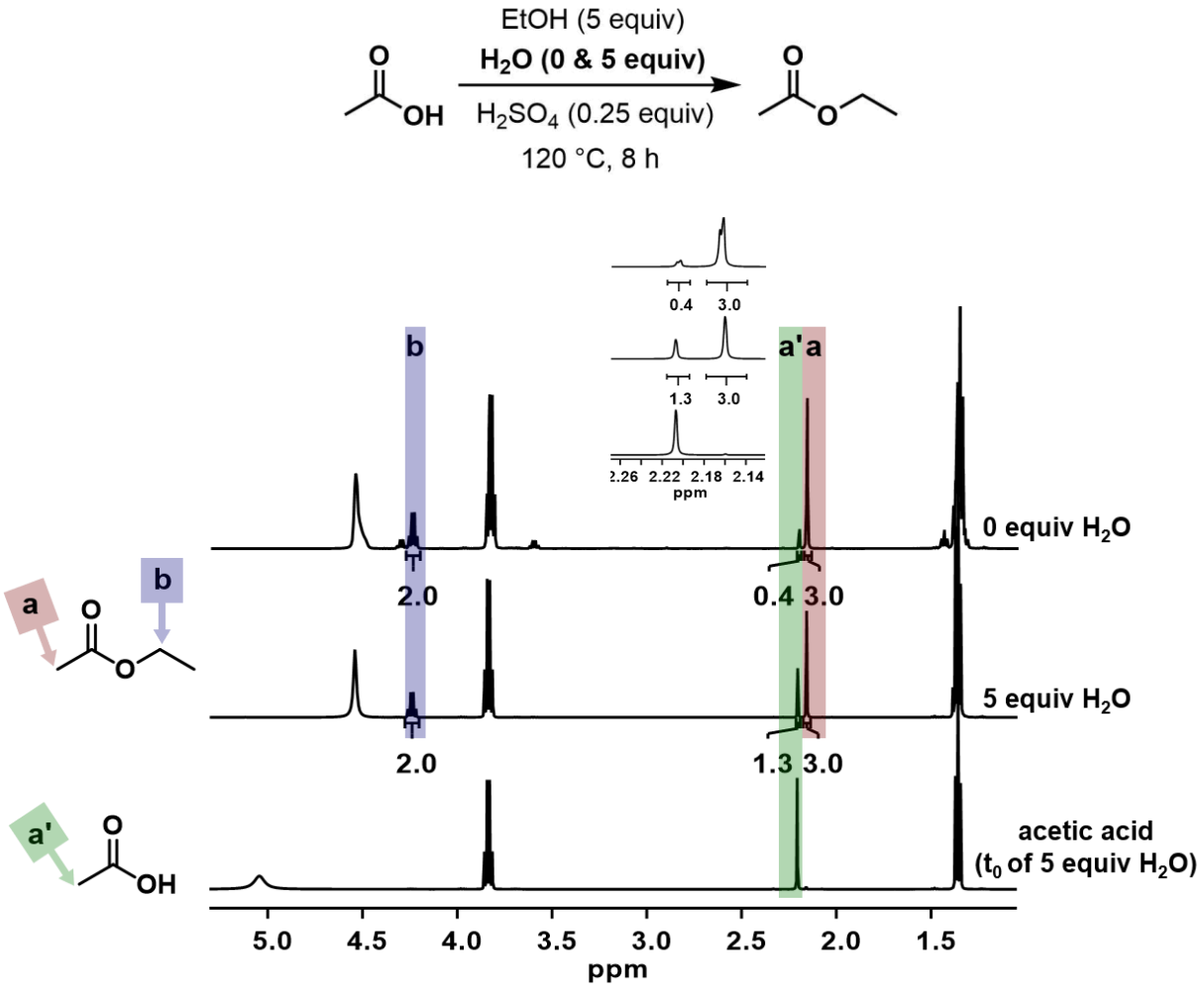

Figure A2-16. ^{1}H NMR spectra of acetic acid esterification with EtOH in the presence (middle) and absence (top) of water (500 MHz, $CDCl_3$/pyridine-d_5 at 2:1).

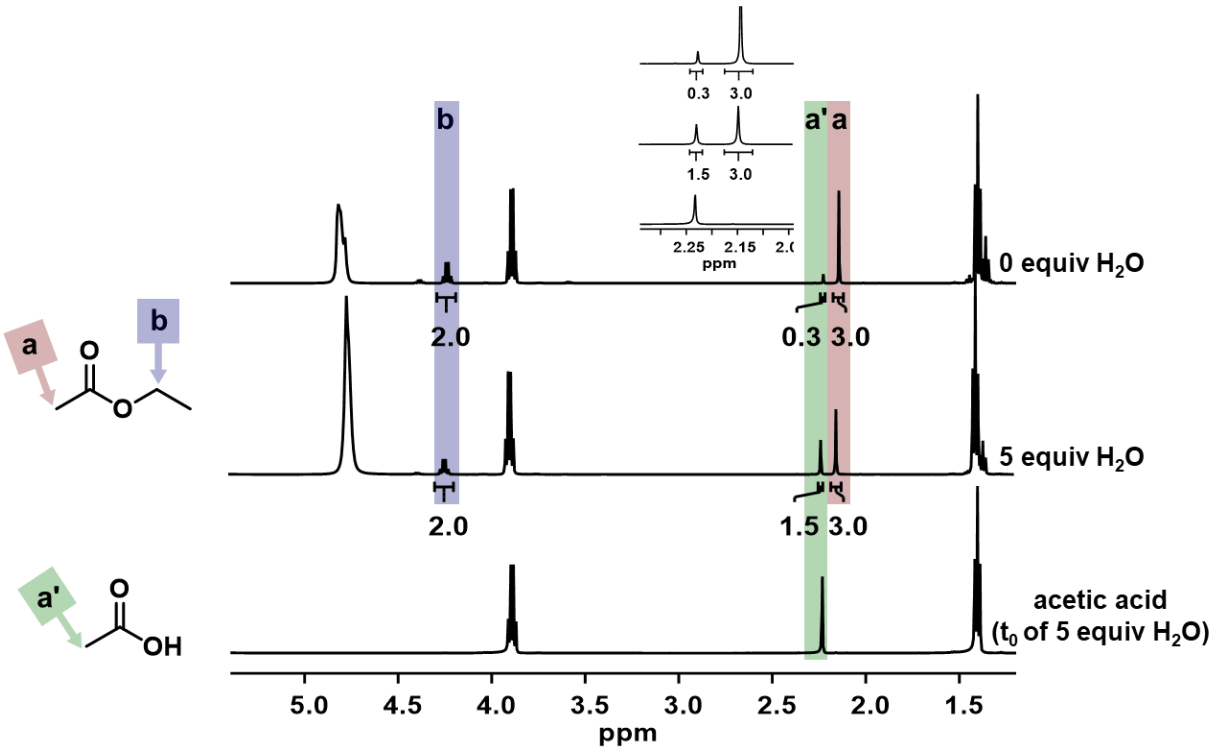

Figure A2-17. ^{1}H NMR spectra of acetic acid esterification with EtOH in the presence (middle) and absence (top) of water (500 MHz, $CDCl_3$/pyridine-d_5 at 2:1).

Table A2-7. Calculated conversions for H_2O (0 or 5 equiv) esterification conditions

	a'	a	% conversion
H_2O (0 equiv)	0.4	3.0	88%
H_2O (5 equiv)	1.3	3.0	70%

	average
H_2O (0 equiv)	90%
H_2O (5 equiv)	68%

	a'	a	% conversion
H_2O (0 equiv)	0.3	3.0	91%
H_2O (5 equiv)	1.5	3.0	67%

To two 15 mL pressure vessels equipped with stir bars, 2-EHOH (1.8 mL, 12. mmol, 5.0 equiv.), H_2SO_4 (0.031 mL, 0.58 mmol, 0.25 equiv.) and undecanoic acid (433 mg, 2.30 mmol, 1.00 equiv.) were added. Then, DI H_2O (0.21 mL, 12 mmol, 5.0 equiv.) was added to one vessel. Both vessels were sealed and stirred at 120 °C for 8 h. Thereafter, the vessels were cooled in a rt water bath and aliquots (0.1 mL) were diluted with 2:1 $CDCl_3$/pyridine-d_5 (0.4 mL) for ^{1}H NMR spectroscopic analysis.

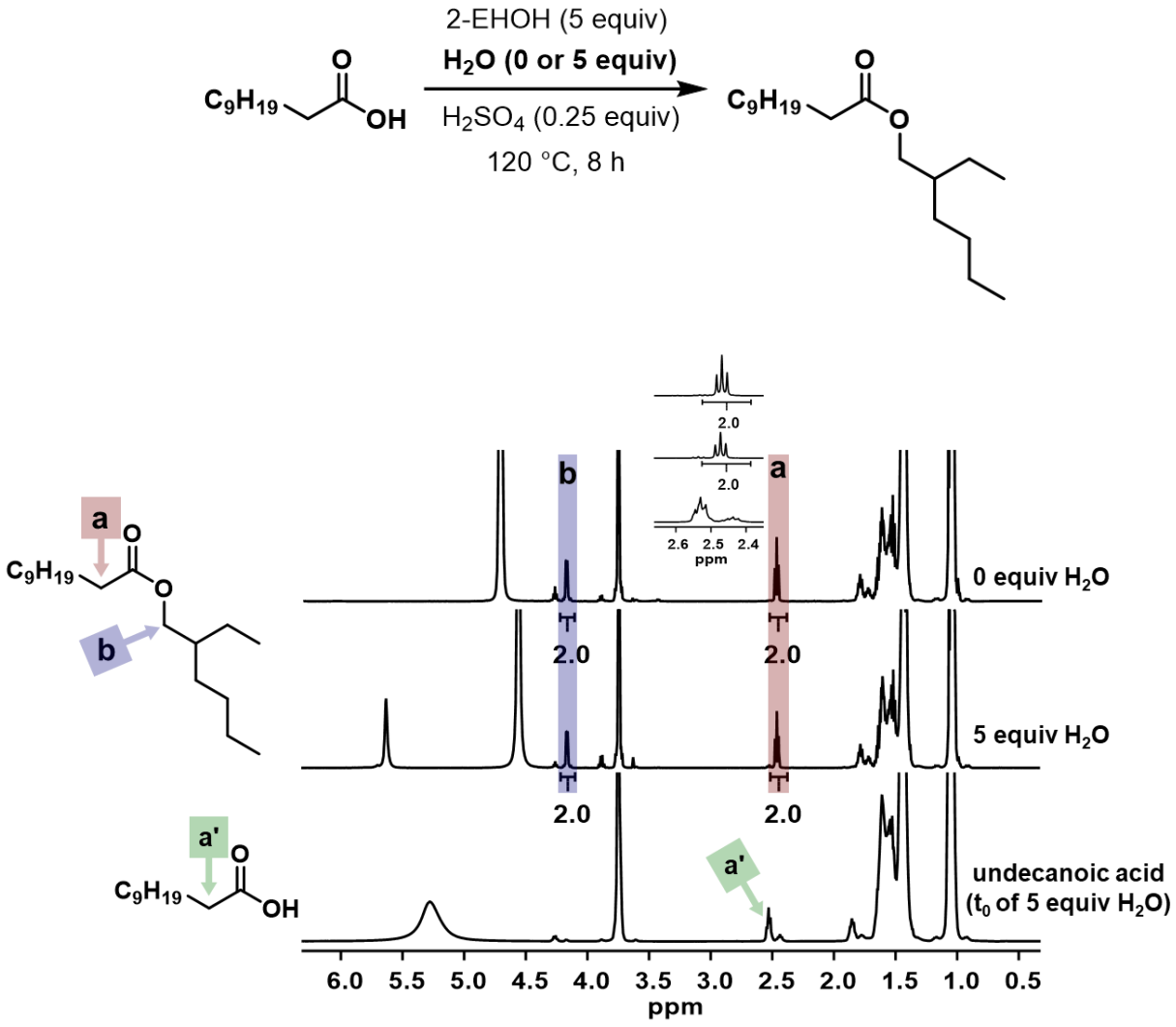

Figure A2-18. ^{1}H NMR spectra of undecanoic acid esterification with 2-ethylhexanol in the presence (middle) and absence (top) of water (500 MHz, $CDCl_3$/pyridine-d_5 at 2:1).

To two 15 mL pressure vessels equipped with stir bars, 2-EHOH (1.8 mL, 12 mmol, 5.2 equiv.), H_2SO_4 (0.031 mL, 0.58 mmol, 0.25 equiv.) and decanoic acid (400 mg, 2.32 mmol, 1.00 equiv.) were added. Then, DI H_2O (0.21 mL, 12 mmol, 5.2 equiv.) was added to one vessel. Both vessels were sealed and stirred at 120 °C for 8 h. Thereafter, the vessels were cooled to rt in a water bath and aliquots (0.1 mL) were diluted with 2:1 $CDCl_3$/pyridine-d_5 (0.4 mL) for ^{1}H NMR spectroscopic analysis.

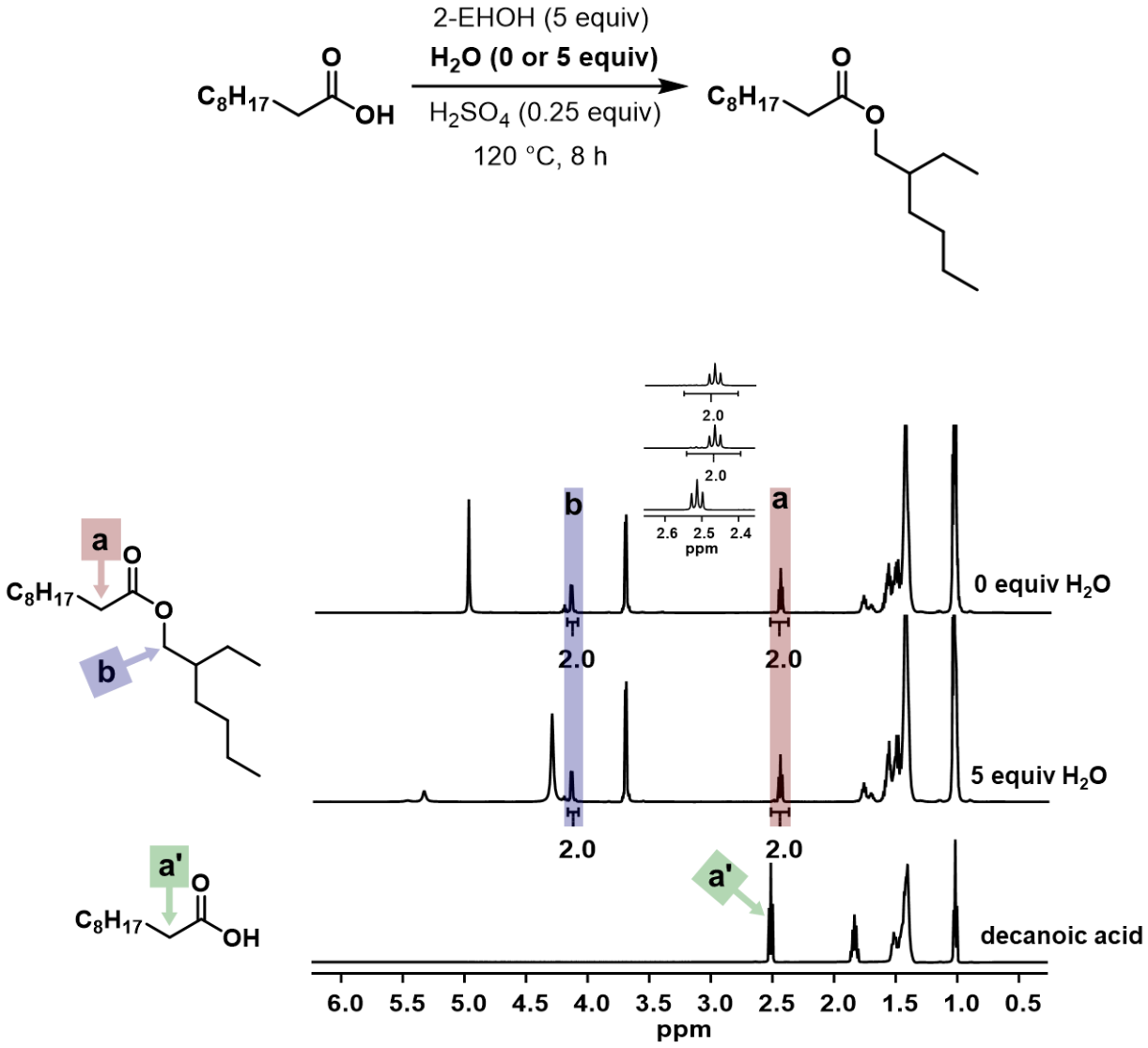

Figure A2-19. ^{1}H NMR spectra of decanoic acid esterification with 2-ethylhexanol in the presence (middle) and absence (top) of water (500 MHz, $CDCl_3$/pyridine-d_5 at 2:1).

Table A2-8. Calculated conversions for H_2O (0 or 5 equiv) esterification conditions

	a'	a	% conversion
H_2O (0 equiv)	0	2.0	100%
H_2O (5 equiv)	0	2.0	100%

	average
H_2O (0 equiv)	100%
H_2O (5 equiv)	100%

	a'	a	% conversion
H_2O (0 equiv)	0	2.0	100%
H_2O (5 equiv)	0	2.0	100%

To two 15 mL pressure vessels equipped with stir bars, EtOH (0.58 mL, 9.98 mmol, 5.0 equiv), sulfuric acid (0.027 mL, 0.50 mmol, 0.25 equiv) and undecanoic acid (400 mg , 2 mmol, 1.0 equiv) were added. Then, DI H_2O (0.18 mL , 9.98 mmol, 5.0 equiv) was added to one vessel. Both vessels were sealed stirred at 120 °C for 8 h. Thereafter, the vessels were cooled to rt in a water bath and aliquots (0.1 mL) were diluted with 2:1 $CDCl_3$/pyridine-d_5 (0.4 mL) for ^{1}H NMR spectroscopic analysis.

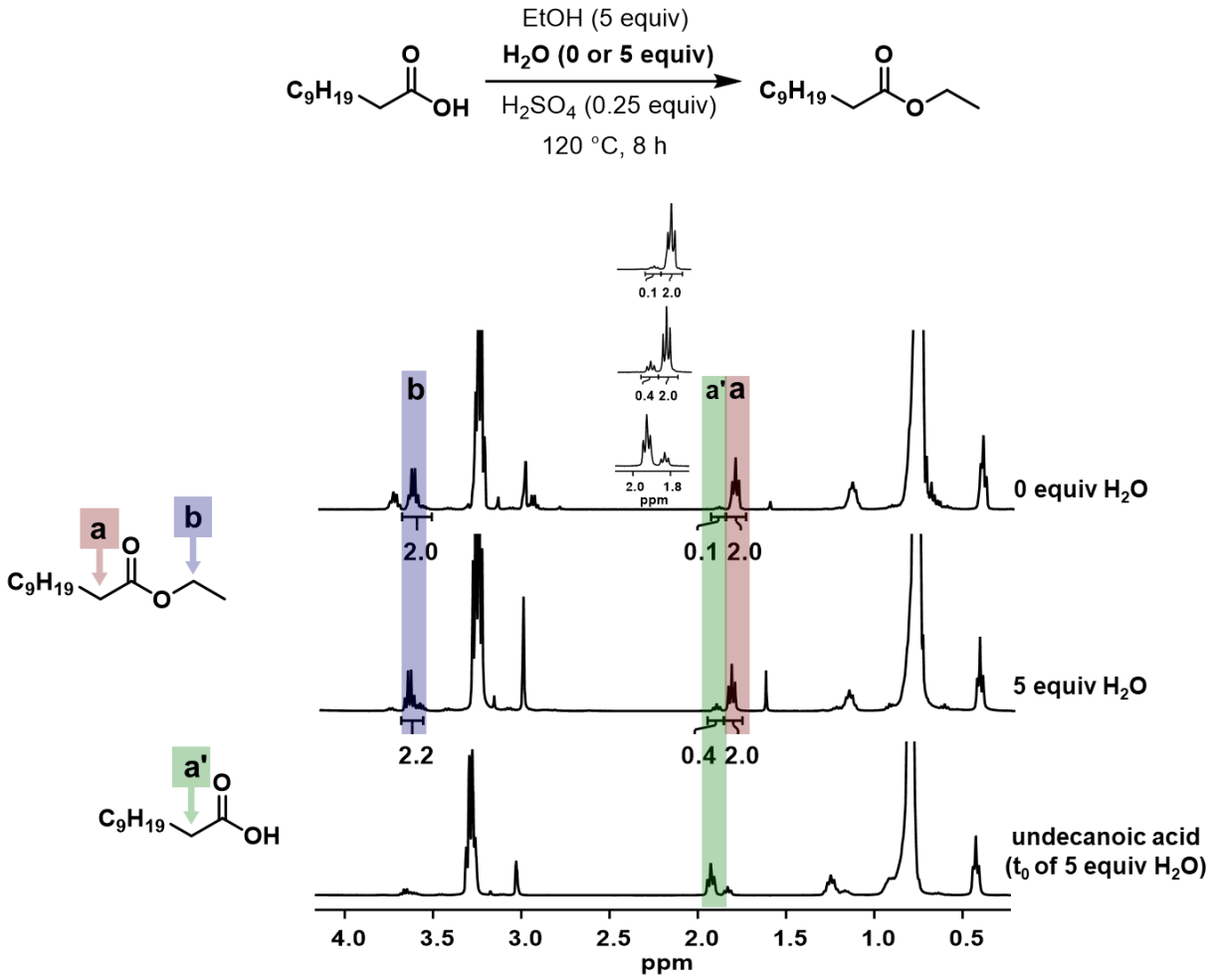

Figure A2-20. ^{1}H NMR spectra of undecanoic acid esterification with EtOH in the presence (middle) and absence (top) of water (500 MHz, $CDCl_3$/pyridine-d_5 at 2:1).

To two 15 mL pressure vessels equipped with stir bars, EtOH (0.74 mL, 12.6 mmol, 5.0 equiv), sulfuric acid (0.034 mL, 0.63 mmol, 0.25 equiv), and undecanoic acid (470 mg , 2.52 mmol, 1.0

equiv) were added. Then, DI H_2O (0.23 mL , 12.6 mmol, 5.0 equiv) was added to one vessel. Both vessels were sealed and stirred at 120 °C for 8 h. Thereafter, the vessels were cooled to rt in a water bath and aliquots (0.1 mL) were diluted with 2:1 $CDCl_3$/pyridine-d_5 (0.4 mL) for ^{1}H NMR spectroscopic analysis.

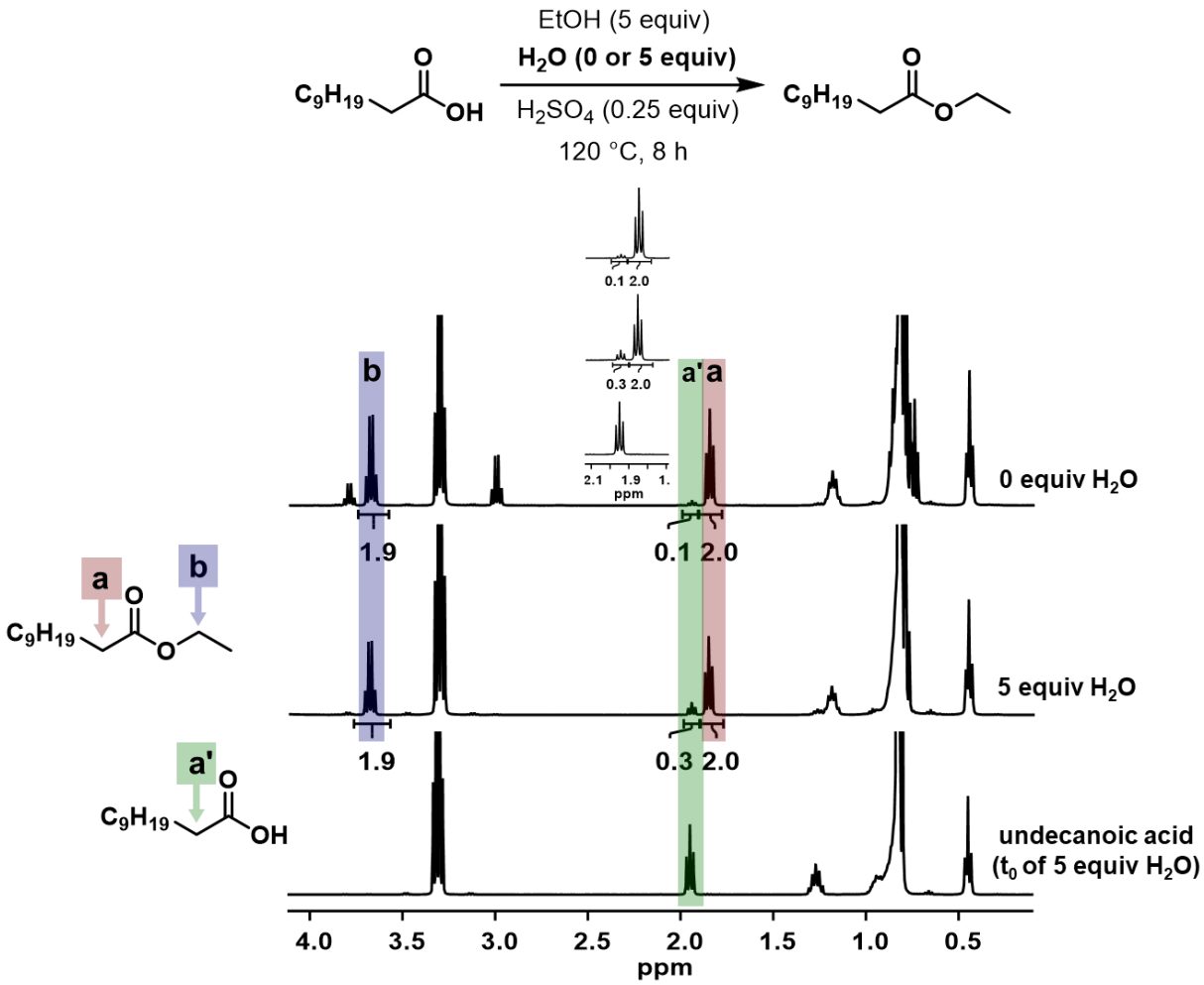

Figure A2-21. ^{1}H NMR spectra of undecanoic acid esterification with EtOH in the presence (middle) and absence (top) of water (500 MHz, $CDCl_3$/pyridine-d_5 at 2:1).

Table A2-9. Calculated conversions for H_2O (0 or 5 equiv) esterification conditions.

	a'	a	% conversion
H_2O (0 equiv)	0.1	2.0	95%
H_2O (5 equiv)	0.4	2.0	83%

	a'	a	% conversion
H_2O (0 equiv)	0.1	2.0	95%
H_2O (5 equiv)	0.3	2.0	87%

	average
H_2O (0 equiv)	95%
H_2O (5 equiv)	85%

Free-energy calculations

Background on free energy calculations

The calculation of free-energy differences between two states is a common and widely adopted method in computational chemistry.[2] To assess the difference between two states, the states must have a configurational overlap large enough for a comparison to be made. In practice, most end states do not have such an overlap, necessitating the use of bridge states that are a mix of both systems of interest. Herein the degree of perturbation is denoted as λ.

System construction

Nonamers AA_9, BA_8AA_1, AA_8BA_1, and BA_9 were constructed using Avogadro[3] and then solvated in a 3:1 butanol:water cuboid using PACKMOL,[4] providing a 12 Å buffer between the nonamer and the edge of the cuboid. This resulted in a 41.841 x 44.981 x 45.167 Å box with 480 butanols and 160 waters for BA_8AA_1 and BA_9, and a 37.678 x 40.876 x 35.483 Å box with 333 butanols and 111 waters for AA_9 and AA_8BA_1. All of the nonamers studied were isotactic. TIP3P parameters[5] were used for water, and parameters for butanol and the nonamers were derived from CGenFF[6] using MATCH.[7]

Molecular Dynamics

Molecular dynamics studies were performed using the CHARMM molecular mechanics platform (developmental version 44a1)[8] with the domain decomposition (DOMDEC) computational kernels on graphics processing units (GPUs).[9] Molecular dynamics were performed using the canonical ensemble (NVT) at 298.15 K using a Langevin thermostat. The Leapfrog Verlet integrator was used with an integration time of 2 fs. Electrostatic interactions were modeled using a particle-mesh Ewald method[10,11,12] with a grid spacing of 1 Å, interpolation order of 6,

and a κ-value of 0.32 $Å^{-1}$. Van der Waals interactions were modelled using a 9 Å switching radius, 10 Å cutoff radius, and a 12 Å neighbor list.

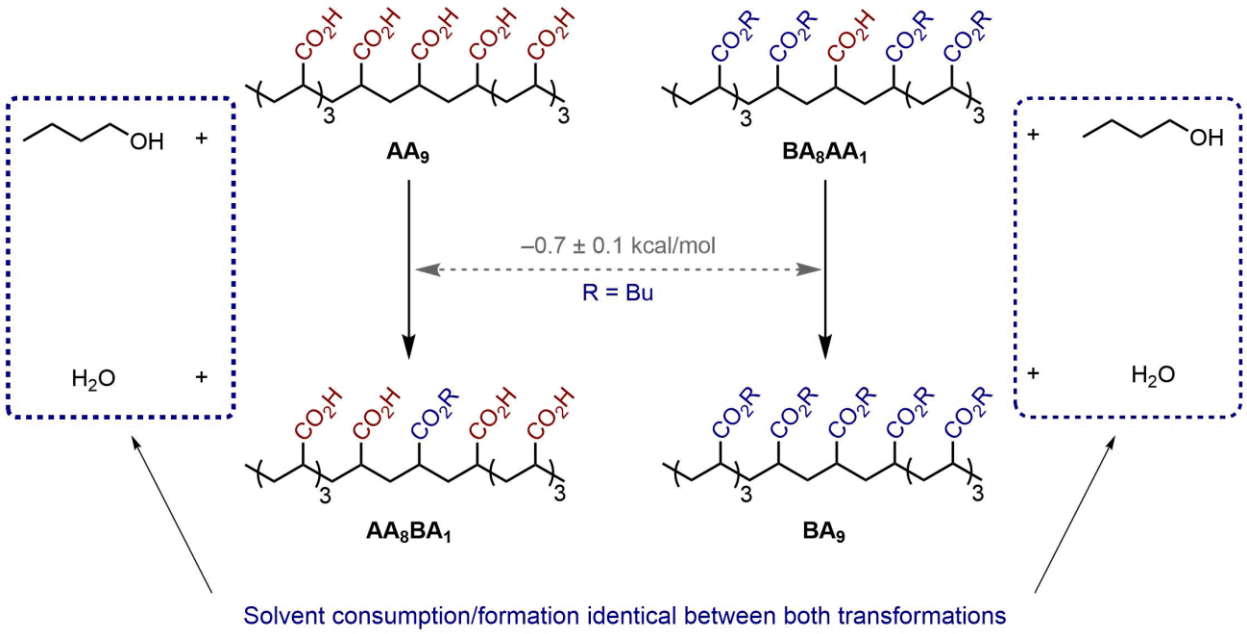

Figure A2-22. The full thermodynamic cycle used to evaluate the free energy of esterification.

Calculating the difference in free energy of esterification (ΔΔA)

The difference in free energy of esterification (ΔΔA) was calculated using the Multistate Bennet Acceptance Ratio method[13] using a dual topology approach. Both AA_9 and BA_8AA_1 were perturbed to AA_8BA_1 and BA_9, respectively, using 11 discrete λ states, $0 \rightarrow 1$, in steps of $\Delta\lambda = 0.1$. Perturbation of λ was achieved using the block module of CHARMM, λ values held constant using the MSλD ffix keyword.[14] Non-bonding interactions were scaled by λ using a soft-core potential.[15] Prior to molecular dynamics simulations, a system was subjected to 200 steps of steepest descent minimization. Each λ state was subjected to 200 steps of steepest descent minimization, followed by equilibration for 5 ns. Production runs consisted of 50 ns of simulation, with trajectory frames saved every 2,500 timesteps (yielding 10,000 frames total).

Energy Calculation Results

The free energy difference between the λ=0 and other lambda states (0.1 to 1.0) for the AA_9 and BA_8AA_1 systems are shown in Table S5. From the ΔA value for when λ=1 for both systems, the ΔΔA of esterification is calculated to be -0.7 ± 0.1 kcal/mol. As the consumption of butanol and the evolution of water is expected to be identical in AA_8BA_1 and BA_9, the ΔA of butanol consumption and water formation during the process of esterification was ignored, as those terms would cancel out in the calculation of ΔΔA of esterification (Figure S22).

Table A2-10. Values for the difference in free energy between λ=0 and other λ values for the AA_9 and BA_8AA_1 systems.

	$AA_9 \rightarrow AA_8BA_1$ ΔA relative to λ=0		**$BA_8AA_1 \rightarrow BA_9$ ΔA relative to λ=0**	
λ	**in k_BT**	**in kcal/mol**	**in k_BT**	**in kcal/mol**
0.0	0.0 ± 0.0	0.0 ± 0.0	0.0 ± 0.0	0.0 ± 0.0
0.1	22.5 ± 0.1	13.35 ± 0.07	21.2 ± 0.1	12.58 ± 0.06
0.2	36.8 ± 0.1	21.78 ± 0.08	35.1 ± 0.1	20.74 ± 0.06
0.3	48.4 ± 0.1	28.70 ± 0.08	46.4 ± 0.1	27.51 ± 0.06
0.4	58.5 ± 0.1	34.65 ± 0.08	56.4 ± 0.1	33.44 ± 0.06
0.5	67.4 ± 0.1	39.92 ± 0.08	65.4 ± 0.1	38.75 ± 0.06
0.6	75.6 ± 0.1	44.76 ± 0.08	73.7 ± 0.1	43.66 ± 0.06
0.7	83.1 ± 0.1	49.24 ± 0.08	81.4 ± 0.1	48.21 ± 0.06
0.8	90.0 ± 0.1	53.31 ± 0.08	88.4 ± 0.1	52.37 ± 0.06
0.9	96.1 ± 0.1	56.93 ± 0.08	94.7 ± 0.1	56.10 ± 0.06
1.0	101.3 ± 0.1	60.04 ± 0.08	100.2 ± 0.1	59.35 ± 0.06

Comparing the difference in free energy of esterification between poly(acrylic acid) and poly(butyl acrylate) with the effects of changing solvent composition.

The free energy of a given reaction is dependent on the free energy of the reaction at standard conditions (calculated when the concentration of both products and reactants is 1M), and concentration of reagents in the given conditions (equation 2).

$$\Delta A=\Delta A°+k_BTln\left(\frac{[Products]}{[Reactants]}\right) \quad (2)$$

In an esterification reaction, the concentration of water increases over time, and the concentration of alcohol decreases. Using the right-hand term of equation 2, we can estimate the effect of changing solvent composition on the free energy of the reaction (equation 3).

$$\Delta\Delta A_{solv}=k_BT\left(ln\left(\frac{[Water]_{end}}{[Alcohol]_{end}}\right)-ln\left(\frac{[Water]_{Start}}{[Alcohol]_{Start}}\right)\right) \quad (3)$$

Using the starting conditions of the reaction, and the expected conditions if full conversion is achieved (1 unit of alcohol is replaced by 1 unit of water), we can estimate the energetic effect that the change in solvent composition has on ΔA, denoted as $\Delta\Delta A_{solv}$ (Table S6.)

Table A2-11. Expected $\Delta\Delta A_{solv}$ values for select reaction conditions.

Scenario	**Alcohol : Water at start**	**Alcohol : Water at end**	**$\Delta\Delta A_{solv}$ in units of k_BT**
Figure S21, esterification conditions	5:3	4:4	0.51
Figure S21, small molecule testing	5:5	4:6	0.41
Free energy calculation	3:1	2:2	1.10

In all of the scenarios listed in Table S6, the $\Delta\Delta A_{solv}$ is less than or comparable in magnitude to the change in free energy of esterification due the change in hydrophobicity (-1.16 units of k_BT). This shows that the increase in hydrophobicity as esterification progresses counters the free energy

contribution due to buildup of water, allowing the reaction to continue to proceed forward in a free-energy favorable fashion.

Esterifying PAA $_{P\&G}$ fragments to make PSAs

PAA $_{P\&G\_5\%\text{-}0min}$: To a 75 mL pressure vessel, 2-EHOH (3.80 mL, 24.3 mmol, 5.00 equiv.) and H_2SO_4 (0.065 mL, 1.21 mmol, 0.25 equiv.) were added and stirred at 120 °C. While stirring, PAA $_{P\&G\_5\%\text{-}0min}$ (350 mg, 4.90 mmol, 1.00 equiv.) was subsequently added and the vessel was sealed and stirred for 10 h at 120 °C. Thereafter, the vessel was cooled in a rt water bath. The poly(2-ethylhexyl acrylate)$_{P\&G\text{-}0min}$ ((P(2-EHA))$_{P\&G\_5\%\text{-}0min}$) was isolated by precipitating into MeOH (20 mL) and removing the supernatant. Then, the polymer was purified by dissolving in minimal amounts of THF (5 mL), precipitating into MeOH (20 mL), and removing the supernatant. This process was repeated three times. The resulting solid was dried under high vacuum at 80 °C for 10 h. The isolated yield was 81%. A portion of the P(2-EHA)$_{P\&G\_5\%\text{-}0min}$ (600 mg) was used for frequency sweep measurements.

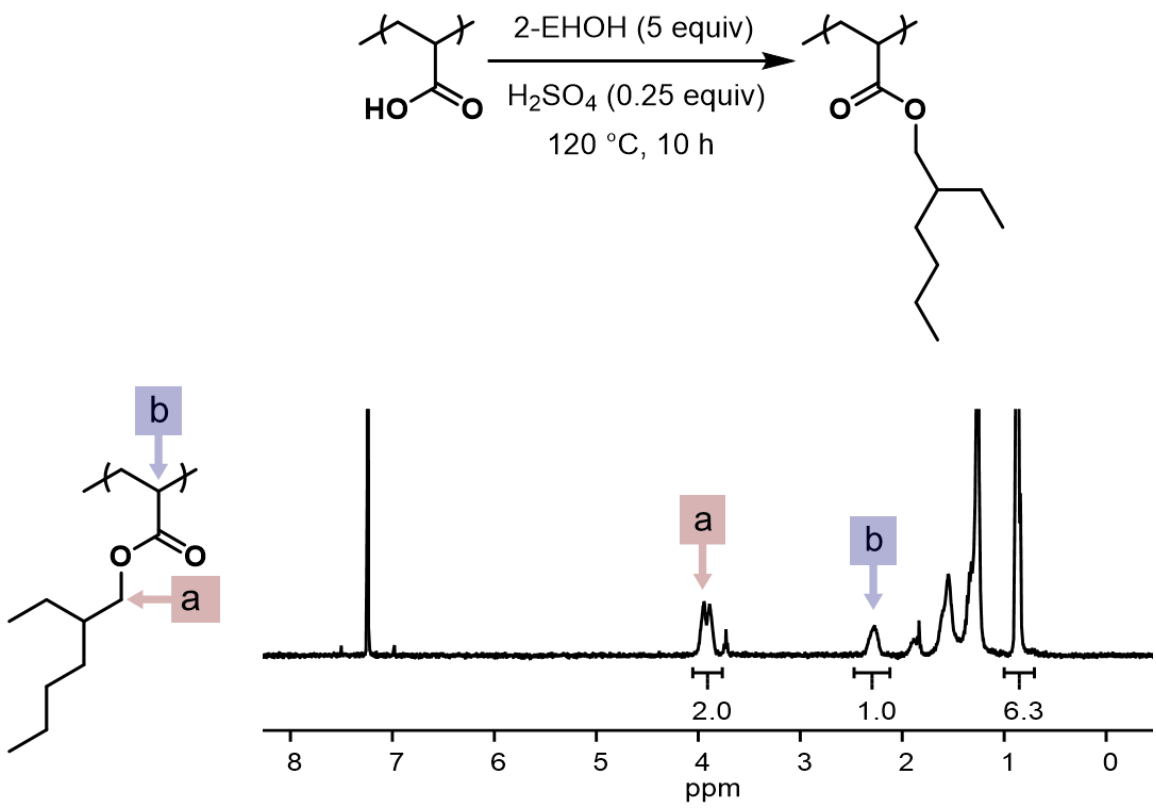

Figure A2-23. ^{1}H NMR spectrum for P(2-EHA)$_{P\&G\_5\%\text{-}0min}$ (500 MHz, $CDCl_3$).

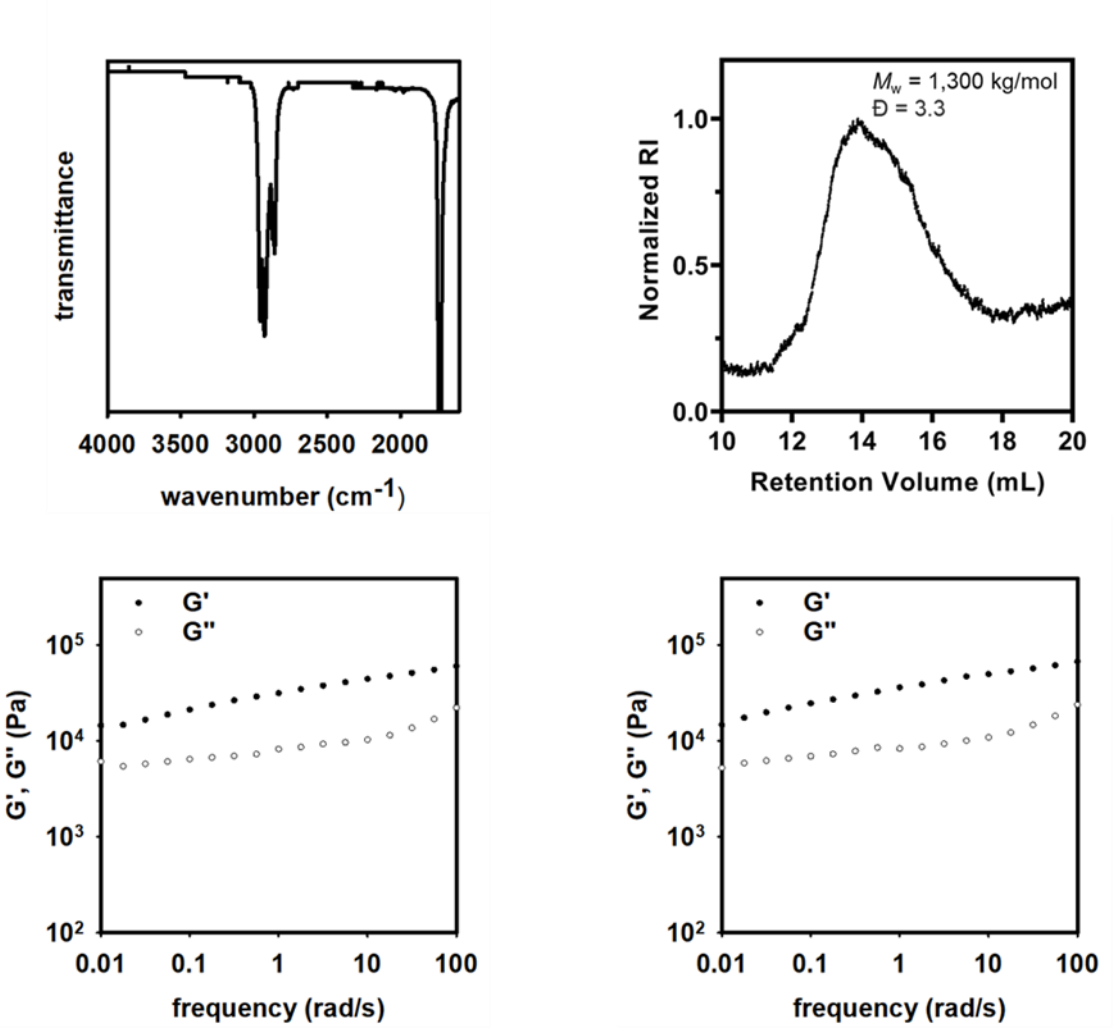

Figure A2-24. IR spectrum (top left), SEC trace (top right), and frequency sweeps (bottom) of P(2-EHA) $_{P\&G\_5\%\text{-}0min}$, made via esterifying decrosslinked $PAA_{P\&G\_5\%\text{-}0min}$.

P(2-EHA)$_{P\&G\_5\%-2min}$: To a 75 mL pressure vessel, 2-EHOH (4.34 mL, 27.8 mmol, 5.00 equiv.) and H_2SO_4 (0.074 mL, 1.39 mmol, 0.25 equiv.) were added and stirred at 120 °C. While stirring, PAA$_{P\&G_5\%-2min}$ (400 mg, 5.60 mmol, 1.00 equiv.) was subsequently added and the vessel was sealed and stirred for 10 h at 120 °C. Thereafter, the vessel was cooled in a rt water bath. The poly(2-ethylhexyl acrylate)$_{P\&G\_5\%-2min}$ ((P(2-EHA))$_{P\&G\_5\%-2min}$) was isolated by precipitating into MeOH (20 mL) and removing the supernatant. Then, the polymer was purified by dissolving in minimal amounts of THF (5 mL), precipitating into MeOH (20 mL), and removing the supernatant. This process was repeated three times. The resulting solid was dried under high vacuum at 80 °C for 10 h. The isolated yield was 78%. A portion of the P(2-EHA)$_{P\&G\_5\%-2min}$ (600 mg) was used for frequency sweep measurements.

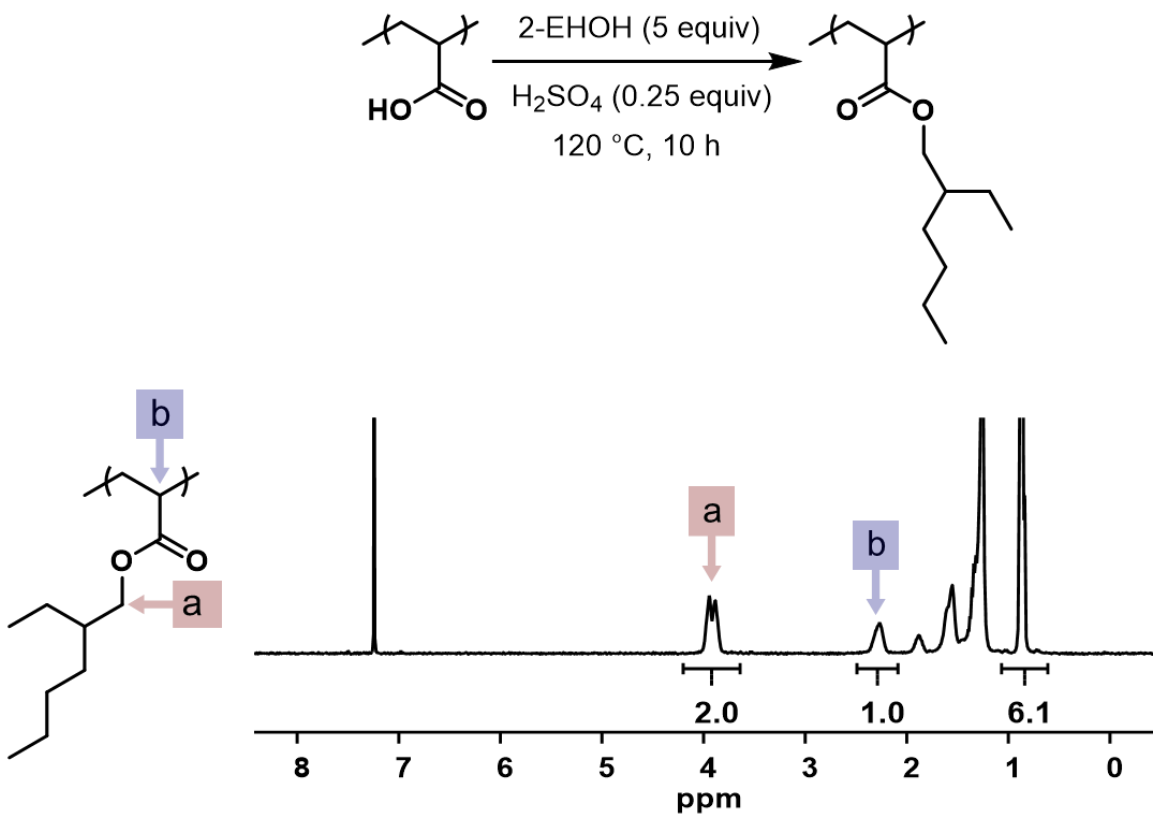

Figure A2-25. ^{1}H NMR spectrum for P(2-EHA)$_{P\&G\_5\%-2min}$ (500 MHz, $CDCl_3$).

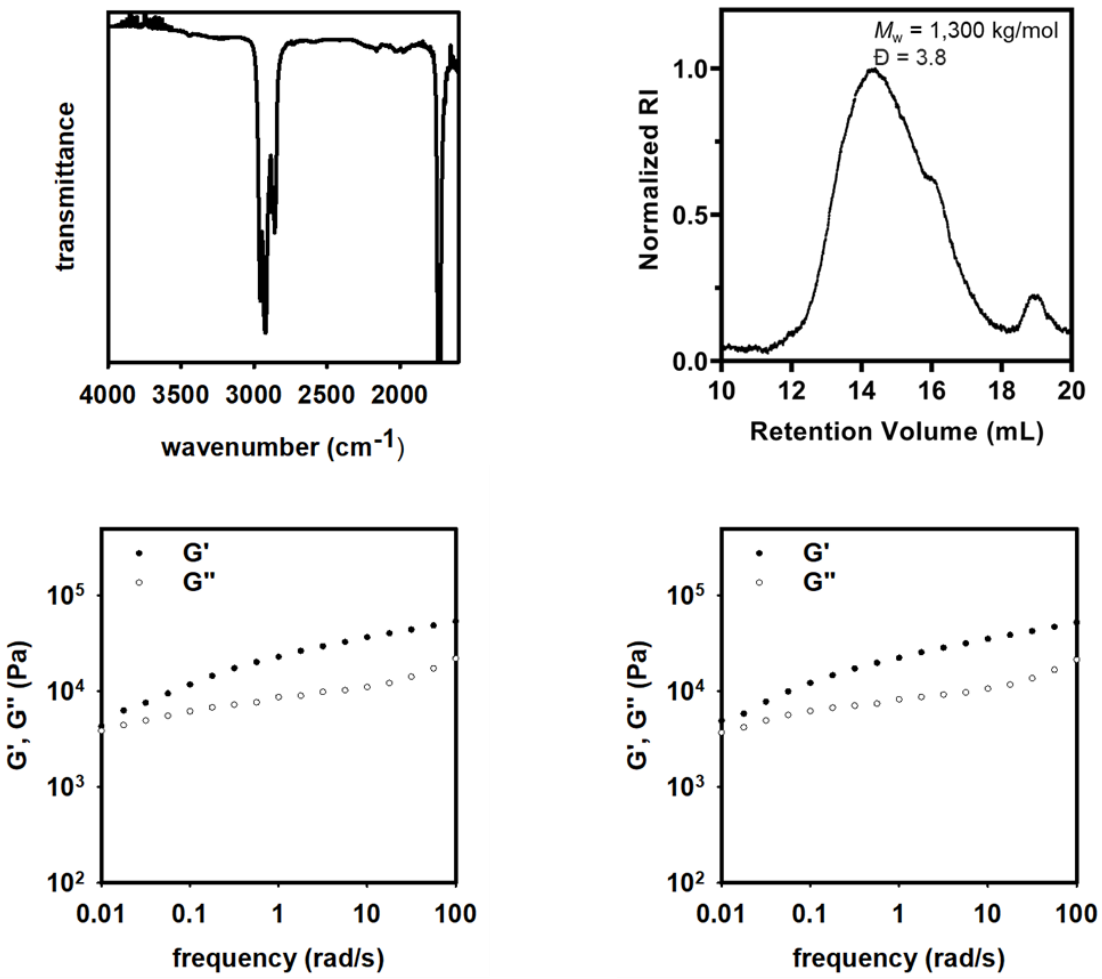

Figure A2-26. IR spectrum (top left), SEC trace (top right), and frequency sweeps (bottom) of P(2-EHA) $_{P\&G\_5\%\text{-}2min}$ made by esterifying decrosslinked PAA$_{P\&G_5\%\text{-}2min}$.

P(2-EHA)$_{P\&G\_2.5\%-1min}$: To a 75 mL pressure vessel, 2-EHOH (6.51 mL, 41.6 mmol, 5.00 equiv.) and H_2SO_4 (0.111 mL, 2.08 mmol, 0.25 equiv.) were added and stirred at 120 °C. While stirring, PAA$_{P\&G_2.5\%-1min}$ (600 mg, 10.4 mmol, 1.0 equiv.) was subsequently added and the vessel was sealed and stirred for 10 h at 120 °C. Thereafter, the vessel was cooled in a rt water bath. The poly(2-ethylhexyl acrylate)$_{P\&G\_2.5\%-1min}$ ((P(2-EHA))$_{P\&G\_2.5\%-1min}$) was isolated by precipitating into MeOH (20 mL) and removing the supernatant. Then, the polymer was purified by dissolving in minimal amounts of THF (5 mL), precipitating into MeOH (20 mL), and removing the supernatant. This process was repeated three times. The resulting solid was dried under high vacuum at 80 °C for 10 h. The isolated yield 73%. A portion of the P(2-EHA)$_{P\&G\_2.5\%-1min}$ (600 mg) was used for frequency sweep measurements.

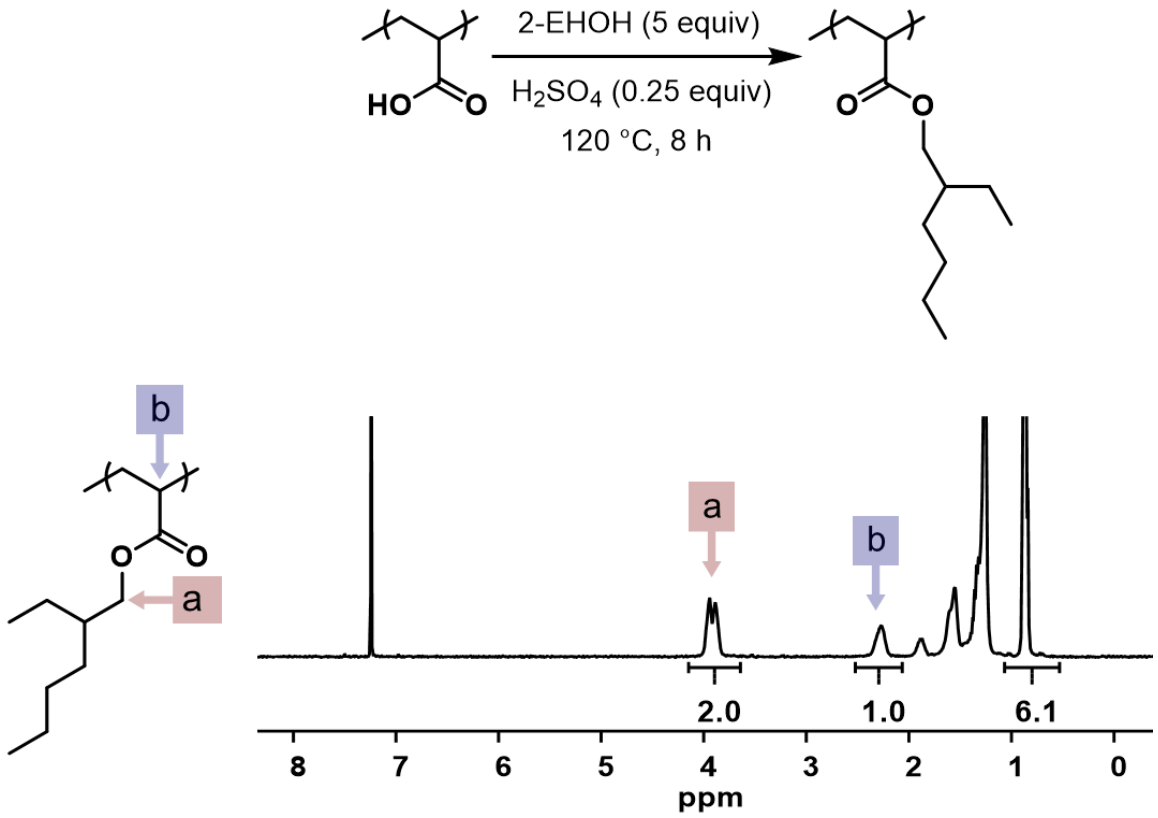

Figure A2-27. ^{1}H NMR spectrum for P(2-EHA)$_{P\&G\_2.5\%-1min}$ (500 MHz, $CDCl_3$).

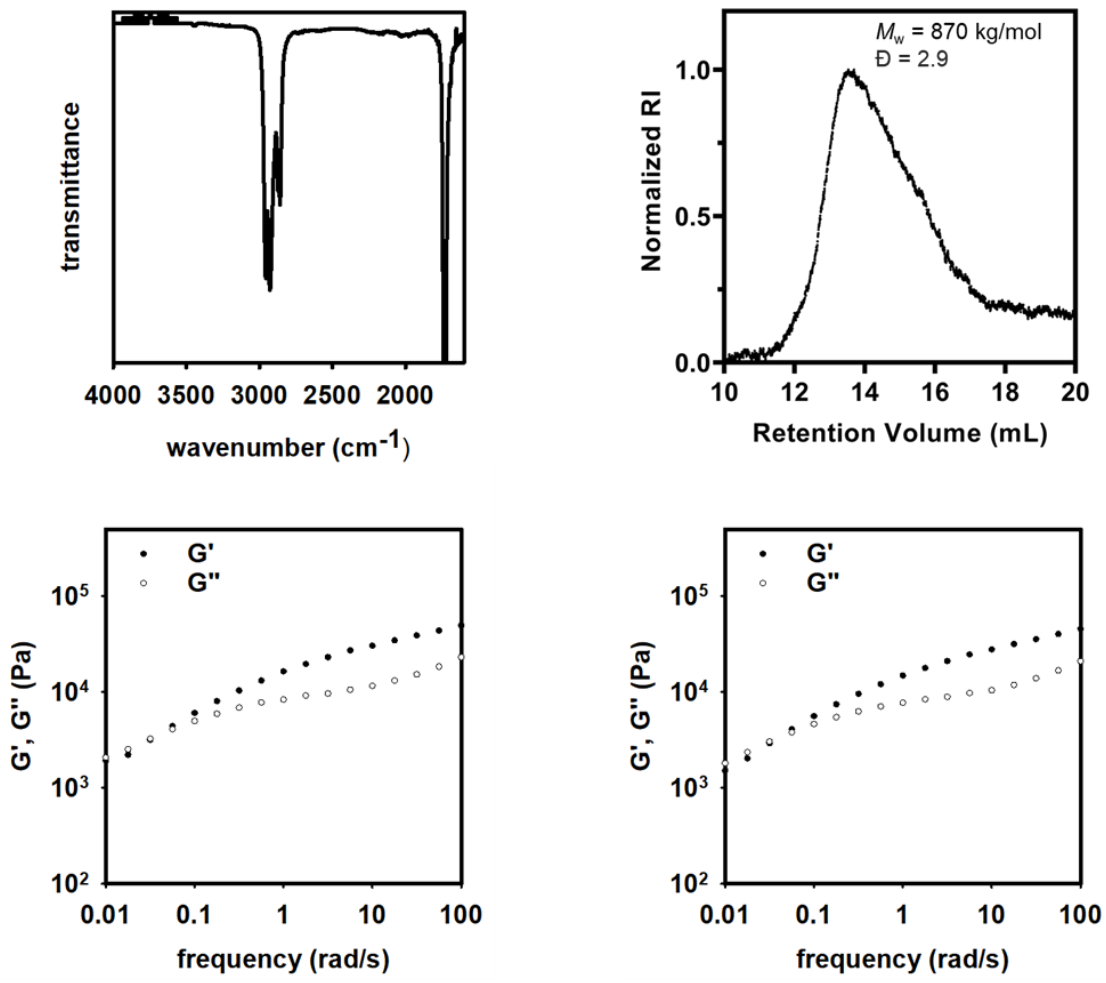

Figure A2-28. IR spectrum (top left), SEC trace (top right), and frequency sweeps (bottom) of P(2-EHA) $_{P\&G\_2.5\%\text{-}1min}$, made by esterifying decrosslinked PAA $_{P\&G\_2.5\%\text{-}1min}$.

Life cycle assessment

We applied a life cycle assessment (LCA) to evaluate the environmental impacts of these novel repurposing methods in comparison to business-as-usual production of poly(2-ethylhexyl acrylate) (P(2-EHA)).

Methods

Modeling of different disposal scenarios was done using the software SimaPro version 9.0.0.48 and the ecoinvent database version 3.5[16] and impacts were calculated using the ReCiPe 2016 v1.1 midpoint method, hierarchist version.[17] Processes and material production were assumed to take place in the US and therefore all ecoinvent processes were specific to a US scenario. LCA results for all impact categories are reported, paying specific attention to cumulative energy demand (CED) and global warming potential (GWP).

Goal and scope

The main goal of the LCA was to quantify the potential environmental impacts of the novel recovery processes and compare them to commercial production of P(2-EHA). Four total scenarios were investigated: 1) the reference scenario of P(2-EHA) production from ethanol and acrylic acid, 2) hydrolysis of reused superabsorbent poly(acrylic acid) with sonication for 1 min followed by esterification 3) hydrolysis of reused superabsorbent poly(acrylic acid) with sonication for 2 min followed by esterification, and 4) hydrolysis with no sonication, followed by esterification. For scenarios 2–4, we assume that superabsorbent poly(acrylic acid) is recovered from used diapers. Given the hypothetical nature of this LCA, we did not take impacts regarding transportation or distribution of the recovered superabsorbent poly(acrylic acid) or any other materials into account. In this LCA, the functional unit is 5000 mg of P(2-EHA). The inventory data for the sonication

and no-sonication processes are specific to the production of 5000 mg of P(2-EHA); therefore, we compare these scenarios to business-as-usual production of 5000 mg of P(2-EHA).

Inventory Data

The following tables contain the inputs for the LCA scenarios. Energy to model the 2-ethylhexanol to produce P(2-EHA) and the 2-ethylhexanol used in the sonication and no sonication scenarios was taken from Poulikidou et al.[18], given the absence of data in ecoinvent. In the P(2-EHA) scenario, we calculate that 391 g of acrylic acid are required in tandem with 1 kg 2-ethylhexanol (1000 grams) to produce P(2-EHA) based on the relative composition of P(2-EHA). In the sonication and no-sonication scenarios, we assume that the excess of the 5 equiv. of 2-ethylhexanol used is recoverable and therefore only included the emissions associated with the use of 1 equiv. of 2-ethylhexanol. Importantly, given the energy required in 2-ethylhexanol production, failure to re-use 2-ethylhexanol will likely favor business-as-usual production of (P-2EHA) over the repurposing scenarios. Emissions data for the extraction of superabsorbent poly(acrylic acid) from diapers was taken from a recent LCA of novel diaper recycling technology in Japan.[19] We account for the collection, separation, wastewater treatment, organic acid recovery, and ozone treatment required to recover (~80%) of the superabsorbent poly(acrylic acid) in one diaper. Since LCA data for these steps was reported per diaper, we multiplied each value by 19%, the percent composition of superabsorbent poly(acrylic acid) . These numbers were then adjusted to account for 80% recovery (i.e., per 9.04 g superabsorbent poly(acrylic acid) not the 11.3 g superabsorbent poly(acrylic acid) in a diaper before recycling). Lastly, to account for the freeze-drying of superabsorbent poly(acrylic acid) in our process, we included data from a freeze-drying LCA.[20]

Table A2-12. Inventory data for reference P(2-EHA scenario).

Material	Amount	Comments
Poly(2-Ethylhexyl Acrylate)*	5000 mg	
*modeled as follows; per 1 kg P(2-EHA)		
Electricity, US grid	117 MJ	Taken from Poulikidou et al., 2019 (17)
Acrylic Acid	391 g	Required acrylic acid to make 1kg P(2-EHA) based on fraction of acrylic acid in P(2-EHA)

Table A2-13. Inventory data for sonication scenarios.

Material	Amount	Comments
Sulfuric acid for protonation and decrosslinking	3.91 g	
Sulfuric acid for esterification	0.65 g	
2-Ethylhexanol [a]	0.00346 kg	1 equivalent. Assuming remainder recycled
Electricity, low voltage, US grid for sonication	34.8 kJ	For sonication 2 min scenario: 2 minutes, 290 watts
or --->	33.6 kJ	For sonication 1 min scenario: 1 minute, 280 watts
Electricity, low voltage, US grid for decrosslinking heat	20.92 kJ	
Electricity, low voltage, US grid for esterification heat	2.976 kJ	
Superabsorbent Poly(acrylic acid) extraction [b]	2500mg	
Lyophilization [c]	50g	
[a] modeled as follows; per 1 kg 2-Ethylhexanol		Taken from Poulikidou et al., 2019 (17)
Electricity, US grid	117 MJ	
[b] modeled as follows; per 9.04 grams of superabsorbent poly(acrylic acid) (80% recovery from 1 diaper)		Taken from Itsubo et al., 2019 (18)
Land use	7.9 cm^2a	
CO2eq	6.8 g	
Water	0.22 m^3	
[c] modeled as follows; per 2.43 kg of water		Taken from Prosapio et al., 2017 (19)
Electricity, US grid	1.98E-01	
Electricity, US grid	4.36E-01	
Electricity, US grid	2.67E-01	
Wastewater to treatment	2437 cm^3	

Table A2-14. Inventory data for No Sonication scenario.

Material	Amount	Comments
Sulfuric acid for protonation and decrosslinking	3.91 g	
Sulfuric acid for esterification	0.65 g	
2-Ethylhexanol [a]	0.00346 kg	1 equivalent. Assuming remainder recycled
Electricity, low voltage, US grid for decrosslinking heat	20.92 kJ	
Electricity, low voltage, US grid for esterification heat	2.976 kJ	
Superabsorbent Poly(acrylic acid) extraction [b]	2500mg	
Lyophilization [c]	50g	
[a] modeled as follows; per 1 kg 2-Ethylhexanol		Taken from Poulikidou et al., 2019 (17)
Electricity, US grid	117 MJ	
[b] modeled as follows; per 9.04 grams of superabsorbent poly(acrylic acid) (80% recovery from 1 diaper)		Taken from Itsubo et al., 2019 (18)
Land use	7.9 cm^2a	
CO2eq	6.8 g	
Water	0.22 m^3	
[c] modeled as follows; per 2.43 kg of water removed		Taken from Prosapio et al., 2017 (19)
Electricity, US grid	1.98E-01	
Electricity, US grid	4.36E-01	
Electricity, US grid	2.67E-01	
Wastewater to treatment	2437 cm^3	

Results

Table A2-15. Impact assessment results for all four scenarios. Conditional formatting is applied for ease of comparison.

Impact Category	Unit	Industrial	2.5%_1min	5%_2min	5%_0min
Nonrenewable fossil	MJ	3.11E+02	2.48E+02	2.49E+02	2.30E+02
Nonrenewable nuclear	MJ	1.07E+02	9.10E+01	9.13E+01	8.43E+01
Nonrenewable biomass	MJ	5.93E-05	5.43E-05	5.45E-05	5.04E-05
Renewable biomass	MJ	4.38E+00	3.74E+00	3.75E+00	3.45E+00
Renewable wind solar geothermal	MJ	5.11E-01	4.32E-01	4.33E-01	4.00E-01
Renewable water	MJ	9.59E+00	8.15E+00	8.17E+00	7.54E+00
CED	MJ	4.33E+02	3.51E+02	3.52E+02	3.25E+02
Global warming	kg CO2 eq	2.58E+01	2.18E+01	2.19E+01	2.03E+01
Stratospheric ozone depletion	kg CFC11 eq	7.04E-06	6.24E-06	6.26E-06	5.68E-06
Ionizing radiation	kBq Co-60 eq	2.40E-01	2.04E-01	2.05E-01	1.89E-01
Ozone formation Human health	kg NOx eq	4.82E-02	4.12E-02	4.13E-02	3.81E-02
Fine particulate matter formation	kg PM2.5 eq	4.45E-02	4.14E-02	4.15E-02	3.85E-02
Ozone formation Terrestrial ecosystems	kg NOx eq	4.88E-02	4.16E-02	4.17E-02	3.85E-02
Terrestrial acidification	kg SO2 eq	1.47E-01	1.37E-01	1.38E-01	1.28E-01
Freshwater eutrophication	kg P eq	1.47E-03	1.31E-03	1.32E-03	1.20E-03
Marine eutrophication	kg N eq	9.40E-05	1.42E-04	1.43E-04	1.36E-04
Terrestrial ecotoxicity	kg 1,4-DCB	9.36E+00	1.09E+01	1.09E+01	8.86E+00
Freshwater ecotoxicity	kg 1,4-DCB	1.52E-02	1.33E-02	1.33E-02	1.22E-02
Marine ecotoxicity	kg 1,4-DCB	2.68E-02	2.46E-02	2.47E-02	2.22E-02
Human carcinogenic toxicity	kg 1,4-DCB	7.93E-02	9.51E-02	9.59E-02	7.43E-02
Human non carcinogenic toxicity	kg 1,4-DCB	2.79E+00	2.52E+00	2.53E+00	2.29E+00
Land use	m2a crop eq	2.27E-01	1.97E-01	1.97E-01	1.82E-01
Mineral resource scarcity	kg Cu eq	1.75E-02	1.86E-02	1.87E-02	1.61E-02
Fossil resource scarcity	kg oil eq	6.78E+00	5.40E+00	5.42E+00	5.00E+00
Water consumption	m3	9.53E+01	9.38E+01	9.40E+01	8.77E+01

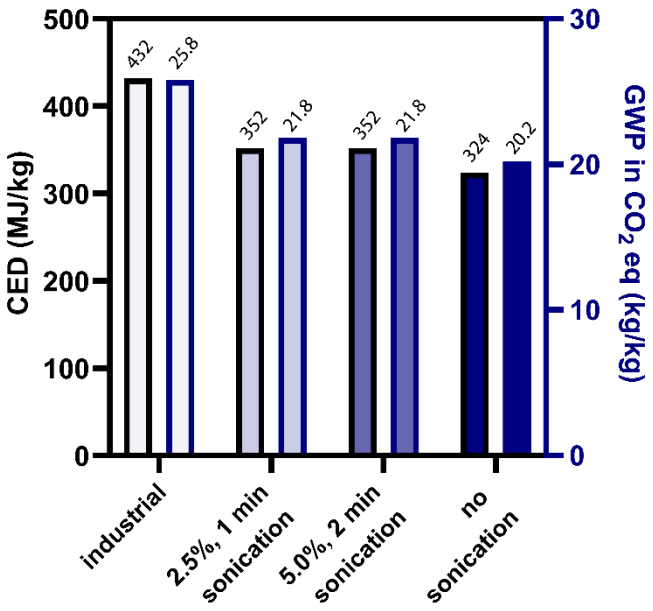

Figure A2-29. Plot of global warming potential and cumulative energy demand for the different LCA scenarios.

LCA results indicate that the PSA repurposing scenarios show improvement in almost all LCA impact categories. Moderate decreases in GWP and CED are indicated for the two sonication scenarios in comparison to conventional P(2-EHA) (~13% reduction in GWP and ~18% reduction in CED). The no sonication scenario (5%, 0min) outperforms the sonication scenarios, unsurprisingly, given the reduction in electricity required. More specifically, the no sonication scenario shows a ~20% reduction in GWP and ~25% reduction in CED compared to conventional P(2-EHA).

One-pot pressure-sensitive adhesive synthesis process combining protonation, decrosslinking, and esterification

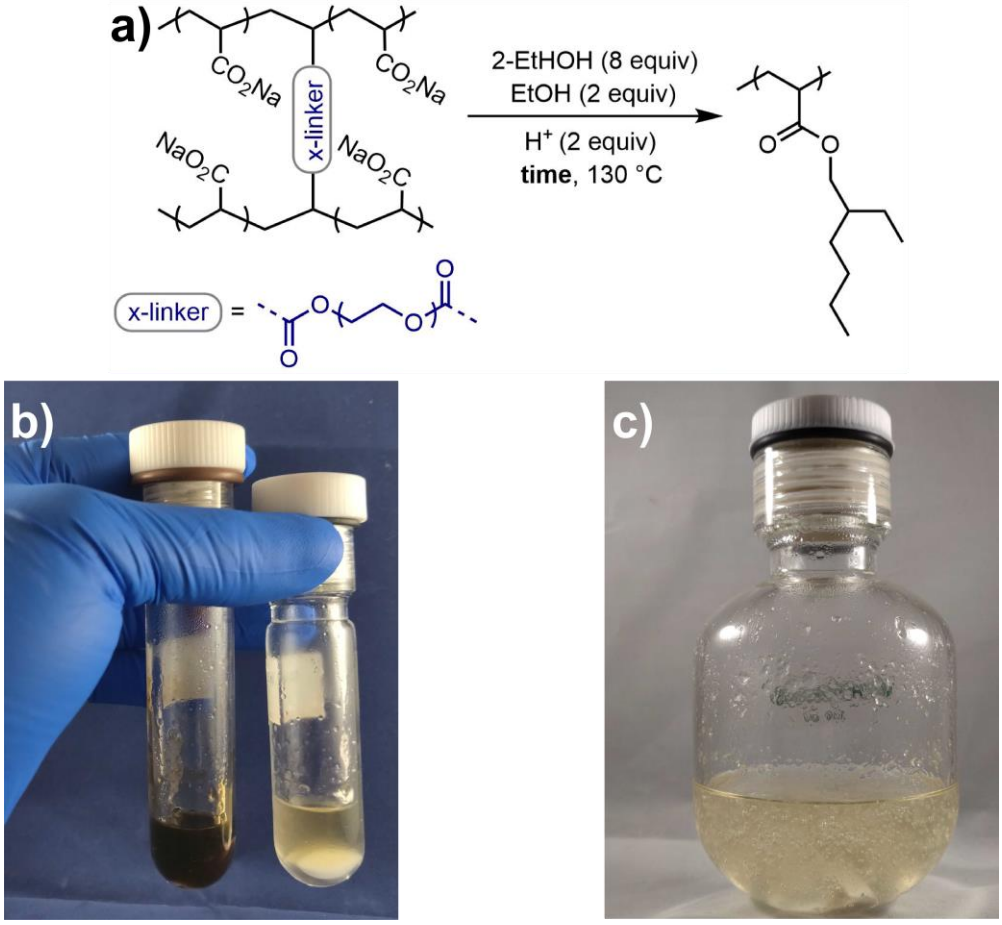

Figure A2-30. Plot of global warming potential and cumulative energy demand for the different LCA scenarios.

2-ethylhexanol (6.65 mL, 42.5 mmol, 8.00 equiv) and $PAA_{P\&G}$ (500 mg, 5.30 mmol, 1.00 equiv) were each added to four 15 mL pressure vessels equipped with stir bars. The top was capped with a septum and the contents were bubbled with N_2 for 20 min using a long needle. Thereafter, ethanol (0.620 mL, 10.6 mmol, 2.0 equiv) and sulfuric acid (0.567 mL, 10.6 mmol, 2.0 equiv) were added. The vessels were placed onto a heating block at 130 °C and was left to stir at 350 rpm. The reaction vessels were quenched at varying time points (1.5, 5, 9, and 21 h).

2-ethylhexanol (13.3 mL, 85.1 mmol, 8.00 equiv) and $PAA_{P\&G}$ (1000 mg, 10.6 mmol, 1.00 equiv) were each added to a 75-pressure vessel equipped with a stir bar. The vessel was covered with aluminum foil and the contents were bubbled with N_2 for 20 min using a long needle. Thereafter, ethanol (1.24 mL, 21.3 mmol, 2.00 equiv) and sulfuric acid (1.13 mL, 21.3 mmol, 2.00 equiv) were added. The vessels were placed onto a heating block at 130 °C and was left to stir at 350 rpm. The reactions were quenched at varying time points (i.e., 15 and 25 h).

Thereafter, the vessels were cooled in a rt water bath. The polymer was isolated by precipitating into MeOH (10–20 mL) followed by centrifugation at 4500 rpm for 5 min and decanting off the supernatant. To the precipitated polymer, warm DI water (30 mL, 80 °C) was added followed by capping and vigorously handshaking (3 shakes per second) for 30 s to wash off the $NaHSO_4$ by-product. This process was repeated 3 times. After the final wash, the pH paper reading of the water changed from ~1 to 4. The polymer was washed with methanol (20 mL) to remove the H_2O. Further purification was done by dissolving/swelling the polymer in minimal amounts of THF (15 mL) and precipitating with MeOH (30 mL) twice. The polymer was dried under high vacuum at 100 °C for 3–5 h. 600 mg of each polymer was used for rheological measurements.

Table A2-16. Recoveries for one-pot esterifications at different timepoints.

reaction time (h)	1.5	5	9	15	21	25
recovered mass (g)	0.65	0.84	0.88	1.90	0.89	1.84
% recovery	66	85	89	96	91	93

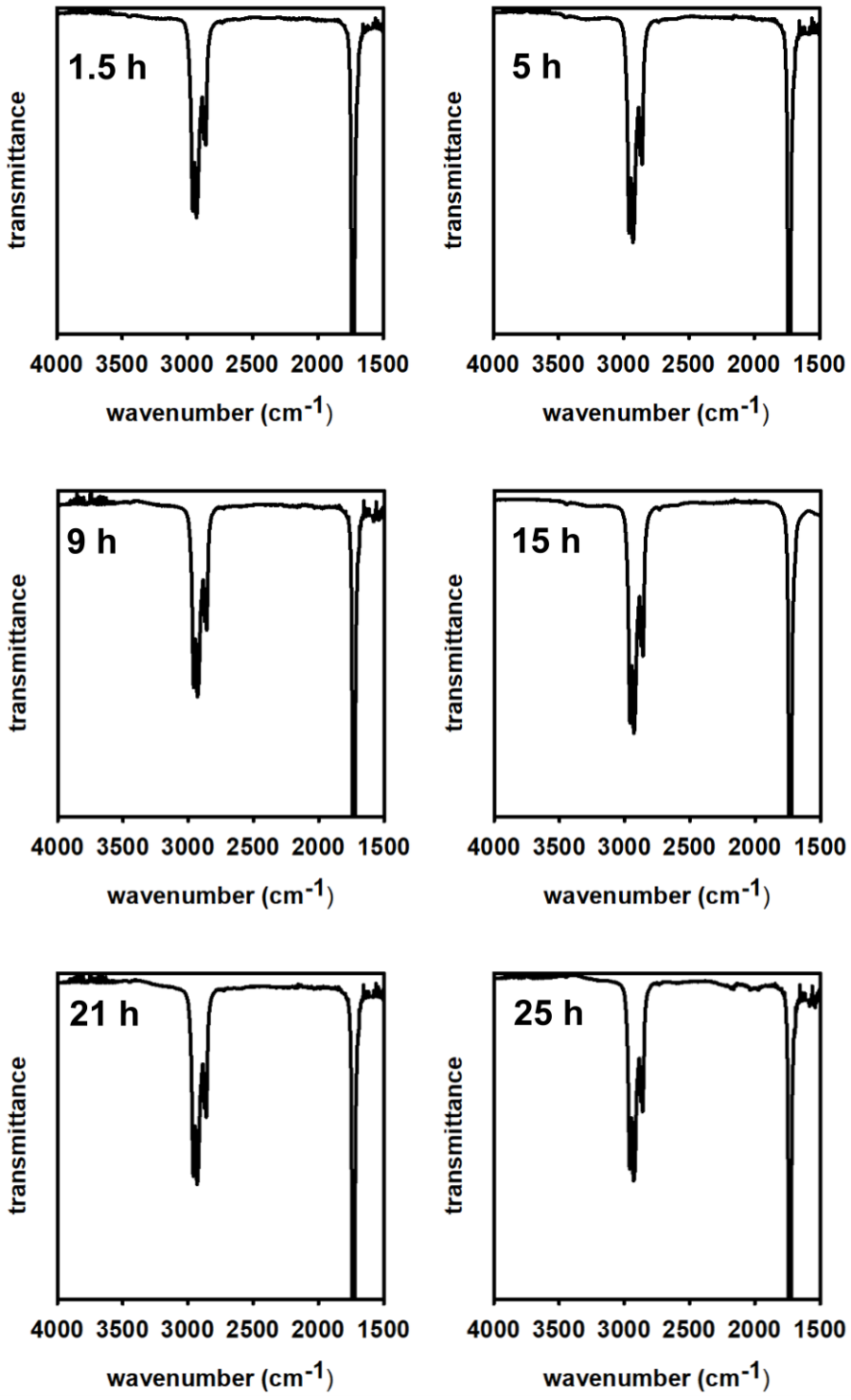

Figure A2-31. Infrared spectra for one-pot esterifications at different timepoints.

Decrosslinking/esterification was used to convert $PAA_{P\&G}$ into pressure sensitive adhesives in one pot. Data was collected for reactions run for various time points up to 25 h. Due to their hardness, samples run for times below 9 h were not characterized via rheology. All samples were characterized via IR.

Frequency sweeps (0.01–100 Hz) were done at 25 °C using a 20 mm cross-hashed geometry using a gap of 1250 µm (600 mg of polymer). Due to their hardness at 25 °C, samples run for times below 9 h were not characterized via rheology.

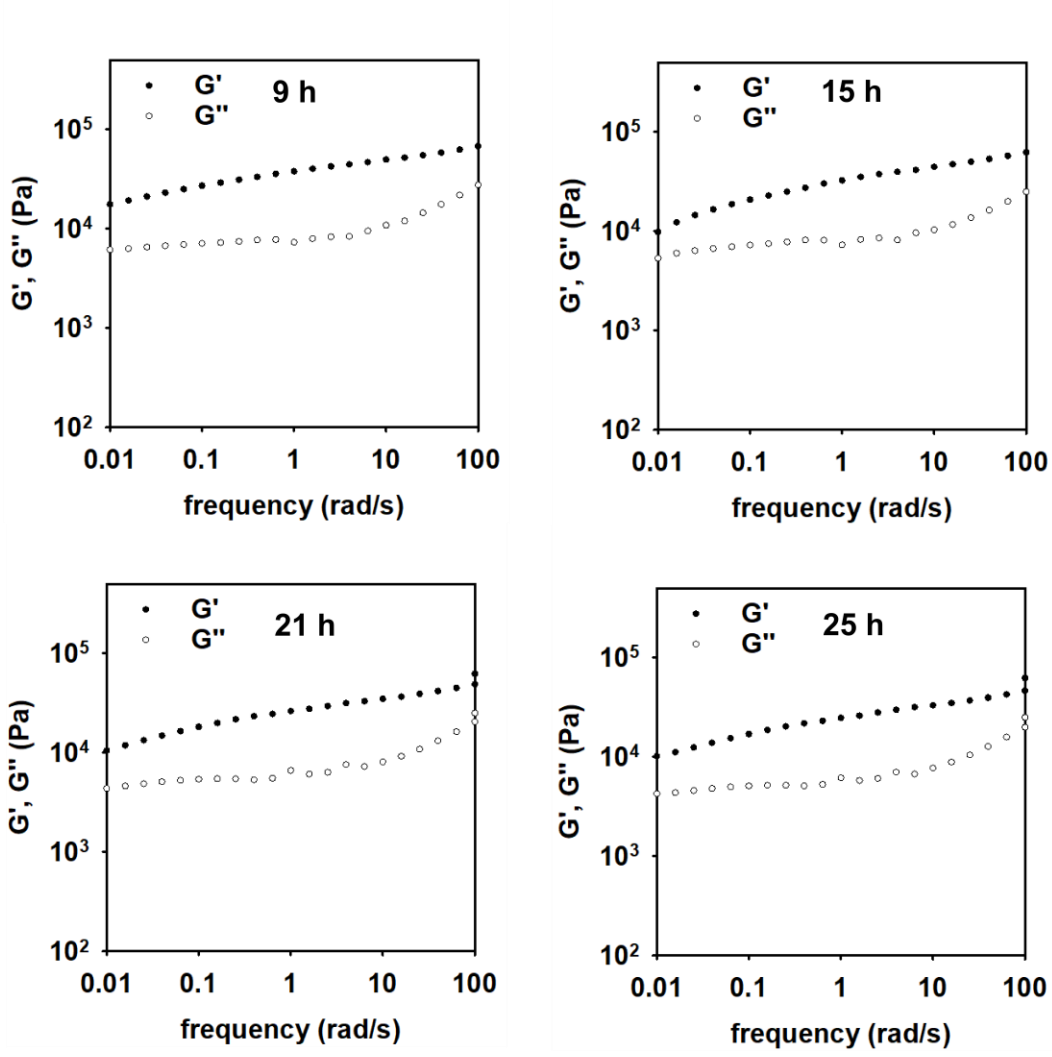

Figure A2-32. Frequency sweeps for one-pot esterifications at different timepoints.

References

1 Moriguchi, T.; Arita, Y. Process for Producing Acrylic Acid. U.S. Patent 8404887B2. March 26, 2013.

2 Christ, C. D.; Mark, A. E.; Van Gunsteren, W. F. Basic Ingredients of Free Energy Calculations: A Review. *J. Comput. Chem.* **2010**, *31*, 1569–1582. https://doi.org/10.1002/jcc.21450.

3 Hanwell, M. D.; Curtis, D. E.; Lonie, D. C.; Vandermeerschd, T.; Zurek, E.; Hutchison, G. R. Avogadro: An Advanced Semantic Chemical Editor, Visualization, and Analysis Platform. *J. Cheminform.* **2012**, *4*, 17. https://doi.org/10.1186/1758-2946-4-17.

4 Martínez, L.; Andrade, R.; Birgin, E. G.; Martínez, J. M. PACKMOL: A Package for Building Initial Configurations for Molecular Dynamics Simulations. *J. Comput. Chem.* **2009**, *30*, 2157–2164. https://doi.org/10.1002/jcc.21224.

5 Jorgensen, W. L.; Chandrasekhar, J.; Madura, J. D.; Impey, R. W.; Klein, M. L. Comparison of Simple Potential Functions for Simulating Liquid Water. *J. Chem. Phys.* **1983**, *79*, 926–935. https://doi.org/10.1063/1.445869.

6 Vanommeslaeghe, K.; Hatcher, E.; Acharya, C.; Kundu, S.; Zhong, S.; Shim, J.; Darian, E.; Guvench, O.; Lopes, P.; Vorobyov, I.; Mackerell, A. D. CHARMM General Force Field: A Force Field for Drug-like Molecules Compatible with the CHARMM All-Atom Additive Biological Force Fields. *J. Comput. Chem.* **2009**, *31*, NA-NA. https://doi.org/10.1002/jcc.21367.

7 Yesselman, J. D.; Price, D. J.; Knight, J. L.; Brooks, C. L. MATCH: An Atom-Typing Toolset for Molecular Mechanics Force Fields. *J. Comput. Chem.* **2012**, *33*, 189–202. https://doi.org/10.1002/jcc.21963.

8 Brooks, B. R.; Brooks, C. L.; Mackerell, A. D.; Nilsson, L.; Petrella, R. J.; Roux, B.; Won, Y.; Archontis, G.; Bartels, C.; Boresch, S.; Caflisch, A.; Caves, L.; Cui, Q.; Dinner, A. R.; Feig, M.; Fischer, S.; Gao, J.; Hodoscek, M.; Im, W.; Kuczera, K.; Lazaridis, T.; Ma, J.; Ovchinnikov, V.; Paci, E.; Pastor, R. W.; Post, C. B.; Pu, J. Z.; Schaefer, M.; Tidor, B.; Venable, R. M.; Woodcock, H. L.; Wu, X.; Yang, W.; York, D. M.; Karplus, M. CHARMM: The Biomolecular Simulation Program. *J. Comput. Chem.* **2009**, *30*, 1545–1614. https://doi.org/10.1002/jcc.21287.

9 Hynninen, A.-P.; Crowley, M. F. New Faster CHARMM Molecular Dynamics Engine. *J. Comput. Chem.* **2014**, *35*, 406–413. https://doi.org/10.1002/jcc.23501.

10 Darden, T.; York, D.; Pedersen, L. Particle Mesh Ewald: An N·log(N) Method for Ewald Sums in Large Systems. *J. Chem. Phys.* **1993**, *98*, 10089–10092. https://doi.org/10.1063/1.464397.

11 Essmann, U.; Perera, L.; Berkowitz, M. L.; Darden, T.; Lee, H.; Pedersen, L. G. A Smooth Particle Mesh Ewald Method. *J. Chem. Phys.* **1995**, *103*, 8577–8593. https://doi.org/10.1063/1.470117.

12 Huang, Y.; Chen, W.; Wallace, J. A.; Shen, J. All-Atom Continuous Constant PH Molecular Dynamics with Particle Mesh Ewald and Titratable Water. *J. Chem. Theory Comput.* **2016**, *12*, 5411–5421. https://doi.org/10.1021/acs.jctc.6b00552.

13 Shirts, M. R.; Chodera, J. D. Statistically Optimal Analysis of Samples from Multiple Equilibrium States. *J. Chem. Phys.* **2008**, *129*, 124105. https://doi.org/10.1063/1.2978177.

14 Vilseck, J. Z.; Sohail, N.; Hayes, R. L.; Brooks, C. L. Overcoming Challenging Substituent Perturbations with Multisite λ-Dynamics: A Case Study Targeting β-Secretase 1. *J. Phys. Chem. Lett.* **2019**, *10*, 4875–4880. https://doi.org/10.1021/acs.jpclett.9b02004.

15 Hayes, R. L.; Armacost, K. A.; Vilseck, J. Z.; Brooks, C. L. Adaptive Landscape Flattening Accelerates Sampling of Alchemical Space in Multisite λ Dynamics. *J. Phys. Chem. B* **2017**, *121*, 3626–3635. https://doi.org/10.1021/acs.jpcb.6b09656.

16 Wernet, G.; Bauer, C.; Steubing, B.; Reinhard, J.; Moreno-Ruiz, E.; Weidema, B., The Ecoinvent Database Version 3 (Part I): Overview and Methodology. *The International Journal of Life Cycle Assessment* **2016,** *21*, 1218–1230.

17 LCIA: the ReCiPe Model.

18 Poulikidou, S.; Heyne, S.; Grahn, M.; Harvey, S., Lifecycle Energy and Greenhouse Gas Emissions Analysis of Biomass-Based 2-Ethylhexanol as an Alternative Transportation Fuel. *Energy Science & Engineering* **2019,** *7*, 851–867.

19 Itsubo, N.; Wada, M.; Imai, S.; Myoga, A.; Makino, N.; Shobatake, K., Life Cycle Assessment of the Closed-Loop Recycling of Used Disposable Diapers. *Resources* **2020,** *9*, 34.

20 Prosapio, V.; Norton, I.; De Marco, I., Optimization of Freeze-Drying Using a Life Cycle Assessment Approach: Strawberries' Case Study. *Journal of Cleaner Production* **2017,** *168*, 1171–1179.

Appendix 3: Removing MPs Pollutants from Water via Adhesive Induced Van der Waals Interactions

Materials

All chemicals were used as received unless otherwise mentioned. Polyacyrlic acid (PAA) with molecular weight listed as 1,033 kg/mol ($PAA_{SPP\text{-}1000k}$) was purchased from Scientific Polymer Products. Poly(2-ethylhexyl acrylate) (P(2-EHA)) solution in toluene listed as 92 kg/mol ($P(2\text{-}EHA)_{Sigma\text{-}93k}$), $PAA_{Sigma\text{-}240k}$ (listed as 240 kg/mol), $PAA_{Sigma\text{-}370k}$ (listed as 450 kg/mol), decanoic acid, sulfuric acid (H_2SO_4), sodium dodecyl sulfate (SDS) and sodium nitrate ($NaNO_3$) were purchased from Millipore Sigma. Methanol (MeOH) and ethanol (EtOH) were purchased from Fisher Scientific. Tetrahydrofuran (THF) was purchased from OmniSolv. Glacial acetic acid was purchased from Acros Organics. Deuterated solvents: chloroform ($CDCl_3$), pyridine-d_5, and deuterium oxide (D_2O) were purchased from Cambridge Isotopes. Micronized rubber was provided by Entech and Lehigh technologies. The superabsorbent polymer ($PAA_{P\&G}$) provided by Procter & Gamble is 70% neutralized (i.e., % sodium form) and contains up to 1% by weight ethylene glycol diacrylate crosslinker relative to the acrylic acid monomer. Sonicated polymer fragments were dialyzed in deionized (DI) water using Spectra/Por molecular porous membrane tubing (molecular weight cut-off: 3.5 kg/mol). Pressure vessels were purchased from Thomas Scientific. Jacketed beakers were purchased from Sigma Aldrich (cat#: Z202738-1EA).

Preparing adhesives

A. P(2-EHA)$_{Sigma\text{-}93k}$

A commercial solution of P(2-EHA)$_{Sigma\text{-}93k}$ in toluene (20 mL) was purified by precipitating into MeOH (30 mL) once and washing with MeOH (30 mL) 3 times. Centrifugation was used to separate the polymer from the supernatant. The polymer was dried under high vacuum at 60 °C for 3 h. yield?

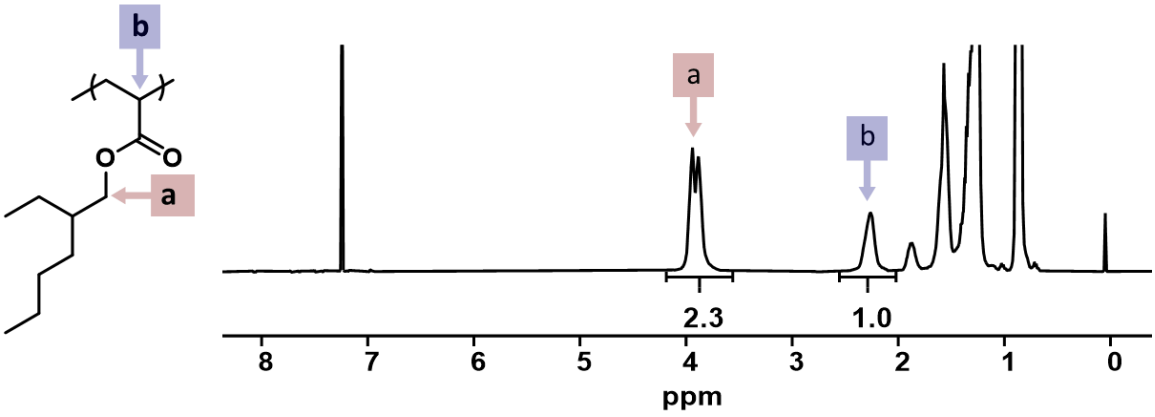

Figure A3-1. ^{1}H NMR spectra of P(2-EHA)$_{Sigma\text{-}93k}$ (500 MHz, $CDCl_3$).

B. P(2-EHA)$_{Sigma\text{-}370k}$ and P(2-EHA)$_{SPP\text{-}950k}$

(i) Chain-Shortening PAA$_{SPP\text{-}1000k}$

PAA$_{SPP\text{-}1000k}$ (2,500 mg, 34.7 mmol) and DI water (50 mL) was added to a jacketed beaker (3.5 cm inner diameter, 9 cm height) equipped with a stir bar and left to stir (500 rpm) for 12 h. Then, cold water (10–15 °C) was flowed through the jacket. The contents were sonicated for 5 min at 100% amplitude (300 W based on a kill-a-watt device) using a Sonics and Materials Vibra-cell VCX 600 Ultrasonic Liquid Processor equipped with a 13 mm replaceable tip probe. A thermocouple was immersed into the polymer solution to monitor temperature, which rose from 15 to 60 °C.

After sonication, the polymer was dialyzed using DI water (~1 gallon), switching the DI water three times over 12–18 h. Then, the polymer was freeze-dried and ground to a fine powder using a mortar and pestle. More specifically, while wearing cryogenic gloves, a piece of freeze-dried polymer was put into a mortar, which was then immersed into a bath of liquid N_2. A small amount of liquid N_2 was poured into the mortar and the polymer was ground using a pestle. The fine powder was immediately transferred to a 20 mL vial and held under high vacuum for 10 min as the polymer warmed to rt to avoid water condensation. SEC? yield?

(ii) Esterifying PAA$_{SPP\text{-}1000k}$ and PAA$_{Sigma\text{-}240k}$

Note that PAA$_{Sigma\text{-}240k}$ was used for esterification without chain-shortening.

2-EHOH (16.27 mL, 104.1 mmol, 5.00 equiv), H_2SO_4 (0.277 mL, 5.20 mmol, 0.25 equiv), and chain-shortened PAA$_{SPP\text{-}1000k}$ or PAA$_{Sigma\text{-}240k}$ (1,500 mg, 20.8 mmol, 1.00 equiv) were added to a 75 mL pressure vessel, along with a stir bar. The vessels were sealed with a Teflon screw cap and

heated to 120 °C for 8 h. Thereafter, the vessel was cooled to rt in a water bath. Next, the reaction mixture was poured into MeOH (~50 mL) to precipitate the P(2-EHA). The resulting $P(2\text{-EHA})_{SPP\text{-}950k}$ or $P(2\text{-EHA})_{Sigma\text{-}370k}$ obtained was purified by dissolving in minimal amounts of THF (~10 mL) and precipitating with MeOH (~50 mL). The polymer was isolated by centrifugation and decanting off the supernatant. This precipitation process was repeated three times. Aft the final isolation, the polymer was dried under high vacuum with heating at 60 °C for 3 h. The isolated yield was 73% $P(2\text{-EHA})_{SPP\text{-}950k}$ and 82% for $P(2\text{-EHA})_{Sigma\text{-}370k}$.

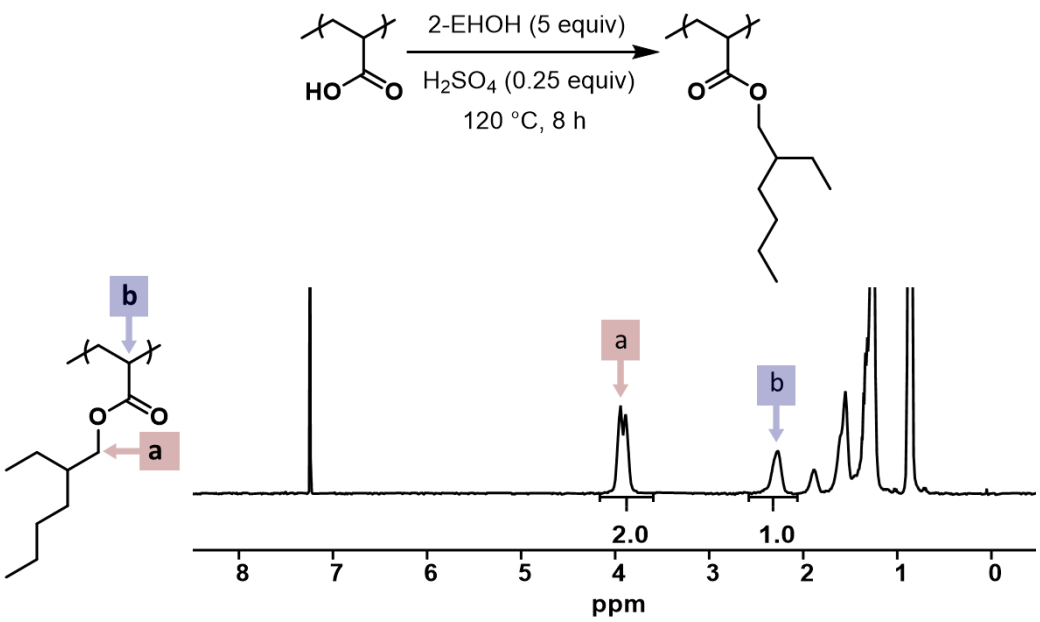

Figure A3-2. ^{1}H NMR spectra of $P(2\text{-EHA})_{SPP\text{-}950k}$ (500 MHz, $CDCl_3$).

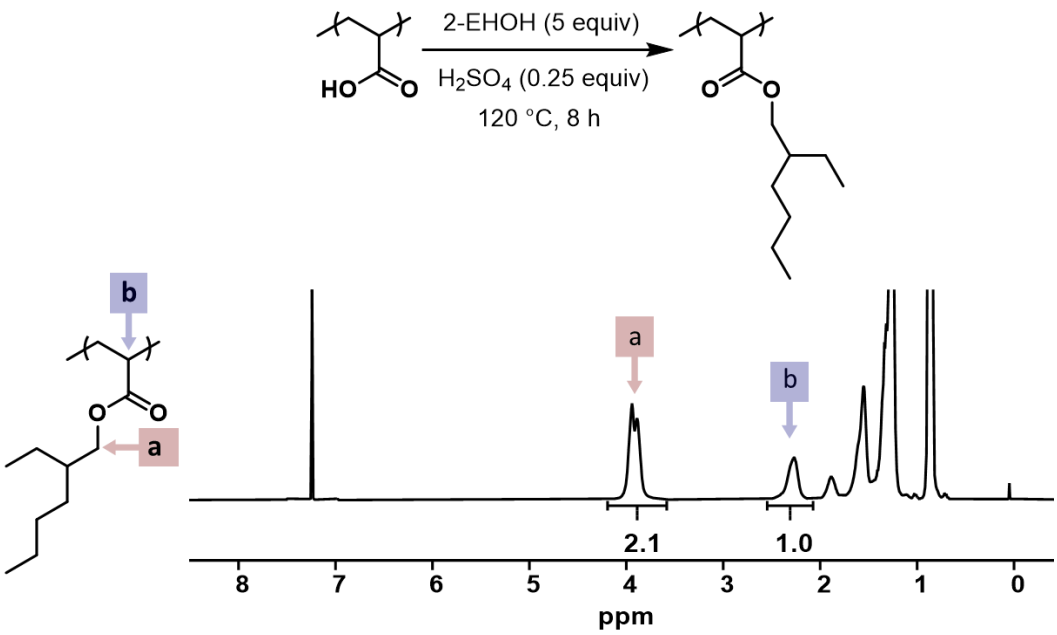

Figure A3-3. ^{1}H NMR spectra of P(2-EHA)$_{\text{Sigma-370k}}$ (500 MHz, $CDCl_3$).

C. P(2-EHA)$_{P\&G\text{-}590k}$

(i) Decrosslinking: A 0.8 M aq. H_2SO_4 solution was prepared by adding H_2SO_4 (6.84 mL, 128 mmol, 1.5 equiv) to a 350 mL pressure vessel containing DI H_2O (160 mL) stirring at 350 rpm. Thereafter, $PAA_{P\&G}$ (8,000 mg, 85.1 mmol, 1 equiv) was added. The vessel was sealed, and the reaction stirred at 120 °C for 24 h. The resulting reaction mixture was used directly in the subsequent sonication experiments.

(ii) Chain-shortening: Decrosslinked $PAA_{P\&G}$ solution (~50 mL) was poured into a jacketed beaker (3.5 cm inner diameter, 9 cm height) equipped with a stir bar. While flowing cold water (10–15 °C) through the jacket, the decrosslinked $PAA_{P\&G}$ was sonicated for 5 min at 100% amplitude (290 W based on a kill-a-watt device) using a Sonics and Materials Vibra-cell VCX 600 Ultrasonic Liquid Processor equipped with a 13 mm replaceable tip probe. A thermocouple was immersed into the polymer solution to monitor temperature, which rose from 23 °C to 45 °C.

After sonication, the polymer was dialyzed using DI water (~1 gallon), switching the DI water three times over 12–18 h. Then, the polymer was freeze-dried and ground to a fine powder using a mortar and pestle. More specifically, while wearing cryogenic gloves, a piece of freeze-dried polymer was put into a mortar, which was then immersed into a bath of liquid N_2. A small amount of liquid N_2 was poured into the mortar and the polymer was ground using a pestle. The fine powder was immediately transferred to a 20 mL vial and held under high vacuum for 10 min as the polymer warmed to rt to avoid water condensation. The polymer was isolated in 91% yield (over both steps).

(iii) Esterification: To a 75 mL pressure vessel, 2-EHOH (4.34 mL, 27.8 mmol, 5.00 equiv.) and H_2SO_4 (0.074 mL, 1.39 mmol, 0.25 equiv.) were added and stirred at 120 °C. While stirring, chain-

shortened $PAA_{P\&G}$ (400 mg, 5.60 mmol, 1.00 equiv.) was subsequently added and the vessel was sealed with a Teflon screw cap and stirred for 10 h at 120 °C. Thereafter, the vessel was cooled in a rt water bath. The $P(2\text{-EHA})_{P\&G\text{-}590k}$ was isolated by precipitating into MeOH (20 mL) and removing the supernatant. Then, the polymer was purified by dissolving in minimal amounts of THF (5 mL), precipitating into MeOH (20 mL), and removing the supernatant after centrifugation. This process was repeated three times. The resulting solid was dried under high vacuum at 80 °C for 10 h. The isolated yield was 79%.

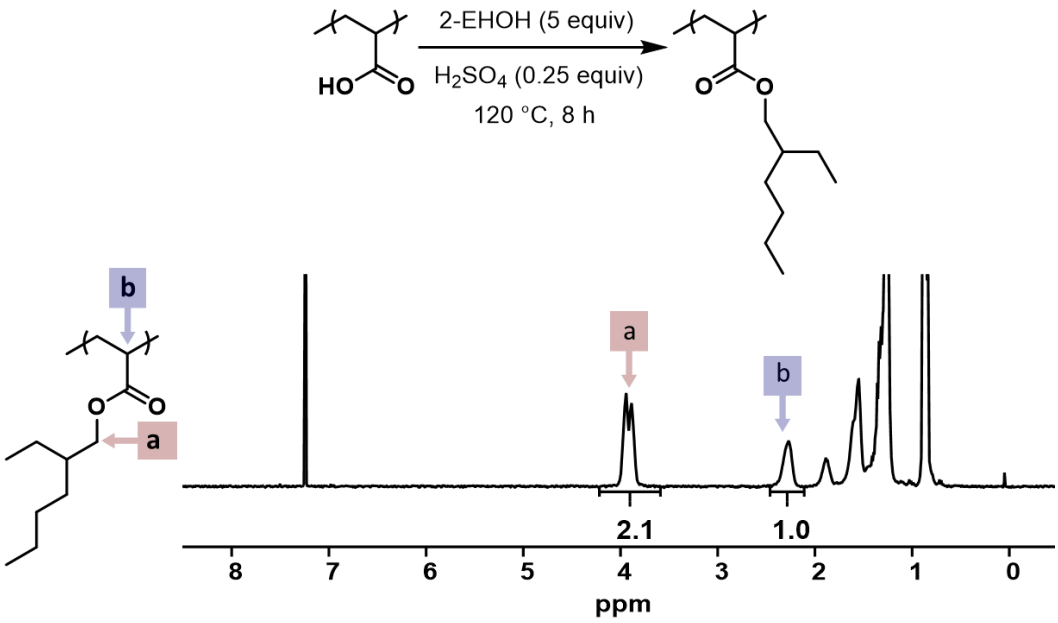

Figure A3-4. ^{1}H NMR spectra of $P(2\text{-EHA})_{P\&G\text{-}590k}$ (500 MHz, $CDCl_3$).

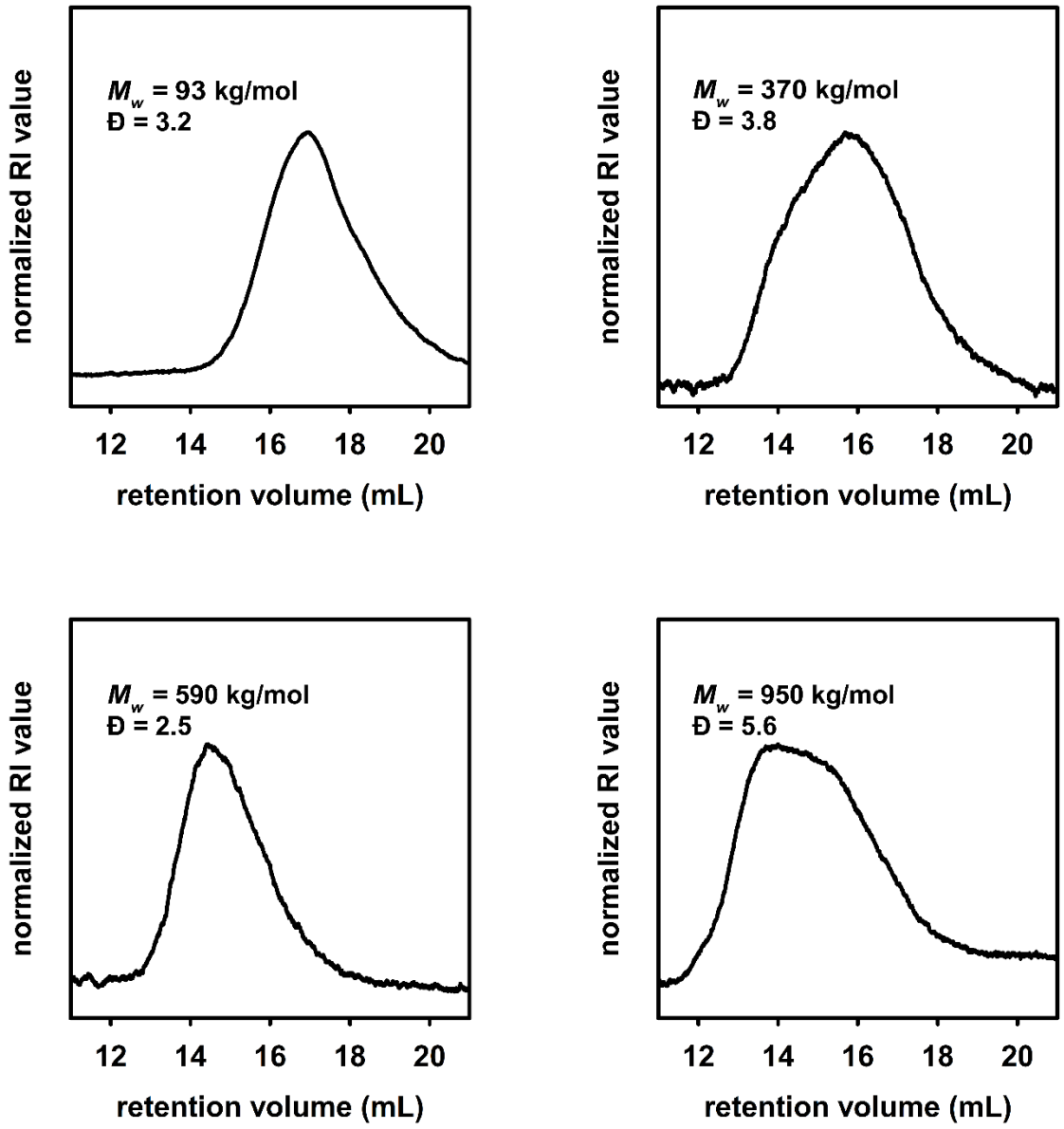

Figure A3-5. Size-exclusion chromatography traces of the synthesized P(2-EHA)s.

Confirming MPs capture in deionized water

A stir bar was coated with pressure-sensitive adhesive by dipping a solution of $P(2\text{-EHA})_{Sigma\text{-}93k}$ (5.0% w/v in tetrahydrofuran) followed by oven drying at 120 °C for 10 min. Two MPs suspensions were prepared my mixing micronized rubber (15 mg) and DI H_2O (5 mL) followed by vortex mixing at the 10/10 setting for 30 s and handshaking (3 shakes per second) for 1 min. To the control and experiment sample, a bare and coated stir bar were added, respectively. The suspensions were hand-shaken (3 shakes per second) for 1.0 min and MPs removal was evaluated by eye inspection.

Figure A3-6. Comparing capturing MPs micronized rubber using adhesive bare (left) versus coated (right) stir bar.

Adhesive coated beads as substrates for MPs removal

Used dry molecular sieves (2.0 mm, 10.0 g) were PSA coated by adding $PAA_{SPP\text{-}950k}$ solution (1 mL, 5.0% w/v.). The beads were hand-shaken (3 shakes per second) for 2 min, oven dried (120 °C) for 10 min, and left to cool to ambient temperature.

A PET suspension in water (1.5 mg/mL) was prepared by adding PET (7.5 mg, 300 µm) and DI H_2O (5 mL) to an 8 mL vial. The mixture was vortex mixed at the 10/10 setting for 30 seconds. Adhesive coated beads (0.100 mg, ~10 beads) were added to the PS suspension and the sample was hand-shaken (3 shakes per second) for 1 min. The beads were transferred to a separate 8 mL vial and washed by adding 5 mL of DI H_2O, hand-shaking for 10 seconds, and removing the water using a needle and syringe. The beads were left to dry overnight and then analyzed using scanning electron microscopy (SEM).

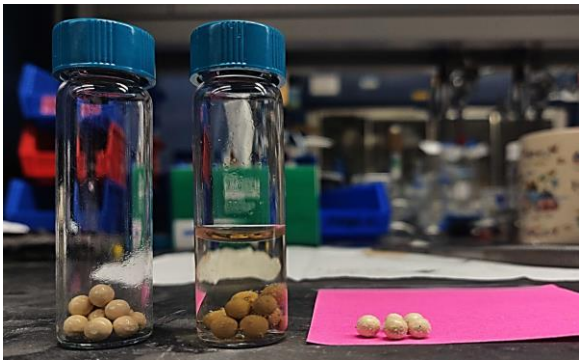

Figure A3-7. Visualization of adhesive-coated post-use 2 mm molecular sieves before (left), and after (right) MPs removal.

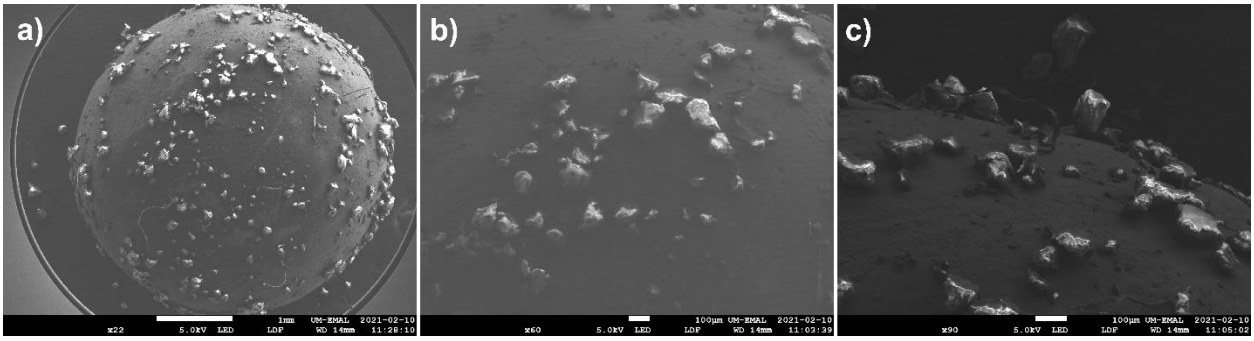

Figure A3-8. SEM images of 2 mm post-use molecular sieves after capturing 300 µm PET in water.

A PS suspension in water (1.5 mg/mL) was prepared by adding PS latex (300 mg, 2.5% wt., 90 µm) and DI H_2O (5 mL) to an 8 mL vial. The mixture was vortex mixed at the 10/10 setting for 30 seconds. Adhesive coated beads (0.100 mg, ~10 beads) were added to the PS suspension and the sample was hand-shaken (3 shakes per second) for 1 min. The beads were transferred to a separate 8 mL vial and washed by adding 5 mL of DI H_2O, hand-shaking for 10 seconds, and removing the water using a needle and syringe. The beads were left to dry overnight and then analyzed using scanning electron microscopy (SEM).

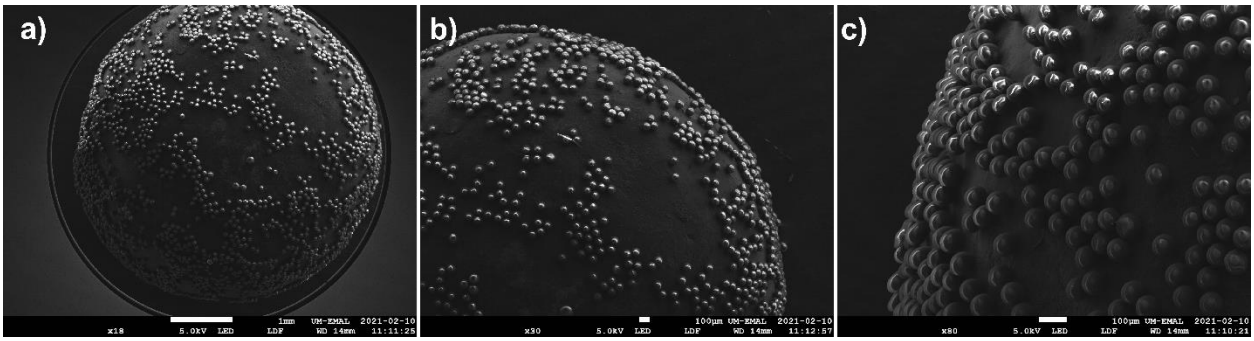

Figure A3-9. SEM images of 2 mm post-use molecular sieves after capturing 90 µm PS in water.

Comparing performance of adhesive coated beads versus glass slides

Zirconium silicate beads (0.5 mm, 20.0 g) were added to a 40 mL vial and washed by adding 10 mL acetone and shaking for 30 seconds followed removing the solvent using a needle and syringe. The beads were spread onto aluminum foil and oven dried (120 °C) for 10 min. After cooling to ambient temperature, $PAA_{SPP\text{-}950k}$ (0.50 mL, 10% w/v.) was added and the beads were hand-shaken (3 shakes per second) for 2 min. The beads were dried under high vacuum for 3 h.

A stock PS suspension in water (50 mL, 0.38 mg/mL) was prepared by adding PS latex (760 mg, 2.5% wt., 90 µm) and DI H_2O (50 mL) to a 50 mL centrifuge tube. The mixture was vortex mixed at the 10/10 setting for 30 seconds. The stock solution was vortex mixed at the 10/10 setting for 30 seconds before taking aliqouts and stored in the refrigerator after each use.

To 8 mL vials containing PS suspension (3.5 mL, 0.38 mg/mL) was added adhesive coated beads (50 mg) followed by vortex mixing at the 10/10 setting for the appropriate time in duplicates (i.e., 0.5, 1.0, and 2 min). The beads were transferred to a separate 8 mL vial and washed by adding 5 mL of DI H_2O, hand-shaking for 10 seconds, and removing the water using a needle and syringe. The beads were left to air dry for 1 h and then analyzed using optical microscopy.

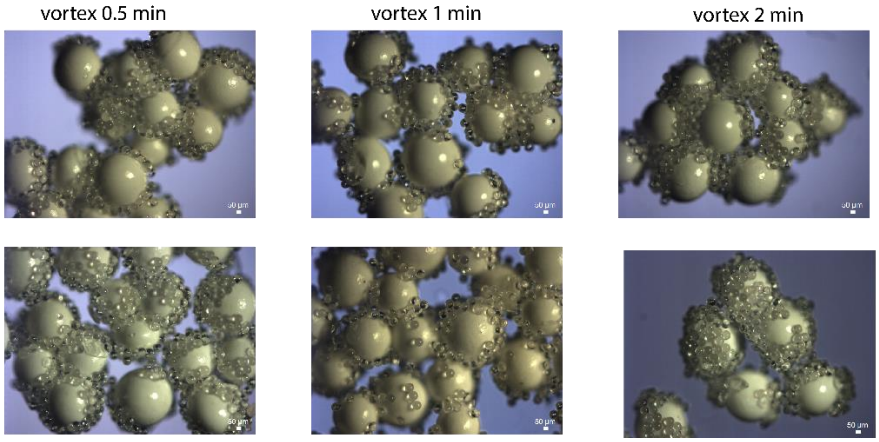

Figure A3-10. Optical microscope images showing 90 µm PS captured by $PAA_{SPP\text{-}950k}$ coated 0.5 mm beads at different time points.

To prepare the substrates for MPs capture, 2 droplets of a 10% wt. solution of $PAA_{SPP\text{-}950k}$ in THF (10 µL) was drop-cast onto glass slides (0.8x3.75 cm) using a 10–100 µL micropipette. The droplets on the glass slides were left to dry in air for 5 min before placing inside the oven (120 °C) to further dry for 10 min. After allowing the slide to cool (ca 10 min), the glass slides were immersed into 8 mL vials containing PS suspension (3.5 mL, 0.38 mg/mL) followed by vortex mixing at the 10/10 setting for the appropriate time (i.e., 0.5, 1.0, 2.0, and 4 min). The glass slides were washed by squirting them with DI H_2O. The glass slides were left to air dry for 1 h and then analyzed using optical microscopy. The optical microscopy images were analyzed using ImageJ.

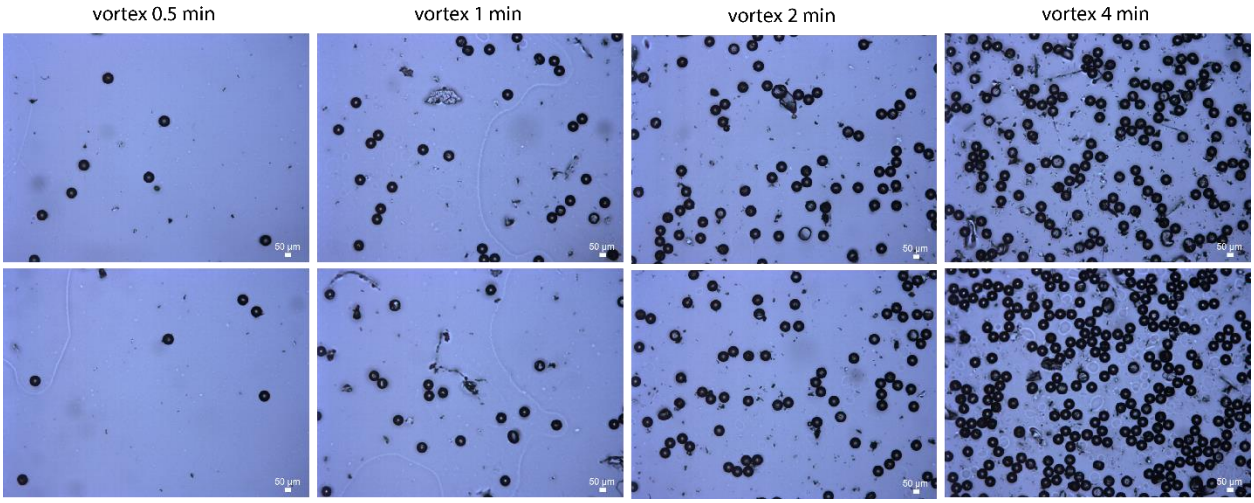

Figure A3-11. Optical microscope images showing 90 µm PS captured by $PAA_{SPP\text{-}950k}$ coated glass slides at different time points.

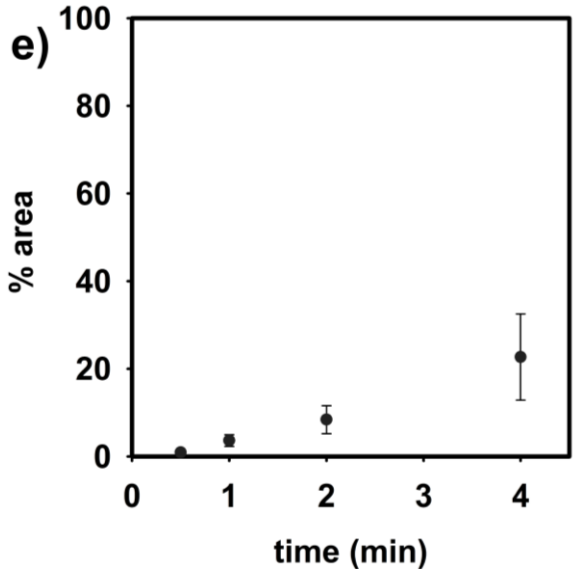

Figure A3-12. Percent area covered by captured 90 µm PS over time on $PAA_{SPP\text{-}950k}$ coated glass slides calculated using ImageJ.

Methods and molecular dynamics sampling

Molecular dynamic simulations were conducted using the cgenff molecular mechanics forcefield and the GPU-enabled c45a2 version of CHARMM package. Initial structures for microplastic surfaces were generated using the CHARMM-GUI.[1] Initial structures for adhesives were generated by an in-house python code algorithm which produces CHARMM ready input structures of R-group modified polyacrylate adhesives from monomer geometries. The algorithm works by taking CHARMM optimized polyacrylate monomer geometries and generating a linear sequence of bonded residues, analogous to unrelaxed protein strands. Both types of structures were then equilibrated at 298.15 K under NVT conditions for 10 ns. The Packmol program[2] was used to create adhesive-water and adhesive-plastic interfaces, starting from the pre-equilibrated initial structures. Adhesive-water systems were equilibrated at 298.15 K under NPT conditions for 50 ns before production runs for 10 ns with NVT conditions with frame sampling every 50 ps. Adhesive-plastic systems were equilibrated at 298.15 K under NVT conditions for 50 ns before productions runs under the same conditions for 10 ns with frame sampling every 50 ps. Interfacial surface tension was calculated with the Lee-Richards method to determine interfacial surface area and energies.[3] Each simulation provided 200 frames with interfacial surface tension analysis, from which the mean was taken for the value and standard deviation for error bars.

Adhesive models and statistical sampling

As 2-EHA is a chiral monomer, statistical sampling of the polymer structure was used to prevent unintentional clustering of monomeric chirality in residue sequences which would cause outlier results. As such, the adhesive construction algorithm was used to independently construct three P(2-EHA) adhesive chains, of approximately the same molecular weight, which were then relaxed

to their equilibrium state. Each of these three adhesives was then simulated with the aqueous and plastic surfaces 10 separate times to produce 30 total simulations of 200 frames each. Simulation γ values were averaged, and errors combined with any outliers removed based on Dixon's Q-test method.[4] Final γ and work of adhesion value are reported in SI TABLE S1 below.

Table A3-1. Computed γ values and work of adhesion values for plastics with P(2-EHA).

plastic material	$\gamma_{adhesive-water}$ ***(mN/m)***‡	$\gamma_{adhesive-plastic}$ ***(mN/m)***	$WoA_{(aq)}$ ***(mN/m)***
Polyethylene terephthalate	-49.19 ± 0.27	-27.97 ± 0.20	21.22 ± 0.34
Polystyrene	-49.19 ± 0.27	-19.31 ± 1.30	29.87 ± 1.32
Polyethylene	-49.19 ± 0.27	-18.75 ± 1.09	30.44 ± 1.12
Nylon-6	-49.19 ± 0.27	-24.52 ± 1.05	24.67 ± 1.08

‡ This value is constant for a given adhesive composition and size.

Evaluating microplastics removal efficiency

A. Coating the beads

Four types of adhesive coated beads ($P(2\text{-EHA})_{SPP\text{-}950k}$, $P(2\text{-EHA})_{Sigma\text{-}370k}$, $P(2\text{-EHA})_{P\&G\text{-}590k}$, and $P(2\text{-EHA})_{Sigma\text{-}93k}$) were prepared independently. $ZrSiO_4$ beads (0.5 mm, 20.0 g) were added to a 20 mL vial and washed by adding acetone (10 mL) and shaking for 30 s. Then, the solvent was removed using a needle and syringe. The beads were spread onto aluminum foil and oven dried (120 °C) for 10 min. After cooling to ambient temperature, adhesive solution, (1.0 mL, 5% w/v.) was added and the beads were hand-shaken (3 shakes per second) for 2 min. The solvent was removed by drying under high vacuum for 3 h.

B. Preparing microplastics suspension

Two stock suspensions of PS (1.0 mg/mL) in 80/20 H_2O/EtOH were prepared by adding PS (40.1 mg, 10 µm), nano pure H_2O (32.0 mL), and EtOH (8.00 mL) to 50 mL centrifuge tubes. The mixture was vortex mixed at 10 setting for 30 s and sonicated for 15 min.

C. Microplastics removal

Four time points (0.5, 1, 3, and 5 min) and four replications for each time point (i.e., each time point was run 4x) were collected (i.e., 64 samples) for each of the four adhesives. To accomplish this goal, adhesive-coated beads (400 mg) were added to sixty-four 4 mL vials, which were labeled accordingly.

The stock PS suspension (40.0 mL, 1.0 mg/mL) was hand-shaken to homogenize followed by transferring 1.00 mL using a needle (18 gauge) and syringe (1 mL) into the 4 mL vials containing the adhesive-coated beads. Immediately after transferring the suspension, the vials were hand-

shaken (approx. 3 shakes per s) for the appropriate time (0.5, 1, 3, and 5 min). After shaking, a needle (18 gauge) and syringe (3 mL) was used to transfer the remaining microplastic suspensions into a 1.5 mL Eppendorf tubes and stored in the refrigerator until quantification via flow cytometry was performed (within 2 d).

Note: For each time point, Julie Rieland performed the hand-shaking on replicates number 2 and 3 while Takunda Chazovachii did the hand-shaking on replicates number 1 and 4.

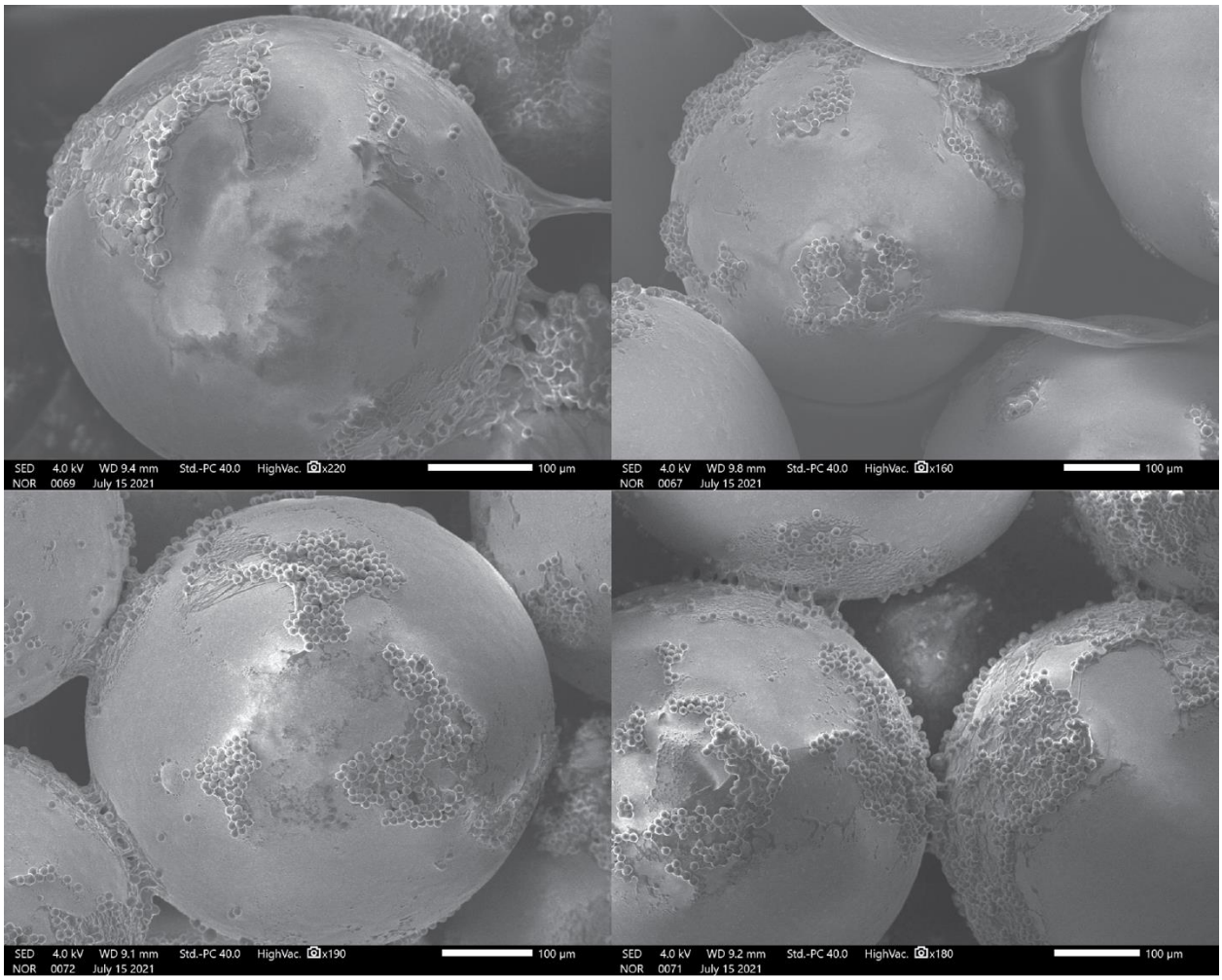

Figure A3-13. Additional SEM images of P(2-EHA)$_{590}$-coated beads after a 5 min exposure to the PS microplastic solution.

D. Flow cytometry analysis

Flow cytometry was used to quantify the concentration of microplastics in aqueous suspension. The technique is traditionally used to study physiochemical properties of cells (size, granularity, antibody expression, etc.) and sort different cellular populations according to their differences and/or similarities. Fluorescent staining is usually an integral part of the analysis since the complexity of cells would necessitate a variety of fluorophore for each dimension under observation. However, for the purposes of this work (solely particle quantitation), fluorescent staining was not necessary as a single class of microplastics (10 micron polystyrene) was under inspection. The instrument used is an Attune NXT Flow Cytometer. The settings are as follows: forward scatter detector gain (200 mV), sample flow rate (25 µl/min), and sample volume (30 µl).

Table A3-2. Processed data from the flow cytometry experiments plotted in Figures A3-15–35. Note that the raw data was first multiplied by a factor of 33.3 to convert the 30 µL injection volume to a count/mL for this table.

sample information	singlets/mL	doublets/mL	triplets/mL	other/mL[a]	sum/mL	% removal
PS stock 1	923774.28	225707.4	25474.5	5766.09	1174956.18	0
PS stock 2	908309.16	233566.2	28571.4	5799.42	1170446.76	0
PS stock 3	781955.13	286380	42557.4	5832.75	1110892.53	0
PS stock 4	673999.26	357642	93006.9	7665.9	1124648.16	0
PS stock 5	674065.92	345853.8	79420.5	7765.89	1099340.22	0
Sigma-93k 5min 1	5866.08	1065.6	399.6	28597.14	7331.28	99.4
Sigma-93k 5min 2	10998.9	3196.8	999	17798.22	15194.7	98.7
Sigma-93k 5min 3	14798.52	3130.2	799.2	13631.97	18727.92	98.4
Sigma-93k 5min 4	12665.4	4129.2	1098.9	18998.1	17893.5	98.4
Sigma-93k 3min 1	29697.03	12387.6	5994	20764.59	48078.63	95.8
Sigma-93k 3min 2	30430.29	6460.2	2297.7	13431.99	39188.19	96.6
Sigma-93k 3min 3	33230.01	11122.2	4095.9	16898.31	48448.11	95.7
Sigma-93k 3min 4	25530.78	11322	3396.6	21164.55	40249.38	96.5
Sigma-93k 1min 1	101589.84	33433.2	18481.5	34229.91	153504.54	86.5
Sigma-93k 1min 2	101389.86	35697.6	16683.3	13198.68	153770.76	86.5
Sigma-93k 1min 3	110155.65	46153.8	35164.8	9732.36	191474.25	83.1
Sigma-93k 1min 4	75525.78	30769.2	18081.9	21797.82	124376.88	89.1
Sigma-93k 0.5min 1	110855.58	41292	19780.2	34629.87	171927.78	84.9
Sigma-93k 0.5min 2	130786.92	51415.2	35364.6	10598.94	217566.72	80.8
Sigma-93k 0.5min 3	179582.04	68464.8	42357.6	12765.39	290404.44	74.4
Sigma-93k 0.5min 4	133153.35	43223.4	21078.9	20897.91	197455.65	82.6
P&G-590k 5min 1	12865.38	865.8	199.8	2299.77	13930.98	98.8
P&G-590k 5min 2	11498.85	1332	99.9	2766.39	12930.75	98.9
P&G-590k 5min 3	19598.04	1864.8	399.6	1866.48	21862.44	98.1
P&G-590k 5min 4	13865.28	1598.4	199.8	3033.03	15663.48	98.6
P&G-590k 3min 1	40995.9	8058.6	899.1	2666.4	49953.6	95.6
P&G-590k 3min 2	98790.12	15651	2397.6	2899.71	116838.72	89.7
P&G-590k 3min 3	64260.24	9390.6	1198.8	1933.14	74849.64	93.4
P&G-590k 3min 4	48928.44	8325	999	1533.18	58252.44	94.9
P&G-590k 1min 1	187381.26	41625	7992	2066.46	236998.26	79.1
P&G-590k 1min 2	250441.62	74791.8	11188.8	2833.05	336422.22	70.4
P&G-590k 1min 3	192980.7	52081.2	7392.6	2366.43	252454.5	77.8
P&G-590k 1min 4	171516.18	25108.2	2997	2766.39	199621.38	82.4
P&G-590k 0.5min 1	271039.56	72460.8	13486.5	3866.28	356986.86	68.6
P&G-590k 0.5min 2	391627.5	92574	11988	1866.48	496189.5	56.3
P&G-590k 0.5min 3	421524.51	139393.8	24175.8	2966.37	585094.11	48.5
P&G-590k 0.5min 4	315601.77	76257	18481.5	2799.72	410340.27	63.9
Sigma-370k 5min 1	48295.17	11655	2797.2	2666.4	62747.37	94.5

Sigma-370k 5min 2	66893.31	18381.6	3296.7	2499.75	88571.61	92.2
Sigma-370k 5min 3	88457.82	32434.2	11688.3	2066.46	132580.32	88.3
Sigma-370k 5min 4	47961.87	14718.6	2497.5	3266.34	65177.97	94.3
Sigma-370k 3min 1	89891.01	39094.2	16183.8	2666.4	145169.01	87.2
Sigma-370k 3min 2	189581.04	60939	16583.4	2966.37	267103.44	76.5
Sigma-370k 3min 3	143585.64	44888.4	12087.9	3366.33	200561.94	82.3
Sigma-370k 3min 4	78792.12	38361.6	17682.3	3699.63	134836.02	88.1
Sigma-370k 1min 1	290604.27	110822.4	43356.6	2499.75	444783.27	60.8
Sigma-370k 1min 2	391127.55	140059.8	34065.9	2766.39	565253.25	50.2
Sigma-370k 1min 3	336266.37	123409.8	35264.7	2333.1	494940.87	56.4
Sigma-370k 1min 4	257940.87	94705.2	37462.5	2733.06	390108.57	65.7
Sigma-370k 0.5min 1	400259.97	138661.2	39660.3	2866.38	578581.47	49.1
Sigma-370k 0.5min 2	407159.28	163902.6	50349.6	1766.49	621411.48	45.3
Sigma-370k 0.5min 3	558144.18	178155	39860.1	3566.31	776159.28	31.7
Sigma-370k 0.5min 4	366363.36	138461.4	47452.5	2533.08	552277.26	51.4
SPP-950k 5min 1	10232.31	1398.6	299.7	20064.66	11930.61	98.9
SPP-950k 5min 2	9132.42	1798.2	499.5	22164.45	11430.12	99.0
SPP-950k 5min 3	85458.12	17316	1698.3	3033.03	104472.42	90.8
SPP-950k 5min 4	28397.16	5927.4	699.3	4299.57	35023.86	96.9
SPP-950k 3min 1	73359.33	24175.8	5394.6	4166.25	102929.73	90.9
SPP-950k 3min 2	185081.49	51015.6	7492.5	2366.43	243589.59	78.6
SPP-950k 3min 3	146885.31	24975	3496.5	2566.41	175356.81	84.6
SPP-950k 3min 4	77758.89	27639	7892.1	3666.3	113289.99	90.0
SPP-950k 1min 1	254807.85	77122.8	20079.9	4932.84	352010.55	69.0
SPP-950k 1min 2	328900.44	107359.2	19980	2233.11	456239.64	59.8
SPP-950k 1min 3	362230.44	115950.6	18381.6	2199.78	496562.64	56.3
SPP-950k 1min 4	255841.08	66799.8	9990	2433.09	332630.88	70.7
SPP-950k 0.5min 1	369063.09	123210	30569.4	2266.44	522842.49	54.0
SPP-950k 0.5min 2	430590.27	123676.2	21978	2233.11	576244.47	49.3
SPP-950k 0.5min 3	447221.94	176290.2	43956	2833.05	667468.14	41.2
SPP-950k 0.5min 4	396560.34	107825.4	20379.6	2833.05	524765.34	53.8

[a,b] The doublets and triplets were multiplied by the 2 and 3, respectively, in the “sum” calculation. [c] The “other” counts were not included in the “sum.”

Table A3-3. Average counts from the flow cytometry data presented in Figures A3-15–35 and Table A1-2

sample information	singlets/mL	doublets/mL[a]	triplets/mL[b]	other/mL[c]	sum/mL	% removal
PS stock suspension	792421	289830	53806	6566	1136057	0.0
Sigma-93k 0.5min	138594	51099	29645	19723	219339	80.7
Sigma-93k 1min	97165	36513	22103	19740	155782	86.3
Sigma-93k 3min	29722	10323	3946	18065	43991	96.1
Sigma-93k 5min	11082	2880	824	19756	14787	98.7
P&G-590k 0.5min	349948	95171	17033	2875	462153	59.3
P&G-590k 1min	200580	48402	7393	2508	256374	77.4
P&G-590k 3min	63244	10356	1374	2258	74974	93.4
P&G-590k 5min	14457	1415	225	2491	16097	98.6
Sigma-370k 0.5min	432982	154795	44331	2683	632107	44.4
Sigma-370k 1min	318985	117249	37537	2583	473771	58.3
Sigma-370k 3min	125462	45821	15634	3175	186918	83.5
Sigma-370k 5min	62902	19297	5070	2625	87269	92.3
SPP-950k 0.5min	410859	132750	29221	2541	572830	49.6
SPP-950k 1 min	300445	91808	17108	2950	409361	64.0
SPP-950k 3 min	120771	31951	6069	3191	158792	86.0
SPP-950K 5 min	33305	6610	799	12390	40714	96.4

[a,b] The doublets and triplets were multiplied by the 2 and 3, respectively, in the "sum" calculation. [c] The "other" counts were not included in the "sum."

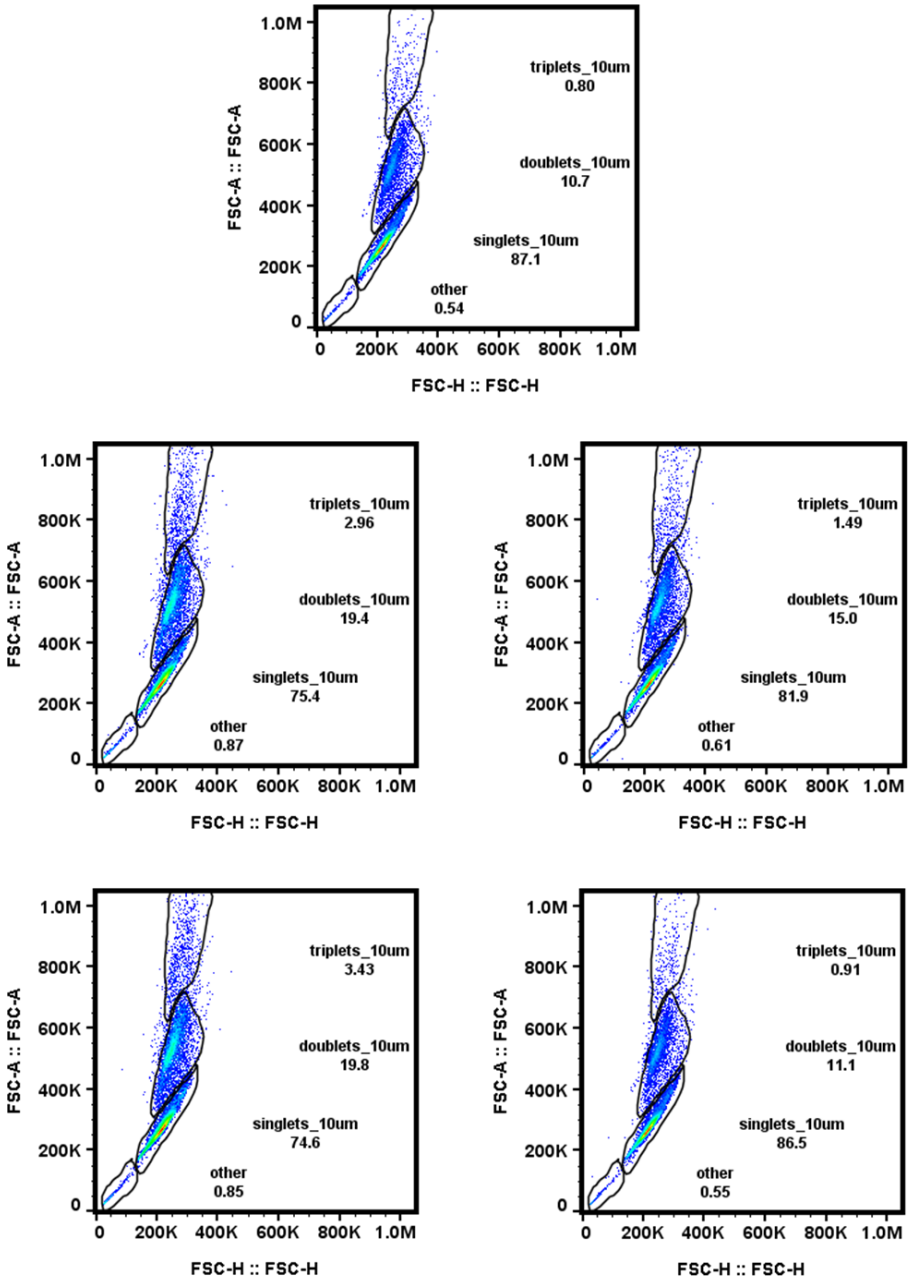

Figure A3-14. Flow cytometry data for stock PS microplastics suspensions.

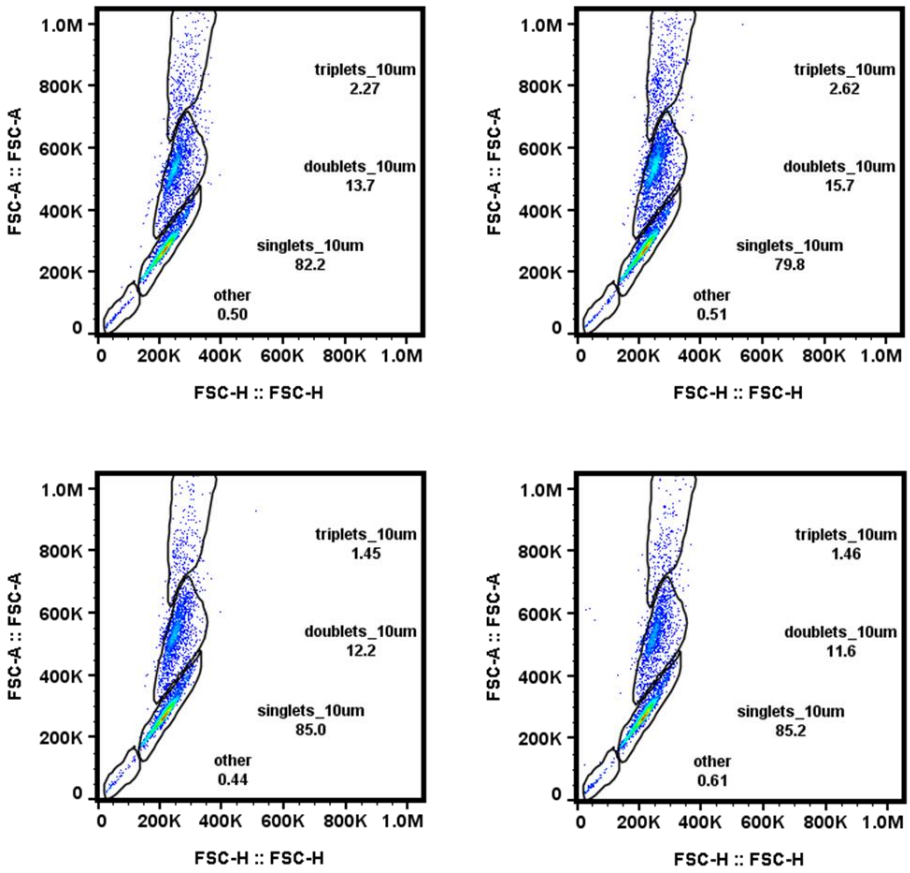

Figure A3-15. Flow cytometry data at **0.5 min** for capturing PS microplastics using P(2-EHA)$_{950K}$ coated onto beads

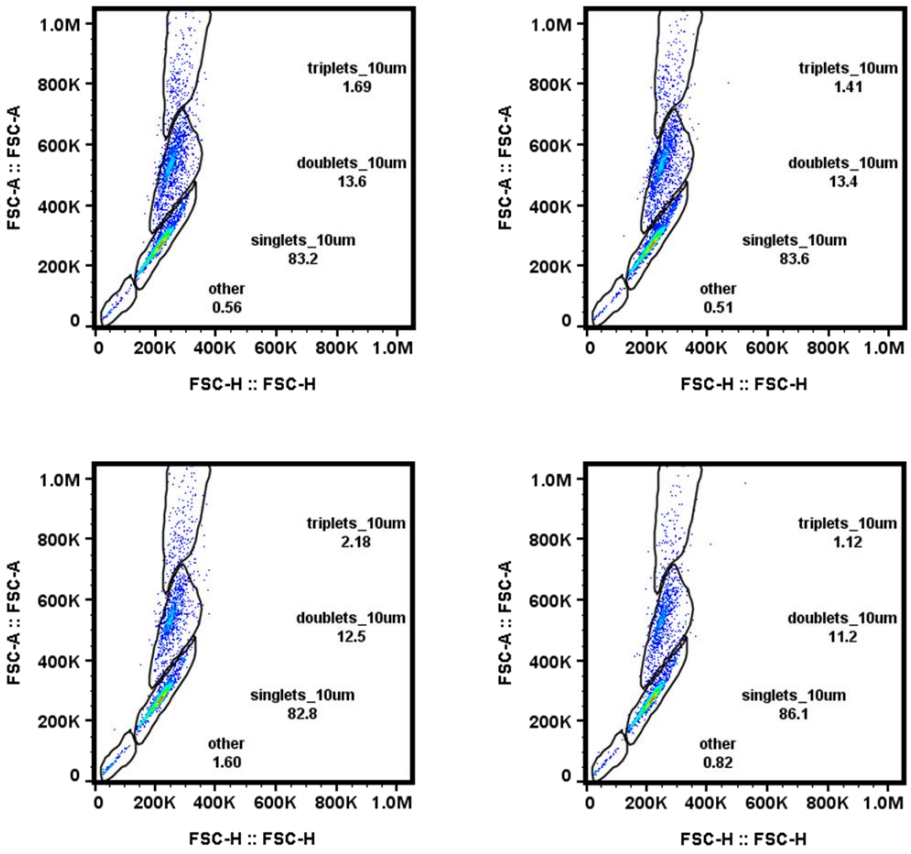

Figure A3-16. Flow cytometry data at 1 min for capturing PS microplastics using P(2-EHA)$_{950K}$ coated onto beads

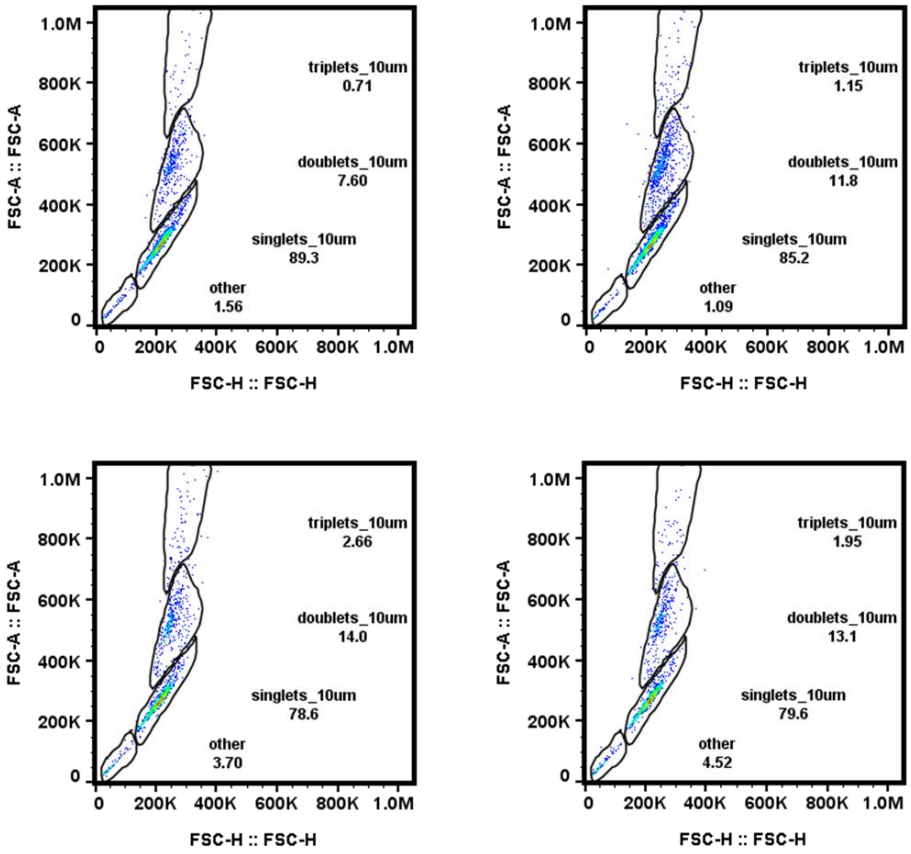

Figure A3-17. Flow cytometry data at **3 min** for capturing PS microplastics using P(2-EHA)$_{950K}$ coated onto beads

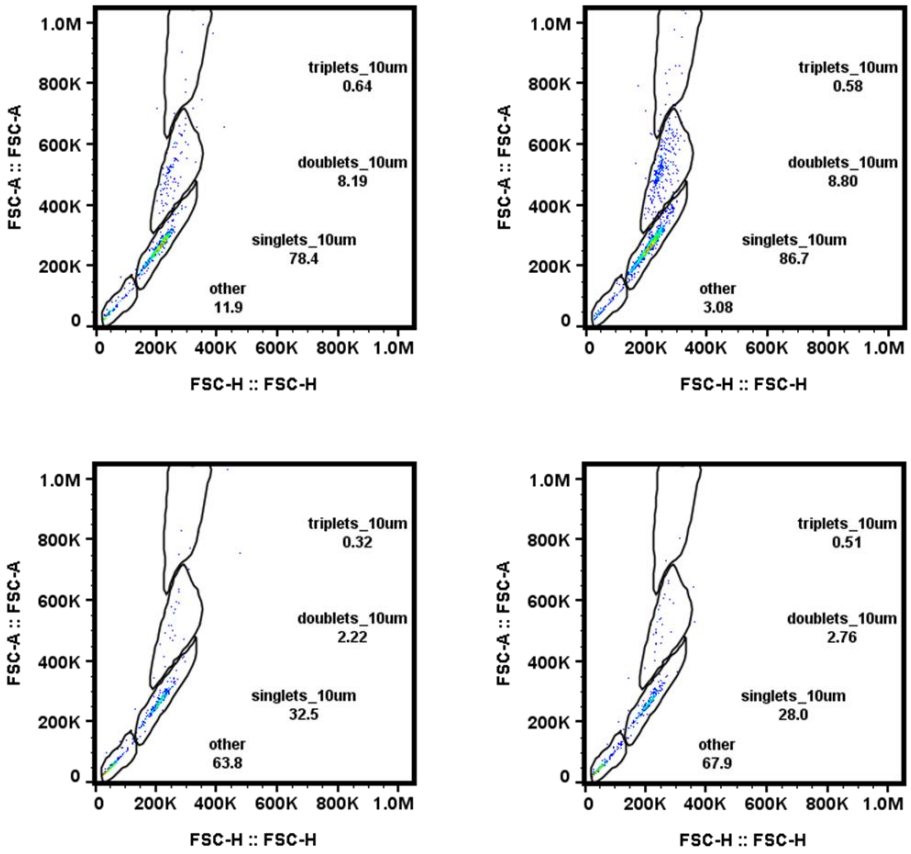

Figure A3-18. Flow cytometry data at **5 min** for capturing PS microplastics using P(2-EHA)$_{950K}$ coated onto beads

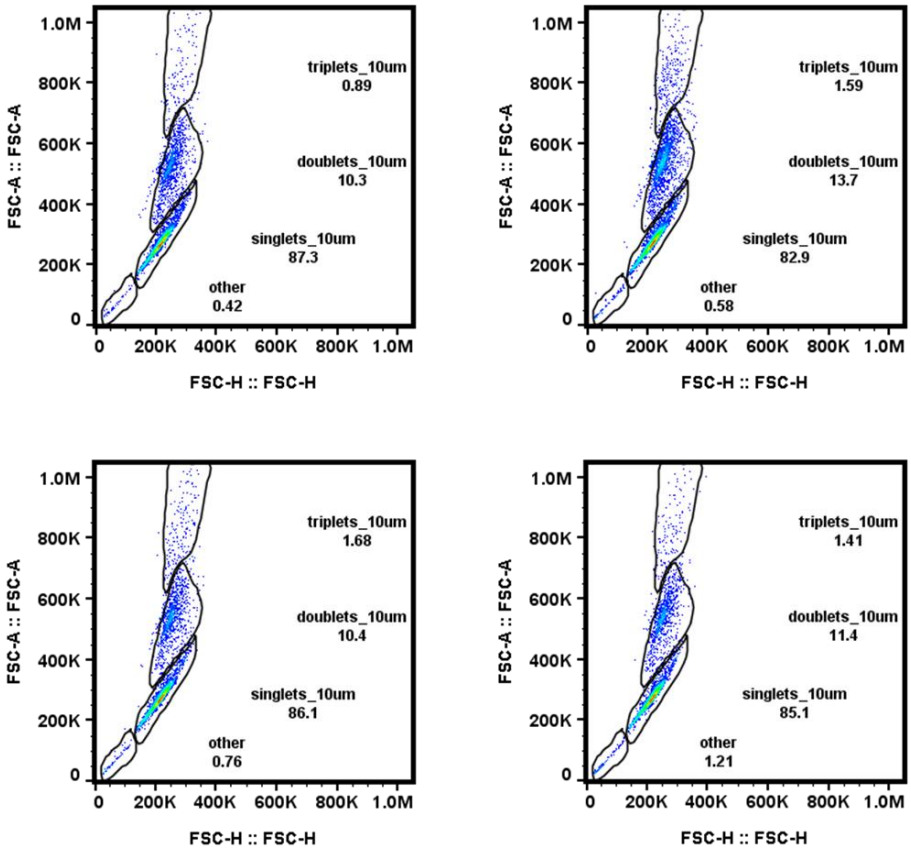

Figure A3-19. Flow cytometry data at **0.5 min** for capturing PS microplastics using P(2-EHA)$_{590K}$ coated onto beads

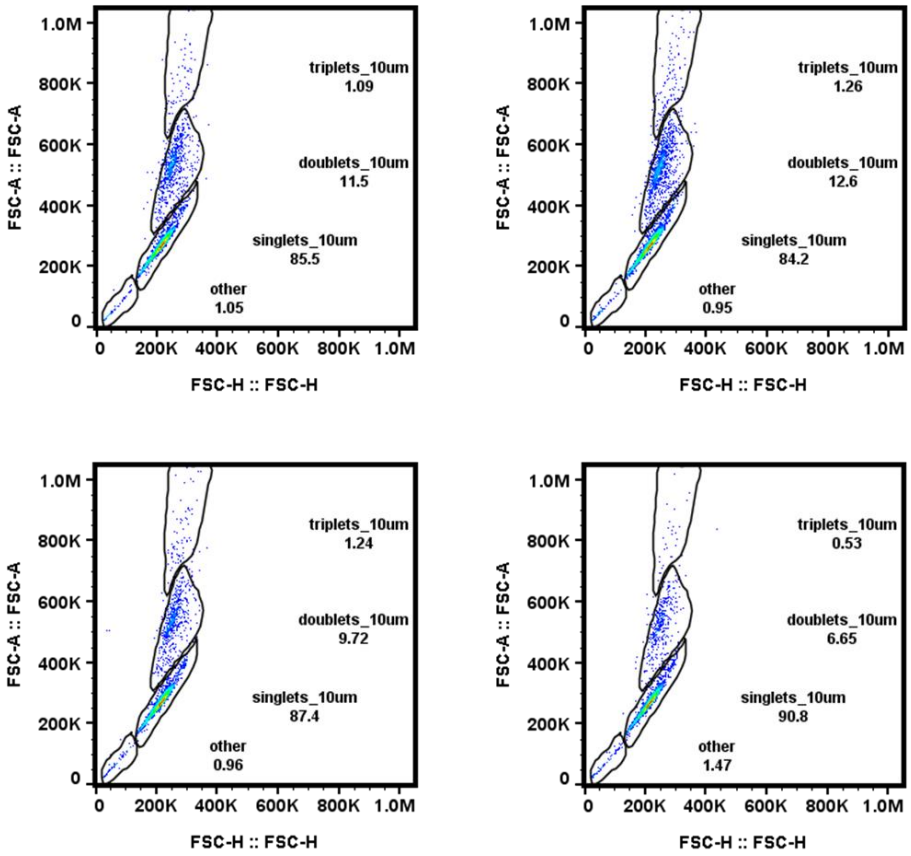

Figure A3-20. Flow cytometry data at **1 min** for capturing PS microplastics using P(2-EHA)$_{590K}$ coated onto beads

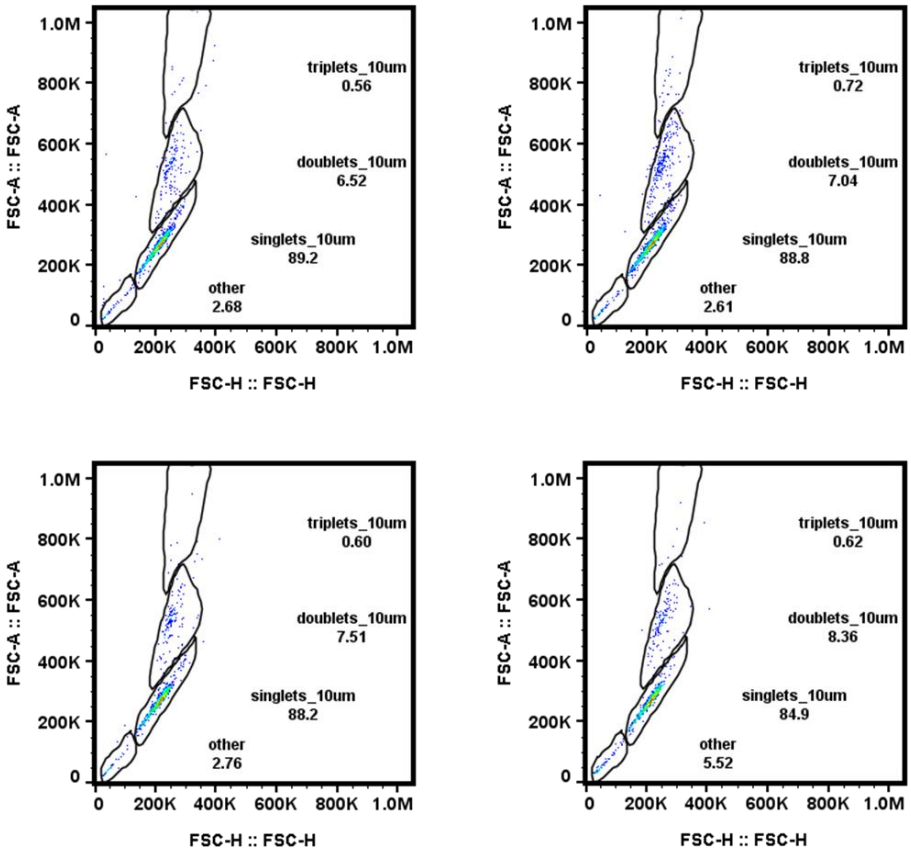

Figure A3-21. Flow cytometry data at **3 min** for capturing PS microplastics using P(2-EHA)$_{590K}$ coated onto beads

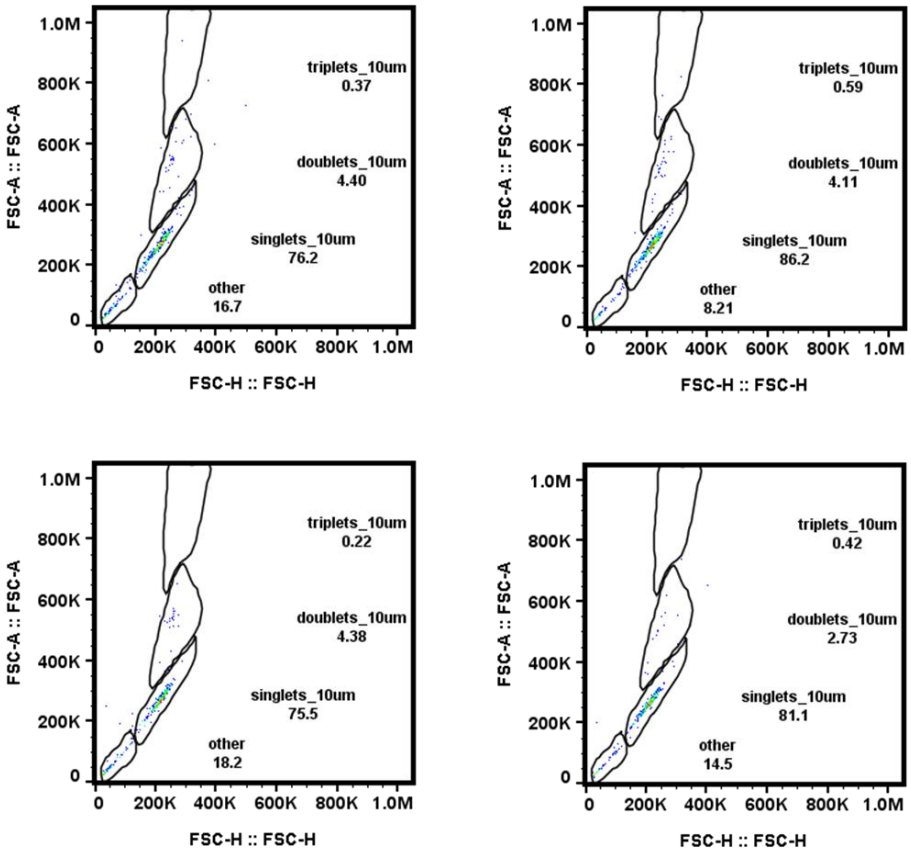

Figure A3-22. Flow cytometry data at **5 min** for capturing PS microplastics using P(2-EHA)$_{590K}$ coated onto beads

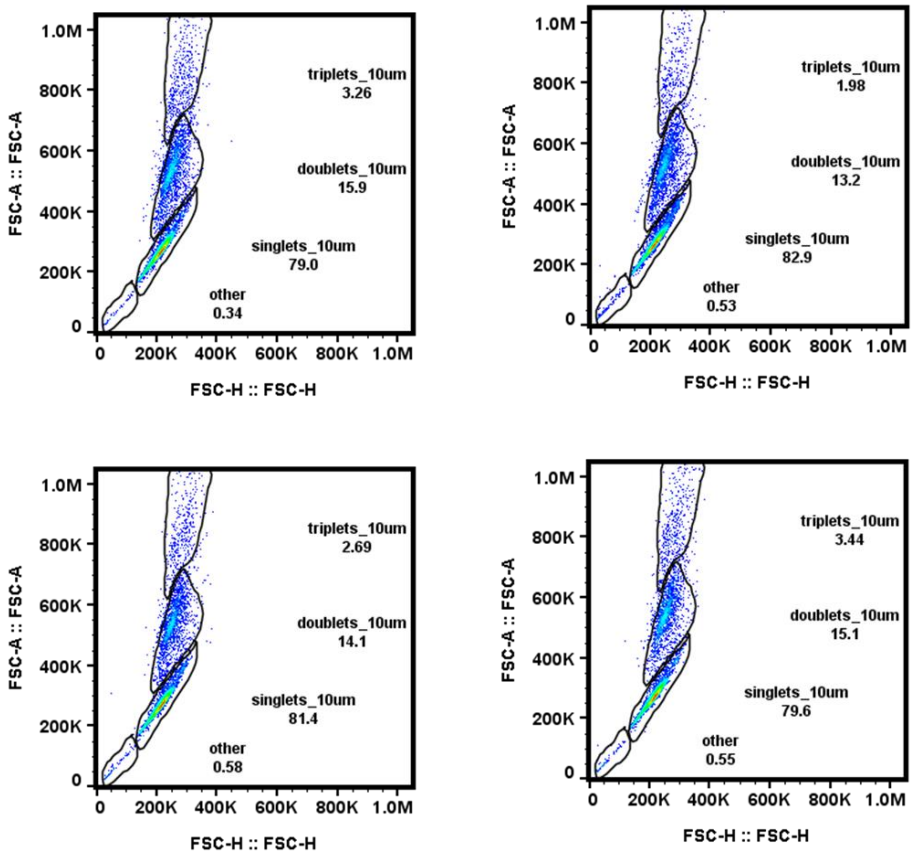

Figure A3-23. Flow cytometry data at **0.5 min** for capturing PS microplastics using P(2-EHA)$_{370K}$ coated onto beads

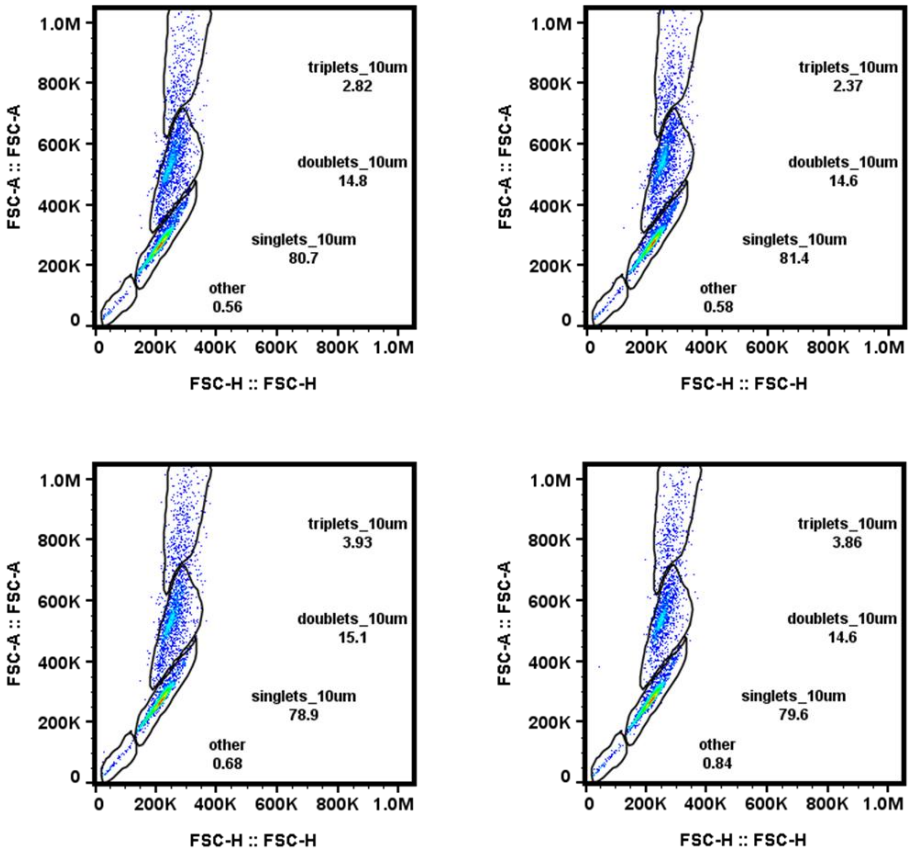

Figure A3-24. Flow cytometry data at **1 min** for capturing PS microplastics using P(2-EHA)$_{370K}$ coated onto beads

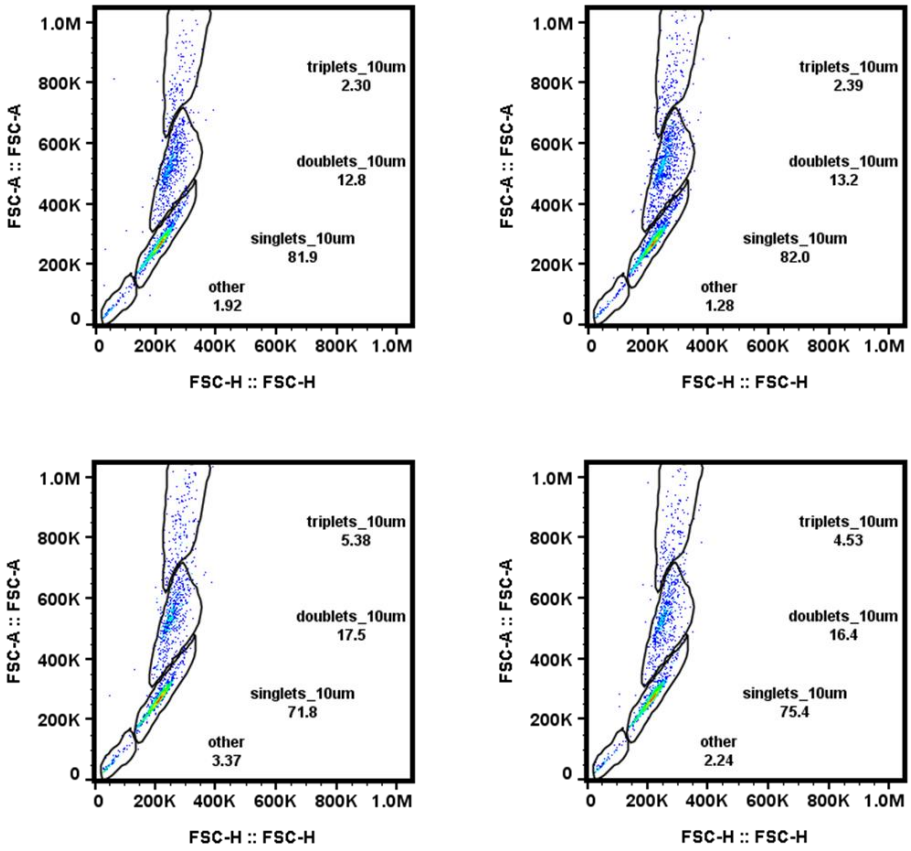

Figure A3-25. Flow cytometry data at **3 min** for capturing PS microplastics using $P(2\text{-EHA})_{370K}$ coated onto beads

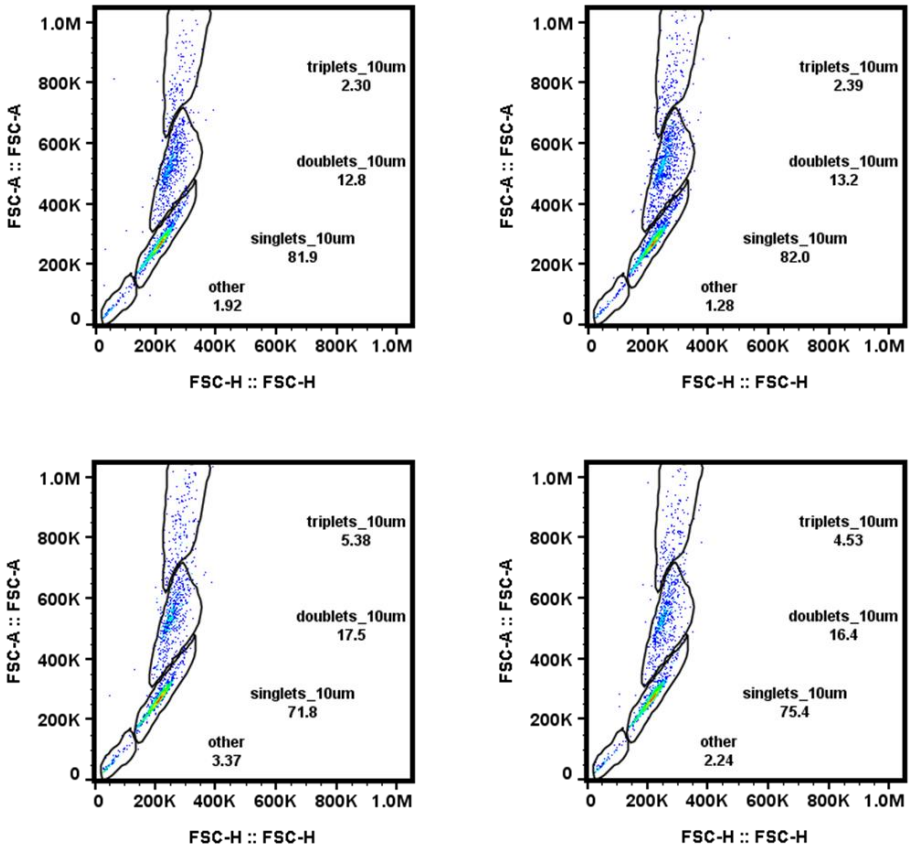

Figure A3-26. Flow cytometry data at **5 min** for capturing PS microplastics using P(2-EHA)$_{370K}$ coated onto beads

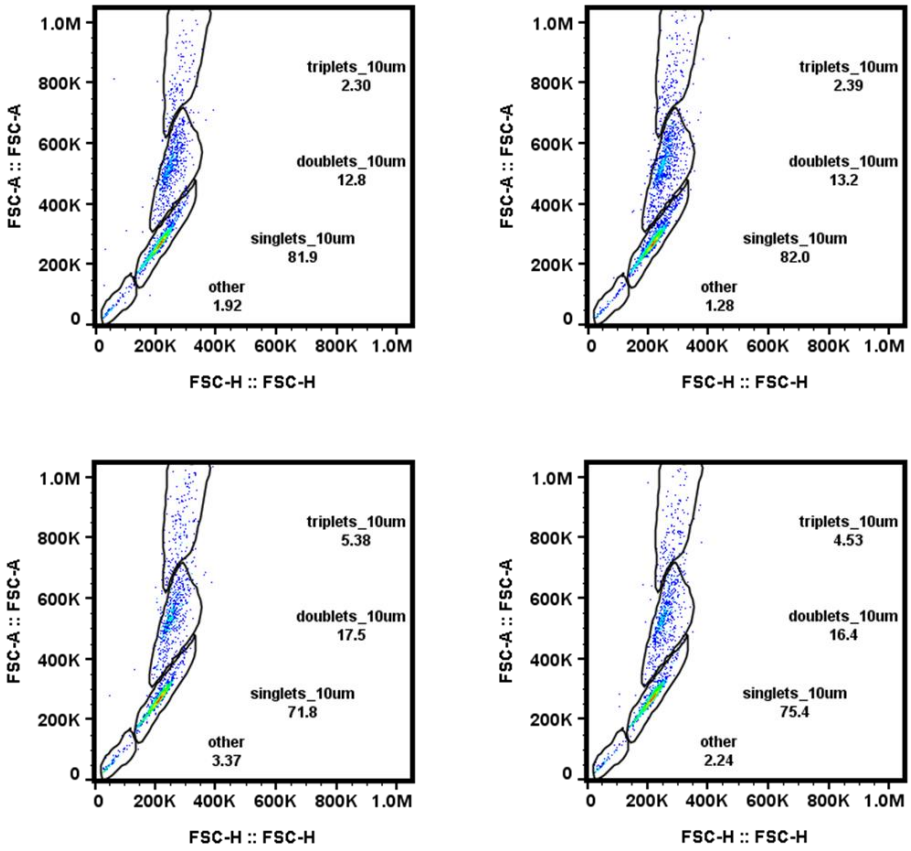

Figure A3-27. Flow cytometry data at **0.5 min** for capturing PS microplastics using P(2-EHA)$_{93K}$ coated onto beads

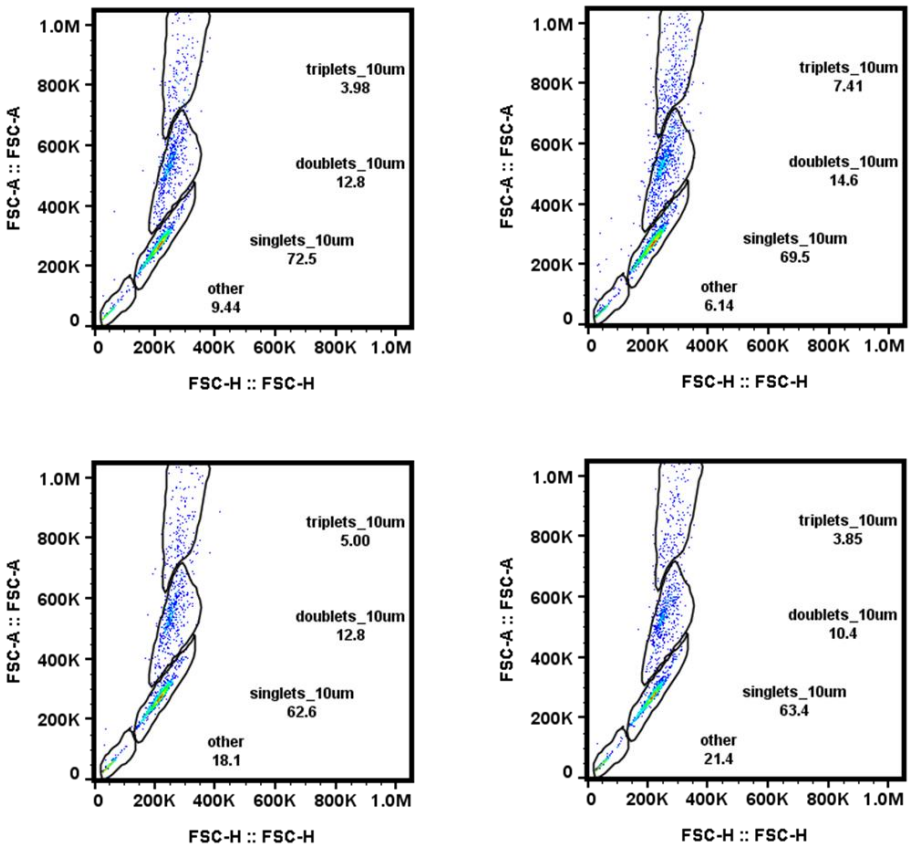

Figure A3-28. Flow cytometry data at **1 min** for capturing PS microplastics using P(2-EHA)$_{93K}$ coated onto beads

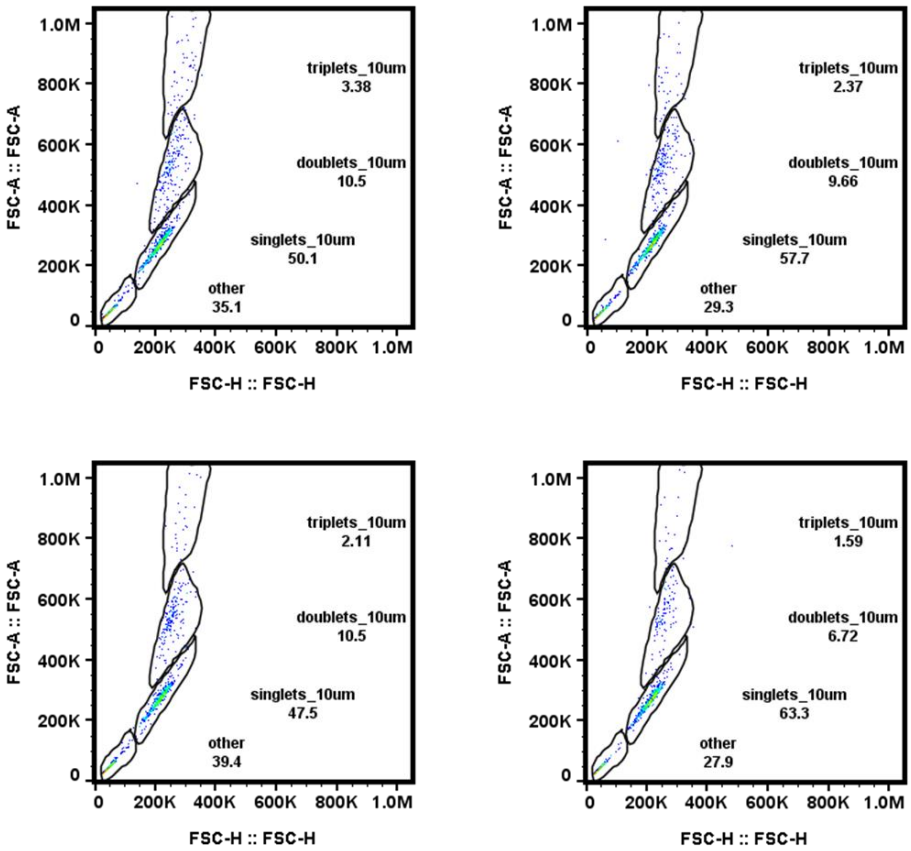

Figure A3-29. Flow cytometry data at **3 min** for capturing PS microplastics using P(2-EHA)$_{93K}$ coated onto beads

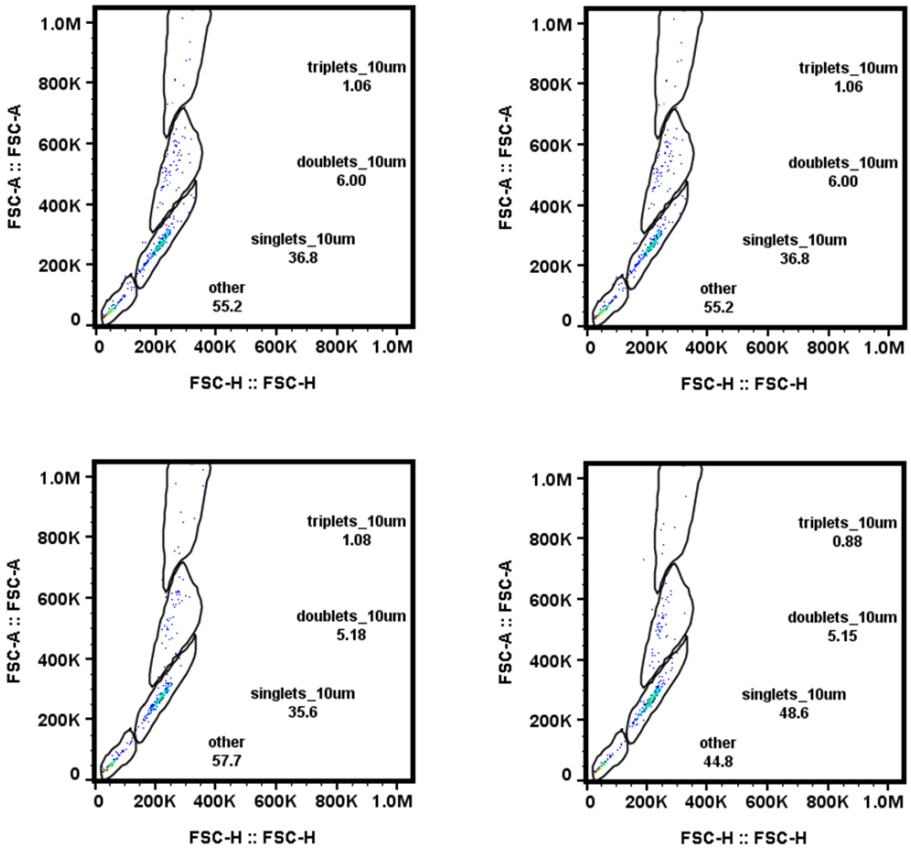

Figure A3-30. Flow cytometry data at **5 min** for capturing PS microplastics using P(2-EHA)$_{93K}$ coated onto beads

E. Microplastics removal efficiency without EtOH

Five PS suspensions in H_2O (1.0 mg/mL) were prepared by adding PS (1.0 mg, 10 μm) and H_2O (1.00 mL) to a 4 mL vial followed by vortex mixing for 1 min.

Four of the five suspensions prepared were used for the removal experiment. To each of the four suspensions, $P(2\text{-EHA})_{P\&G\text{-}590k}$ coated beads (400 mg) were added and the suspensions were hand-shaken at 3 shakes per second for 5 min. After hand-shaking, EtOH (200 μL) was added to each sample to homogenize the suspension, and then a needle (18 gauge) and syringe (3 mL) was used to transfer the remaining microplastic suspension into 1.5 mL Eppendorf tube, which was stored in the refrigerator until quantification (~10 h).

Note: Julie Rieland performed the hand-shaking on replicates number 1 and 2 while Takunda Chazovachii performed the hand-shaking on replicates number 3 and 4.

Table A3-4. Summary of flow cytometry data for experiments with EtOH added before analysis. Note that the raw data was first multiplied by a factor of 40 to convert the 30 μL injection volume to a count/mL for this table.

sample	**singlets/mL**	**doublets/mL**[a]	**triplets/mL**[b]	**other/mL**[c]	**sum/mL**	**average**	**stdev**	**% removal**
P&G-590k 1	3640	400	120	3240	4160			
P&G-590k 2	1080	240	0	4240	1320			
P&G-590k 3	1040	320	240	3600	1600			
P&G-590k 4	480	400	360	4080	1240	2080	1208	99.83
PS stock 1	902640	330400	37080	6000	1270120			
PS stock 2	952080	267360	27840	4560	1247280			
PS stock 3	964240	261520	29280	5640	1255040			
PS stock 4	857440	316160	24960	5000	1198560	1242750	26802	0

[a,b] The doublets and triplets were multiplied by the 2 and 3, respectively, in the "sum" calculation.
[c] The "other" counts were not included in the "sum."

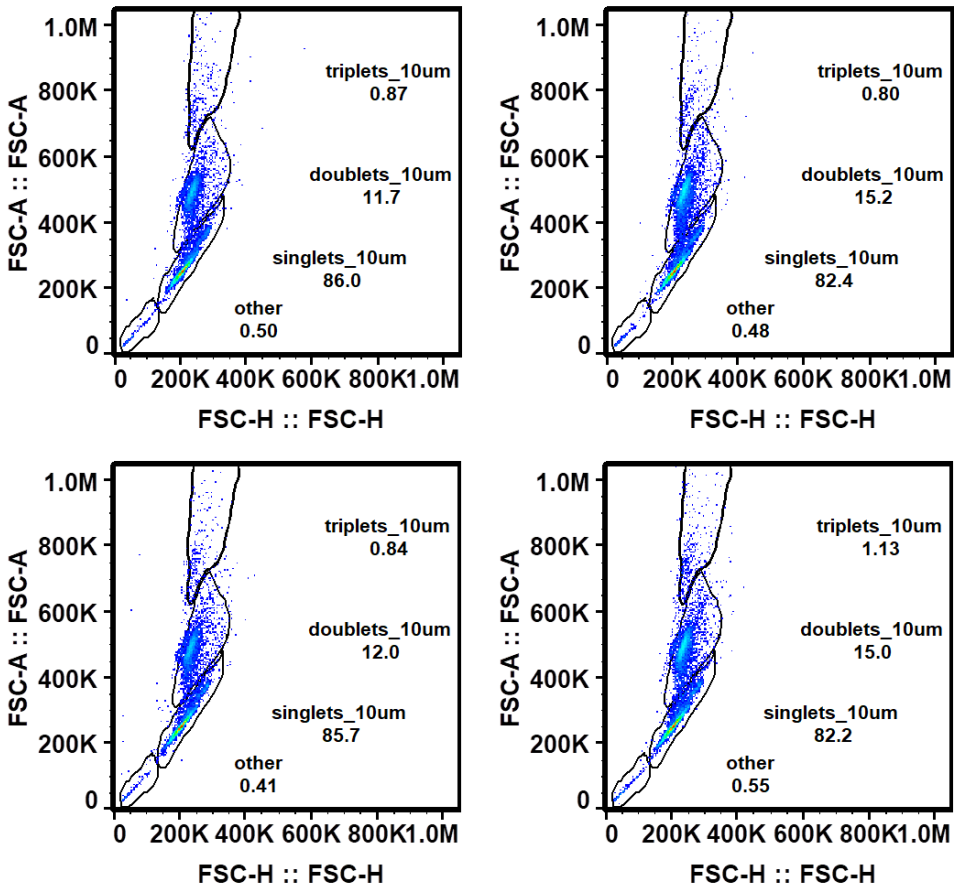

Figure A3-31. Flow cytometry data for PS stock solution with EtOH added for sample analysis only.

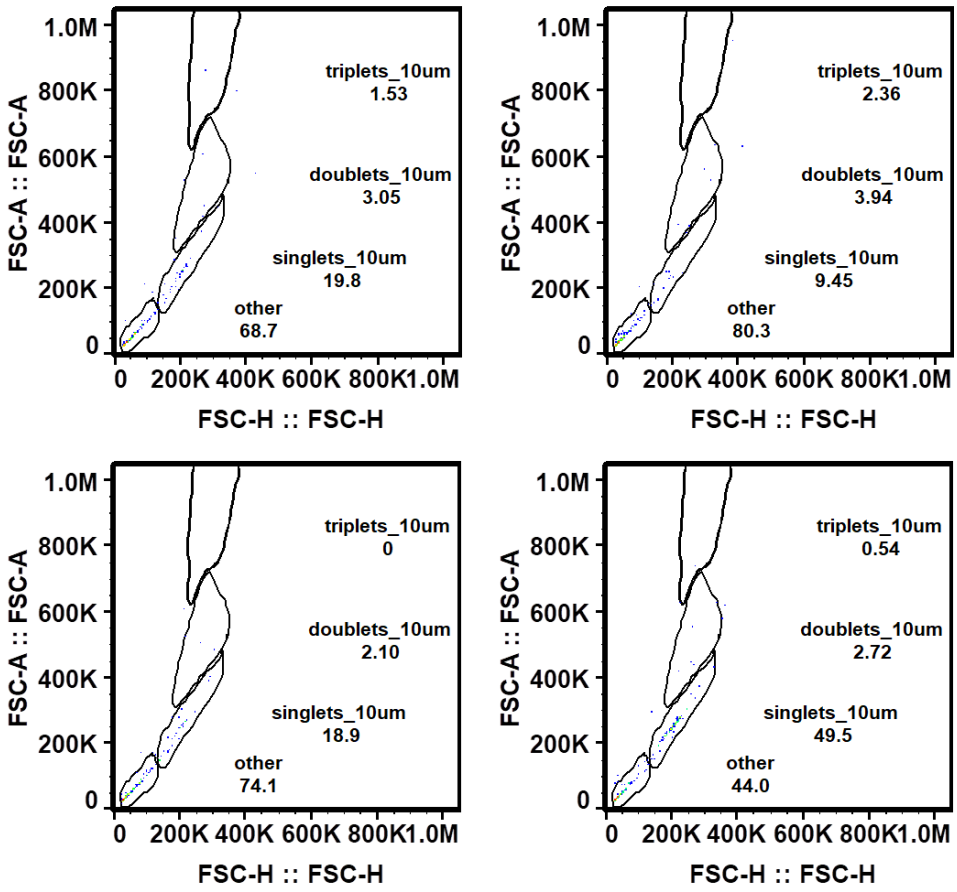

Figure A3-32. Flow cytometry data at **5 min** for capturing PS microplastics using P(2-EHA)$_{590K}$ coated onto beads with EtOH added only for analysis.

Testing MPs removal using glass slides

A. Coating glass slides

Onto five glass slides (1.2 x 4.0 cm), a $P(2\text{-EHA})_{P\&G\_590k}$ solution in THF (10 µL, 5% w/v) was dispensed using a micropipette. The slides were then held for 2 min at room temperature and then further dried at 125 °C in the oven for 2 min. The slides were then cooled to room temperature for about 5 min.

B. Preparing microplastics suspensions

Microplastic suspensions (final conc = 2.0 mg/mL) of nylon (30 µm), poly(ethylene) (PE, 50 µm), micronized rubber (MR, 100 µm), and poly(ethylene terephthalate) (300 µm) were prepared by adding the microplastics (10 mg) and ultrafiltered H_2O (5.00 mL) to 20 mL vials followed by vortex mixing for 1 min.

C. Microplastics capture

To each microplastics suspension, an adhesive-coated glass slide was added, and the suspensions were hand-shaken for 5 min at 3 shakes per second. Thereafter, the glass slides were removed using tweezers and washed with DI H_2O (20 mL) using a squirt bottle to remove unadhered MPs. The slides were then air-dried for 30 min and analyzed using optical microscopy.

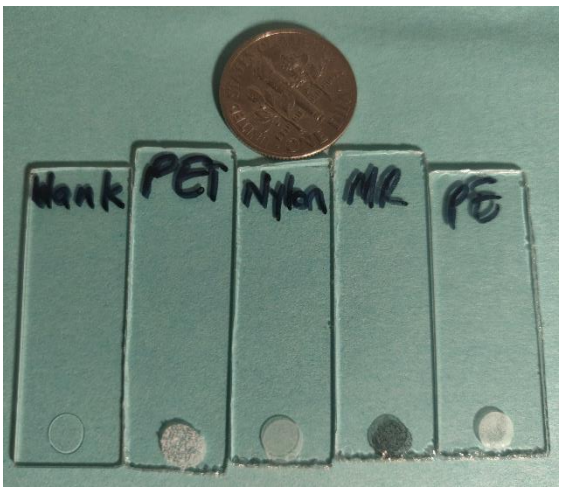

Figure A3-33. Glass slides with drop-cast P(2-EHA)$_{P\&G\_590k}$ after microplastics capture.

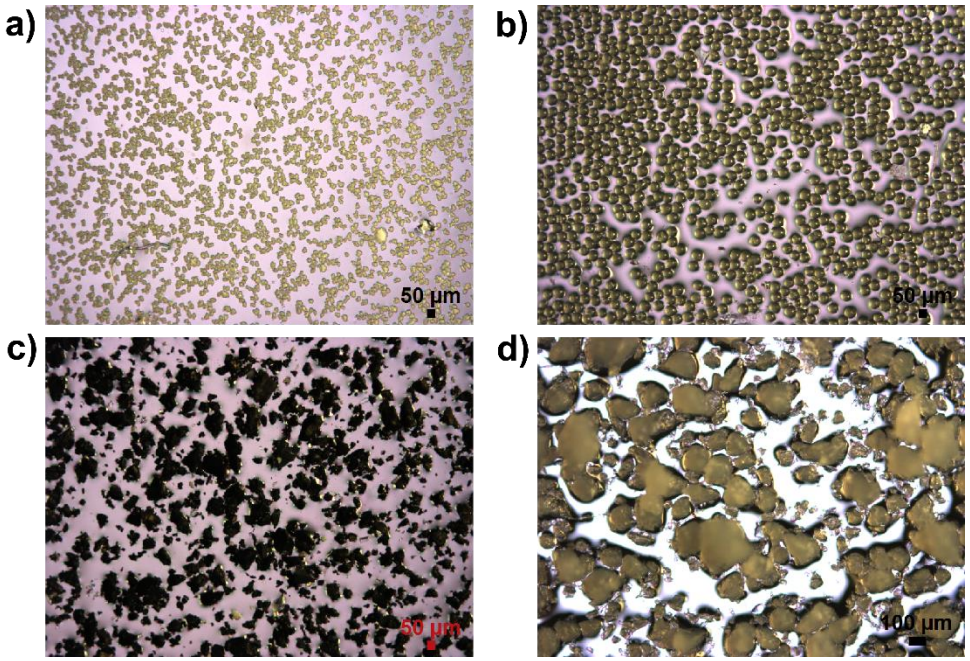

Figure A3-34. Optical microscope images of adhesive-coated glass slides that captured other microplastics: (a) nylon (30 µm), (b) poly(ethylene) (PE, 50 µm), (c) micronized rubber (MR, 100 µm), and (d) poly(ethylene terephthalate) (300 µm).

Effect of surfactant on microplastics removal

A stock dispersion of PS in DI H_2O (5 mg/mL) was prepared by adding PS (200 mg, 40 µm) and DI water (40 mL) to a 50 mL centrifuge tube. The mixture was vortex mixed at 10/10 setting for 30 seconds and sonicated for 5 min. While handshaking (3 shakes per second) for 10 s between aliquot transfers, aliquots (2 mL) were transferred into four 8 mL vials, which were subsequently used in MPs removal experiments.

In a 4 mL vial, sodium dodecyl sulfate (SDS, 20 mg) was dissolved with DI H_2O (1.0 mL) to make a 2.0% w/v stock solution. Serial dilutions were performed to make a 1.0% (500 µL of 2.0% sln plus 500 µL of DI H_2O) and 0.2% (100 µL of 1.0% sln plus 400 µL of DI H_2O). To prepare samples with varying concentrations of surfactant (i.e., 0.10%, 0.05%, and 0.01% w/v), 100 uL of the 2.0%, 1.0%, and 0.20% w/v surfactant solutions were added to the 2 mL MPs suspensions.

10% w/v solution in THF of $P(2\text{-EHA})_{P\&G\_780k}$ were prepared and used for MPs removal. Onto each glass substrate (0.8x20 mm), a droplet (10 uL) of adhesive was dispensed using a micropipette (Figure A3-12). The THF was allowed to evaporate for 2 minutes under ambient conditions and then further dried at 125 C in the oven for 2 min. The slides were left to cool to ambient temperature for about 5 min.

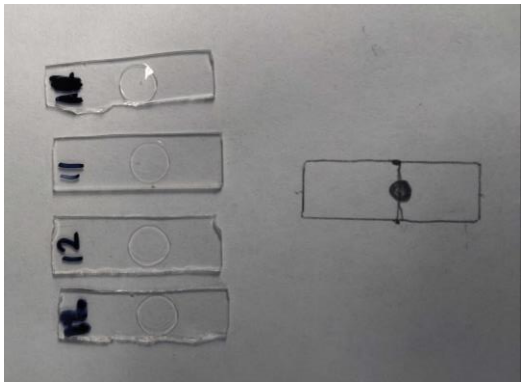

Figure A3-35. Glass slides coated with $P(2\text{-EHA})_{P\&G\_780k}$ for MPs removal.

For MPs removal, the adhesive coated glass slide was dropped into the 8 mL containing the microplastics dispersion and immediately vortex mixed at the 6/10 setting for 1 min. Afterwards, the glass slide was washed by squirting with DI water and then left to air dry for 20 min. The slides were analyzed by taking optical microscopic images of the center of each spot.

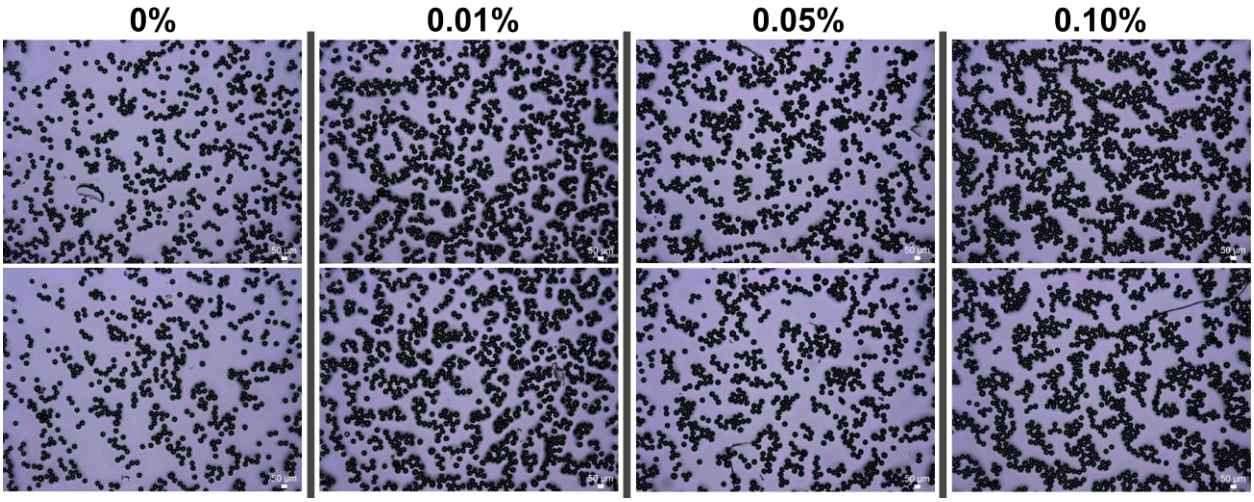

Figure A3-36. Optical microscopic images on the effect of surfactant on microplastics removal.

References

1 Jo, S.; Kim, T.; Iyer, V.G.; Im, W. CHARMM-GUI: A Web-based Graphical User Interface for CHARMM. *J. Comput. Chem.* **2008**, 29, 1859–1865.

2 Martìnez, L.; Andrade, R.; Birgin, E.G.; Martìnez, J.M. Packmol: A package for building initial configurations for molecular dynamics simulations. *J. Comput. Chem.* **2009**, 30, 2157–2164.

3 Lee, B.; Richards, F.M. The interpretation of protein structures: estimation of static accessibility. *J. Mol. Biol.* **1971**, 55, 379–400.

4 Dean, R.B.; Dixon, W.J. Simplified Statistics for Small Numbers of Observations. *Anal. Chem.* **1951**, 23, 636–638.